

**STUDIES ON THE ROLE OF AMMONIA IN THE CONTROL OF BREATHING IN THE
PACIFIC HAGFISH (*Eptatretus stoutii*) AND RAINBOW TROUT (*Oncorhynchus mykiss*)**

by

Junho Eom

B.Sc., Kangwon National University, 2003

M.Sc., University of British Columbia, 2016

A DISSERTATION SUBMITTED IN PARTIAL FULFILLMENT OF
THE REQUIREMENTS FOR THE DEGREE OF

DOCTOR OF PHILOSOPHY

in

THE FACULTY OF GRADUATE AND POSTDOCTORAL STUDIES

(Zoology)

THE UNIVERSITY OF BRITISH COLUMBIA

(Vancouver)

March 2021

© Junho Eom, 2021

The following individuals certify that they have read, and recommend to the Faculty of Graduate and Postdoctoral Studies for acceptance, the dissertation entitled:

Studies on the role of ammonia in the control of breathing in the Pacific hagfish (*Eptatretus stoutii*) and rainbow trout (*Oncorhynchus mykiss*)

submitted by Junho Eom in partial fulfillment of the requirements for

the degree of Doctor of Philosophy

in Zoology

Examining Committee:

Chris Wood, Department of Zoology, UBC
Co-Supervisor

Patricia Schulte, Department of Zoology, UBC
Co-Supervisor

William K. Milsom, Department of Zoology, UBC
Supervisory Committee Member

Eric B. Taylor, Department of Zoology, UBC
University Examiner

Scott Reid, Department of Biology, UBC
University Examiner

Additional Supervisory Committee Members:

Anthony Farrell, Department of Zoology, UBC
Supervisory Committee Member

Abstract

Ammonia, which is excreted across the gills, is the major nitrogenous waste of fish. It is also a toxicant. My thesis focuses on how and why ammonia influences breathing in fish, using the phylogenetically ancient Pacific hagfish (an agnathan) and the rainbow trout (a teleost) as models. I first characterized the unique breathing mechanism of hagfish, demonstrating a two-phase unidirectional system with a fast suction velar pump for inhalation through the nostril and a much slower force pump for exhalation through gill pouches. High environmental ammonia (HEA) causes an initial hypoventilation, sometimes apnea, and a later sustained hyperventilation. The hypoventilation is independent from responses to O₂ and CO₂ and is mediated by external receptors. The hyperventilation is mediated by increased blood ammonia, detected internally, similar to previous findings on teleosts. In trout, I confirmed an assumption in the literature that ventilation would not affect ammonia excretion. However, I then used chronic internal ammonia loading to upregulate the ammonia transport system (rhesus glycoproteins) in the gills. This removed diffusion limitation so that ammonia excretion became sensitive to ventilation. Hyperventilating trout, therefore, excrete more ammonia. After developing a new less invasive system for the direct measurement of ventilation, I used it to show that HEA hyperventilation is not immediate, but develops gradually, mediated by internal receptors. Indeed, specific application of HEA to the external surface of the gills causes a transient acute hypoventilation, again as in hagfish. Direct application of ammonia to the hindbrain causes hyperventilation by the stimulation of central chemoreceptors, while peripheral chemoreceptors in the gills (neuroepithelial cells) sense increased plasma ammonia. In humans, ammonia buildup in the brain similarly stimulates breathing. I conclude that a role for ammonia in ventilatory control is probably ubiquitous in vertebrates, including the oldest extant representatives (hagfish). Initial hypoventilation is protective against the uptake of a toxicant, while sustained hyperventilation is beneficial at times of internal ammonia loading such post-exercise recovery, and after feeding. This hyperventilation will facilitate not only greater ammonia excretion, but also the greater O₂ uptake needed to recover from exercise and to metabolically process food.

Lay Summary

Ammonia is a toxic metabolic waste product excreted across the gills of fish, and a common pollutant. In both the primitive hagfish and modern rainbow trout, breathing is initially inhibited by high water ammonia. This protective response, mediated by external receptors, minimizes uptake of the toxicant. As exposure continues, ammonia builds up in the bloodstream, stimulating internal receptors in gills and brain, causing increased breathing. An ammonia transport system across the gills is also activated, preventing blood ammonia levels from rising too high. These responses also occur naturally when the fish has high internal ammonia levels from feeding or exercise. Increased breathing helps the fish to excrete more ammonia and take up more oxygen. Ammonia buildup in the brain also stimulates breathing in humans, which helps survival during liver failure. I conclude that the effects of ammonia on breathing are beneficial, and probably ubiquitous in vertebrate animals.

Preface

Chapter 1 is a General Introduction focused on how and why ammonia may influence ventilation in fish. While the original idea was to study this mainly in trout, my work evolved so that in the end I placed an equal emphasis on hagfish to study these questions in a fish of ancient lineage and evolutionary importance. For both species, part of my focus became understanding their basic ventilatory mechanisms and developing methods to study them. This chapter reviews the background and ideas behind the work, and provide brief summaries of the individual experimental chapters.

Chapter 2 has been published as Eom J and Wood CM (2019) entitled “The ventilation mechanism of the Pacific hagfish *Eptatretus stoutii*” in the Journal of Fish Biology 94, 261-276. Doi.org/10.1111/jfb.13885. I performed all the experiments and analysed the data in consultation with Dr. CM Wood. I wrote the first draft of the manuscript, which was edited by Dr. Wood.

Chapter 3 has been published as Eom J, Giacomini M, Clifford AM, Goss GG, and Wood CM (2019) entitled “Ventilatory sensitivity to ammonia in the Pacific hagfish (*Eptatretus stoutii*), a representative of the oldest extant connection to the ancestral vertebrates” in the Journal of Experimental Biology 222, jeb199794. DOI: 10.1242/jeb.199794. I performed most of the experiments, with help from Dr. Marina Giacomini for blood sampling and plasma ammonia assays, and Dr. Alex Clifford and Dr. Greg Goss for oxygen consumption measurements. I analysed the data in consultation with all co-authors. I wrote the first draft of the manuscript, which was edited by Dr. Wood, and revised critically by all authors.

Chapter 4 has been published as Eom J and Wood CM (2021b) entitled “Understanding ventilation and oxygen uptake of Pacific hagfish (*Eptatretus stoutii*), with particular emphasis on responses to ammonia and interaction with other respiratory gases” in the Journal of Comparative Physiology B 191, 255–271 doi.org/10.1007/s00360-020-01329-7. I performed all the experiments and analysed the data in consultation with Dr. CM Wood. I wrote the first draft of the manuscript which was edited by Dr. Wood.

Chapter 5 has been published as Eom J, Fehsenfeld S, and Wood CM (2020) entitled “Is ammonia excretion affected by gill ventilation in the rainbow trout *Oncorhynchus mykiss*?” in Respiratory Physiology & Neurobiology 275, 103385. Doi.org/10.1016/j.resp.2020.103385. I performed all the experiments and Dr. Sandra Fehsenfeld performed the mRNA expression

analysis. I analysed the data in consultation with Dr. Wood. I wrote the first draft of the manuscript which was edited by Dr. Wood, and revised critically by all authors.

Chapter 6 has been published as Eom J and Wood CM (2020) entitled “A less invasive system for the direct measurement of ventilation in fish” in the *Canadian Journal of Fisheries and Aquatic Sciences* 77, 1870–1877. Doi.org/10.1139/cjfas-2020-0177. I designed the apparatus, performed the experiments, and analyzed the data in consultation with Dr. Wood. I wrote the first draft of the manuscript, which was edited by Dr. Wood.

Chapter 7 has been published as Eom J and Wood CM (2021a) entitled “Brain and gills as internal and external ammonia sensing organs for ventilatory control in rainbow trout *Oncorhynchus mykiss*” in *Comparative Biochemistry and Physiology A* 254, 110896. Doi: 10.1016/j.cbpa.2021.110896. I performed the experiments and analysed the data in consultation with Dr. Wood. I wrote the first draft of the manuscript which was edited by Dr. Wood.

Chapter 8 provides Conclusions and Future Directions. This chapter summarizes the major findings of my work and points to research questions arising from it.

Please note that there is a change in convention between Chapters 2 and 3 *versus* Chapters 4, 6, and 7, reflecting the original versions of the papers which were published in different journals. Inhalation ventilatory flow measured by the ultrasonic ventilation probe is considered negative in Chapters 2 and 3, but positive in Chapters 4, 6, and 7.

All experiments performed for this thesis followed the guidelines of the Canada Council for Animal Care, under joint approval of the animal care committees at the University of British Columbia (AUP#: A14-0251, A17-0301, A18-0271) and Bamfield Marine Sciences Centre (AUP #: RS-17-20, RS-18-20, RS-19-15).

Table of Contents

Abstract.....	iii
Lay summary	iv
Preface	v
Table of contents.....	vii
List of tables.....	xv
List of figures.....	xvi
Abbreviations.....	xxii
Acknowledgements.....	xxvii
Chapter 1: Introduction	1
1.1 Overview.....	1
1.2 Mechanisms of ventilation.....	3
1.3 Control of ventilation, with a particular focus on ammonia	4
1.4 Ammonia production and chemistry in fish.....	8
1.5 Ammonia excretion in fish	10
1.6 Is there a relationship between ventilation and ammonia excretion in fish?	12
1.7 Study organisms	13
1.7.1 The Pacific hagfish (<i>Eptatretus stoutii</i>)	13
1.7.2 The rainbow trout (<i>Oncorhynchus mykiss</i>)	13
1.8 Thesis objectives and chapter summaries	14

1.8.1 Chapter 2: “The ventilation mechanism of the Pacific hagfish <i>Eptatretus stoutii</i> ” ...	14
1.8.2 Chapter 3: “Ventilatory sensitivity to ammonia in the Pacific hagfish (<i>Eptatretus stoutii</i>), a representative of the oldest extant connection to the ancestral vertebrates”	15
1.8.3 Chapter 4: “Understanding ventilation and oxygen uptake of Pacific hagfish (<i>Eptatretus stoutii</i>), with particular emphasis on responses to ammonia and interactions with other respiratory gases”	15
1.8.4 Chapter 5: “Is ammonia excretion affected by gill ventilation in the rainbow trout <i>Oncorhynchus mykiss</i> ?”	15
1.8.5 Chapter 6: “A less invasive system for the direct measurement of ventilation in fish”	17
1.8.6 Chapter 7: “Brain and gills as internal and external ammonia sensing organs for ventilatory control in rainbow trout <i>Oncorhynchus mykiss</i> ”	17
Chapter 2: The ventilation mechanism of the Pacific hagfish <i>Eptatretus stoutii</i>	23
2.1 Summary	23
2.2 Introduction.....	23
2.3 Materials and Methods.....	25
2.3.1 Experimental animals	25
2.3.2 Anatomical studies	26
2.3.3 Physiological recording from various sites in the cardio-respiratory system	26
2.3.4 Calibration of the recording systems	29
2.3.5 Experimental procedures	29
2.3.6 Statistical analyses	29
2.4 Results.....	30
2.4.1 Anatomical observations	30
2.4.2 Ventilation of <i>E. stoutii</i> under control resting conditions.....	31
2.4.3 Analysis of ventilatory flow and pressure relationships	32

2.4.4 Simultaneous recordings from nostril duct, mouth cavity, velum chamber, and pharyngo-cutaneous duct (PCD)	33
2.5 Discussion.....	35
2.5.1 Anatomical observation.....	35
2.5.2 Patterns of ventilation.....	35
2.5.3 Coughing	38
2.5.4 Ventilation during swimming.....	39
2.5.5 Coughing remarks.....	40

Chapter 3: Ventilatory sensitivity to ammonia in the Pacific hagfish (*Eptatretus stoutii*), a representative of the oldest extant connection to the ancestral vertebrates 54

3.1 Summary.....	54
3.2 Introduction.....	54
3.3 Materials and Methods.....	56
3.3.1 Experimental animal and chemicals	56
3.3.2 Physiological recording from the nostril duct in the respiratory system	56
3.3.3 Blood sampling.....	58
3.3.4 Series I – Ventilation changes in hagfish loaded externally with ammonia - high environmental ammonia (HEA)	58
3.3.5 Series II – The effect of HEA on oxygen consumption rate.....	59
3.3.6 Series III – Relationship between ventilation and altered blood chemistry in hagfish loaded externally with ammonia	59
3.3.7 Series IV – Relationship between ventilation and altered blood chemistry in hagfish loaded internally with ammonia.....	60
3.3.8 Blood and water chemistry analyses.....	61
3.3.9 Statistical analyses	62
3.4 Results.....	62

3.4.1 Series I – Ventilation changes in hagfish loaded externally with ammonia – high environmental ammonia (HEA)	62
3.4.2 Series II – The effect of HEA on oxygen consumption rate.....	63
3.4.3 Series III – Relationship between ventilation and changes in blood chemistry in hagfish loaded externally with ammonia	63
3.4.4 Series IV – Relationship between ventilation and changes in blood chemistry in hagfish loaded internally with ammonia.....	64
3.5 Discussion.....	66
3.5.1 Overview	66
3.5.2 Ventilation changes in hagfish loaded externally with ammonia	66
3.5.3 Ventilation changes in hagfish loaded internally with ammonia.....	68
3.5.4 Summary and future directions.....	70

Chapter 4: Understanding ventilation and oxygen uptake of Pacific hagfish (*Eptatretus stoutii*), with particular emphasis on responses to ammonia and interactions with other respiratory gases..... 85

4.1 Summary	85
4.2 Introduction.....	85
4.3 Materials and Methods.....	88
4.3.1 Experimental animals	88
4.3.2 Ventilation flow recording from the nostril duct.....	89
4.3.3 Series I. Measurement of oxygen partial pressure (PO ₂) from gill openings including the pharyngo-cutaneous duct (PCD)	90
4.3.4 Series II. Basic ventilatory responses to high environmental ammonia (HEA)	91
4.3.5 Series III. Ventilatory responses to other respiratory gases and interactive effects of exposure to HEA	92
4.3.6 Statistical analyses.....	92

4.4 Results.....	93
4.4.1 Series I - Measured expired O ₂ tensions and calculated O ₂ utilization under normoxia and in various respiratory gas treatments	93
4.4.2 Series II - Ventilation changes in 10 mM high environmental ammonia (HEA)	95
4.4.3 Series III - Ventilation changes in 1% hypercapnia, hypoxia, hyperoxia, and 10 mM HEA.....	95
4.5 Discussion	96
4.5.1 Overview	96
4.5.2 Ventilation, utilization, and $\dot{M}O_2$ under normoxia	97
4.5.3 Ventilation, utilization, and $\dot{M}O_2$ under respiratory gas treatments	99
4.5.4 The relationship between $\dot{M}O_2$ and ventilation under different respiratory gas treatments.....	102

Chapter 5: Is ammonia excretion affected by gill ventilation in the rainbow trout

<i>Oncorhynchus mykiss?</i>	113
5.1 Summary.....	113
5.2 Introduction	114
5.3 Materials and Methods.....	116
5.3.1 Experimental animals	116
5.3.2 Fish operations	116
5.3.3 Experimental series.....	117
5.3.3.1 Series I – Relationship between ventilation and ammonia excretion in fish under baseline conditions	118
5.3.3.2 Series II – Relationship between ventilation and ammonia excretion in ammonia-loaded fish	119

5.3.3.3 Series III – Influence of ammonia-loading on gene expression in the gills	119
5.3.4 Analytical techniques.....	119
5.3.5 Data analysis.....	120
5.4 Results.....	121
5.4.1 Series I – Relationship between ventilation and ammonia excretion in fish under baseline conditions.....	121
5.4.2 Series II – Relationship between ventilation and ammonia excretion in ammonia- loaded fish.....	121
5.4.3 Series III – The influence of ammonia loading on gene expression in the gills	123
5.5 Discussion.....	123
5.5.1 Overview	123
5.5.2 Ammonia permeability in gills	124
5.5.3 Possible ammonia sensing organs in fish	125
5.5.4 Interaction of ammonia with O ₂ in ventilatory control	126
5.5.5 Perspectives	126
Chapter 6: A less invasive system for the direct measurement of ventilation in fish	136
6.1 Summary	136
6.2 Introduction.....	136
6.3 Materials and Methods.....	138
6.3.1 Experimental animals	139
6.3.2 Rainbow trout operations.....	139
6.3.3 System set-up for rainbow trout	140
6.3.4 System set-up for goldfish	140

6.3.5 Flow-meter calibration	141
6.3.6 Experimental procedures	142
6.3.7 Data analysis.....	142
6.4 Results	143
6.5 Discussion.....	143

Chapter 7: Brain and gills as internal and external ammonia sensing organs for ventilatory control in rainbow trout, *Oncorhynchus mykiss*..... 153

7.1 Summary	153
7.1 Introduction.....	153
7.2 Materials and Methods.....	155
7.2.1 Experimental animals	155
7.2.2 Fish cannulations and analytical techniques	155
7.2.3 Experimental series.....	158
7.2.3.1 Series I – Acute responses to high environmental ammonia (HEA) in the external water	158
7.2.3.2 Series II – Ammonia perfusion to external gill arches	158
7.2.3.3 Series III– Ammonia injection onto the hindbrain	159
7.2.3.4 Statistical analysis	159
7.3 Results.....	159
7.3.1 Series I - Acute responses over time to high environmental ammonia (HEA) in the external water.....	160
7.3.2 Series II – Ammonia perfusion to external gill arches	160
7.3.3 Series III – Ammonia injection into the hind-brain cavity.	161
7.4 Discussion	161
7.4.1 Overview	161

7.4.2 External and internal ammonia sensing in gills	162
7.4.3 Nociceptors as possible external ammonia-sensing receptors	163
7.4.4 Internal ammonia sensing in the central nervous system.....	164
7.4.5 Why do fish regulate ventilation in response to elevated external or internal ammonia?	165
Chapter 8: General discussion and conclusions	172
8.1 Role of ammonia in controlling ventilation of hagfish	172
8.2 Role of ammonia in controlling ventilation of trout	174
8.3 Evolutionary perspective	178
8.4 Future directions	179
References.....	185

List of Tables

Table 2.1 Ventilatory parameters collected under resting control conditions from 64 Pacific hagfish.....	52
Table 2.2 Simultaneous recordings of ventilatory parameters from the nostril duct, velum chamber, mouth cavity, and 13 th gill of three Pacific hagfish under control resting conditions.	53
Table 3.1 Blood acid-base chemistries of hagfish before (control) and 0.5h and 1h after (post) injection of the respective doses of salts into the venous sinus, in Series IV.	83
Table 3.2 Ammonia flux and urea-N flux rates of hagfish after injection at a dose of 1,000 $\mu\text{mol kg}^{-1}$ NH_4HCO_3 (N = 18) or 1,000 $\mu\text{mol kg}^{-1}$ NaHCO_3 (N = 11) into the venous sinus, in Series IV.	84
Table 5.1 Heart rates (beats sec^{-1} , <i>via</i> ECG) under baseline conditions in Series I and ammonia-loading in Series II.	135

List of Figures

Figure 1.1 Cranial nerves leaving or entering the hindbrain which consists of pons and medulla where rhythmic respiratory patterns are thought to be generated in fish.	19
Figure 1.2 Location of neuroepithelial cells in fish gills and their functional mechanism in response to changed ambient respiratory gas levels such as hypoxia (redrawing of figures from Coolidge et al. 2008 and Zachar and Jonz 2012).	20
Figure 1.3 Ammonia movements in enterocytes (intestine), hepatocytes (liver), brain, muscle, and gill cells, and the purine nucleotide cycle in fish.	21
Figure 1.4 Current model for the ammonia excretion mechanism in the fish gill (update and redrawing of figure from Wright and Wood 2009).	22
Figure 2.1 Schematic diagram of recording attachments to nostril, mouth cavity, velum chamber, and pharyngo-cutaneous duct and a simple model summarizing our current understanding of the unidirectional ventilatory water flow mechanism in the Pacific hagfish at rest and during swimming.	41
Figure 2.2 Dissection of a freshly euthanized Pacific hagfish injected with dyed silicone.	42
Figure 2.3 Observational experiments in live Pacific hagfish.	43
Figure 2.4 Dye injection to the mouth cavity of a live Pacific hagfish.	44
Figure 2.5 Simultaneous recording of flow and pressure in the nostril duct of Pacific hagfish. .	45
Figure 2.6 Simultaneous ventilation recordings of nostril flow, mouth cavity pressure, velum chamber impedance, and pharyngo-cutaneous duct pressure in a resting Pacific hagfish under control conditions.	46
Figure 2.7 , Plots of nostril flow against frequency, stroke volume, pressure amplitude, and ventilatory index in Pacific hagfish (using 3134 data points).	47

Figure 2.8 Ventilatory parameters recorded simultaneously under control conditions, during nostril coughing, during mouth coughing, and during spontaneous swimming in the same three hagfish.	48
Figure 2.9 Simultaneous recordings of nostril flow, mouth cavity pressure, velum chamber impedance, and pharyngo-cutaneous duct pressure in a Pacific hagfish where nostril coughing was induced by dye inhalation into the nostril.	49
Figure 2.10 Simultaneous recordings of nostril flow, mouth cavity pressure, velum chamber impedance, and pharyngo-cutaneous duct pressure in a Pacific hagfish where mouth coughing was induced by dye injection into the mouth cavity.	50
Figure 2.11 Simultaneous recordings of nostril flow, mouth cavity pressure, velum chamber impedance, and pharyngo-cutaneous duct pressure prior to and during a period of spontaneous swimming in a Pacific hagfish.	51
Figure 3.1 Responses over time in ventilatory frequency, ventilatory pressure amplitude, and ventilatory index of hagfish exposed to 10 mM NaHCO ₃ and two high environmental ammonia (HEA) treatments, 10 mM NH ₄ HCO ₃ and 10 mM NH ₄ Cl.	72
Figure 3.2 Changes in oxygen consumption rate of hagfish in response to two different HEA treatments, 10 mM NH ₄ Cl or 10 mM NH ₄ HCO ₃ , as well as a control treatment with 10 mM NaHCO ₃ in Series II.	73
Figure 3.3 Flowmeter recordings of nostril ventilatory parameters in hagfish exposed to 10 mM NH ₄ HCO ₃ (HEA) in Series III.	74
Figure 3.4 Changes in plasma total ammonia concentration, plasma ammonia partial pressure, plasma pH, plasma carbon dioxide partial pressure, and plasma bicarbonate concentration in hagfish in response to exposure to 10 mM NH ₄ HCO ₃ for 5 min or 180 min, in Series III.	75
Figure 3.5 Changes in ventilatory parameters of hagfish in response to injections of ammonium salts or appropriate sodium salt controls into the venous sinus, in Series IV.	76
Figure 3.6 Changes in plasma total ammonia concentration and plasma ammonia partial pressure of hagfish in response to injections of ammonium salts or appropriate sodium salt controls into the venous sinus, in Series IV.	77

Figure 3.7 Changes in ventilatory frequency and ventilatory flow of hagfish in response to injections at a dose of 1,000 $\mu\text{mol kg}^{-1}$ NH_4HCO_3 and 1,000 $\mu\text{mol kg}^{-1}$ NaHCO_3 into the venous sinus, in Series IV.	78
Figure 3.8 Responses over time in ventilatory parameters of hagfish exposed to 0, 5, 10, and 20 mM NH_4HCO_3 as high environmental ammonia treatments, in Series I (Supplementary Figure in original publication).	79
Figure 3.9 Changes in pH over time of sea water containing either 10 mM NH_4HCO_3 , 10 mM NH_4Cl , or 10 mM NaHCO_3 , and continuously bubbled with air, in Series I (Supplementary Figure in original publication).	80
Figure 3.10 Two examples of flowmeter recordings of nostril ventilatory flow rate in hagfish exposed to 10 mM NH_4HCO_3 in Series III (Supplementary Figure in original publication).	81
Figure 3.11 Correlation of ventilatory index with total plasma ammonia concentration and gaseous ammonia tension in individual hagfish injected at a dose of 1,000 $\mu\text{mol kg}^{-1}$ or 70 $\mu\text{mol kg}^{-1}$ of ammonium salts in Series IV (Supplementary Figure in original publication).	82
Figure 4.1 On the flipped over hagfish, which was submerged in water, expired oxygen tension was measured at the gill openings including the pharyngo-cutaneous duct by a needle-type oxygen probe attached on a micro-manipulator, which was magnetically mounted on an iron plate.	104
Figure 4.2 Expired O_2 tensions and % utilization of O_2 from the respective gill openings including the pharyngo-cutaneous duct in control normoxic hagfish.	105
Figure 4.3 Expired oxygen tension and % utilization of O_2 from the respective gill openings including pharyngo-cutaneous duct of hagfish treated with high environmental ammonia, hypercapnia, severe hypoxia (<15% air saturation), and hyperoxia (>200% air saturation).	106
Figure 4.4 Routine $\dot{\text{M}}\text{O}_2$ calculated by Equation 2 using the $\text{P}_\text{I}\text{O}_2$, mean $\dot{\text{V}}_\text{w}$, and overall mean $\text{P}_\text{E}\text{O}_2$ values for each fish under each experimental condition.	107

Figure 4.5 Changes in ventilatory parameters (frequency, total ventilatory flow, and ventilatory stroke volume) in hagfish acutely exposed to 10 mM high environmental ammonia in normoxia.	108
Figure 4.6 Changes in ventilatory parameters (frequency, total ventilatory flow, and ventilatory stroke volume) in hagfish exposed to hypercapnia and then subsequently acutely exposed to 10 mM high environmental ammonia in the continuing presence of hypercapnia.	109
Figure 4.7 Changes in ventilatory parameters (frequency, total ventilatory flow, and ventilatory stroke volume) in hagfish exposed to severe hypoxia and then subsequently acutely exposed to 10 mM high environmental ammonia in the continuing presence of hypoxia.	110
Figure 4.8 Changes in ventilatory parameters (frequency, total ventilatory flow, and ventilatory stroke volume) in hagfish exposed to hyperoxia and then subsequently acutely exposed to 10 mM high environmental ammonia in the continuing presence of hyperoxia.	111
Figure 4.9 Regressions between routine oxygen consumption rate and total ventilatory flow in hagfish under different respiratory gas treatments.	112
Figure 5.1 Changes in ventilation pressure amplitude, frequency, total ventilatory index, and ammonia excretion flux rate in non-infused rainbow trout during hypoxia in Series I.	128
Figure 5.2 Changes in ventilation pressure amplitude, frequency, total ventilatory index, and ammonia excretion flux rate in non-infused rainbow trout during hyperoxia in Series I.	129
Figure 5.3 Changes in ventilation pressure amplitude, frequency, total ventilatory index, and ammonia excretion flux rate in non-infused rainbow trout in response to ammonia infusion and subsequent treatment with hypoxia during continuing ammonia infusion in Series II.	130
Figure 5.4 Changes in ventilation pressure amplitude, frequency, total ventilatory index, and ammonia excretion flux rate in non-infused rainbow trout in response to ammonia infusion and subsequent treatment with hyperoxia during continuing ammonia infusion in Series II.	131

Figure 5.5 Hyperventilation or hypoventilation in Series I did not affect ammonia excretion flux rate in non-infused fish that were not loaded with ammonia.	132
Figure 5.6 After ammonia infusion in Series II, plasma ammonia significantly increased in rainbow trout.	133
Figure 5.7 Expression levels of genes (Rhcg2, HAT, and NHE2) in the gills of rainbow trout infused with 140 mM NH_4HCO_3 or 140 mM NaCl for 33 h in Series III.	134
Figure 6.1 A diagram of a less invasive system set-up, in rainbow trout and goldfish.	146
Figure 6.2 Ventilatory flow parameters measured during control normoxia, during 1h in either hypoxia or hyperoxia, and during recovery in normoxia, in rainbow trout and goldfish.	147
Figure 6.3 Changes in buccal pressure amplitude, breathing frequency, and ventilatory index in rainbow trout with or without the silicone collapsible funnel and balloon piece layer in place.	148
Figure 6.4 Ventilatory flow traces of rainbow trout and goldfish in hypoxia and hyperoxia. Note the episodic breathing patterns in hyperoxia-treated goldfish.	149
Figure 6.5 An example of a manual calibration curve for the flow-probe (Supplementary Figure in original publication).	150
Media 6.1 System set-up procedure in 350-g rainbow trout (Supplementary material in original publication). https://cdnsiencepub.com/doi/10.1139/cjfas-2020-0177	151
Media 6.2 System set-up procedure in 10-g goldfish (Supplementary material in original publication). https://cdnsiencepub.com/doi/10.1139/cjfas-2020-0177	152
Figure 7.1 Schematic diagram of the experimental setups for external ammonia perfusion to gills and ammonia injection to brain cavity of rainbow trout.	166
Figure 7.2 The immediate time course of ventilatory responses to 1 mM HEA exposure in rainbow trout in Series I.	167
Figure 7.3 Representative recordings of buccal ventilatory index in a single trout of Series II in response to perfusion of a logarithmic series of increasing ammonia concentrations directly to the external surfaces of the 1 st gill arches.	168

Figure 7.4 Mean ventilatory parameters in Series II in response to perfusion of increasing ammonia concentrations to the external surfaces of the 1 st gill arches.	169
Figure 7.5 Representative ventilation traces in three trout of Series III after random injections of mock EDF solutions, and ammonia concentrations in mock EDF, directly to the hind-brain cavity of rainbow trout.	170
Figure 7.6 Variations of ventilatory parameters after randomly ordered injections of ammonia concentrations to the hind-brain cavity in Series III.	171
Figure 8.1 Hypothetical model of the role of external high environmental ammonia (HEA) in controlling hagfish ventilation.	181
Figure 8.2 Hypothetical model of the role of internal ammonia in controlling hagfish ventilation after feeding and/or exercise (swimming).	182
Figure 8.3 Hypothetical model of the role of external high environmental ammonia (HEA) in controlling ventilation in trout.	183
Figure 8.4 Hypothetical model of the role of internal ammonia in controlling ventilation in trout after feeding and/or exercise (swimming).	184

Abbreviations

5-HT	serotonin
aba	afferent branchial artery
apa	afferent primary artery
AC	accessory cell
ADP	adenosine diphosphate
AMP	adenosine monophosphate
ATP	adenosine triphosphate
AUP	animal utilization protocols
bv	branchial vein
BMSC	Bamfield Marine Sciences Centre
BPL	balloon piece layer
BW	body weight
cl	collagen layer
cvs	central venous sinuses
cDNA	complementary deoxyribonucleic acid
C	control
Ca _v	Ca ²⁺ channel
CaCl ₂	calcium chloride
CA	carbonic anhydrase
Cer	cerebellum
CFTR	cystic fibrosis transmembrane conductance regulator
Cl	chloride
CMA	celiacomesenteric artery

CO ₂	carbon dioxide
DCV	dense-cored vesicles
DNase	deoxyribonuclease
eba	efferent branchial artery
epa	efferent primary artery
ECG	electro-cardiogram
EDF	extradural fluid
FM	fast mode
FP	flow probe
fr	frequency
FW	freshwater
g	gill pouches
GDH	glutamate dehydrogenase
GDP	guanosine diphosphate
GLN	glutaminase
GO	gill openings
GS	glutamine synthetase
GTP	guanosine triphosphate
HEA	high environmental ammonia
HF	hagfish
IMP	inosine monophosphate
kPa	kilopascal
K _B	potassium channel

KCl	potassium chloride
LGA	left gill arches
mmHg	millimetre of mercury
MC	mouth cough
Med	medulla
MgSO ₄	magnesium sulphate
$\dot{M}O_2$	oxygen consumption rate
MRC	mitochondria rich cell
mRNA	messenger ribonucleic acid
MS-222	tricaine methanesulfonate
N	needle
n	nostril tube
NaCl	sodium chloride
NaHCO ₃	sodium bicarbonate
NaOH	sodium hydroxide
NBC	sodium bicarbonate co-transporter
NC	nostril cough
NECs	neuroepithelial cells
NH ₃	gaseous ammonia
NH ₄ ⁺	ionic ammonium
NH ₄ Cl	ammonium chloride
NHE	sodium-proton exchanger
NH ₄ HCO ₃	ammonium bicarbonate
(NH ₄) ₂ SO ₃	ammonium sulphate

NKA	sodium-potassium adenosine triphosphatase
NKCC	sodium-potassium-2 chloride co-transporter
O ₂	oxygen
Olf	olfactory bulb
ONS	oronasohypophyseal septum
p	pharynx
pgl	primary gill lamellae
P _{crit}	critical oxygen tension below which oxygen consumption becomes dependent on
PO ₂	
PC	pillar cell
PCD	pharyngo-cutaneous duct
PCO ₂	carbon dioxide partial pressure
P _E O ₂	oxygen partial pressure of expired water
P _I O ₂	oxygen partial pressure of inspired water
PNH ₃	ammonia partial pressure
PO ₂	oxygen partial pressure
PE tubing	polyethylene tubing
PNA	peanut lectin agglutinin
PVC	polyvinyl chloride
PVCs	pavement cells
qPCR	real-time polymerase chain reaction
RBC	red blood cell
RGA	right gill arches
Rh	rhesus glycoproteins

Rhag	rhesus glycoproteins type a
Rhbg	rhesus glycoproteins type b
Rgcg	rhesus glycoproteins type c
RS	rubber stopper
sgl	secondary gill lamellae
sph	sphincter
SCF	silicone collapsible funnel
SDA	specific dynamic action
SM	slow mode
SP	stainless-steel pin
ST	silicone tubing
SV _w	stroke volume
SW	seawater
T _{Amm}	total ammonia concentration
T _{CO2}	total carbon dioxide
TCA	tricarboxylic acid
Tel	telencephalon
TEP	transepithelial potential
UBC	University of British Columbia
v	velum chamber
V-H ⁺ -ATPase	vacuolar-type proton adenosine triphosphatase
\dot{V}_w	ventilatory flow

Acknowledgements

Chris teaches me how to think in science, this lesson has given me the opportunity to enlarge my knowledge of science from every single challenge during my PhD. The way how to make my thinking in science more logically structured has been provided by my official supervisor, Trish and my two other committee members, Bill and Tony. It is great honour to work with them.

Past and current Wood lab members are the joy of my life in science. Thank you.

Chapter 1: Introduction

Section 1.1 provides an overview of the thesis, while Sections 1.2 to 1.6 provide brief reviews of the background knowledge that led to the investigations in this thesis. Section 1.7 provides background information on the two different animal species used in this thesis. Section 1.8 provides brief summaries of the major findings in each experimental chapter.

1.1 Overview

My thesis focuses on how and why ammonia influences ventilation in fish. The original idea was to study these questions mainly in the rainbow trout (*Oncorhynchus mykiss*), a model species in which there is a rich background of knowledge on both ammonia metabolism and ventilatory control. A small comparative component was also planned to investigate these same topics in the Pacific hagfish (*Eptatretus stoutii*), where the knowledge base is much smaller. The goal was to see if similar principles applied in a fish of ancient lineage and evolutionary importance. However, as the investigation of the latter evolved, it became clear that there were interesting questions to pursue in the hagfish which has a unique ventilatory system very different from that of the rainbow trout. Part of my focus became understanding the basic mechanics of the hagfish ventilation, and developing methods to evaluate its respiratory physiology. Similarly, I also developed an improved method to measure ventilation in the rainbow trout and other teleosts. In the end, my thesis places approximately equal emphasis on the trout and the hagfish, with three experimental chapters on each. Over the four years, trout and hagfish studies were performed alternately, with hagfish studied at Bamfield Marine Sciences Centre (BMSC) in late summer and early fall, and trout studied at University of British Columbia (UBC) at other times of the year. However, for coherence, Chapters 2, 3, and 4 deal with the hagfish, and Chapters 5, 6, and 7 deal with trout.

In hagfish, prior to studying its responses to ammonia, I first had to understand its breathing system. These animals employ a unique ventilatory system which is fundamentally different from those of teleosts and other fishes, and which to date has been only sparsely investigated (Strahan 1958; Johansen and Strahan 1963; Malte and Lomholt 1998). In order to answer the above questions, I employed anatomical observations, dye flow measurements, and recordings of pressure, flow, and impedance relationships at nostril, mouth, velum, and gill pouches. Chapter 2 (Eom and Wood 2019) describes a two-phase unidirectional pumping system with a fast suction pump (the velum) for inhalation and a much slower force pump (gill pouches) for exhalation. The hagfish breathing system is capable of very large changes in ventilatory flow, including periods of complete apnea. With this background

knowledge, in Chapter 3 (Eom et al. 2019), I exposed hagfish to both external and internal ammonia loading while measuring blood ammonia levels, acid-base status, and ammonia excretion rates. I discovered dual responses to high environmental ammonia (HEA). The initial response is hypo-ventilation, sometimes complete apnea, which is a novel finding. A later response of hyper-ventilation was also observed, and I showed that this later hyper-ventilation is mediated by increased blood ammonia levels that are detected internally, similar to previous findings on teleost fish (Zhang et al. 2009, 2011). I concluded that ammonia-sensing and a role for ammonia in ventilatory control is probably ubiquitous in fish, including the oldest extant ancestral vertebrates. In Chapter 4 (Eom and Wood 2021b), I further characterized the hagfish respiratory system, showing differential O₂ utilization by the various gill pouches, and quantifying how this changed with changes in ventilatory flow in different respiratory gas treatments. I also examined the interaction of the acute hypo-ventilatory response to HEA with the ventilatory responses to hypoxia, hyperoxia, and hypercapnia, and concluded that the acute hypoventilatory response to ammonia was independent from responses to other respiratory gases.

The trout studies started by addressing a conundrum. It was previously believed that ventilation would not affect ammonia excretion due to diffusion limitation on ammonia movement across the gills (Randall and Ip 2006). Why then should internal ammonia stimulate breathing if it would not help increase ammonia excretion? In Chapter 5, I showed diffusion limitation to be present in “resting” trout, but once this limitation was removed *via* upregulation of the Rh channel system (channels which facilitate ammonia diffusion) in the gills by ammonia loading (Wright and Wood 2009), ammonia excretion became sensitive to ventilation. Hyperventilating trout excreted more ammonia, showing that the response is beneficial at times of internal ammonia loading (e.g. meal digestion, post-exercise recovery, post-exposure to HEA). These experiments used proxy measures (buccal pressure amplitude and frequency) of ventilatory flow (\dot{V}_w), whereas I wished to directly measure \dot{V}_w in future studies. Therefore, in Chapter 6 (Eom and Wood 2020), I invented a device to quantify \dot{V}_w , so as to replace the original method of van Dam (1934). The new system is based on the same principle, but replaces mechanical overflow devices with an ultrasonic flowmeter, and is far less stressful to the fish. Chapter 6 demonstrates its use to directly measure \dot{V}_w during experimental hypoxia and hyperoxia in trout and goldfish. Finally, in Chapter 7 (Eom and Wood 2021a), I discovered that trout, like hagfish, show an immediate hypo-ventilatory response to water-borne high environmental ammonia (HEA) that is sensed externally in the gills. As HEA continues, ventilation increases, due to internal ammonia build-up which is sensed internally. Part of this internal sensing appears to be in the brain, in addition to the previously established role of the gill neuro-epithelial cells (NECs) (Zhang et al. 2011). Chapter 8 summarizes key findings of the thesis and points to research questions arising from it.

1.2 Mechanisms of ventilation

The basic principles of ventilation in teleost fish were worked out by Hughes (1961) and Hughes and Shelton (1962). In most teleosts, the combined serial pumping action of the buccal cavity and the opercular covers generate unidirectional, more or less continuous water movement across the gills. In the opercular suction phase, ventilation is initiated by opening the mouth, enlarging the buccal cavity by lowering the jaw and floor of the mouth so the pressure in the buccal cavity decreases below ambient; as a result, water is inspired into the mouth. At the same time, the opercular covers are closed but the opercular chamber is expanded, creating a pressure in the opercular chamber which is more negative than in the buccal cavity, so water flows across the gills into the expanded opercular chamber. This is followed by the buccal force phase in which the fish then closes the mouth, elevating the jaw and floor, thereby shrinking the buccal cavity and increasing the buccal pressure above ambient. Almost simultaneously, the volume of the opercular cavity is decreased and its pressure increases by movements of the opercular covers. As a result, the overall pressure of the opercular cavity is now higher than ambient so that water is expired through the opercular openings, but lower than that in the buccal cavity so that the inspired water continues to move from buccal cavity to opercular cavity across the gill lamellae. The flow of water through the lamellar channels is countercurrent to the flow of blood through the lamellae themselves. Meanwhile, the exchange of the traditional respiratory gases (O_2 , CO_2) occurs by simple diffusion along PO_2 gradients and PCO_2 gradients between inspired water and the blood in the vascularized gill lamellae. Overall, ventilation is achieved by continuously cycling pressures in the buccal cavity and opercular cavity by opening or closing mouth and opercular covers, so that more or less continuous unidirectional water movement occurs in the fish respiratory system.

The breathing mechanism and branchial structure of the jawless hagfish are fundamentally different from those of most other fish (Bartels 1998; Johansen and Strahan 1963; Malte and Lomholt 1998). Unlike teleosts, where the gills are grouped together bilaterally, covered by symmetrical operculae and ventilated *via* the mouth by a buccal force – opercular suction pump as described above (Hughes and Shelton 1962), or elasmobranchs which operate a similar system with separate gill slits (Piiper and Schumann 1968), the hagfish have multiple separate gill pouches on each side, and water flow through the gill lamellae is thought to be countercurrent as in teleosts (Mallatt 1984). The gill pouches are internal structures surrounded by cartilaginous plates, muscle, and connective tissues, and each has a separate exit to the outside (Marinelli and Strenger 1956). Water is inhaled through the single separate nostril tube, as a result of the suction created by up-and-down pumping action of a central velar scroll (Bartels 1998). It

has been unclear whether or not inhalation also occurs *via* the mouth (Johansen and Hol 1960), a point that is clarified in the present thesis. The velum chamber contracts rhythmically, forcing water down a long pharynx and into the separate afferent branchial ducts leading to the separate gill pouches, as well as into an apparent bypass shunting system, the pharyngo-cutaneous duct (PCD) which has a single exit on the left side in *E. stoutii*. A pumping role of the gill pouches for exhalation has been proposed for the Atlantic hagfish, *Myxine glutinosa* (Goodrich 1930; Johansen and Hol 1960), another point which is addressed in the present thesis on *Eptatretus stoutii*.

1.3 Control of ventilation, with a particular focus on ammonia

In teleosts, rhythmic ventilatory movement is controlled by co-ordinated interaction between the central nervous system (brain) and the peripheral chemoreceptors (Fig. 1.1). The central respiratory pattern generator is located in the hindbrain which consists of the medulla and pons. It is unclear whether central chemoreceptors are present. Two studies on different holostean species produced conflicting results (Hedrick et al. 1991; Wilson et al. 2000), and there appear to be no studies on teleosts (Milsom 2012). The peripheral chemoreceptors are located along the respiratory passages in fish - within the walls of the orobranchial cavity, spiracle (if present), pseudobranch, and especially the gills - and they sense the variations of ambient and/or internal respiratory gases such as O₂ and CO₂. O₂ is generally considered to be the primary controller of breathing, because it is more difficult for the fish to obtain O₂ from the water (because of its much lower solubility) than it is to excrete CO₂ into the water (e.g. Perry et al. 2009a). To date, there are only a few studies on the role of ammonia (reviewed by Zhang et al. 2015). The sensed signals from the peripheral chemoreceptors (neuroepithelial cells or NECs) are transmitted *via* afferent fibres in the cranial nerves (facial VIIth, glossopharyngeal IXth, and vagal Xth) to the brain respiratory centre, which lies in the hindbrain (Milsom and Burleson 2007). The transmitted signals scatter between longitudinal long narrow pieces of nuclei within the hindbrain, where integration is thought to occur. Efferent signals are then sent back to the ventilatory muscular regions, for example, the jaw-closing muscles, with the maxillary branch and the mandibular branches of the trigeminal Vth cranial nerve serving the upper and lower jaws respectively. The hyomandibular region and the branchial muscles in the hyoid arch including the spiracle (if present) and the opercular muscles receive motor signals *via* the facial VIIth. The intrinsic respiratory muscles and the gill arches receive motor signals *via* the glossopharyngeal IXth and the vagus Xth. As a result, the fish controls its ventilation. The transmitted signals in the hindbrain also scatter between the spinal cord and the more rostral parts of the brain *via* the reticular formation and back to respective muscular and skeletal regions, so the fish increases not only

ventilation but also the general level of activity in response to hypoxia or hypercapnia (Hughes and Ballintijn 1965; Randall and Taylor 1988; Taylor 1992).

Fish show hyperventilation in acute hypoxia (also decreasing heart rate) and hypoventilation in acute hyperoxia, as well as hyperventilation in response to hypercarbia (high CO₂) and high ammonia. These changes of ventilation appear to be primarily initiated by peripheral chemoreceptors, neuroepithelial cells (NECs) of the gills, which detect the levels of respiratory gases in arterial blood and/or environmental water. The NECs are known to be located in the primary (i.e. filaments) and/or secondary lamellae in fish gills (Coolidge et al. 2008). The NECs are peripheral chemoreceptors and appear to sense at least three respiratory gases, for example, O₂ and CO₂ in zebrafish (Jonz et al. 2004), O₂ in catfish (Burlison et al. 2006), and ammonia in rainbow trout (Zhang et al. 2011) and zebrafish (Porteus et al. 2020). The NECs on the 1st and 2nd gill arches affect neighboring afferent nerves supplied by the glossopharyngeal IXth and the vagus Xth, so they are considered analogous to mammalian chemoreceptors, the carotid bodies and the aortic bodies respectively which are similarly innervated by cranial nerve IXth and Xth respectively (Milsom and Burlison 2007). The NECs are found within the epithelial layer of primary and secondary gill lamellae, and at filament tip-ends, where the countercurrent exchange occurs, so the NECs are thought to sense the ambient respiratory gases. In addition, the NECs are also found around the efferent primary arteries and basal lamina close to the central venous sinus, where the arterialized blood flows after countercurrent exchange, therefore, the NECs are considered as internal chemoreceptors as well. The number of NECs range between 781 and 3252 per filament in rainbow trout (Laurent 1984), however, their specific locations and abundance are varied and species-specific (Coolidge et al. 2008) (Fig. 1.2A). In the NECs, dense-cored vesicles (DCV) of 80 to 100 nm are well characterized, especially for the cells in the basal lamina. The DCV contains the neurotransmitter serotonin (5-HT) which can be released to adjacent neurons, thereby triggering afferent action potentials back to the brain (Coolidge et al. 2008; Zachar and Jonz 2012). It is thought that this occurs in response to changes in ambient and/or internal levels of the respiratory gases.

A current model of respiratory gas sensing in the NECs of teleost fish has been well described by Zachar and Jonz (2012), Perry and Tzaneva (2016), and Jonz (2018) (Fig. 1.2B). The electrogenic Na⁺-K⁺-ATPase (NKA) transporters actively pump in K⁺ ions and pump out Na⁺ ions across the cell membranes of the NECs. Therefore, intracellular K⁺ levels are kept high, leading to outward diffusion of K⁺ along the electrochemical gradient, and thus the resting potential of NECs is generated. In hypoxia or hypercapnia, however, the variations of external (media) or internal (blood) respiratory gases are sensed by the unidentified sensors which will inhibit outward K⁺ movement *via* “background” K⁺ channels (K_B),

so the resting membrane potential is disturbed, leading to membrane depolarization in the NECs. The depolarized membrane activates inward Ca^{2+} movement *via* voltage-gated Ca^{2+} channels (Ca_v), and intracellular Ca^{2+} concentration is increased. Abdallah et al. (2012) also proposed a model whereby endoplasmic reticulum releases stored Ca^{2+} to the cytosol during hypercapnia (instead of inward Ca^{2+} movement *via* voltage-gated Ca^{2+} channels), but the exact releasing mechanism requires further study. Increased intracellular Ca^{2+} induces DCV fusion to the polarized NEC cell membrane, stimulating the release of 5-HT neurotransmitter to adjacent nerve fibres. As a result, action potentials are triggered and transmitted to the central nervous system through afferent fibres in cranial nerves VIIth (facial), IXth (glossopharyngeal) and Xth (vagus). The transmitted signals provide information to the respiratory control area in the hindbrain and to the reticular formation; as a result, the fish increase their ventilation and their general activity levels in response to hypoxia or hypercapnia. After that, the intracellular $[\text{Ca}^{2+}]$ mediated K^+ channels (K_{Ca}) are also activated, so the depolarized membrane of the NEC becomes hyperpolarized and then returns to resting potential, and the signal transmission is terminated.

Elevations in both external and internal ammonia also trigger hyperventilation in fish and the overall processes are thought to be mediated by rhesus glycoproteins (Rh proteins), especially Rhbg and Rhcg1 located in basolateral and apical membranes of gill epithelial cells, and basal Rhbg in the NECs respectively, at least in rainbow trout (Zhang and Wood 2009; Zhang et al. 2011; Zhang et al. 2015). In the HEA treatment, trout showed delayed hyperventilation, and the interpretation offered was that the ambient HEA first diffuses to the internal blood plasma through apical Rhcg1 and basolateral Rhbg serving as specialized ammonia channels in the gill epithelium. As a result, plasma ammonia levels increase and ammonia then diffuses into the NECs through their basal Rhbg ammonia channels, mobilizing intracellular Ca^{2+} and releasing 5-HT from the DCV which triggers action-potentials in neighbouring afferent nerve fibres. These action potentials are then transmitted to the central nervous system especially the hindbrain so that the fish generates hyperventilation in HEA (Perry and Tzaneva 2016). However, in zebrafish, Porteus et al. (2020) have recently provided evidence against a role for Rh proteins in mediating ammonia entry into NECs. The brain is also considered as a potential internal chemosensory organ. Notably during HEA exposure in trout, increases in ventilation directly paralleled increases in brain intracellular ammonia concentrations (Zhang et al. 2013). Ammonia directly permeates through the blood-brain barrier and accumulates in the brain (Fig. 1.3A). Ammonia is toxic to neural function, and one of its effects appears to be the depletion of ATP reserves. As a detoxification mechanism, glutamine synthetase in the fish brain reacts ammonia with glutamate, converting them into glutamine (Randall and Tsui 2002). However, the ammonia detoxification process itself is ATP-dependent, so the ATP-depletion process may block the ammonia detoxification, leading to increasing

ammonia concentration in the brain simultaneous with the hyperventilation response (Zhang et al. 2015). The specific region(s) of the brain where ammonia accumulation may serve as a stimulant for hyperventilation is not known.

In contrast to the fairly rich background information on this topic in teleosts, relatively little is known about the control of breathing in hagfish, and prior to this thesis, nothing about the possible role of ammonia. Braun and Perry (2010) and Edwards et al. (2015), however, proved the presence of Rh proteins in the gills (*see* Section 1.5) and there is some evidence that these are involved in high rates of ammonia excretion after experimental ammonia loading. They may also be responsible for high rates of ammonia excretion after feeding (Wilkie et al. 2017; Weinrauch et al. 2018) and for apparent active ammonia excretion against gradients (Clifford et al. 2015, 2017). Oxygen consumption is also elevated after feeding (Weinrauch et al. 2018; Glover et al. 2019). Similar to teleosts, hagfishes show hyperventilation in response to hypoxia (Malte and Lomholt 1998; Perry et al. 2009b) and hypercapnia (Perry et al. 2009b). According to both studies, only ventilatory frequency changes, and ventilatory stroke volume cannot be modified. It is not known yet whether hagfish sense those respiratory gases by NECs or other receptors, or whether there are chemoreceptors in the central nervous system.

Another possible mechanism by which ammonia may be sensed is through external nociceptors. These polymodal sensors are known to detect noxious chemicals in mammals (Lynn 1996; Yeomans and Proudfit 1996), amphibia (Spray 1976), birds (Gentle 2000), and fish (reviewed by Sneddon 2019). They initiate defensive responses to prevent damage to their sensory and other systems (Walters 1996) and in fish, their activation may increase opercular movements (Sneddon 2003). They are distributed throughout the head region in fish, innervated by the trigeminal nerve (cranial nerve V) (Sneddon 2019). A variety of substances (e.g. acetic acid, high NaCl) appear to be detected by nociceptors in the head region of trout, including high CO₂ (Mettam et al. 2012). Mettam et al. (2012) reported a lack of response to a relatively low concentration of NH₄Cl (0.02 mM), but it remains unclear whether a higher level of waterborne ammonia would be detected by nociceptors in fish.

1.4 Ammonia production and chemistry in fish

The primary routes of ammonia production in teleost fish are the oxidation and accompanying deamination of amino acids, and the breakdown of purines in the purine nucleotide cycle (Fig. 1.3A, B). Fish digest prey items (food) after ingestion, and break them down into simple chemical compounds such as amino acids (from proteins), mono- and disaccharides (from carbohydrates), and fatty acids and

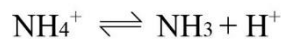
glycerol (from lipids) in the intestinal tract, including stomach and intestine. The amino acids enable the fish to keep their body maintenance and sustain protein growth, but also participate in the production of toxic ammonia, some of which may be generated in the chyme during digestion, and some of which may be produced in the intestinal epithelial cells, the enterocytes (Fig. 1.3A). Ballantyne (2001), Taylor et al. (2011) and Jung et al. (2020) provide overviews of the role of the intestine and the fate of ingested amino acids. Here, some of the absorbed glutamine is utilized directly by the intestinal epithelial cells as a primary energy source for transport processes, protein synthesis and cellular proliferation, thereby liberating ammonia, but most of the other absorbed free amino acids, including glutamine, are transferred to the liver by the portal venous blood circulation. In the liver, most amino acids are transaminated, such that their amino groups are transferred to α -keto acids generating glutamate and carbon skeletons such as pyruvate which can be used for gluconeogenesis or respired directly by the tricarboxylic acid (TCA) cycle. Subsequently, the oxidative deamination of glutamate occurs, catalyzed by glutamate dehydrogenase, regenerating α -ketoglutarate for recycling or respiration, and liberating toxic ammonia. The latter, together with the ammonia absorbed from the chyme and produced by the enterocytes, enters the venous blood stream and is ultimately excreted *via* the gills, unless it is trapped elsewhere by glutamine synthetase. The carbon skeletons from the amino acids are channeled into the TCA cycle to produce ATP and GTP. When overall fish energy levels are high, these ATP and GTP molecules act as allosteric inhibitors to glutamate dehydrogenase, thus inhibiting glutamate deamination and ammonia production. Conversely, when energy levels are low, ADP and GDP act as allosteric activators and stimulate glutamate dehydrogenase activity, so that carbon skeletons are generated to feed into the TCA cycle; as a result, ATP and ammonia production are increased.

During intense exercise in fish, the net breakdown of ATP, ADP, and AMP, which powers muscle contraction, results in excess ammonia production by the purine nucleotide cycle (Fig. 1.3B). In the first step of this cycle catalyzed by AMP deaminase, AMP is converted to inosine monophosphate (IMP), liberating ammonia (Mommensen and Hochachka 1988). Some of this ammonia diffuses into the venous bloodstream. As a result, both plasma ammonia levels and overall ammonia excretion rates at the gills increase after exercise (Wood 1988).

In hagfish, the pathways for ammonia production by oxidative deamination of amino acids, and *via* the purine nucleotide cycle are both present (Peters and Gros 1988). However, hagfish are known as deep sea animals, feeding only intermittently, and spending much of their time coiled on the sediments (*Eptatretus stoutii*) or buried in the mud or sand (*Myxine glutinosa*). This coincides with reports that their overall metabolic rates are much lower than in teleosts (e.g. Munz and Morris 1965; Clifford et al. 2016).

Ammonia production rates appear to be similarly low (e.g. Clifford et al. 2017; Giacomini et al. 2019a; Giacomini et al. 2019b). Glover et al. (2011) proposed that ammonia production would occur mostly *via* amino acid breakdown after feeding, not as a result of exercise. Indeed, later studies showed that both ammonia excretion rates and plasma ammonia levels are greatly elevated after feeding (Wilkie et al. 2017; Weinrauch et al. 2018), and their normally low O₂ consumption rates may increase 2-to 3-fold after a meal (Weinrauch et al. 2018; Glover et al. 2019). Hagfish sometimes burrow into carcasses to feed, where the external environment would be rich in nutrients. In this context, it is interesting that amino acids (as well as other nutrients) are taken up not only by ingestion through the mouth, but also by transport across external epithelia such as gills and skin (Clifford et al. 2015; Glover et al. 2011; Glover et al. 2015; Glover and Bucking 2016).

Therefore, after feeding or during and after exercise, fish may experience greatly increased plasma total ammonia levels, both in the form of ionized ammonium (NH₄⁺) and dissolved gaseous ammonia (NH₃). However, at the pH of the plasma and intracellular fluids, > 95% ammonia is present as NH₄⁺ and only <5% is present as NH₃, reflecting the difference between fish body fluid pH (7.0 ~ 8.2) and the ammonia pK (~9.5 at 15°C water temperature). NH₃ acts as a weak base while NH₄⁺ acts as a weak acid in fish plasma:



While there has been controversy as to whether metabolic reactions produce NH₃ (the weak abase) or NH₄⁺ (the weak acid), there is an agreement that on a net basis, the metabolic production of ammonia is acid-base neutral in animals, because the relevant reactions produce equal amounts of NH₄⁺ and HCO₃⁻ (or NH₃ and CO₂) on a net basis (Hills 1973). The association constant (K) is derived from the law of mass action and is described in the equation below.

$$K = \frac{[\text{NH}_3][\text{H}^+]}{[\text{NH}_4^+]}$$

Using the logarithmic transformation of the above equation, K is transformed into pK (-logK) which is analogous to pH (-log[H⁺]), thus the equation is rearranged as the *Henderson-Hasselbach equation*:

$$-\log[\text{H}^+] = -\log K + \log \frac{[\text{NH}_3]}{[\text{NH}_4^+]} \quad \text{or} \quad \text{pH} = \text{pK} + \log \frac{[\text{NH}_3]}{[\text{NH}_4^+]}$$

The *Henderson-Hasselbach equation* allows us to calculate the molar ratio of the pair of $[\text{NH}_3]$ and $[\text{NH}_4^+]$ given the pK and pH values. For example, if the fish plasma pH is similar to pK , then the $\log([\text{NH}_3] / [\text{NH}_4^+])$ closes to zero, because the molar concentration ratio of $[\text{NH}_3]/[\text{NH}_4^+]$ will be 1.0. However, the blood plasma pH of most teleosts is typically around 7.8 at 15°C , while the ammonia pK is around 9.5, so the $\log([\text{NH}_3] / [\text{NH}_4^+])$ is approximately -1.7; theoretically, this means that that most teleost fish contains >97% of $[\text{NH}_4^+]$ and <3% of $[\text{NH}_3]$ in their plasma at 15°C water temperature.

1.5 Ammonia excretion in fish

Since ammonia excretion was first measured in the fish gills by Homer Smith (1929), the transport mechanisms have been variously explained by simple diffusion of NH_3 along PNH_3 gradients, by NH_4^+ diffusion along electrochemical gradients, by direct exchange of Na^+ for NH_4^+ (first suggested by August Krogh 1939), or NH_4^+ movement *via* K^+ channels and transporters (*see* Evans and Cameron 1986; Evans et al. 2005; Wilkie 2002; Wood 1993 for reviews) - but it has been controversial. However, the discovery that Rhesus glycoproteins (Rh proteins) are expressed in fish gills (Hung et al. 2007; Nakada et al. 2007b; Nawata et al. 2007) revolutionized understanding. The Rh proteins are now thought to play key roles in current models for branchial ammonia excretion in both teleost fish (Ito et al. 2013; Wright and Wood 2009) and hagfish (Braun and Perry 2010; Clifford et al. 2017; Edwards et al. 2015). While some ammonia may pass by simple diffusion through the lipoprotein cell membranes, a significant portion may also pass by facilitated diffusion through Rh protein channels, and this fraction is thought to increase when Rh protein expression is induced by ammonia loading. In current models (Weihs et al. 2009; Wright and Wood 2009, 2012), three family types of Rh proteins participate in ammonia excretion in fish gills: Rhag in red blood cells, Rhbg and Rhcg in basal and apical epithelial cell membranes respectively (Fig. 1.4). Their overall gene expression levels are increased when the fish are exposed to high environmental ammonia (HEA) or infused by ammonia directly into their blood circulation. Increased internal plasma ammonia is transferred to fish gills by red blood cells (RBCs) that contain ammonia transport channels, Rhag proteins, in their membranes, which facilitate the diffusive movement of ammonia between RBCs and plasma. Due to gradient differences, ammonia is released by the RBCs, transferred to the intracellular compartments of gill epithelial cells *via* basal Rhbg channels, and subsequently excreted to the external media *via* apical Rhcg channels. The ammonia excretion across the apical membrane of fish gills *via* Rhcg channels is thought to be coupled to H^+ excretion and Na^+ uptake mechanisms (Fig. 1.4). Most H^+ (metabolic acid) and HCO_3^- (metabolic base) originates from CO_2 hydrolysis which is catalyzed by the enzyme carbonic anhydrase (CA). The resulting H^+ is excreted *via*

apical H⁺-ATPase (HAT) and/or the Na⁺-/H⁺-exchanger (NHE) into the gill boundary layer, so the boundary layer is acidified; this helps protonation of NH₃ to NH₄⁺ as it emerges from the Rhcg protein. These H⁺ ions are simultaneously exchanged against external Na⁺ *via* NHE (direct exchange) or the Na⁺ channel energized by the apical HAT (indirect exchange). HCO₃⁻ may be exchanged directly against external Cl⁻ *via* specialized apical anion exchange proteins in the apical membranes. As a result, freshwater fish take up external Na⁺ and Cl⁻ which are essential to preserving their internal osmolarity. Although direct Na⁺/NH₄⁺ exchange may not occur (still controversial), CO₂ excretion after hydrolysis to H⁺ and HCO₃⁻ and ammonia excretion after protonation to NH₄⁺ occur simultaneously, such that Na⁺ and Cl⁻ uptake are coupled to CO₂ and ammonia excretion in fish gills. Thus, the Na⁺/NH₄⁺ exchange originally suggested by August Krogh (1938) is explained by a more complicated “exchange complex” or metabolon (Ito et al. 2013; Wright and Wood 2009).

With respect to the mechanism of ammonia transport through the Rh proteins, they are generally thought of as NH₃ transport channels, due to the structural similarity between animal Rh proteins and bacterial AmtB proteins (Knepper and Agre 2004). The protein AmtB is known as a specialized NH₃ transport channel in the bacterial inner membrane between cytoplasmic and periplasmic spaces. In bacteria, the ionic ammonium (NH₄⁺) is deprotonated in the periplasm so that NH₄⁺ is transformed into gaseous ammonia (NH₃) which penetrates the bacterial membrane *via* a pore formed by amino acid residues (AmtB). The transported NH₃ is then protonated back to NH₄⁺ because of higher ammonia pK relative to bacterial pH. Similar to AmtB, and the related AMT proteins of some invertebrates (Weihrauch and Allen 2018), the Rh proteins are thought to facilitate the transport of ammonia from the blood plasma to the external media through the epithelial membranes in fish gills by the action of deprotonation of NH₄⁺ to form into gaseous NH₃, so the ammonia penetrates through the fish gills and is then protonated back to NH₄⁺ by the mechanisms outlined in the previous paragraph. The study of Nawata et al. (2010b) which investigated the transport characteristics of trout Rh proteins expressed in *Xenopus* oocytes provided direct support for this NH₃ diffusion plus H⁺ deprotonation / protonation model, and in Fig. 1.4, this concept has been incorporated into the original model of Wright and Wood (2009).

1.6 Is there a relationship between ventilation and ammonia excretion in fish?

There are many reports that teleost fish hyperventilate during and after exposure to HEA (Fivelstad and Binde 1994; Knoph 1996; Lang et al. 1987; Smart 1978). While this is often interpreted as

a general stress response to a toxicant, it may in fact reflect the specific role of ammonia as a ventilatory stimulant discussed in Section 1.3. In HEA, it appears that external ammonia gradually diffuses into fish plasma due to chemical gradients, resulting in elevation of fish plasma ammonia levels, and some minutes to hours later, the fish increases ventilation (e.g. DeBoeck and Wood 2015; Zhang et al. 2011). Internal administration of ammonia directly into the bloodstream stimulates almost immediate hyperventilation (McKenzie et al. 1993; Zhang and Wood 2009; Zhang et al. 2011). This hyperventilation can occur independently from changes in blood O₂, CO₂, and acid-base status (Zhang and Wood 2009).

However, a key uncertainty is whether the elevated ventilation elicited by high internal ammonia levels actually helps to increase ammonia excretion, an idea which was tested experimentally in the present thesis. Randall and Ip (2006) argued that ammonia excretion in fish is probably limited by diffusion rather than by blood perfusion or water convection, so “*that increases in ventilation would have negligible effect on the rate of ammonia excretion, and therefore represent a non-physiological response on the part of the fish*”. However, it is important to note that this was a theoretical prediction formulated in the absence of any evidence whether (or not) changes in ventilation affected ammonia excretion, and it was made just one year before the discovery of Rh proteins in fish gills (Hung et al. 2007; Nakada et al. 2007b; Nawata et al. 2007). If Rh proteins serve to facilitate ammonia movement through the gill epithelium, diffusion limitation may not apply, and this argument may be invalid. Ammonia-stimulated ventilation would be important in elevating ammonia excretion after natural ammonia loading scenarios such as feeding or exhaustive exercise. Furthermore, it could be particularly important during and after HEA exposure, as there is evidence that the Rh system also allows active ammonia excretion against unfavourable NH₃ partial pressure gradients and [NH₄⁺] electrochemical gradients in trout (Nawata et al. 2007; Wood and Nawata 2011; Sinha et al. 2013).

Prior to this thesis, there was no evidence on whether or not ammonia stimulates ventilation in hagfish. However, it has been demonstrated that Rh proteins occur in the gills and skin of hagfish (Braun and Perry 2010; Edwards et al. 2015; Clifford et al. 2017), and respond to internal and external ammonia loading (Edwards et al. 2015; Clifford et al. 2017). There is also evidence of potential active ammonia excretion in the Pacific hagfish so as to keep internal ammonia levels low during HEA exposure (Braun and Perry 2010; Clifford et al. 2015; Clifford et al. 2017). This ability for active excretion may be a very important factor in the tolerance of hagfish to very high levels of HEA. Certainly, if ammonia does stimulate ventilation in hagfish, the response would likely facilitate increased ammonia excretion.

1.7 Study organisms

I have used two very different, phylogenetically distant fish species with fundamentally different breathing mechanisms in order to understand the role of ammonia in the control of breathing: *Eptatretus stoutii* (“Pacific hagfish”) and *Oncorhynchus mykiss* (“Rainbow trout”).

1.7.1 The Pacific hagfish (*Eptatretus stoutii*)

Little was known about the control of breathing in hagfish when I started my research. Perry et al. (2009b) had demonstrated that ventilation was increased by both hypoxia and hypercarbia, as well as in response to injections of cyanide to the inhaled water or circulatory system, and this represents indirect evidence for the presence of chemoreceptors somewhere in the system. However, it was not known whether peripheral (e.g. NECs) or central chemoreceptors were present, or whether breathing responded to ammonia. Some relevant information was available on the acid-base response to very high levels of environmental PCO_2 where hagfish rapidly regulate plasma pH levels by increasing HCO_3^- uptake from the ambient water while excreting internal Cl^- ions which are abundant because the fish is both an osmo- and an iono-conformer of plasma Na^+ and Cl^- concentrations (Clifford et al. 2014; Baker et al. 2015). It was also known that hagfish excrete ammonia mainly at the gills (Clifford et al. 2016), that they possess Rh proteins in gills and skin (Braun and Perry 2009; Edwards et al. 2017; Clifford et al. 2017; Suzuki et al. 2017), that they are able to excrete ammonia at high rates (Wilkie et al. 2017) and against external gradients (Edwards et al. 2015; Clifford et al. 2015; Clifford et al. 2017), processes in which Rh proteins could be involved. Therefore, it seemed reasonable to investigate the possible role of ammonia in ventilatory control in this species.

1.7.2 The rainbow trout (*Oncorhynchus mykiss*)

The rainbow trout has been used as the premier model fish in respiratory physiology for several decades, and their ventilatory responses to changed levels of the traditional respiratory gases (O_2 and CO_2) in ambient water and in the bloodstream have been well-described, as detailed in Section 1.3. When I started, there was much less information on the role of ammonia in the control of breathing, and virtually all of this had been established using the rainbow trout model (Hillaby and Randall 1979; McKenzie et al. 1993; Zhang and Wood 2009; Zhang et al. 2011; Zhang et al. 2013; Zhang et al. 2015). There was also substantial information on the role of Rh proteins in branchial ammonia excretion in the

rainbow trout (Nawata et al. 2007; Nawata and Wood 2009; Nawata et al. 2010b; Wood and Nawata 2011; Sinha et al. 2013; Zimmer et al. 2010). However, although gill NECs were clearly implicated in ammonia-sensing (Zhang et al. 2011; Zhang et al. 2015), the details of detecting internal *versus* external ammonia remained unclear, and the possible role of central chemo-sensing of ammonia by the brain was only speculated (Zhang et al. 2013). It was also unclear whether or not changes in ventilation had any effect on ammonia excretion (Randall and Ip 2006). Therefore, much remained unknown, so it was logical to continue to use the trout model system to investigate these further questions.

1.8 Thesis objectives and chapter summaries

The objectives of this thesis are to investigate the role of ammonia in controlling ventilation in fish, the possible adaptive significance of this control (e.g. for avoiding ammonia uptake, for promoting ammonia excretion, and/or for promoting the exchange of the other respiratory gases), the mechanisms involved, and the phylogenetic basis of the phenomena.

1.8.1 Chapter 2: “The ventilation mechanism of the Pacific hagfish *Eptatretus stoutii*”

The goal of this chapter was to clarify the breathing mechanism of the Pacific hagfish. Hagfish are the extant vertebrate group with the most ancient lineage, and thus of great evolutionary importance. However, there was little prior information on breathing in hagfish, which appears to be fundamentally different from that in teleosts. Therefore, prior to starting my investigation of the influence of ammonia on ventilation in *Eptatretus stoutii*, it was first necessary to understand it. The anatomy of the respiratory passageway was investigated, the flow rate through the nostril, the pressures at the nostril, mouth, gill pouches, and pharyngo-cutaneous duct (PCD), and the movements of the heart and velum were recorded, together with observations of dye flow in various parts of the system. During normal breathing, water flow was powered largely by the action of the complex scroll-like velum. The complete system comprises two-phase unidirectional pumping with a fast suction pump, the velum, for inhalation, and a slow force pump at gill pouches and PCD for exhalation. The mouth joins the pharynx posterior to the velum and plays no role in ventilation. Normal breathing patterns can range from prolonged periods of complete apnea to very high flow rates, achieved by increases in both velum frequency and stroke volume. The ventilatory index (product of frequency x nostril pressure amplitude) provides a useful proxy for true ventilatory flow rate. Two types of coughing (flow reversals) through the nostril duct and mouth cavity

respectively were described. These flow reversals would help to protect the soft respiratory tract and gills by removing debris. Observations on the feeding mechanism and ventilation during swimming were also made.

1.8.2 Chapter 3: “Ventilatory sensitivity to ammonia in the Pacific hagfish (*Eptatretus stoutii*), a representative of the oldest extant connection to the ancestral vertebrates”

The main objective of this chapter was to evaluate whether or not *Eptatretus stoutii*, a representative of the most primitive extant vertebrates, exhibits ventilatory sensitivity to ammonia. Specifically, the ventilatory responses to both external high environmental ammonia (HEA) in the water and to internal ammonia loading to the bloodstream were evaluated, together with changes in blood ammonia and acid-base status, using techniques developed in Chapter 2 (Eom and Wood 2019) to measure breathing. Hagfish showed immediate apnea or extreme hypoventilation (“breath-holding”) in response to the HEA treatment, interpreted as a protective response to minimize ammonia uptake. However, this changed to later hyperventilation by 3h as plasma ammonia levels eventually increased. The ammonia-injected hagfish exhibited rapid hyperventilation. In both cases plasma total ammonia and PNH_3 levels increased, while blood acid-base status remained unchanged, indicating specific responses to internal ammonia. Therefore, hyperventilation in HEA appeared to be an indirect response to internal ammonia elevation, rather than a direct response to external ammonia. This investigation discovered a previously undetected response (immediate hypoventilation) to HEA in fish, whereas the later hyperventilation indicated that the stimulatory effect of internal ammonia on breathing was present very early in vertebrate evolution.

1.8.3 Chapter 4: “Understanding ventilation and oxygen uptake of Pacific hagfish (*Eptatretus stoutii*), with particular emphasis on responses to ammonia and interactions with other respiratory gases”

The two major objectives in this chapter were: (i) to further characterize the respiratory system of the hagfish by examining its performance in O_2 utilization (the percentage extraction of O_2 from the ventilatory flow) and O_2 uptake, and (ii) to understand how other respiratory gases (O_2 : hypoxia and hyperoxia, and CO_2 : hypercapnia) interact with the acute hypoventilation response to HEA exposure (discovered in Chapter 3, Eom et. al., 2019), as well as how all these treatments affect O_2 uptake. Similar to previous chapters, the ventilatory performance was assessed by measuring total ventilatory flow and

frequency at the nostril. In addition, inspired and expired O₂ tensions were simultaneously measured at the exits of all 12 gill pouches plus the pharyngo-cutaneous duct (PCD). Oxygen utilization was greater in more posterior pouches and the PCD. Overall O₂ utilization remained constant between normal and spontaneous hyperventilation, and increased greatly during hypoventilation. Environmental hypoxia caused hyperventilation, but neither hyperoxia nor hypercapnia altered ventilation flow. The acute hypoventilation response to HEA still occurred during hypoxia and hyperoxia, but was blunted during hypercapnia, likely because of the lower water pH which decreased the PNH₃. Under all treatments, O₂ consumption increased with increases in ventilation flow. There was a lower convection requirement for O₂ during hyperoxia, higher requirements during hypoxia and hypercapnia, but unchanged requirements during acute HEA. In conclusion, the “primitive” hagfish operates a flexible respiratory system with considerable reserve capacity, adaptive to its deep-sea environment.

1.8.4 Chapter 5: “Is ammonia excretion affected by gill ventilation in the rainbow trout *Oncorhynchus mykiss*?”

The major goal of this chapter was to address the assumption of Randall and Ip (2006) that ammonia excretion in fish is limited by diffusion rather than by convection, so that increases in ventilation would have a negligible effect on the rate of ammonia excretion. If this were the case, why then should elevated internal ammonia stimulate breathing if it would not help increase ammonia excretion? However, this statement was made before the discovery of the Rh protein metabolon that can facilitate ammonia excretion across the gills (Nawata et al. 2007; Wright and Wood 2009). The rainbow trout was used in the present experiments, as it has been the principal teleost model for studies on breathing and ammonia excretion. “Voluntary” changes were induced in the ventilation of trout using moderate hypoxia (for hyperventilation) and hyperoxia (for hypoventilation). The experiments were performed in a relatively non-invasive fashion, using a buccal catheter to record breathing frequency and pressure amplitude (product = ventilatory index), thereby providing a semi-quantitative indicator of ventilation flow. In “resting” trout, in which plasma ammonia levels and gill Rh protein expression were low, ammonia excretion was insensitive to ventilation, in accord with the diffusion limitation idea of Randall and Ip (2006). However, in ammonia-loaded fish in which plasma ammonia levels and gill Rh protein expression were both high, ventilation was greatly elevated. Furthermore, in these fish, ammonia excretion became sensitive to ventilation, increasing with further experimentally induced hyperventilation, and decreasing with experimental hypoventilation. Therefore, once diffusion limitation was removed *via* upregulation of the Rh metabolon, ammonia excretion became sensitive to convection.

The hyperventilation response would be beneficial at times of internal loading (e.g. meal digestion, post-exercise recovery, post-exposure to HEA) to increase the excretion of potentially toxic ammonia.

1.8.5 Chapter 6: “A less invasive system for the direct measurement of ventilation in fish”

This chapter introduces a newly developed, less invasive method for the direct measurement of ventilation. This was accomplished by modification of the original design of the “Van Dam chamber” (Van Dam 1938) by incorporation of an ultrasonic blood flow probe to measure the ventilatory water flow in real time on a breath-to-breath basis. No anaesthesia, surgery, or gluing/sewing of membranes to the lips is involved, so the fish can be quickly moved in and out of the apparatus, facilitating repeated measurements on the same animal after different treatments. Using both 400-g rainbow trout and 10-g goldfish, hyperventilatory responses to environmental hypoxia and hypoventilatory responses to hyperoxia were recorded, matching previously reported responses to these treatments in buccal pressure amplitude, breathing frequency, and ventilatory index. The apparatus was used in Chapter 7 (Eom and Wood 2021a) and in other studies not reported in this thesis. Due to the absence of anesthesia and difficult surgery, this less invasive methodology may prove more acceptable to animal ethics committees.

1.8.6 Chapter 7: “Brain and gills as internal and external ammonia sensing organs for ventilatory control in rainbow trout *Oncorhynchus mykiss*”

The main purpose of this chapter was to factor out the roles of possible ammonia sensing organs for ventilatory control in teleosts, using the rainbow trout as a model. More or less immediate hyperventilation after direct ammonia injection to blood circulation (Zhang et al. 2011) suggests that fish are sensing internal ammonia elevations in the plasma, probably *via* the NECs. However, uncertainties remain about the possible role of central chemoreceptors in the brain in internal ammonia sensing, and also about the detectors involved in the ventilatory responses to external HEA. A time course analysis using the less invasive system developed in Chapter 6 (Eom and Wood 2020) revealed that the hyperventilatory response to external HEA developed gradually over 20 min. This suggests that as in the hagfish, acute hyperventilation is a response to gradually rising internal ammonia rather than a direct response to external ammonia elevation. When a Y-shaped tubing was used to introduce HEA directly to the external surfaces of the 1st gill arches, an immediate hypoventilatory response occurred. This has not previously been reported in teleosts, but may be similar to the acute hypoventilatory response discovered

in hagfish in Chapters 3 (Eom et al. 2019) and 4 (Eom and Wood 2021b). Again, it may be may be a short-term protective response to minimize the uptake of toxic ammonia. Finally, injections of physiologically relevant concentrations of ammonia in mock extradural fluid (EDF) directly onto the surface of the hindbrain induced immediate hyperventilation. This is the first evidence of central chemoreception in teleost fish. The results suggest that there are three sites of ammonia sensing, an external one on the gill surfaces for hypoventilation in HEA, and two internal ones, branchial NECs and brain, for hyperventilation in response to elevated internal ammonia levels.

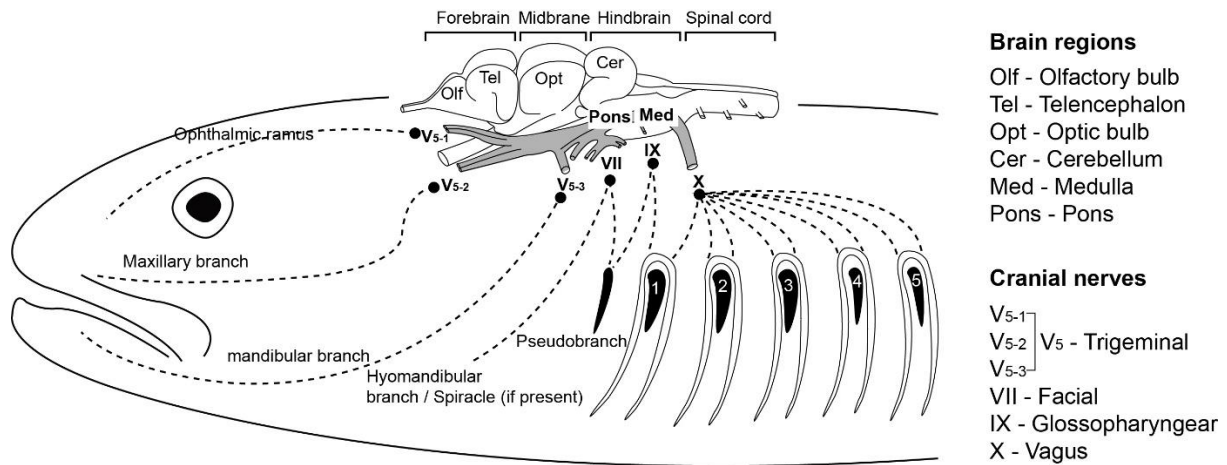


Figure 1.1 Cranial nerves leaving or entering hindbrain which consists of pons and medulla where the rhythmic respiratory pattern is thought to be generated in fish (communication with Dr. William Milsom).

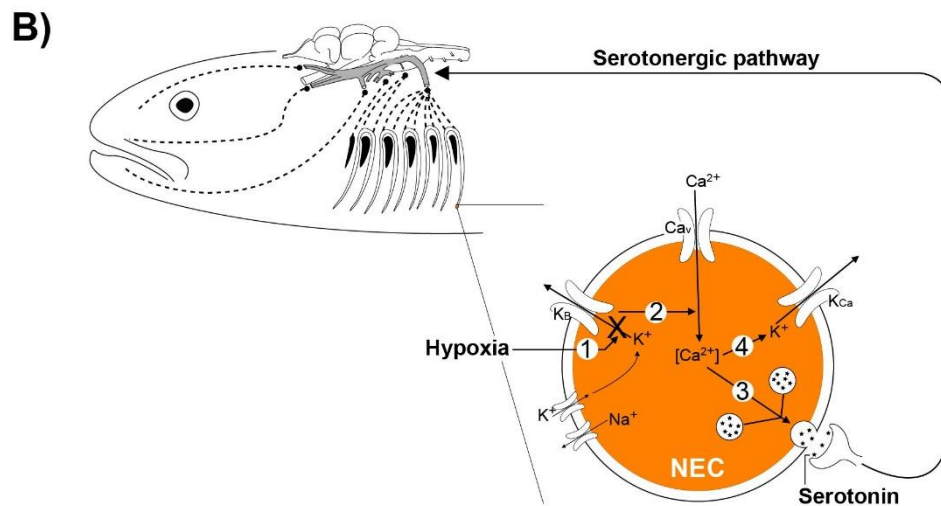
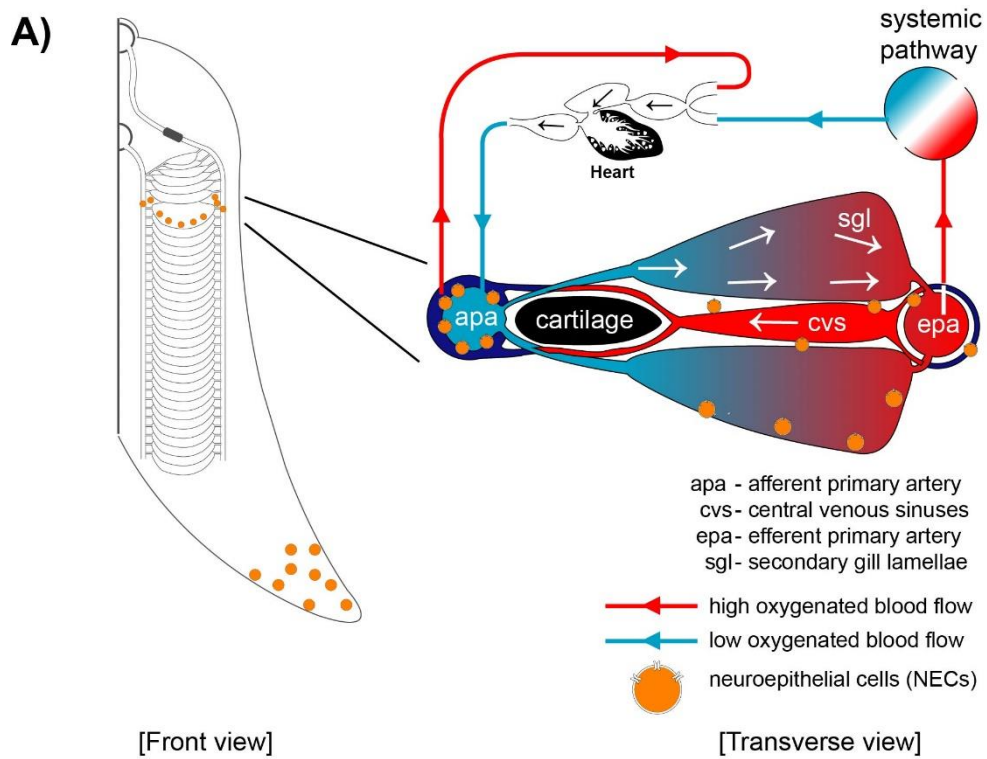


Figure 1.2 A) Location of neuroepithelial cells (NECs) in fish gills and B) their functional mechanism in response to changed ambient respiratory gas levels such as hypoxia (Re-drawings of figures from Coolidge et al. 2008, and Zachar and Jonz 2012).

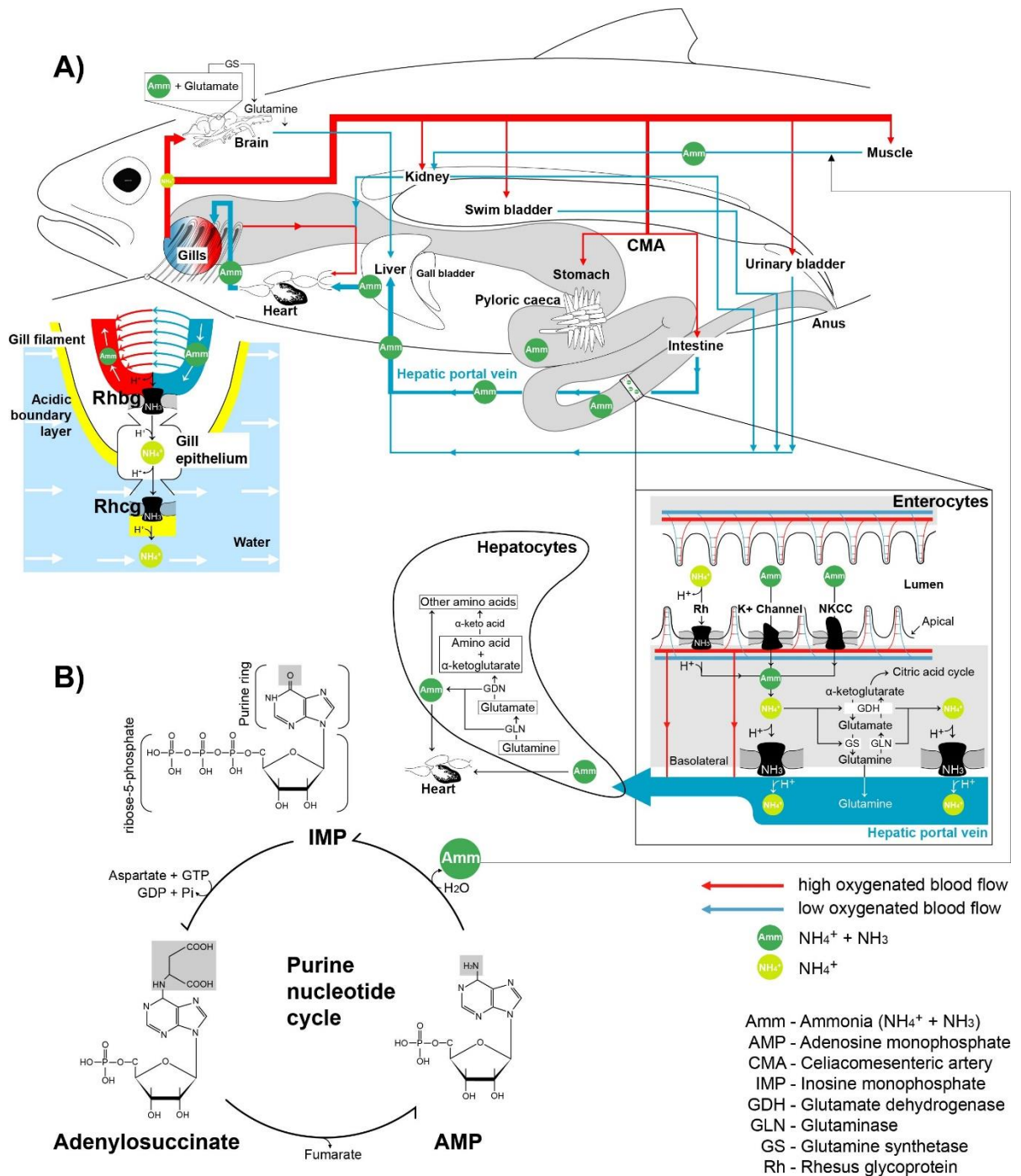


Figure 1.3 A) Ammonia movements in enterocytes (intestine), hepatocytes (liver), brain, muscle, and gill cells, and B) purine nucleotide cycle in fish (communication with Ellen Jung).

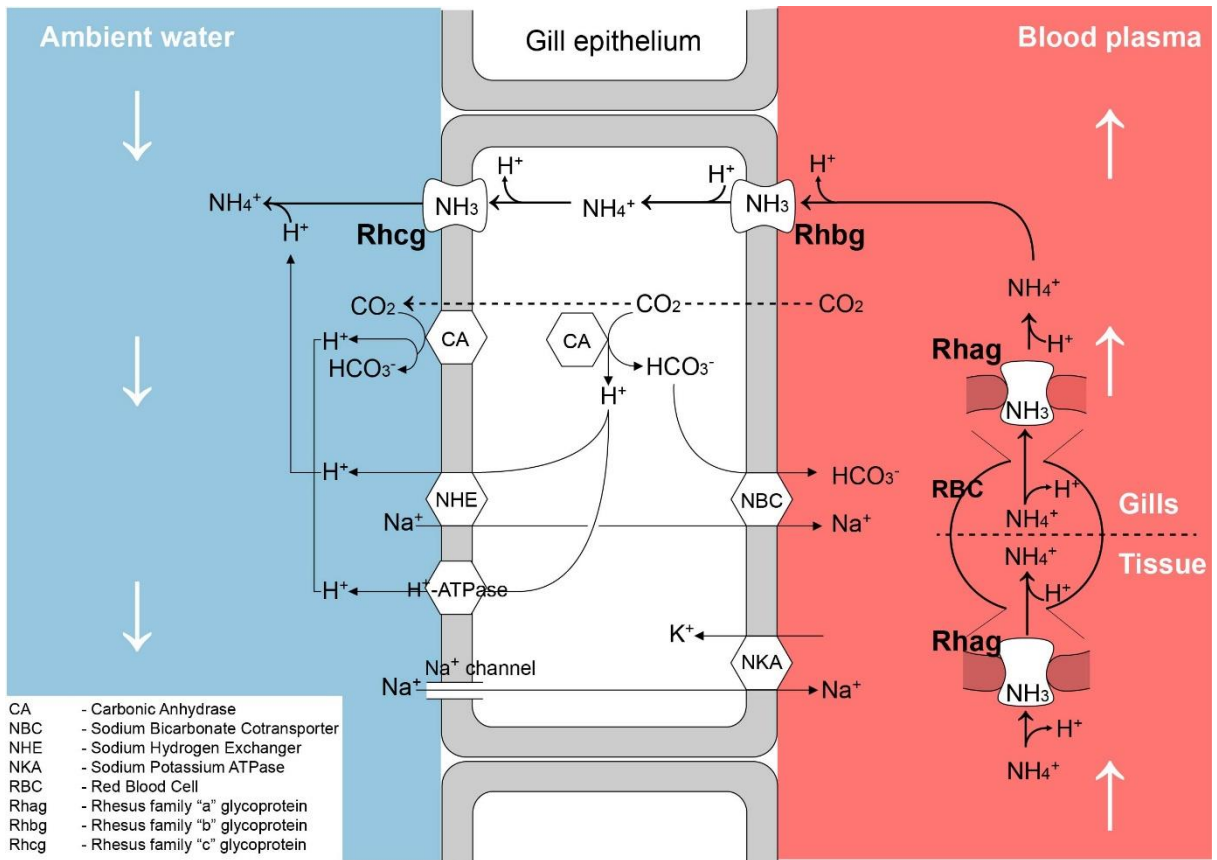


Figure 1.4 Current model for the ammonia excretion mechanism in the fish gill (update and re-drawing of figure from Wright and Wood 2009). Please see text for details.

Chapter 2: The ventilation mechanism of the Pacific hagfish *Eptatretus stoutii*

2.1 Summary

Anatomical and physiological observations of the breathing mechanisms were performed in Pacific hagfish *Eptatretus stoutii*, with measurements of nostril flow and pressure, mouth and pharyngo-cutaneous duct (PCD) pressure and velum and heart impedance and observations of dye flow patterns. Resting animals frequently exhibit spontaneous apnea. During normal breathing, water flow is continuous at a high rate ($\sim 125 \text{ ml kg}^{-1} \text{ min}^{-1}$ at 12°C) powered by a two-phase unidirectional pumping system with a fast suction pump (the velum, $\sim 22 \text{ min}^{-1}$) for inhalation through the single nostril and a much slower force pump (gill pouches and PCD $\sim 4.4 \text{ min}^{-1}$) for exhalation. The mouth joins the pharynx posterior to the velum and plays no role in ventilation at rest or during swimming. Increases in flow up to $>400 \text{ ml kg}^{-1} \text{ min}^{-1}$ can be achieved by increases in both velum frequency and stroke volume and the ventilatory index (product of frequency x nostril pressure amplitude) provides a useful proxy for ventilatory flow rate. Two types of coughing (flow reversals) are described. During spontaneous swimming, ventilatory pressure and flow pulsatility become synchronised with rhythmic body undulations.

2.2 Introduction

The breathing mechanism of hagfishes (Class Myxini), which are arguably the extant vertebrates of the most ancient lineage, is fundamentally different from those in other fishes (Bartels 1998; Johansen and Strahan 1963; Malte and Lomholt 1998). To date, most studies have been on the Family Myxinidae, with only two studies on the Family Eptatretidae (Coxon and Davison 2011; Perry et al. 2009b). For both families, there is general agreement that the rhythmic up and down movement of the scroll-like velum in the velum chamber of the anterior pharynx serves as the major ventilatory pump, inhaling the ambient water *via* the single anterior nostril duct to the pharynx. This idea that the velum is responsible for the ventilatory water current was first suggested by Cole (1905) based on anatomical studies. Gustafson (1935) and Strahan (1958) added a detailed description of the cartilaginous skeleton and muscles that constitute the velum chamber. Later, Johansen and Hol (1960) applied x-ray analysis with water-soluble contrast media and confirmed that the velum structure moved dorsoventrally as the major pump for the ventilatory water current as Cole (1905) had originally suggested. The inhaled water is then expelled through pairs of gill pouches (variable in number both within and between species) and a pharyngo-cutaneous gill duct (PCD). The Eptatretidae differ from the Myxinidae in having separate gill pouch

openings to the outside on each side in addition to the exit of the common PCD on the left side *via* an enlarged posterior gill slit.

There have been only two direct measurements of ventilatory water flow in hagfishes, both using blood flow meters in novel configurations. Steffensen et al. (1984) measured a resting ventilatory flowrate of about $45 \text{ ml kg}^{-1} \text{ min}^{-1}$ in *Myxine glutinosa* L. 1758 at 15°C by mounting the flow-probe on a cone overlying the partially buried animal. Perry et al. (2009b) reported a much higher value of about $235 \text{ ml kg}^{-1} \text{ min}^{-1}$ in *Eptatretus stoutii* (Lockington 1878) at 12°C fitted with a flow-probe attached to a tube tied into the nostril of the non-buried animal. It is unclear whether these very different values reflect differences between the species or the methods used. Furthermore Perry et al. (2009b), using hypoxia and hypercapnia as experimental stimuli, concluded that changes in ventilatory flow rate occurred only *via* changes in velum frequency and that stroke volume did not vary. This conclusion was supported by Coxon and Davison (2011) who recorded the ventilatory frequency response to temperature in *Eptatretus cirrhatus* (Forster 1801) by electromyography of velum contraction, but no direct measurements of ventilatory flow rate were made.

Other elements of the hagfish breathing mechanism also remain incompletely understood. For example, various researchers have questioned the role of gill pouches and their associated ducts as active pumps *versus* passive conduits and have even raised the possibility of bidirectional water flow. For example, Goodrich (1930) suggested the gill pouches served as an active water pump in series with the velum chamber for unidirectional water flow and he believed that the gill pouches could even generate a bidirectional water current (inhalation and exhalation) when the nostril was occluded, as might for example occur during feeding. Strahan (1958), however, did not observe the active contraction of gill pouches in live *M. glutinosa* so he concluded that the role of the gill pouches was entirely passive. Subsequently, using x-ray analysis in the same species, Johansen and Hol (1960) observed contraction of the gill pouches during normal unidirectional ventilation. They concluded that water in the pharynx was expelled actively through the gill pouches while valve-like muscular sphincters located in the efferent and afferent gill ducts regulated the amount of expelled water and this was later accepted by Strahan (in Johansen and Strahan 1963). Another uncertainty is the possible role of the mouth as a conduit, or even a pump, for inhalation; i.e., additional to the well accepted roles of the nostril and velum chamber for these functions. This does not appear to have been directly investigated, though in *M. glutinosa*, Johansen and Hol (1960) observed that x-ray contrast media injected *via* a tube in the mouth subsequently appeared in the gill pouches and gill ducts, suggesting a functional connection. Various types of flow reversals (coughing and sneezing) either spontaneously, or in response to waterborne particles, have been described in *M. glutinosa* (Johansen and Hol 1960; Johansen and Strahan 1963; Steffensen et al. 1984;

Strahan 1958). However, in the Eptatretidae, to our knowledge, the potential roles of the gill pouches and the mouth in ventilation have never been investigated and flow reversals have not been described in members of this family (Coxon and Davison 2011; Perry et al. 2009b).

With this background in mind, the goal of the present study was to describe the basic breathing mechanisms in *E. stoutii* as a prelude to subsequent studies on its ventilatory responses to temperature (Giacomin et al. 2019b) and ammonia (Eom et al. 2019 – now Chapter 3). We started with the simple assumption that any organ connected to the pharynx such as the nostril, the velum chamber, the mouth cavity and the pairs of gill pouches including the PCD exiting through the left posterior gill slit, could serve as ventilatory organs in *E. stoutii*. In order to understand the system, the hagfish were dissected and we collected water flow data from the nostril, pressure data from the nostril, mouth and PCD, impedance data from the velum chamber and the heart for velum and cardiac rates, and dye flow patterns were observed. The focus was on normal ventilatory physiology in resting animals and how this changed during experimental disturbances, during ventilatory reversals (here referred to as nostril coughing and mouth coughing) and during spontaneous bouts of exercise.

2.3 Materials and Methods

2.3.1 Experimental animals

Pacific hagfish *E. stoutii*, body mass 53.9 ± 3.3 g, N = 149] were captured in August and September by 22 L sized Korean cone traps that were baited with strips of Pacific hake *Merluccius productus* (Ayres 1855) and anchored on the bottom at a depth of 100 m in Trevor channel (48° 50.8440 N, 125° 08.3210 W) located close to the Bamfield Marine Sciences Centre (BMSC), off the southwest coast of Vancouver Island, BC, Canada. The captured *E. stoutii* were housed at BMSC in fibreglass tanks (20 m³) served with flow-through seawater and furnished with PVC pipes for shelter. Although hake strips were provided, the animals generally did not feed during the 2 months period of holding. The animals were collected under permits from the Department of Fisheries and Oceans Canada (XR-202-2016 and 194-2017) and the experiments were approved by the University of British Columbia (UBC) (Animal Use Protocol A14-0251) and BMSC Animal Care Committees (AUP RS-17-20) and followed the guidelines of the Canadian Council of Animal Care. Holding and experimental temperature was 11 to 13°C and salinity was 30 to 31 ppt. After experimentation, animals were euthanized by an overdose of 5 g L⁻¹ neutralised MS-222 followed by evisceration to ensure death.

2.3.2 Anatomical studies

In freshly euthanized *E. stoutii*, the head and gill pouch regions were dissected and photographed in order to describe the anatomy of the ventilatory system. In order to further understand anatomical features of the mouth cavity, 9 ml of silicone (Silicone I, GE Sealants and Adhesives, Huntersville, NC, USA) dyed with red food colouring were injected into the anterior opening of the nostril cavity of euthanized *E. stoutii* and 3 ml of green or blue silicone into the anterior opening of the mouth cavity respectively. A plastic syringe with attached plastic tube that fit snugly into the respective openings was used for silicone injection. The fish were then immediately dissected to ascertain the distribution of the coloured silicone dyes. In order to further understand functional features of the hagfish mouth cavity, the fish were anaesthetised with MS-222 (see section 2.3), a #18-gauge needle was inserted at an angle of 45° through the ventral side of head into the mouth cavity, a 30-cm length of polyethylene tubing (PE160, 1.57 mm O.D. and 1.14 mm I.D., Clay-Adams, Sparks, MD, USA) was inserted through the hole and then heat-flared using a butane lighter so it was properly secured inside the mouth cavity.

After the fish recovered from anaesthesia in flowing sea water, a 300 µl volume of red food dye was gently injected into the mouth cavity *via* the PE160 cannula and the fish was monitored over the following 24 h with a surveillance camera system (Pro-Series HD 720P, Swann Communications; www.swann.com). Food dye was also injected into the water in front of the nostril, in front of the mouth and in front of the gill pouch openings in order to visually observe the direction of ventilatory flow in *E. stoutii*. In order to study the effect of nostril blockage as might occur when the *E. stoutii* immerses its head in its prey, the hagfish nostril was manually occluded and we observed the fate of dye that had been injected into the pharynx *via* the PCD cannula described in the following section.

2.3.3 Physiological recording from various sites in the cardio-respiratory system

Prior to operation for attachment of sensors, the fish were anaesthetized in MS-222 (0.6 g L⁻¹, neutralized to pH 7.8 with 5 M NaOH) and placed on an operating table. As hagfish are very hypoxia-tolerant, it was not necessary to maintain gill irrigation. Simple silk sutures (26 mm 1/2C taper, Perma-Hand Silk, Ethicon, Somerville, NJ, USA) fastened to the skin were used to hold recording devices in place. The following recording devices were implanted in various combinations (Fig. 2.1A); not all devices were installed on all animals:

- (i) For impedance recording of velum movements, a pair of ~15-cm laminated copper wires (AWG #32, Belden, Chicago, IL, USA), with ~1-cm stripped of their insulation at the recording ends were inserted under the skin as “fish-hook” electrodes, knotted externally, and secured laterally to the skin around the velum chamber. The entries were made with a #21-

- gauge needle ~2-cm posterior to the simple eye spots. The other ends of the copper wires, also stripped of insulation, could be connected to an impedance converter (2991, Transmed Scientific, San Luis Obispo, CA, USA).
- (ii) For impedance recording of heart contractions, a similar pair of copper wire electrodes were implanted ventrally under the skin around the heart (~1-cm posterior to the PCD). The hagfish were very sensitive to attachment of wires in the heart region, frequently showing anti-predation knotting behavior, so the attached wires as well as other catheters etc. were easily tangled or displaced. Therefore, heart rate recordings were taken from a separate group of hagfish fitted only with these heart electrodes.
 - (iii) In order to measure ventilatory flow, a 3-cm length of transparent silicone tubing (6.35 mm O.D. and 4.32 mm I.D.) was inserted so as to fit snugly into the nostril cavity, and two stitches were made laterally to the skin to secure the tubing in the nostril cavity. The probe of a flow meter was connected directly to the front of the silicone tubing, and used for measuring flow at the nostril associated with ventilation, a technique adapted from that of Perry et al. (2009b).
 - (iv) In order to measure ventilatory pressures at the nostril, a 3-cm length (non-flared) of PE160 polyethylene tubing was inserted 1-cm deep into the transparent silicone tubing of (iii), and secured by two stitches to the silicone tubing. The inserted PE160 tubing occupied 21.4% of the cross-sectional area of the silicone tubing. It could easily be removed and re-inserted with minimal disturbance to the hagfish, unlike a T-junction tubing tried earlier which was frequently tangled and displaced by the anti-predation knotting behavior of the hagfish. The secured PE160 tubing in the silicone tubing could then be connected *via* a #18-gauge needle shaft to another ~30-cm water-filled PE160 tubing which was attached to a medical pressure transducer (DPT-100, Utah Medical Products).
 - (v) In order to monitor pressure events in the mouth cavity, a ~2-cm flared PE160 catheter was fixed into the mouth, as described in Section 2.3.2 (*Anatomical Studies*). This could then be attached *via* a #18-gauge needle shaft to a ~30-cm water-filled PE160 catheter connected to a pressure transducer.
 - (vi) In order to monitor pressure events in the PCD, a ~2-cm non-flared PE160 catheter was gently inserted 1-cm deep into the PCD, and secured in place by two stitches to the skin. As with the mouth and nostril catheters, this could then be attached *via* a #18-gauge needle shaft to a ~30-cm water-filled PE160 catheter connected to a pressure transducer.

The copper wire electrodes were connected to impedance converters (Model 2991, Transmed Scientific) so as to collect the frequency (min^{-1}) of the velum chamber or heart beats (min^{-1}). The PE160 catheters were connected to medical pressure transducers (DPT-100, Utah Medical Products) so as to collect ventilatory pressures (cmH_2O) and velum frequencies (min^{-1}) at the nostril, mouth, and PCD. A microcirculation ultrasonic flow probe (V-series, Transonic Systems Inc., Ithaca, NY, USA) was connected to a dual channel small animal blood flowmeter (T106 series, Transonic Systems Inc.) so as to monitor nostril water flow ($\text{ml kg}^{-1} \text{min}^{-1}$) and velum frequency (min^{-1}) as well as the flow direction (inhalation or exhalation). Inhalation was recorded as negative flow, and exhalation as positive flow. Ventilatory stroke volume ($\text{ml kg}^{-1} \text{velum stroke}^{-1}$) was calculated as nostril water inflow divided by velum frequency. The measured analogue signals were amplified (LCA-RTC, Transducer Techniques, Temecula, CA, USA), converted to digital signals in a PowerLab data integrity system (ADInstruments, Colorado Springs, CO, USA), and were visualized and analyzed in LabChart version 7.0 software (ADInstruments). Two surveillance camera systems (Pro-Series HD 720P, Swann Communications, Santa Fe Springs, CA, USA) simultaneously recorded the hagfish (for monitoring of behavior) and the computer screen (for monitoring physiological parameters) for later correlation of behavior with interpretation of the simultaneously collected physiological data (Fig. 2.1A).

Following implantation of recording devices, most of the hagfish ($N = 119$) were allowed to recover overnight in flowing anaesthetic-free seawater before measurements of nostril ventilatory parameters. In order to collect simultaneous ventilatory signals in the nostril duct, mouth cavity, velum chamber, and PCD at rest and during spontaneous swimming activity, another group of hagfish ($N = 3$) were allowed to recover for only 30 min before physiological recordings commenced. By this time, the hagfish had resumed their normal coiled posture, and ventilatory flows and pressures were at normal resting levels. This much shorter recovery period was necessary to minimize tangling and extrusion of the multiple recording devices by the hagfish. The three animals from which the simultaneous multiple recordings were made successfully in fact represent a small subset of the total number (> 10) which were attempted. In general, Pacific hagfish showed higher activity levels at night-time so the operations were performed in late afternoon and the recordings were made mostly during the night-time. The recording area was screened from the general laboratory by black plastic sheeting, but was next to a window and thus exposed to natural photoperiod.

2.3.4 Calibration of the recording systems

The flow probe detected both the magnitude and direction of flow, so correct orientation was essential. In our recordings, negative values (i.e., below zero flow) represent inhalation through the nostril and positive values represent exhalation, as occurs during coughing, for example. As noted by Perry et al. (2009b), the intrinsic calibration of the flow probe proved to be altered in seawater, so the probe was recalibrated by flowing salinity 30 ppt seawater at 12°C through the probe at known rates (determined gravimetrically), using a peristaltic pump. Voltage outputs were converted into flow units (ml min^{-1}) by the LabChart software. The pressure transducers were zeroed to the water surface and calibrated with a column of water in the range of 0 to 4 cmH_2O . These units were used for parallelism with previous studies on ventilatory pressures in fish. Note that 1 cmH_2O is equivalent to 0.09801 kPa. The impedance measurements gave faithful recordings of frequency of velum and heart contractions but could not be used as indices of contraction strength because amplitude varied with the precise placement of the electrodes.

2.3.5 Experimental procedures

Measurements of cardiorespiratory parameters in resting, undisturbed *E. stoutii* under control conditions (normoxic water, 12°C) were available from 122 animals (99 for various ventilatory variables, 23 for heart rate). Many of these animals ($N = 119$) were subsequently subjected to treatments that altered ventilation such as exposure to various levels of ammonium bicarbonate (NH_4HCO_3) and ammonium chloride (NH_4Cl) in the water or injections of the ammonium salts in isotonic saline. Many also exhibited coughing and periods of spontaneous swimming. Recordings from these periods of altered ventilation were analysed to better understand the overall working of the ventilatory system. In addition, simultaneous measurements were obtained from the three animals fitted with nostril duct, mouth cavity, velum chamber and PCD recording devices for parallel recording at all these sites at rest, during coughing and during spontaneous exercise.

2.3.6 Statistical analyses

Data have been reported as mean \pm SE. Nostril and mouth coughing were repeatedly generated in three animals by dye injection into the respective cavities and these same three animals were used for detailed analysis of the swimming responses. One-way repeated measures ANOVA followed by Dunnett's test were applied to compare the changed respiratory variables against respective control values in GraphPad Prism 6.0 (www.graphpad.com). Relationships (with 95% confidence intervals and

95% prediction intervals) among various ventilatory variables were assessed by simple linear regression. The threshold for statistical significance was $P < 0.05$.

2.4 Results

2.4.1 Anatomical observations

The mouth of the *E. stoutii* is a hollow sac-like structure located ventral to the single anterior nostril and separated horizontally from it by a thin sheet of muscle, which has been termed the oronasohypophyseal septum (ONS) in *Eptatretus burgeri* (Girard 1855) by Oisi et al. (2013). The entrance of the mouth can be sealed by bilaterally paired dental plates that are covered with the lingual teeth used for predation. When the plates are closed, inhalation of water through the mouth would appear to be impossible. The velum chamber, which consists of a complex cartilaginous skeleton and muscular structure that can be expanded and contracted, lies posterior to the nostril and is directly connected to it at the front end and to the anterior pharynx at the back end. Injections of red-dyed silicone into freshly-ethanized animals revealed that the nostril cavity leads directly to the velum chamber and then to the pharynx and gill pouches (Fig. 2.2). Silicone injected into the nostril never appeared in the mouth. In contrast, injections of green or blue-dyed silicone into the mouth revealed that the mouth is not connected to the velum chamber but rather leads directly to the anterior pharynx, just posterior to the velum chamber. The injected dye in the pharynx exited mostly *via* the opening of the PCD posterior and to the left of the gill pouches and partially *via* the paired gill pouches. Thus, the nostril-velum-pharynx route and the mouth-pharynx route lie in parallel.

Injections of dye into the water close to the nostril of live hagfish indicated a steady inhalation powered by the contractions of the velum chamber and indeed the rhythmic velum contractions could sometimes be seen at the body surface. Dye inhaled through the nostril subsequently exited through the posterior gill slits and the PCD in a pulsatile fashion (Fig. 2.3A). In some cases, rhythmic slow pulsatile contractions of the PCD could be observed visually, whereas movement of the paired gill pouches was never detected visually. However, in instances where the dye inhaled into the nostril induced nostril coughing, it was ejected both through the nostril and then through the PCD opening (Fig. 2.3B). Dye placed in the water close to the mouth or directly injected into the mouth was not inhaled into the pharynx, therefore ejection of this dye never occurred through either the paired gill pouches, PCD opening, or nostril duct during normal ventilation. However, in instances where direct dye injection to the mouth cavity stimulated mouth coughing, the injected dye was immediately ejected to the ambient environment through the mouth (Fig. 2.3C). When the injection did not induce mouth coughing, the dye was forced back up the injection tubing and stayed there more than 24 h (Fig. 2.4), indicating that it was

never inhaled in resting *E. stoutii*. Similarly, dye placed just outside the openings of the paired gill pouches and PCD was never inhaled. In addition, we briefly occluded the nostril in some *E. stoutii* (Fig. 2.3d). These animals immediately showed muscular contraction (possibly by the pharyngeal constrictor muscle) in the ventral area, but this did not cause the injected dye in the pharynx (which had been previously injected *via* the PCD cannula) to exit through the gill pouches or PCD (Fig. 2.3E). Eventually, the fish violently coughed the dye out through the mouth (Fig. 2.3F). After release of the nostril occlusion, the *E. stoutii* immediately initiated unidirectional ventilatory inflow through the nostril so the remaining dye in the pharynx was ejected through the gill pouches and PCD.

Thus, there was no evidence of bi-directional flow in *E. stoutii* gill pouches and the PCD. Using chunks of anchovy, feeding behaviour was also observed in a few animals. The *E. stoutii* first oriented its head towards the prey item (Fig. 2.3G), then exposed and opened its paired dental plates in front of the prey item (Fig. 2.3H) and engulfed the chunk of anchovy immediately (Fig. 2.3I). Overall, this sequence of feeding events was completed within 3 s.

2.4.2 Ventilation of *E. stoutii* under control resting conditions

Key parameters are summarised in Table 2.1. After operation, most hagfish (N = 99) were allowed to recover overnight in flowing seawater and their ventilatory movements were recorded *via* the inserted pressure-measuring tubing, flow probes and impedance wires at the respective sites for 5 min, sometimes longer. These recordings are defined as control resting ventilation in this study. Of the healthy 99 animals in which ventilatory measurements were made under control resting conditions, 35 *E. stoutii* (35.4%) exhibited no detectable breathing during the observation period. As most of our recordings were of short duration, the mean duration of apnea is not known, but some animals did not breathe for several hours. In non-breathing animals, ventilation could usually be initiated by stressors such as pinching or prodding. Some of these *E. stoutii* immediately stopped breathing again while others continued to breathe. These 35 non-breathing animals were not included in the averages of Table 2.1, but this observation indicates that prolonged periods of ventilatory arrest are common in *E. stoutii*.

During simultaneous recordings, the frequencies of the nostril duct (pressure and flow), mouth cavity (pressure), velum region (impedance) and PCD (pressure) showed similar values, reflecting the pulsatile movement of the velum chamber. Therefore, averaged frequencies from the nostril duct, mouth cavity and velum chamber have been reported as velum frequency in Table 2.1, averaging about 22 min⁻¹ (range 4.7 to 77.5 min⁻¹). This rhythmic velum contraction and relaxation resulted in a negative absolute pressure in the nostril of about -0.6 cmH₂O (range = -0.89 to -0.35 cmH₂O) with a pressure pulse amplitude of approximately 0.05 cmH₂O (range = 0.01 to 0.10 cmH₂O). Ventilatory index (*see* below),

the product of pressure pulse amplitude times velar frequency, averaged about $1.3 \text{ cmH}_2\text{O min}^{-1}$ (range = 0.11 to $6.22 \text{ cmH}_2\text{O min}^{-1}$). The frequency of spontaneous coughing events under control resting conditions was about 0.65 min^{-1} (range = 0.48 to 0.82 min^{-1}) and heart rate averaged about 16 min^{-1} (range = 3.2 to 20.7 min^{-1}) and was therefore similar to mean velum frequency in *E. stoutii*. As a result of the continuous but fluctuating negative pressure created in the nostril by the velum chamber contraction cycle, water was inhaled into the nostril cavity at a mean flow rate of about $-125 \text{ ml kg}^{-1} \text{ min}^{-1}$ (range = -267 to $-22 \text{ ml kg}^{-1} \text{ min}^{-1}$) in resting animals (Table 2.1). Water flow was continuous, fluctuating with the velum cycle, but never dropping to zero between velum beats. The mean ventilatory stroke volume for each velum contraction cycle was about 7 ml kg^{-1} (range = 2.35 to 10.96 ml kg^{-1}). In simultaneous recordings, the trough (most negative point) in nostril pressure corresponded to the greatest nostril inflow (Fig. 2.5). Water was exhaled through 12 pairs of branchial pouches and the PCD.

The three *E. stoutii* set up to characterize coughing and spontaneous swimming events were also employed to make detailed pressure measurements in the mouth and PCD (13th gill opening), together with recordings of nostril flow (Table 2.2). The absolute mean pressure (about $+0.005 \text{ cmH}_2\text{O}$, range = $+0.002$ to $+0.008 \text{ cmH}_2\text{O}$) in the PCD was very low and variable but slightly above ambient pressure on average. Two types of frequencies were detected in the PCD, one (fast mode; Fig. 2.6D) which was matched to the velum frequency with a mean pressure amplitude of about $0.008 \text{ cmH}_2\text{O}$ (range = 0.007 to $0.009 \text{ cmH}_2\text{O}$) and the other [slow-mode (SM)]; (Fig. 2.6D) with a frequency of about 4.4 min^{-1} (range = 4.13 to 4.73 min^{-1}) and a mean pressure amplitude of about $0.05 \text{ cmH}_2\text{O}$ (range = 0.045 to $0.055 \text{ cmH}_2\text{O}$) which was probably generated by the contraction–relaxation of the gill pouches. The interpretation of this SM ventilation frequency is explored further in Section 2.4; note that this phenomenon was recorded not only in these three fish, but also in an earlier group ($N = 6$; data not shown) where recordings were made from the PCD catheter only. Note also that contraction of the velum chamber (Fig. 2.6C) also created a pulsatile negative absolute pressure in the mouth cavity (Fig. 2.6B; mean = $-0.44 \text{ cmH}_2\text{O}$, range = -0.10 to $-1.24 \text{ cmH}_2\text{O}$) with a pressure amplitude of about $0.2 \text{ cmH}_2\text{O}$ (range = 0.06 to $0.23 \text{ cmH}_2\text{O}$). The trough in mouth cavity pressure (i.e., least negative mouth pressure value) corresponded to the peak in nostril inflow, exactly opposite the pattern in nostril pressure.

2.4.3 Analysis of ventilatory flow and pressure relationships

Over 3000 data points from 42 animals were available where nostril flow and nostril pressures were recorded simultaneously under a variety of conditions (rest, spontaneous activity, ammonia injections, exposure to high environmental ammonia) in which ventilatory flow varied greatly, from close

to 0 ml kg⁻¹ min⁻¹ to over -400 ml kg⁻¹ min⁻¹ (Fig. 2.7). Clearly, changes in both velum frequency (Fig. 2.7A) and stroke volume (Fig. 2.7B) contributed to changes in flow, with the stroke volume explaining a slightly greater percentage of the variance (34%, based on r^2) than did frequency (26%), though both relationships were highly significant ($P < 0.001$). Flow was strongly related to pressure amplitude ($p < 0.001$) which explained 52% of the variance in flow (Fig. 2.7C). Stroke volume was also significantly related to pressure amplitude ($P < 0.001$), which accounted for about 25% of the variance (Fig. 2.7E). Therefore, pressure amplitude and stroke volume are not independent parameters, explaining why the contributions of frequency (Fig. 2.7A), stroke volume (Fig. 2.7B), and pressure amplitude (Fig. 2.7C) appear to explain more than 100% of the variance in flow. The ventilatory index (product of velum frequency times nostril pressure amplitude; Fig. 2.7D) was strongly correlated ($r = 0.64$, $p < 0.001$) with ventilatory flow, and can be employed as a useful proxy, accounting for 42% of the variance in the latter.

2.4.4 Simultaneous recordings from nostril duct, mouth cavity, velum chamber, and pharyngo-cutaneous duct (PCD)

Ventilatory parameters from different respiratory organs were measured simultaneously in a subset of 3 fish to better understand the relationships between them at rest, as well as during coughing and spontaneous exercise (Figs. 2.8, 2.9, 2.10, 2.11). Nostril coughing is defined as coughing stimulated by inhalation of dye into the nostril, while mouth coughing is defined as coughing initiated by injection of dye into the mouth. Under control resting conditions (Table 2.2), the absolute values were similar to those for the larger group of fish in Table 2.1. The changes seen during nostril coughing, mouth coughing, and spontaneous swimming are summarized in Fig. 2.8. Spontaneous nostril coughing occurred far more often than spontaneous mouth coughing.

During nostril coughing the hagfish showed greatly different patterns of ventilatory parameters compared to control resting conditions. For example, they changed the direction of nostril flow from unidirectional inhalation averaging about -155 ml kg⁻¹ min⁻¹ in these 3 fish to unidirectional exhalation, averaging about +100 ml kg⁻¹ min⁻¹, a highly significant change (Fig. 2.8A). Although nostril pressure was not measured in these three hagfish, based on other fish in which nostril coughing occurred, the absolute pressure (and pressure amplitude) increased greatly to highly positive values in the nostril during the flow reversal. Absolute pressures and pressure amplitudes also increased greatly to highly positive values in both the mouth cavity (Figs. 2.8d, e) and PCD (“fast mode”; Figs. 2.8f, g); all of these changes were significant. The “slow mode” pressure waves could not be diagnosed because of the short duration

of the coughing event. However, the velum frequency (measured by impedance; Fig. 2.8B) and the PCD “fast mode” frequency (Fig. 2.8C) did not change. After dye administration to the nostril (1st dashed line in Fig. 2.9) and prior to the actual nostril cough, the apparent frequency slowed and the pressure became more positive and then more negative in the mouth cavity (* in Fig. 2.9B). Then the actual cough (2nd dashed line in Fig. 2.9) occurred with simultaneous pressure increases in the nostril duct (with flow reversal; Fig. 2.9A), the mouth cavity (Fig. 2.9B), and the PCD (Fig. 2.9D), and an indication of velum chamber contraction in the impedance trace (Fig. 2.9C). Dye was immediately ejected anteriorly through the nostril opening, and then posteriorly mainly through the PCD, and to a lesser extent through the gill pouches (Fig. 2.3A, C).

During mouth coughing, the fish essentially stopped nostril flow (Fig. 2.8A), but there were significantly greater pressure amplitudes in both the mouth cavity (Fig. 2.8D) and PCD (“fast mode”; Fig. 2.8F) as well as significantly greater absolute pressures in both locations (Figs. 2.8E, G). Similar to nostril coughing, velar frequency (Fig. 2.8B) and PCD “fast mode” frequency (Fig. 2.8C) were not altered during mouth coughing. Usually (but not always) the fish showed a large reduction (* in Fig. 2.10D) of the PCD pressure to negative values after dye administration and prior to mouth coughing. Just before the cough, the hagfish exhibited contraction of the nostril (Fig. 2.10A), the velum chamber (Fig. 2.10C), and the PCD (Fig. 2.10D) while the mouth cavity was expanded (more negative pressure; Fig. 2.10B) The dye in the mouth cavity was never excreted *via* the paired gill pouches or PCD but rather was immediately excreted to the environment *via* the mouth opening, with the brief opening of the dental plates at this time. This never occurred during nostril coughing.

During spontaneous swimming, mean nostril flow did not change (Fig. 2.8A) despite significant increases of PCD “fast mode” frequency (Fig. 2.8C). The PCD “fast mode” pressure amplitude (Fig. 2.8F) and absolute pressure (Fig. 2.8G) were significantly elevated; however, mouth cavity pressure amplitude (Fig. 2.8D) and mouth cavity absolute pressure (Fig. 2.8E) were not changed. During the transition period, pressure amplitudes gradually increased. Eventually the overall frequencies from nostril duct, mouth cavity, and PCD (fast mode) were synchronized at about 34 min⁻¹ (range = 32.0 to 35.5 min⁻¹). These values were matched to the frequency of body undulation in swimming performed by the animal (average 34.2 min⁻¹). The impedance trace became noisy during swimming events and could not be reliably interpreted, so it is unclear whether velum frequency also changed or not. Our visual observations confirmed that the dental plates were not exposed and remained closed during spontaneous swimming.

2.5 Discussion

Fig. 2.1B provides a simple model of our understanding of the ventilatory mechanism in *Eptatretus stoutii* based on observations made in the present study.

2.5.1 Anatomical observations

Our anatomical studies indicate both similarities and differences in *Eptatretus stoutii* from previous observations in the Myxinidae. As in the latter, the nostril duct lies dorsal to the mouth cavity and is horizontally separated from it by the oronasohypophyseal septum (ONS), a simple muscular membrane-like structure. The nostril duct leads directly to the anterior velum chamber but in contrast to *Myxine glutinosa* which has a short ONS (Strahan 1958; Johansen and Strahan 1963; Dawson 1963), *Eptatretus stoutii* has a relatively longer ONS, so the mouth cavity is connected not to the velum chamber but to the anterior pharynx by a bucco-pharyngeal aperture that lies posterior to the velum (Fig. 2.1B); this was confirmed by the silicone injection experiment of Fig. 2.2. Simultaneous recordings of pressure in the mouth cavity, and pressure and/or flow in the nostril revealed reciprocal patterns of fluctuations at the frequency of velum contraction (dotted line in Fig. 2.6A and 2.6B), presumably due to passive distension and relaxation of the ONS by the action of the velum pump. Due to the ONS barrier and the post-velum connection point of the bucco-pharyngeal aperture, water exchange between the velum chamber and mouth cavity probably does not normally occur (Fig. 2.1B). Furthermore, the mouth cavity is normally completely sealed (Fig. 2.1B; Fig. 2.4) by the paired dental plates, and probably also by contraction of the bucco-pharyngeal aperture when the animal is not feeding. If the “short” ONS model of *Myxine glutinosa* were present, with the anterior connection of the velum chamber to both the nostril duct and mouth chamber, then the rhythmic movement of the velum would generate qualitatively similar pressure patterns in the two chambers, in contrast to the reciprocal patterns seen in the present study.

2.5.2 Patterns of ventilation

In accord with many previous studies on Myxinidae (*see* Introduction), and two on Eptatretidae (Perry et al. 2009b; Cox and Davison 2011), our observations indicate that ventilation in the Pacific hagfish is primarily driven by the rhythmic contraction of the velum apparatus which creates a fluctuating but continuous negative pressure in the nostril (Fig. 2.1B). The resulting inflow through the nostril is pulsatile but continuous, never dropping to zero between velum contractions, in agreement with Steffensen et al. (1984) and Perry et al. (2009b), so water flow through the gills is also probably

continuous. The pressure pulses in the nostril caused by the velum contraction cycle could also be detected in the PCD and in the mouth cavity, where the frequencies (fast mode frequency only for PCD) were the same as those of the impedance recordings from the velum.

Indeed, two types of ventilatory movements were detected in the PCD under resting conditions: a slow mode (SM) frequency of 4 ~ 5 positive pressure fluctuations per min onto which was superimposed very small amplitude pressure fluctuations representing the fast mode (FM) frequency of velum contractions (Fig. 2.6D, Table 2.2). Anatomically, the velum chamber is connected to the paired gill pouches and the PCD *via* the long pharynx (Fig. 2.1B), so the pressure wave from the rhythmic movement of the velum chamber could be transmitted to the measurement site at the PCD. The larger SM pressure pulses were interpreted as evidence of active contraction of the gill pouches and/or PCD and their associated ducts, which thereby help power exhalation (Fig. 2.1B). While this possibility was initially denied in *Myxine glutinosa* (Strahan 1958), it was later proven to occur in this species (Johansen and Hol 1960; Johansen and Strahan 1963). These authors described a “peristaltic wave from the proximal end of the afferent (gill) duct to the proximal end of the efferent duct” which is probably the same as our SM contractions. However, it is not clear from these studies on Myxinidae whether the gill pouch contractions occur at a lower rate than the velum chamber contractions. *Eptatretus stoutii* appears to operate a two-phase ventilatory system with a faster suction pump for inhalation, and a much slower force pump for exhalation (Fig. 2.1B). Water inhalation through the gill pouches or PCD was not observed.

Under control conditions, the Pacific hagfish showed an “all or nothing” pattern of breathing, either ventilating rhythmically or not at all; 35% of the animals examined exhibited no spontaneous ventilation. Regular rhythmic ventilation seemed to be more common after sunset, perhaps reflecting the nocturnal nature of these animals. During periods of apnea, mild stressors such as pinching and/or gently touching the skin would usually cause ventilation to start up, though in some animals it would soon stop again. These periods of ventilatory arrest are in accord with the ability of this species to tolerate anoxia and to suppress metabolic rate for long periods (Cox et al. 2011). As heart rate was not recorded in the same animals, there was no observation whether the heart slowed and kept beating regularly with increased cardiac stroke volume as it does during experimental anoxia (Cox et al. 2010); this is an important topic for future investigation.

When breathing rhythmically, Pacific hagfish exhibited ventilatory flow rates of -125 to -155 ml kg⁻¹ min⁻¹ at rest (Tables 2.1, 2.2). These values are midway between the -45 ml kg⁻¹ min⁻¹ reported for *Myxine glutinosa* by Steffensen et al. (1984) and the -235 ml kg⁻¹ min⁻¹ reported by Perry et al. (2009b)

for *Epratrretus stoutii*, the latter through a method almost identical to that of the current study. However, Perry et al. (2009b) did not report episodes of apnea or coughing, so it is possible that their animals were less settled than those of the present study. Regardless, these resting ventilatory flow rates are very comparable to those of teleost fish (e.g. Wood et al. 1979; Perry et al. 2009a), which is surprising considering that resting $\dot{M}O_2$ is exceptionally low in Pacific hagfish (Munz and Morris 1965; Perry et al. 2009b; Cox et al. 2011; Giacomini et al. 2019b), only about one third of typical rates in comparably sized teleost (e.g. Clarke and Johnston 1999). This anomaly was previously noted by Perry et al. (2009b) and suggests that O_2 extraction efficiency at the gills is very low, which is surprising as it is generally believed that a countercurrent exchange system operates in the gills of hagfish. However, the fact that the resting Pacific hagfish spends substantial periods in apnea suggests that it may hold previously inhaled water in the gill pouches during this time to extract the maximum possible amount of O_2 from that water. Possibly, time-averaged O_2 extraction efficiency could be much higher than during the periods of active ventilation alone. A study of O_2 extraction dynamics at the gills relative to the breathing pattern is required to clarify the situation (now addressed in Chapter 4).

Pacific hagfish were able to increase their ventilatory flow rate to at least $-400 \text{ ml kg}^{-1}\text{min}^{-1}$ during experimental disturbances in the present study (Fig. 2.7), comparable to the elevations reported by Perry et al. (2009b) in response to hypoxia or hypercapnia. Our data clearly show that the hagfish are capable of large variations of ventilatory flow by changing not only velum frequency (Fig. 2.7A) but also stroke volume (Fig. 2.7B) which differs from the conclusion of Perry et al. (2009b) that only changes in frequency occur. Furthermore, increases in stroke volume were correlated with increases in nostril pressure amplitude (Fig. 2.7E), indicating that the velum chamber contraction can become more powerful. Interestingly, most hagfish in this study showed increasing frequency or increasing stroke volume separately, apparently dependent on the nature of the treatment or types of stressors. For example, hagfish mostly increased velum frequency in response to tactile disturbance, similar to the responses reported by Perry et al. (2009b) during hypoxia and hypercapnia, but mostly increased stroke volume first and then velum frequency later under circumstances of high environmental ammonia (HEA) treatment or ammonium salt injection. The ventilatory index (the product of pressure amplitude x frequency) proved useful in capturing this variability and was strongly correlated ($r = 0.64$, $p < 0.001$) with ventilatory flow rate, providing a useful proxy for the latter (Fig. 2.7D). In this regard, the Pacific hagfish, despite its very different breathing mechanism, is similar to many teleost fish, where the ventilatory index is also a useful proxy for ventilatory flow (e.g. Perry et al. 2009a).

2.5.3 Coughing

In the present study, two types of ventilatory flow reversals were seen, termed “nostril coughing” and “mouth coughing” in this manuscript. These were often induced by the presence of dye in the respective cavities. Nostril coughing occurred spontaneously far more often than mouth coughing, and in a related study spontaneous coughing frequency was found to be temperature-dependent (Giacomin et al. 2019b), suggesting that coughing is a normal part of ventilation. Obviously coughing events will serve to clear irritant particles and noxious dissolved substances, but in future studies, it will be of interest to investigate whether they play any direct role in respiratory gas exchange. Hagfish are known to have not only an olfactory-like chemosensory nasal epithelium in the nostril duct but also Schreiner organs scattered on the body surface. These are thought to be sensory cells due to numerous sensory buds composed of microvilli on the apical cell surface (von Doring and Andres 1998). Therefore, dye in the nostril was probably sensed by the nasal epithelium and/or Schreiner organs while dye in the mouth was probably sensed by the Schreiner organs. Interestingly, the two previous investigations on ventilation in the Eptatretidae made no mention of flow reversals (Perry et al. 2009b; Coxon and Davison 2011). However, as discussed below, if only velum frequency is monitored, as in the study of Coxon and Davison (2011), coughing events could well be missed.

Nostril coughing appears to be the same phenomenon as “sneezing” described previously in the Myxinidae (Strahan 1958; Johansen and Hol 1960; Johansen and Strahan 1963; Steffensen et al. 1984). Strahan (1958) hypothesized that this was largely due to contraction of the pharyngeal constrictor muscle which encircled the posterior part of the velum chamber, and this was confirmed by Johansen and Hol (1960) by X-ray cinematography of radio-opaque contrast medium. Their study also implicated contraction of the velum chamber itself.

In *Eptatretus stoutii*, after dye administration to the nostril and prior to the actual nostril cough, pressure recordings in the mouth cavity indicated that the apparent velum frequency in the mouth cavity slowed (even though the true velum frequency did not change) and the mouth pressure first increased then decreased greatly. During the cough itself which ensued within 5 seconds, the fish increased absolute pressures and pressure amplitudes in the nostril duct, mouth cavity, and PCD simultaneously, reversal of flow in the nostril occurred to outflow values comparable to normal inflow values, and the impedance trace suggested contraction of the velum chamber itself (Figs. 2.8, 2.9). This resulted in ejection of the dye first through the nostril duct, then *via* the PCD (major route) and/or paired gill pouches (minor route), after which the fish immediately recovered the unidirectional ventilation. The slowed frequency and the biphasic pressure cycle in the mouth cavity (asterisk in Fig. 2.9B) appeared to

be a key event, and may have reflected tight closure of the bucco-pharyngeal aperture, so that noxious material did not enter the mouth during the nostril cough. The contractile force for the overall event probably originated from contraction of the pharyngeal constrictor muscle and the posterior part of the velum chamber, as deduced by Strahan (1958) and Johansen and Hol (1960).

In mouth coughing, dye was ejected only through the mouth. Johansen and Hol (1960) described an event in *Myxine glutinosa* that may have been the same, where contrast media was ejected through the mouth from the gill area, powered by contraction of the gill pouches and associated ducts, as well as the musculature of the pharynx and body wall. In *Eptatretus stoutii*, the hagfish often (but not always) exhibited a large relaxation of the PCD producing very negative pressures (asterisk in Fig. 2.10D) before the surge of positive pressure in all compartments (Fig. 2.8D, E, F, G) that ejected dye anteriorly through the mouth. None exited posteriorly through the gill pouches, PCD, or nostril. The negative gill pressure perhaps served to drain water from the pharynx into the gill pouches, preparatory to generating back pressure and flow to eject the dye out through the mouth. The bilaterally paired dental plates were opened during ejection, probably by protractor muscles and retractor muscles located ventral to the mouth cavity. The velum chamber must have been shut off from the pharynx at this time, perhaps by the pharyngeal constrictor muscle that encircles the posterior margin of the velum chamber (Strahan 1958; Johansen and Hol 1960). This would explain why there was no ejection through the nostril, and why nostril flow dropped to zero (Fig. 2.8A) while velum frequency continued unchanged (Fig. 2.8B). As the mouth is not used in normal breathing, it may be that mouth coughing is mainly used to clear irritant particles ingested during feeding.

2.5.4 Ventilation during swimming

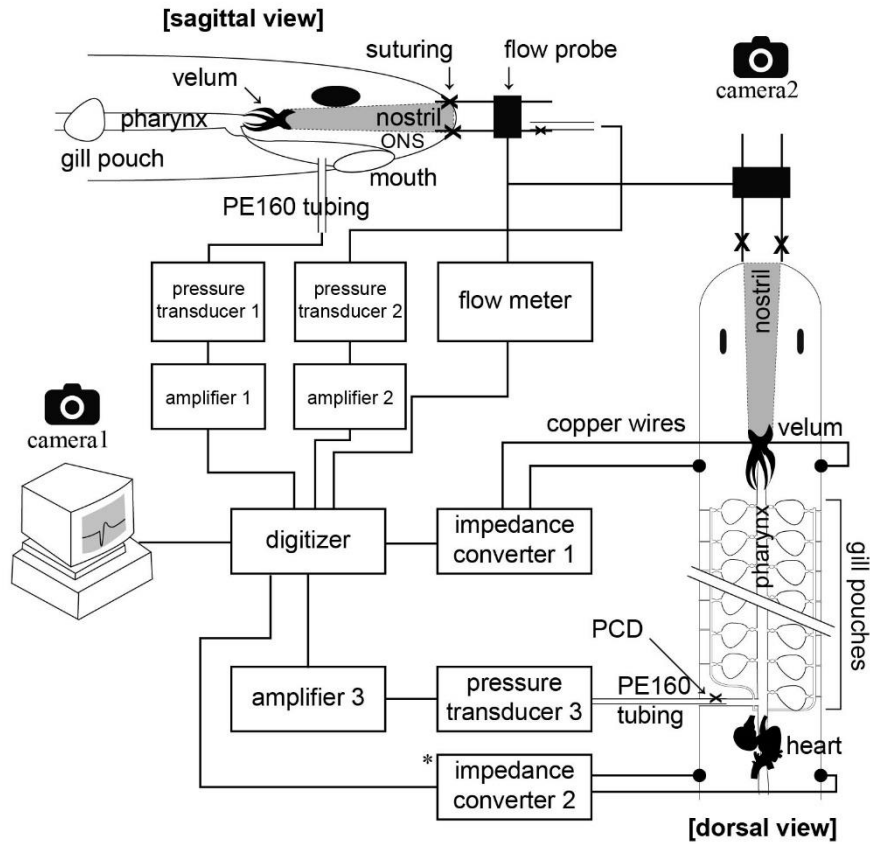
The current observations are the first data on hagfish ventilation during swimming. Hagfish are known as anguilliform locomotors, eel-like swimmers that use lateral oscillations of the posterior 2/3 of the body while the head remains oriented in a straight and forward direction (Long et al. 2002). In our study, the relatively heavy flow-probe attached to the silicone tubing in the nostril duct restricted movement of the fish's head. During spontaneous swimming, frequencies of nostril duct and mouth cavity were synchronized with the frequency of the body undulations. The absolute pressure and pressure amplitude increased in the PCD, and the SM frequency could no longer be seen; only the FM frequency could be detected at this site (Fig. 2.11D), while there were no changes in mouth pressures (Fig. 2.11B). The velar impedance trace usually became noisy and undecipherable during swimming (e.g. Fig. 2.11C), so it is unclear whether velar frequency increased or not (Fig. 2.8B). It seems likely that the increased FM

frequency was generated by body undulation not by velum movement during spontaneous swimming performance, as mean ventilatory flow did not change (Fig. 2.8A and 2.11A). Overall, these observations suggest that the Pacific hagfish may transfer some of the work of breathing to the swimming muscles by using ram ventilation, as first suggested in the Atlantic mackerel by Roberts (1975). This would occur only *via* the nostril as the dental plates remained closed. Otherwise, the ventilatory mechanism appeared to be basically the same as at rest (Fig. 2.1B). However, in future, measurements in truly free-swimming hagfish will be required to confirm these ideas.

2.5.5 Concluding remarks

Overall, our observations indicate that the Pacific hagfish has a complex, unique ventilatory system (Fig. 2.1B) similar but not identical to that of the Myxinidae. Key features include a two-phase unidirectional pumping system with a fast suction pump (the velum) which inhales water through the nostril and a much slower force pump (the gill pouches, PCD, and associated structures) for exhalation. Water flow is continuous. Two types of coughing (flow reversals) occur: nostril coughing (“sneezing”) where water and irritant materials are expelled forcefully through both the nostril and gill pouches, and mouth coughing, where they are expelled only through the mouth. The mouth, which joins the pharynx posterior to the velum chamber, plays no role in ventilation of resting, swimming, and nostril-coughing hagfish as the dental plates remain closed, but is probably an important route for inhalant water and food particles in feeding hagfish. Increases in ventilatory flow can be achieved by both increases in velum frequency and increases in stroke volume, the latter reflected in increases in nostril pressure amplitude. Ventilatory index, the product of velum frequency and nostril pressure amplitude, is strongly correlated with ventilatory flow, and therefore provides a useful index for the latter. When the fish is actively breathing, ventilatory flow rates are relatively high, in the range of those of teleost fish, despite very low O₂ consumption rates, but long periods of spontaneous apnea are common. Ram ventilation powered by the swimming muscles may occur during anguilliform swimming, but this observation remains to be confirmed. In future, it will be of great interest to understand how this complex system is controlled and co-ordinated at a central (CNS) and peripheral level (chemoreceptors), and to study what happens to breathing during feeding, when the hagfish opens its mouth and engulfs or immerses its head its prey.

(A) Experimental set up



(B) Ventilation in resting or swimming hagfish

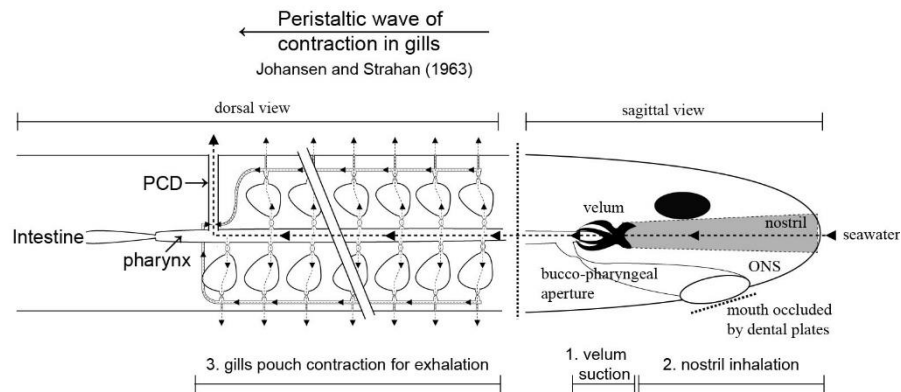


Figure 2.1 Schematic diagram of (A) recording attachments to nostril, mouth cavity, velum chamber, and pharyngo-cutaneous duct (PCD), and heart and (B) a simple model summarizing our current understanding of the unidirectional ventilatory water flow mechanism in the Pacific hagfish at rest and during swimming.

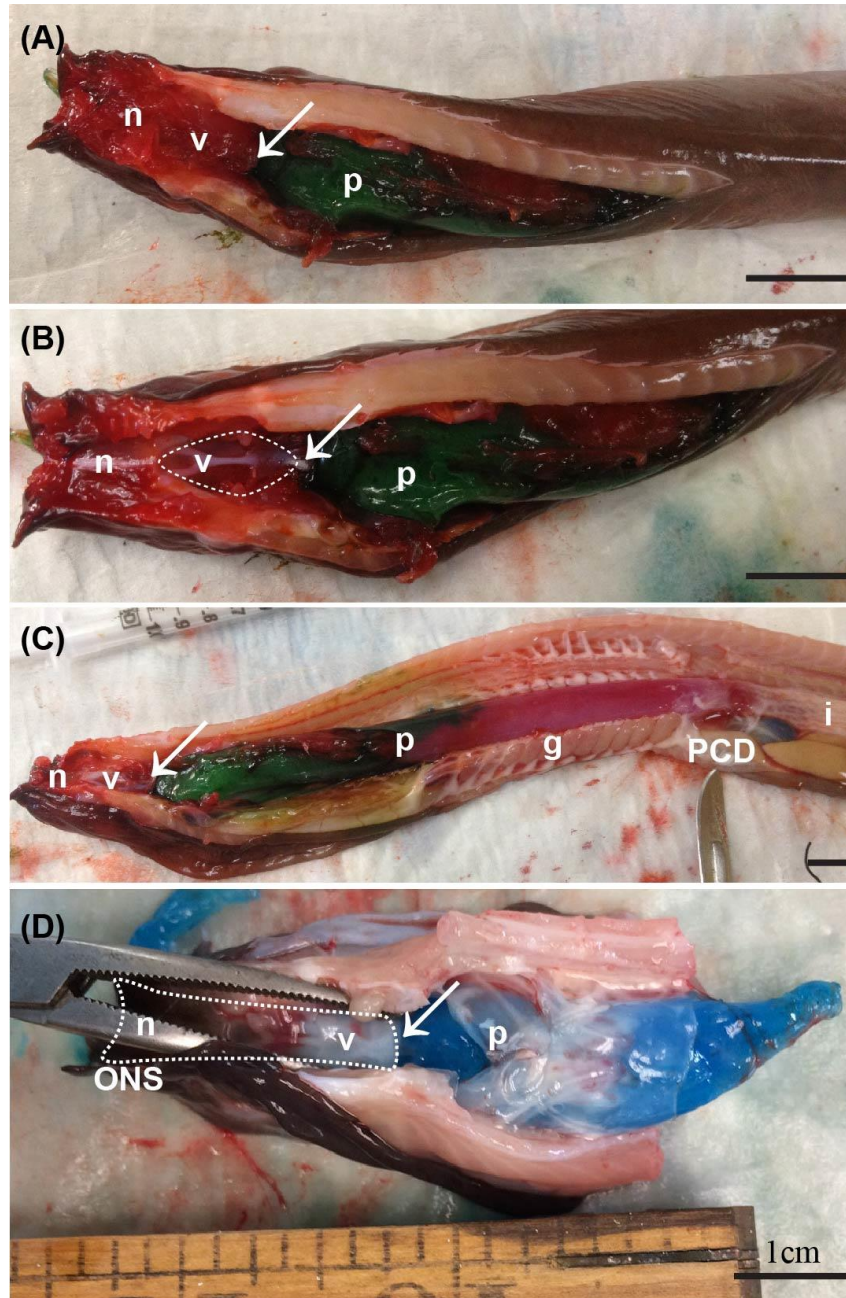


Figure 2.2 Dissection of a freshly euthanized Pacific hagfish injected with dyed silicone. (A, C). Red silicone injected into the nostril was subsequently found between the nostril (n) and velum chamber (v), as well as in the pharynx (p), part of the gill pouches (g), and the pharyngo-cutaneous duct (PCD). Green silicone in (C) or blue silicone in (D) injected into the mouth cavity was subsequently found in the anterior part of pharynx (white arrows) but did not move forward to the velum chamber or nostril. The oronasohypophyseal septum (ONS) is depicted in the white dotted area. After removal of part of the red silicone (B), the nostril cavity and velum chamber were clearly visualized. Scale is 1 cm.

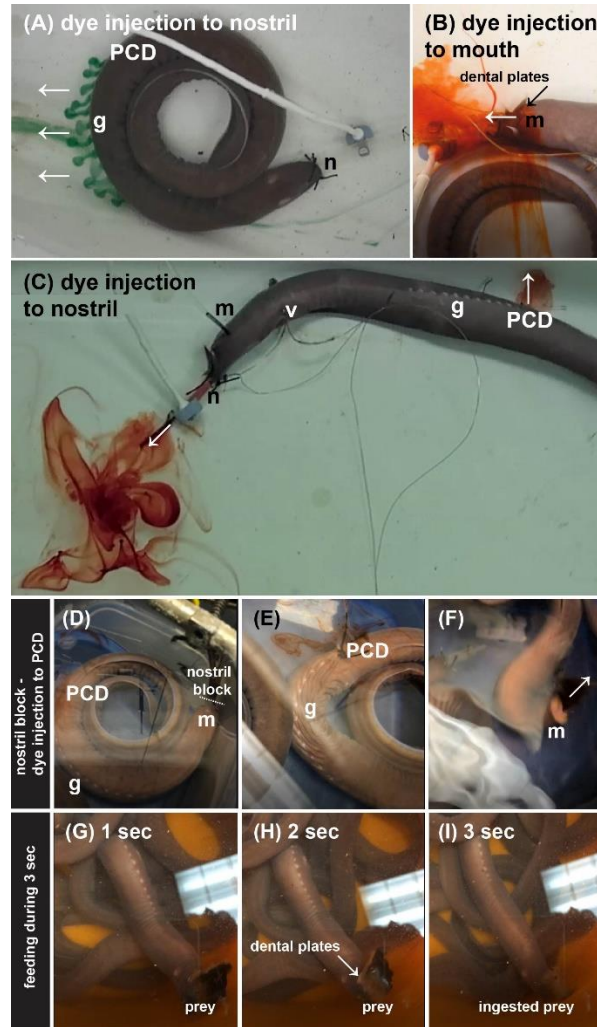
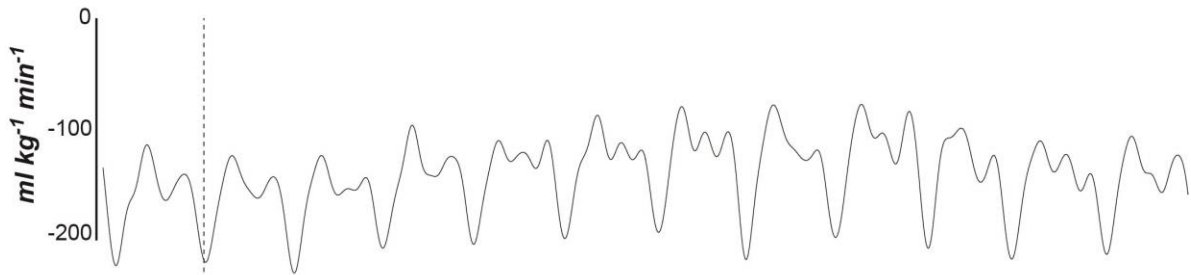


Figure 2.3 Observational experiments in live Pacific hagfish. (A) After dye injection to the nostril (n), the fish excreted dye through 12 pairs of gill pouches (g) or (c) through the pharyngo-cutaneous duct (PCD) in an example where dye injection to the nostril induced nostril coughing, with serial dye ejection from the nostril (n) and then the pharyngo-cutaneous duct (PCD). (B) In contrast, in an example where dye injection into the mouth cavity induced mouth coughing, the dye was ejected only back out through the mouth. In (C), the ventilation measurement sensors can be seen, attached to the nostril (n, flow meter), mouth cavity (m, pressure measuring catheter) and pharyngo-cutaneous duct (PCD, pressure measuring catheter), and skin around the velum chamber (v, wires for impedance measurement). (D) After occluding the nostril, (E) the animals immediately showed muscular contraction in the ventral area but this did not cause the injected dye in the pharynx to exit through the gill pouches or PCD, (F) eventually the fish violently coughed the dye out through the mouth. Panels (G), (H), and (I) depict the time course of feeding by engulfment.



Figure 2.4 Dye injection to the mouth cavity of a live Pacific hagfish. The location of the injected dye was monitored at 0 h (A), 2 h (B), and 24 h (C). In this example, the hagfish immediately flushed the dye back up the tubing (red arrows) and it remained stored in the tubing over 24-h. There was no evidence that it was ever inhaled.

(A) nostril flow recording



(B) nostril pressure recording

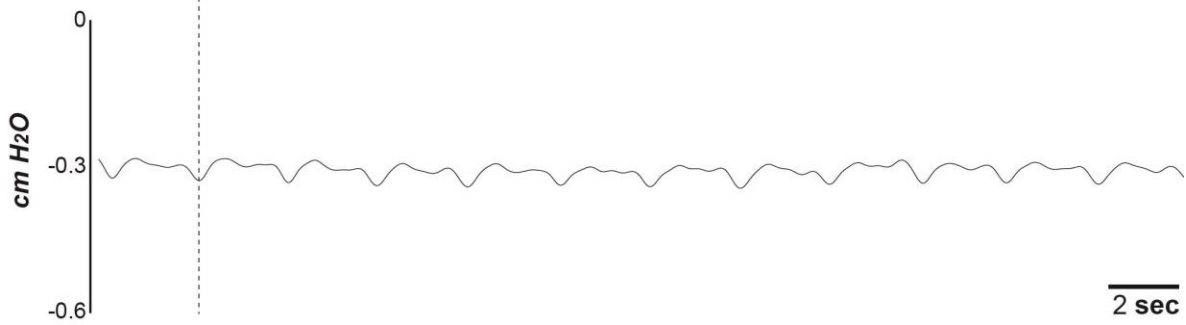


Figure 2.5 Simultaneous recording of (A) flow and (B) pressure in the nostril duct of Pacific hagfish. Note that patterns of greatest flow (most negative value) and lowest pressure (most negative value) were well matched in the nostril duct, as indicated by the dotted vertical line.

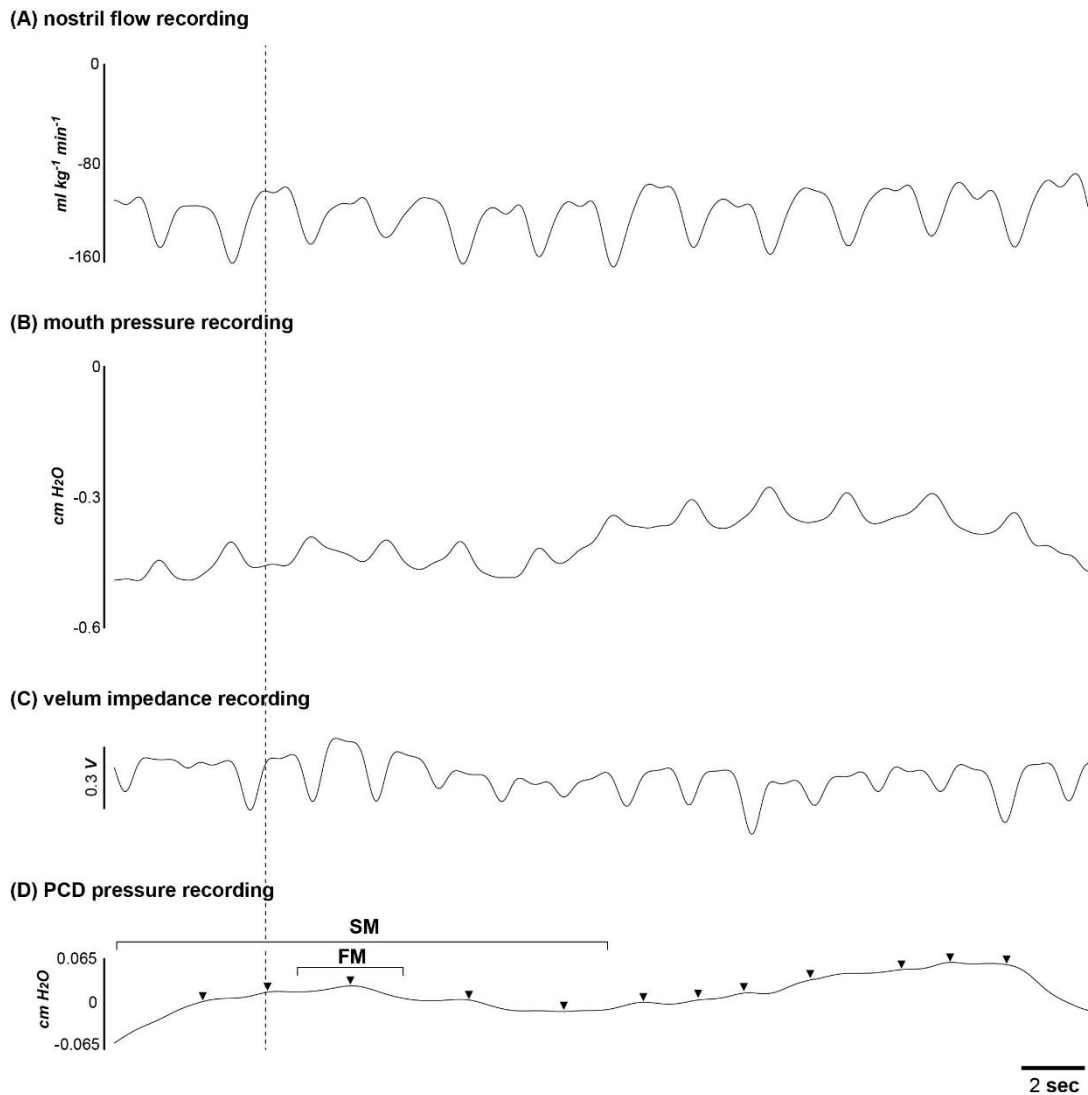


Figure 2.6 Simultaneous ventilation recordings of (A) nostril flow (B) mouth cavity pressure, (C) velum chamber impedance, and (D) pharyngo-cutaneous duct (PCD) pressure in a resting Pacific hagfish under control conditions. In (D) the PCD, two types of ventilatory pressure cycles were detected, “slow mode” (SM) which appeared to be generated by the gill pouches and “fast mode” (FM) which correlated with the velum movement. Note that patterns of lowest nostril flow (least negative value) and lowest mouth pressure (most negative value) were well matched, exactly opposite the pattern with nostril pressure seen in Fig. 2.5 in nostril duct (dotted line). Vertical dotted line indicates simultaneous ventilatory movements – lowest nostril flow, lowest mouth pressure, velum chamber movement, and highest PCD pressure. Arrowheads on the PCD pressure recording (panel d) indicate ventilatory rhythms in fast mode (FM), while the larger brackets indicate the slow pressure wave of slow mode (SM).

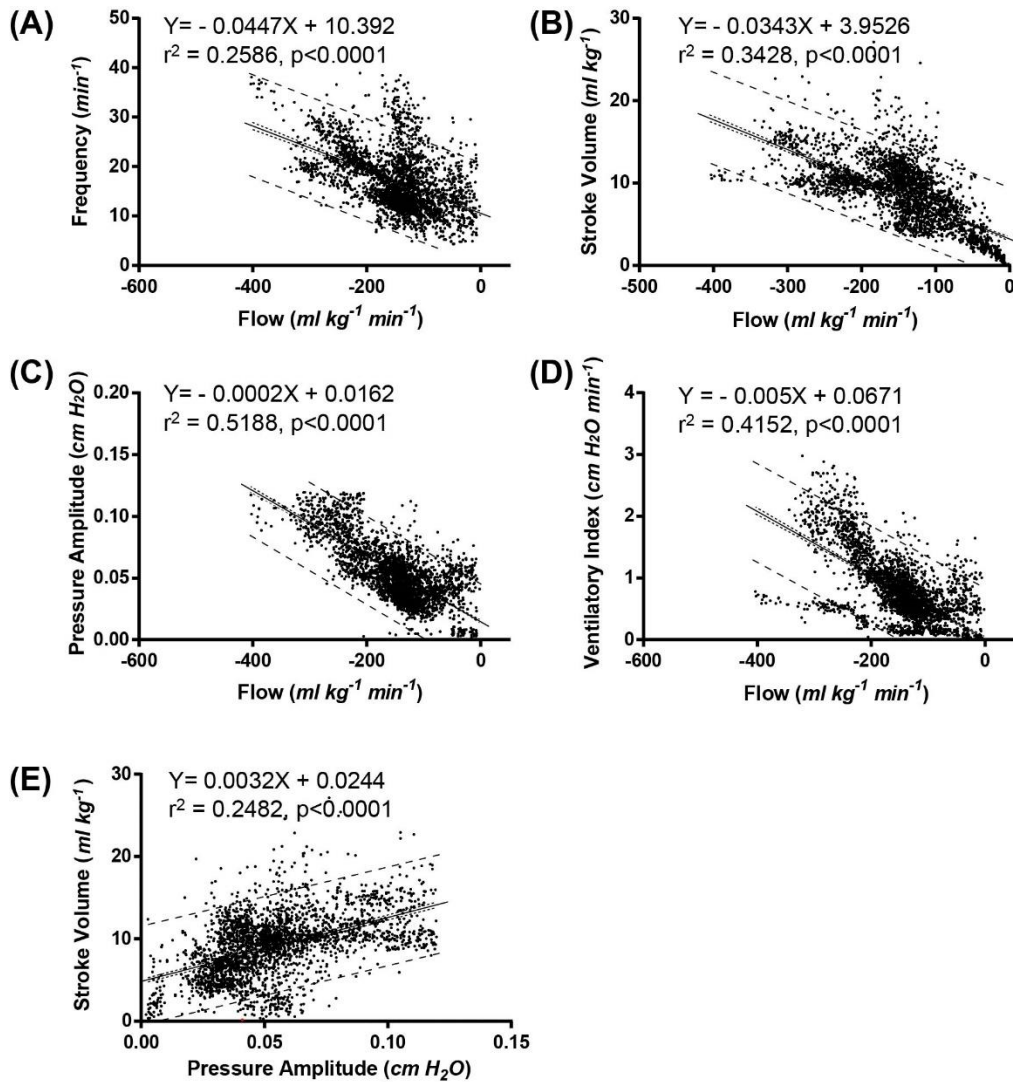


Figure 2.7 Using 3134 data points from $N = 42$ hagfish, nostril flow was plotted against (A) frequency, (B) stroke volume, (C) pressure amplitude, and (D) ventilatory index. (E) Pressure amplitude was also plotted against stroke volume. The equations of the linear regression relationships are given. The 95% confidence intervals are shown as the inner dotted lines, also called the confidence interval for the regression, which describe the range where the regression line values will fall 95% of the time for repeated measurements. The larger outer dashed lines are the 95% prediction intervals, also called the confidence interval for the population, which describe the range where the data values will fall 95% of the time for repeated measurements. The r^2 values are also shown. In all cases, the relationships were highly significant ($p < 0.001$).

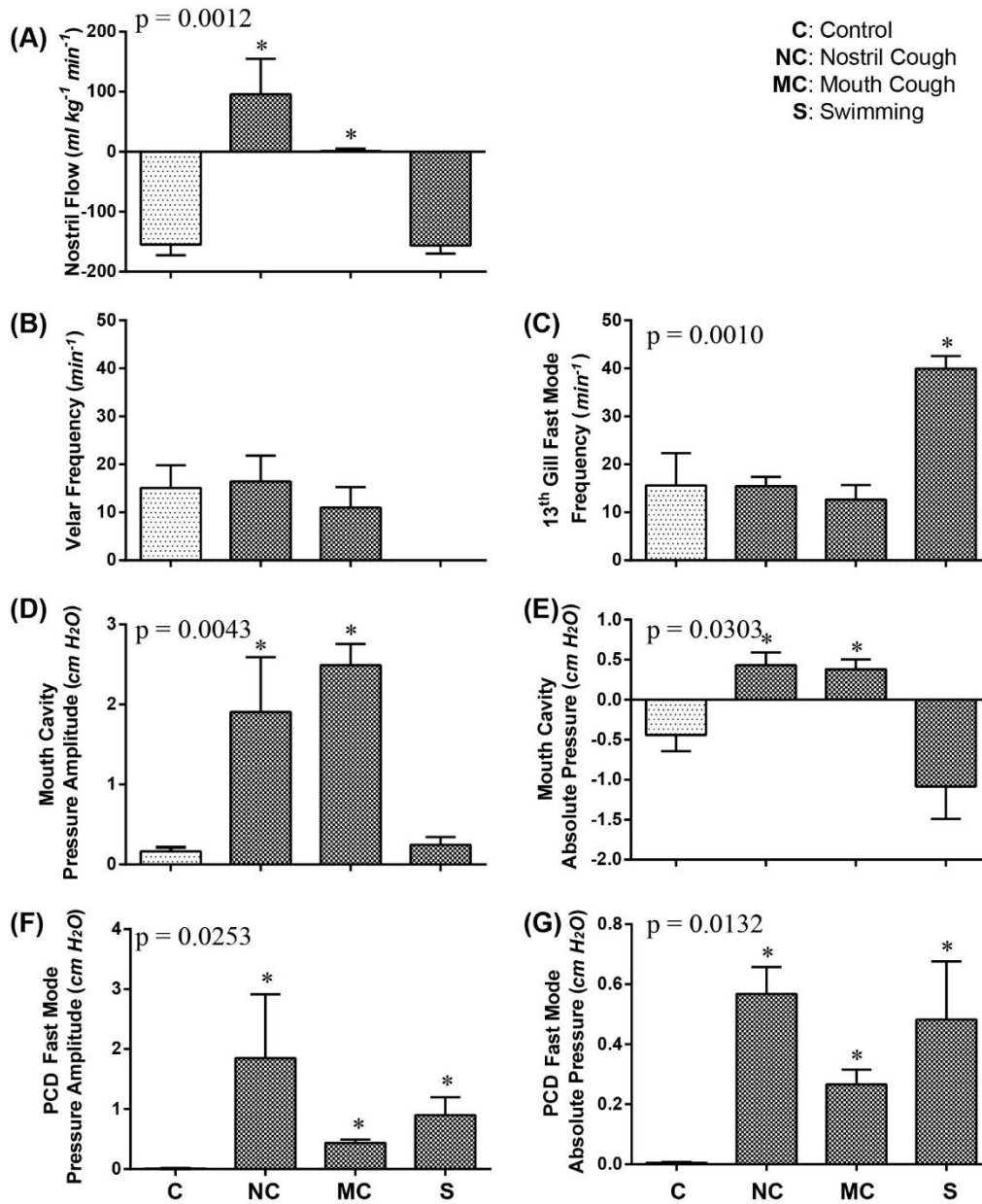
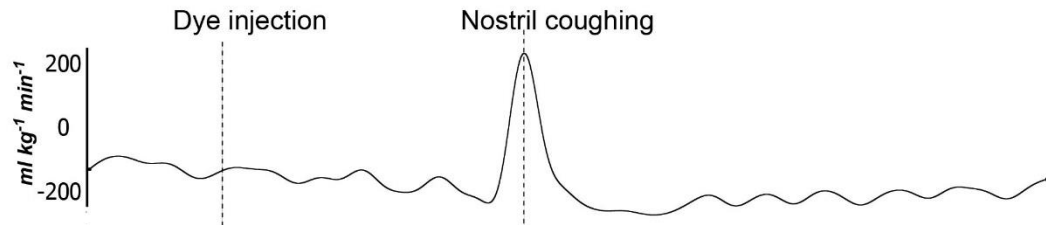


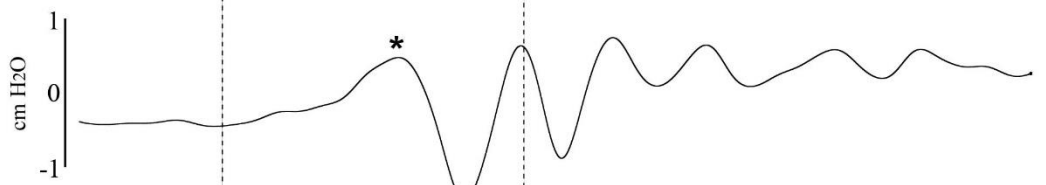
Figure 2.8 Ventilatory parameters recorded simultaneously under control conditions (C), during nostril coughing (NC), during mouth coughing (MC), and during spontaneous swimming (S) in the same three hagfish. (A) Nostril flow rate; (B) velum frequency; (C) pharyngo-cutaneous duct (PCD) fast mode (FM) frequency; (D) mouth cavity pressure amplitude; (E) mouth cavity absolute pressure; (F) PCD FM pressure amplitude; (G) PCD FM absolute pressure. There is no velar frequency for spontaneous swimming in panel (B) as the velum impedance recording became noisy, and the pulsatility of flow and pressure (e.g. fast mode frequency in panel C) became equal to that of body undulations.

[nostril coughing]

(A) nostril flow recording



(B) mouth pressure recording



(C) velum impedance recording



(D) PCD pressure recording

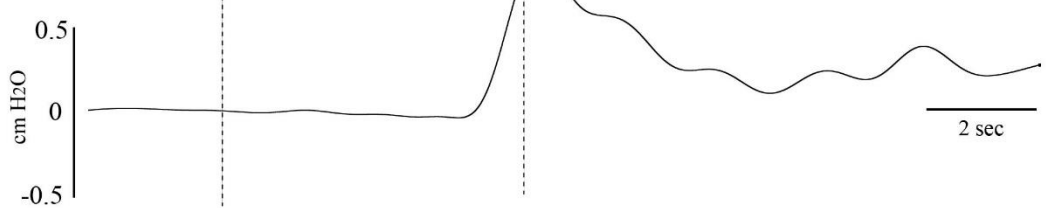
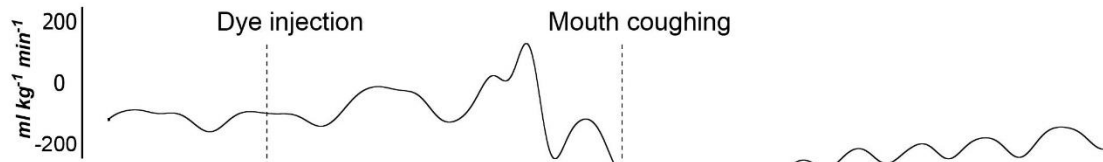


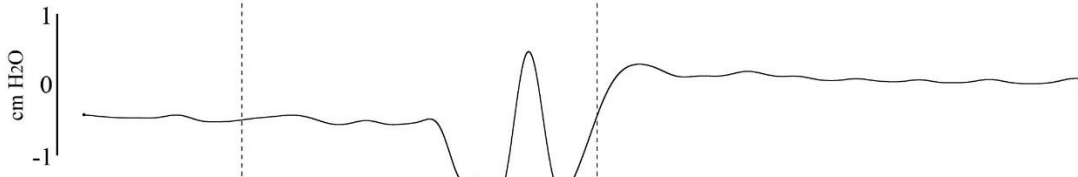
Figure 2.9 Simultaneous recordings of (A) nostril flow (B) mouth cavity pressure, (C) velum chamber impedance, and (D) PCD pressure in a Pacific hagfish where nostril coughing was induced by dye inhalation into the nostril (1st dashed line). Following dye administration and prior to the actual nostril cough, the apparent frequency slowed and the pressure became more positive and then more negative in the mouth cavity (* in panel B). Then the actual cough occurred (2nd dashed line) with simultaneous pressure pulses in the nostril duct (with flow reversal; panel A), the mouth cavity (panel B), and the PCD (panel D), and a rise in the impedance trace from the velar chamber (panel C).

[mouth coughing]

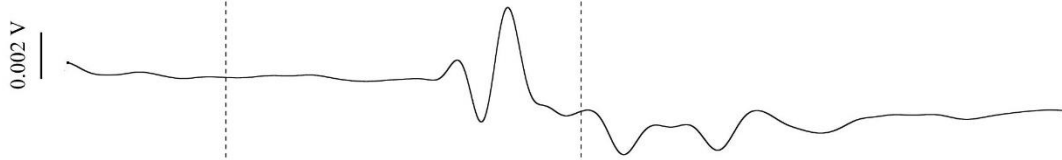
(A) nostril flow recording



(B) mouth pressure recording



(C) velum impedance recording



(D) PCD pressure recording

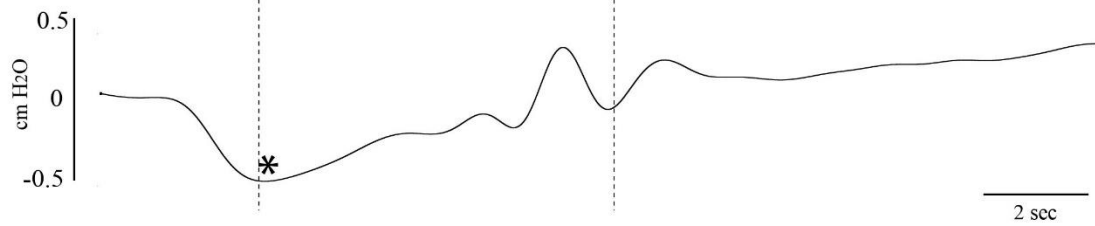
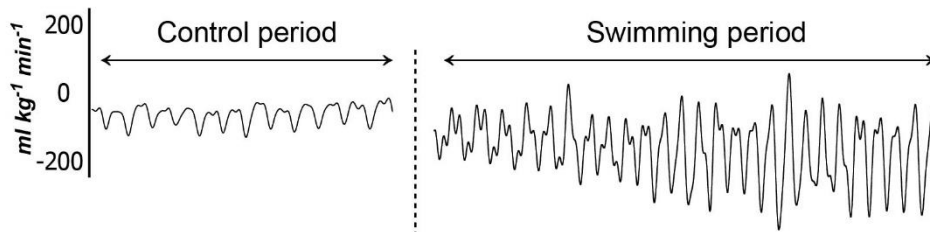


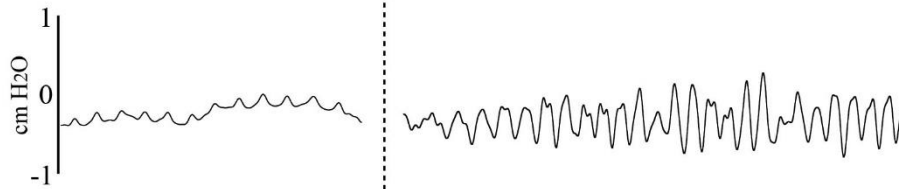
Figure 2.10 Simultaneous recordings of (A) nostril flow (B) mouth cavity pressure, (C) velum chamber impedance, and (D) PCD pressure in a Pacific hagfish where mouth coughing was induced by dye injection into the mouth cavity. Usually (but not always) hagfish showed a large reduction (* in panel D) of the PCD pressure to negative values before mouth coughing.

[swimming performance]

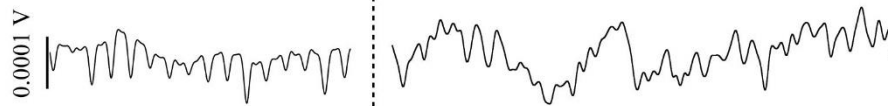
(A) nostril flow recording



(B) mouth pressure recording



(C) velum impedance recording



(D) PCD pressure recording

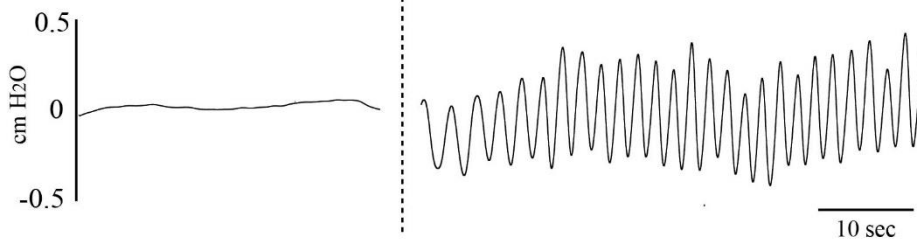


Figure 2.11 Simultaneous recordings of (A) nostril flow, (B) mouth cavity pressure, (C) velum chamber impedance, and (D) PCD pressure prior to and during a period of spontaneous swimming in a Pacific hagfish.

Table 2.1 Ventilatory parameters collected under resting control conditions from 64 Pacific hagfish. During control conditions, 35.4% hagfish (35 out of 99 hagfish) did not breathe spontaneously and are not included here. Heart rates were recorded from an additional 23 hagfish. Data represent means \pm S.E.M. (N).

Nostril Flow (ml kg ⁻¹ min ⁻¹)	-124.6 \pm 25.81 (16)
Stroke Volume (ml kg ⁻¹)	7.11 \pm 1.15 (16)
Velar Frequency (min ⁻¹)	21.84 \pm 1.86 (64)
Nostril Absolute Pressure (cm H ₂ O)	-0.62 \pm 0.27 (11)
Nostril Pressure Amplitude (cm H ₂ O)	0.05 \pm 0.01 (64)
Ventilatory Index (cm H ₂ O min ⁻¹)	1.27 \pm 0.28 (64)
Coughing Frequency (min ⁻¹)	0.65 \pm 0.17 (30)
Heart Rate (min ⁻¹)	16.40 \pm 0.49 (23)

Table 2.2 Simultaneous recordings of ventilatory parameters from the nostril duct, velum chamber, mouth cavity, and 13th gill pouch of three Pacific hagfish under control resting conditions. Velum frequency represents averaged frequency among nostril duct, mouth cavity, velum chamber, and 13th gill fast mode. Data represent means \pm S.E.M. (N = 3).

Velum Frequency (min ⁻¹)	15.07 \pm 1.58
Nostril Flow (ml kg ⁻¹ min ⁻¹)	-154.70 \pm 17.83
Mouth Cavity Absolute Pressure (cm H ₂ O)	-0.44 \pm 0.20
Mouth Cavity Pressure Amplitude (cm H ₂ O)	0.16 \pm 0.05
13 th Gill Absolute Pressure (cm H ₂ O)	0.005 \pm 0.003
13 th Gill Fast Mode Pressure Amplitude (cm H ₂ O)	0.008 \pm 0.001
13 th Gill Slow Mode Pressure Amplitude (cm H ₂ O)	0.050 \pm 0.005
13 th Gill Slow Mode Frequency (min ⁻¹)	4.43 \pm 0.30

Chapter 3: Ventilatory sensitivity to ammonia in the Pacific hagfish (*Eptatretus stoutii*), a representative of the oldest extant connection to the ancestral vertebrates

3.1 Summary

Ventilatory sensitivity to ammonia occurs in teleost, elasmobranchs, and mammals. Here, ventilatory responses to ammonia were investigated in hagfish. Ventilatory parameters (nostril flow, pressure amplitude, velar frequency, and ventilatory index, the latter representing the product of pressure amplitude times frequency), together with blood and water chemistry, were measured in hagfish exposed to either high environmental ammonia (HEA) in the external sea water or internal ammonia loading by intra-vascular injection. HEA exposure (10 mM NH_4HCO_3 or 10 mM NH_4Cl) caused a persistent hyperventilation by 3 h, but further detailed analysis of the NH_4HCO_3 response showed that initially (within 5 min) there was a marked decrease in ventilation (80% reduction in ventilatory index and nostril flow), followed by a later 3-fold increase, by which time plasma total ammonia concentration had increased 11-fold. Thus, hyperventilation in HEA appeared to be an indirect response to internal ammonia elevation, rather than a direct response to external ammonia. HEA-mediated increases in oxygen consumption also occurred. Responses to NH_4HCO_3 were greater than those to NH_4Cl , reflecting greater increases over time in water pH and PNH_3 in the former. Hagfish also exhibited hyperventilation in response to direct injections of isotonic NH_4HCO_3 or NH_4Cl solutions into the caudal sinus. In all cases where hyperventilation occurred, plasma total ammonia and PNH_3 levels increased significantly, while blood acid-base status remained unchanged, indicating specific responses to internal ammonia elevations. The sensitivity of breathing to ammonia arose very early in vertebrate evolution.

3.2 Introduction

Ammonia, the major nitrogenous waste in ammoniotelic fish, can exist in solution as both the dissolved gas (NH_3) and the dissociated ion (NH_4^+), analogous to CO_2 and HCO_3^- , and it can act like a third respiratory gas (Randall and Ip 2006). Here, the term of ammonia refers to the total of these two forms. Ammonia is produced and excreted at a rate of about 10 to 20% of carbon dioxide excretion (MCO_2) in ammoniotelic teleost fish (Wood 2001). Building on pioneering studies by Hillaby and Randall (1979) and McKenzie et al. (1993), Zhang and co-workers have shown that ammonia plays an important role in stimulating ventilation in the freshwater rainbow trout (*Oncorhynchus mykiss*; Zhang and Wood 2009; Zhang et al. 2015), and the same appears to be true in the zebrafish (*Danio rerio*; Perry and Tzaneva 2016). Somewhat surprisingly, breathing is also stimulated by ammonia in a ureotelic

elasmobranch, the Pacific spiny dogfish (*Squalus acanthias suckleyi*; De Boeck and Wood 2015). These studies demonstrated that the hyperventilatory response is specific to elevations in blood ammonia, and not confounded by changes in blood acid-base status that often accompany experimental treatments with ammonia in fish. Hyperventilation occurs in response to both high external ammonia in the environment (HEA) and internal elevation of blood ammonia, but the bulk of the evidence indicates that the latter is major proximate cause – i.e. HEA acts by causing ammonia to diffuse across the body surface, predominantly the gills, into the bloodstream where it acts on internal receptors. At least in part, these internal ammonia receptors are the neuroepithelial cells (NECs) in the gills (Zhang et al. 2011), which are now believed to be trimodal oxygen, carbon dioxide, and ammonia sensors for respiratory sensing (Zhang et al. 2015; Perry and Tzaneva 2016) though there is also some evidence that ammonia may also act centrally on the brain (Wilkie et al. 2011; Zhang et al. 2013; Lissner et al. 2017). Ammonia can also act as a ventilatory stimulant in mammals, which are ureotelic like elasmobranchs, and this stimulation is thought to be important in exercise-induced hyperventilation (Mutch and Bannister 1983), as well as in supporting breathing during severe respiratory acidosis and hepatic coma (Roberts et al. 1956; Warren 1958; Felipo and Butterworth 2002). The detection mechanism is unclear, but the best correlation appears to be with ammonia concentrations in the brain, suggesting a central site of chemo-detection (Wichser and Kazemi 1974).

These findings in groups as diverse as teleosts, elasmobranchs, and mammals, with very different strategies for handling nitrogenous wastes, raise the prospect that ventilatory sensitivity to ammonia arose very early in vertebrate evolution. To evaluate this hypothesis, we examined whether breathing was sensitive to ammonia in the Pacific hagfish, *Eptatretus stoutii*. The exact phylogenetic position of the hagfishes (Class Myxini) is controversial, but there is general agreement that present day hagfishes represent the oldest extant connection to the ancestral vertebrates (e.g. Bardack 1998; Rasmussen et al. 1998; Heimberg et al. 2010; Oisi et al. 2013), though they may be highly derived, evolving on a separate trajectory from jawed vertebrates (Miyashita et al. 2019). Nevertheless, they are important for understanding the evolutionary origin of vertebrate traits. Hagfishes are marine jawless fish possessing a notochord but lacking a proper vertebral column and have a very different breathing mechanism than other fishes, inhaling water through a single nostril by a velar pump, and exhaling it through 18 to 24 separate gill pouches (Kardong 2012). Hagfish are ammoniotelic (Walsh et al. 2001; Giacomini et al. 2019a, b), and feed by burrowing into dead and dying animals (Martini 1998), so are likely exposed periodically to very high levels of environmental ammonia (i.e. HEA) in nature. They are extremely tolerant of HEA in the laboratory (Clifford et al. 2015; Clifford et al. 2017). Their behaviour of writhing and coiling, and releasing vast amounts of slime when disturbed, makes them difficult to work with, but

recently we have developed methods for measuring ventilation in the Pacific hagfish (Eom and Wood 2019; now Chapter 2). In the present study, we applied these methods, together with measurements of blood ammonia levels and acid-base chemistry, to examine whether breathing is sensitive to internal and/or external elevations in ammonia, and whether the response is specific to ammonia.

3.3 Materials and Methods

3.3.1 Experimental animal and chemicals

Pacific hagfish (*Eptatretus stoutii*, 80.9 ± 4.1 g, N = 129) were captured under permits (XR 202 2016 and XR 194 2017) from the Department of Fisheries and Oceans Canada in July ~ September of 2016 and 2017. Bottom-dwelling traps baited with strips of Pacific hake (*Merluccius productus*) were set in Trevor channel (48 50.844 N, 125 08.321 W, depth 100 m). The captured fish were transferred to Bamfield Marine Sciences Centre (BMSC) located on the southwest coast of Vancouver Island, BC, Canada. Hagfish were housed together in fiberglass tanks (20 m³), furnished with PVC pipes for shelter, and served with flowing sea water (temperature 11 to 13°C, salinity 30 to 31 ppt). While hake strips were offered as food, the animals generally did not eat during the holding period which was up to two months. The animal utilization protocols (AUP) for experiments were approved by the University of British Columbia (A14-0251) and Bamfield Marine Sciences Centre (BMSC) Animal Care Committees (AUP RS-17-20) and followed guidelines of the Canadian Council of Animal Care. After experiments, the fish were euthanized by an overdose of tricaine methanesulfonate (MS-222, 5 g L⁻¹ neutralized to pH 7.8 with 5 M NaOH; Syndel laboratories, Parksville, Canada) followed by evisceration to ensure death. All other chemicals were obtained from Sigma-Aldrich, (St. Louis, MO, USA).

3.3.2 Physiological recording from the nostril duct in the respiratory system

Generally, the surgical operations were performed in late afternoon and experiments were carried out mostly during the nighttime, as hagfish are nocturnally active. Procedures were similar to those described by Eom and Wood (2019; Chapter 2). In preparation for ventilatory pressure or ventilatory flow measurements, hagfish were anesthetized in MS-222 (0.6 g L⁻¹, neutralized with NaOH) and placed on an operating table. Gill irrigation was not necessary because the hagfish are hypoxia-tolerant (Sidell et al. 1984; Forster et al. 1992; Perry et al. 2009b), but the fish body was kept moist with wet tissue paper during air exposure. A 3-cm length of transparent silicone tube (6.35 mm O.D. and 4.32 mm I.D.) was snugly fitted into the single nostril duct in the anterior midline and secured by two stitches (26 mm 1/2C

taper; Perma-Hand Silk, Ethicon, Somerville, NJ, USA) which were made laterally to the skin around the nostril entrance. Hagfish were allowed to recover in flowing sea water for several hours before experiments started.

Two different physiological recording methods were applied to the hagfish nostril to measure their ventilatory parameters. In most of the studies, a pressure transducer was used to record the fluctuations in pressure created by velar pumping, in a tube connected to the nostril. In some of the studies (those shown in Figs. 3.3 and 3.7), a blood flow meter was attached to the tube to measure total ventilatory flow. In both methods, analogue ventilatory parameters were amplified (LCA-RTC, Transducer Techniques, Temecula, CA, USA), converted to digital signals in a PowerLab data integrity system (ADInstruments, Colorado Springs, CO, USA), and then visualized and analyzed in LabChart software version 7.0 (ADInstruments). In order to remove non-specific noise, a low-pass type filter was incorporated in the LabChart software while the ventilatory parameters were recorded.

For the ventilatory pressure measurements, a 3-cm non-flared length of polyethylene tubing (PE 160, 1.57 mm O.D and 1.14 mm, I.D., Clay-Adams, Sparks, MD, USA) was inserted 1-cm deep into the transparent silicone tube and secured by two stitches to the silicone tubing. This secured PE160 tubing could then be periodically connected *via* a #18-gauge needle shaft to another ~30-cm water-filled PE 160 tubing which was attached to a medical pressure transducer (DPT-100, Utah Medical Products, Midvale, UT, USA). The pressure transducer was zeroed to the water surface, calibrated with a column of water in the range of 0 to 4 cm, and used for monitoring ventilatory pressure amplitude (cmH₂O) and frequency (min⁻¹) in the nostril. The product of pressure amplitude (cmH₂O) and frequency (min⁻¹) yielded the ventilatory index (cmH₂O min⁻¹). Eom and Wood (2019; Chapter 2) demonstrated that there was a strong correlation between the ventilatory index recorded in this manner and the total ventilatory flow measured directly with a flowmeter.

For the direct measurements of total ventilatory flow, an ultrasonic microcirculation blood flow probe (V-series, Transonic Systems Inc., Ithaca, NY, USA) connected to a dual-channel small animal blood flowmeter (T106 series, Transonic Systems Inc.) was fitted onto the transparent silicone tubing. The pulsatile signal allowed the measurement of velar frequency (min⁻¹) and total water flow rate (ml min⁻¹), from which ventilatory stroke volume (ml stroke⁻¹) could be calculated. Correct orientation of the flow probe was essential; the probe detects both the magnitude and direction of flow, so in our recordings, negative values (i.e. below zero flow) represent inhalation through the nostril, and positive values represent exhalation, as for example, occurs during coughing. Intrinsic calibration and zero of the system were checked by flowing sea water (12°C, 30 to 31 ppt) through the probe at known rates using

an aqua lifter vacuum pump (Cheng Gao Plastic and Hardware Electricity, Dongguan, Guangdong, China). Flow was determined gravimetrically. As noted by Perry et al. (2009b), the intrinsic calibration overestimated true sea water flow. Therefore, voltage outputs were converted into corrected flow units (ml min^{-1}) by the LabChart software.

3.3.3 Blood sampling

It is not possible to reliably sample blood by catheterization in hagfish, so blood samples ($\sim 300 \mu\text{l}$) were taken as described by Clifford et al. (2017) by rapidly anesthetizing the fish in MS-222 (0.6 g L^{-1} , neutralized with NaOH), holding it vertically, and puncturing the caudal blood pool in the subcutaneous venous sinus using a #23-gauge needle attached to a 1-ml gas-tight syringe (Hamilton, Reno, NV, USA). The whole procedure took about 1 ~ 2 min including anesthesia and the fish was air-exposed for < 0.5 min. Upon return to anaesthetic-free sea water, the hagfish resumed its normal coiled behavior within 5 min. The whole blood samples were immediately used for measurement of pH and then centrifuged ($5,000 \text{ g} \times 1 \text{ min}$) for collection of plasma. The plasma was decanted and flash-frozen in liquid N_2 , then stored at -80°C until analysis for total ammonia (T_{Amm}) and total CO_2 (T_{CO_2}).

3.3.4 Series I – Ventilation changes in hagfish loaded externally with ammonia - high environmental ammonia (HEA)

Prior to recording nostril ventilation, the hagfish were anesthetized in neutralized MS-222 (0.6 g L^{-1}) for cannulation of the nostril duct. After recovery from anesthesia, the hagfish were isolated in individual tanks of aerated sea water at 12°C and their nostril ventilation was measured (internal control treatment), then the fish were exposed to 5, 10, or 20 mM ammonium bicarbonate (NH_4HCO_3 , $N = 6$ per treatment) or 10 mM ammonium chloride (NH_4Cl , $N = 6$) over 15 h. Nostril ventilatory parameters (frequency, pressure amplitude, and ventilatory index) were measured immediately after the start of exposure (0 h) and every 3 h thereafter up to 15 h. For controls, a series with no addition ($N = 6$), and one with the addition of 10 mM sodium bicarbonate (NaHCO_3 , $N = 6$) were also performed. The standard protocol was to set the volume of the animal's chamber to 980 ml of aerated sea water for the control measurements, and then add 20 ml of the appropriate salt stock (made in sea water) for the experimental measurements. We previously reported that Pacific hagfish commonly exhibit long periods of spontaneous apnea (Eom and Wood 2019; Chapter 2), so exposures were only performed on animals that

were breathing during the pre-treatment control period. The effects of the addition of the various salts on water pH were also measured (N = 6).

3.3.5 Series II – The effect of HEA on oxygen consumption rate

Hagfish routine oxygen consumption rate ($\dot{M}O_2$) was measured over 15 h in 3-h intervals in HEA environments created with 10 mM NH_4HCO_3 (N = 6), 10 mM NH_4Cl (N = 6) or 10 mM $NaHCO_3$ (control, N = 4). Briefly, each hagfish was placed individually in an air-tight plastic container filled with 1 L of normoxic sea water and containing a magnetic spin-bar to allow for appropriate mixing. Oxygen tension (Torr) was measured intermittently using fiber optic oxygen sensors connected to a WITROX 4 oxygen meter (Loligo, Viborg, Denmark). At the conclusion of each flux period, the chambers were unsealed, refreshed with air-saturated treatment water of the appropriate composition, then resealed to begin the next flux period. At the conclusion of the 15-h experiment, hagfish were anaesthetized, and weighed. Oxygen tensions in Torr were converted to $\mu\text{mol L}^{-1}$ using the oxygen solubility constants described in Boutilier et al. (1984), and $\dot{M}O_2$ was calculated as previously described (Clifford et al. 2016).

3.3.6 Series III – Relationship between ventilation and altered blood chemistry in hagfish loaded externally with ammonia

This series examined ventilation and blood chemistry before and during exposure to high environmental ammonia (HEA) in the external water for 3 h. Based on the results of the previous series, an external concentration of 10 mM NH_4HCO_3 was chosen. Two groups of hagfish were used, one (N = 6) for measurements of total ventilatory flow and the other (N = 6) for blood collection prior to and during exposure to 10 mM HEA. The first group of hagfish had been fitted with nostril tubing for recording of total ventilatory flow and pressure amplitude and were placed in 980 ml of aerated sea water in a plastic chamber. After control records were taken in the absence of added ammonia, the animals were acutely exposed to 10 mM HEA (by the addition of 20 ml of 500 mM reagent grade NH_4HCO_3), and the nostril ventilatory parameters were continuously measured up to 180 min.

The second group of hagfish were used only for collecting blood for analysis of pH, and plasma T_{CO_2} and T_{Amm} . A blood sample was taken under control conditions initially, and then after recovery, the hagfish was exposed to 10 mM HEA prepared with NH_4HCO_3 in the same manner as the first group.

Another blood sample was taken at 5 min of HEA exposure, and a final terminal sample at 180 min of HEA exposure.

3.3.7 Series IV – Relationship between ventilation and altered blood chemistry in hagfish loaded internally with ammonia

This series examined ventilation and blood chemistry before (0 h) and after (0.5 h and 1 h) injection of the following ammonium salts at a dose of either 70 $\mu\text{mol kg}^{-1}$ (low dose) or a 1000 $\mu\text{mol kg}^{-1}$ (high dose). These doses were achieved by preparing ammonium salts as solutions of 35 mM NH_4HCO_3 (N = 6), 500 mM NH_4HCO_3 (N = 18), 35 mM NH_4Cl (N = 6), and 500 mM NH_4Cl (N = 6), and were injected into the subcutaneous venous sinus in the tail at a volume load of 2 $\mu\text{l g}^{-1}$. Additionally, high doses (1,000 $\mu\text{mol kg}^{-1}$) of 500 mM NaCl (N = 6, as a chloride control) and 500 mM NaHCO_3 (N = 11, as a bicarbonate control) were also injected. The low doses using 35 mM ammonium salts were made up in a background concentration of 500 mM NaCl to minimize osmotic disturbance. The predicted initial concentrations (T_{Amm}) in hagfish plasma (14% of body weight) or extracellular fluid (ECF, 30% of body weight; Forster et al. 2001) would range between 500 $\mu\text{mol L}^{-1}$ (low dose) and 7,142 $\mu\text{mol L}^{-1}$ (high dose) in plasma, or 233 $\mu\text{mol L}^{-1}$ (low dose) and 3,330 $\mu\text{mol L}^{-1}$ (high dose) in ECF respectively; these predicted concentrations cover the T_{Amm} range reported in plasma of Pacific hagfish after natural feeding (Wilkie et al. 2017) for the low dose and after exposure to 20 mM HEA for the high dose (Clifford et al. 2015).

The fish were fitted with nostril tubing for recording of ventilatory pressures and flows, allowed to recover, then placed in a plastic chamber containing 1 L of aerated sea water. After recording of control ventilatory parameters, an initial blood sample was taken (0 h) and then 2 $\mu\text{l g}^{-1}$ of the respective salt solution was injected into the venous sinus. The fish was then returned to the 1 L of sea water. Additional ventilation measurements, followed immediately by blood collection, were taken at 0.5 h and 1 h. In the high dose NH_4HCO_3 and 500 mM NaHCO_3 injection experiments, 5-ml water samples were also taken at 0 h, 0.5 h, and 1 h for measurement of ammonia and urea-N excretion rates. The collected water samples were stored in plastic bottles at -20°C until later analysis.

3.3.8 Blood and water chemistry analyses

Freshly collected blood (in the gas-tight Hamilton syringe) and water were transferred to 0.5-mL micro-centrifuge tubes and placed into a 12°C water bath, and pH was immediately (~2 min) measured using a thermo-jacketed Orion ROSS micro pH electrode (Fisher Scientific, Ottawa, ON, Canada), taking care to insert the pH probe to the bottom of the sample so as to minimize any impact of air exposure at the surface on the sample. The blood sample was then centrifuged (2 min at 12,000 x g; Eppendorf, Model 5140C, Hamburg, Germany) and the plasma drawn off and transferred to a second 0.5-mL micro-centrifuge tube and flash-frozen in liquid N₂. The entire blood processing was completed in ~5 minutes. Deep-frozen plasma was later thawed on ice for measurement of plasma total CO₂ (T_{CO2}) and total ammonia (T_{Amm}) concentrations. A Corning 965 CO₂ analyzer (Ciba Corning Diagnostic, Halstead, Essex, UK) was used for T_{CO2}, and an enzymatic reagent kit based on the glutamate dehydrogenase / NAD method (Raichem™ R85446, Cliniqua, San Marcos, CA, USA) for T_{Amm}. In our experience, these procedures yield values identical to those on freshly collected samples, and our measured control plasma ammonia and acid-base data were very close to those reported in previous studies on the same species (Clifford et al. 2015; Clifford et al. 2017; Giacomini et al. 2019a, b). Due to background interference by hagfish plasma in the T_{Amm} measurement, a standard curve was created using the plasma as a matrix spiked with increasing concentrations of NH₄Cl, in order to compensate for the matrix effect. The concentration of T_{Amm} in the plasma was calculated by the standard addition method. The *Henderson-Hasselbalch* equation was applied to T_{CO2} and pH values to calculate hagfish plasma CO₂ tension (PCO₂) and bicarbonate concentration ([HCO₃⁻]), using plasma pK' values and CO₂ solubility coefficients from Boutilier et al. (1984). Plasma ammonia tension (PNH₃) and ionic ammonium concentration ([NH₄⁺]) were similarly calculated from T_{Amm} and pH values by the *Henderson-Hasselbalch* equation using plasma pK' values and NH₃ solubility coefficients from Cameron and Heisler (1983). Full equations and the assumptions made for adjusting the CO₂ and ammonia constants for the ionic strength of hagfish plasma have been given by Giacomini et al. (2019b).

Freshly thawed water samples were employed for measurements of ammonia concentrations by the colorimetric assay of Verdouw et al. (1977) and urea-N concentrations by the colorimetric assay of Rahmatullah and Boyde (1980). Flux rates (μmol-N kg⁻¹ h⁻¹) were calculated by factoring changes in concentration (μmol-N L⁻¹) by water volume (L), body mass (kg) and time (h).

3.3.9 Statistical analyses

Data have been reported as means \pm standard error of the mean (S.E.M.) (N) where N represents the number of fish used in each respective experiment. One-way repeated-measures ANOVA followed by Dunnett's test was used in Series I, III, and IV, and two-way ANOVA followed by Tukey's multiple comparisons test in Series II. Where necessary, data were log-transformed in order to pass normalization and homogeneity of variance tests. The statistical analyses were performed in GraphPad Prism software ver. 6.0 (La Jolla, CA, USA) and in the R project for statistical computing program. The threshold for statistical significance was $p < 0.05$.

3.4 Results

3.4.1 Series I – Ventilation changes in hagfish loaded externally with ammonia – high environmental ammonia (HEA)

In this series, ventilation was measured from the nostril by pressure transducer. There was some variation in the control ventilatory parameters amongst the various treatment groups (Fig. 3.1), reflecting the high variability of hagfish breathing patterns, so the responses in each treatment have been compared against the respective pre-treatment controls in the individual animals.

For simplicity, responses to only three of the experimental treatments are shown in Fig. 3.1, up to 6 h of exposure - 10 mM NaHCO_3 (bicarbonate control), 10 mM NH_4HCO_3 , and 10 mM NH_4Cl . By 3h of exposure, both 10 mM NH_4HCO_3 and 10 mM NH_4Cl caused significant increases in ventilatory index, which persisted at 6 h in the latter (Fig. 3.1C). These were due to significant increases in pressure amplitudes for both salts (Fig. 3.1B), and frequency for NH_4Cl only (Fig. 3.1A). Over the same time frame, there were no changes in ventilation in response to 10 mM NaHCO_3 (Fig. 3.1).

The full data set of all six treatments up to 15 h of exposure, including 0 mM NH_4HCO_3 as a “no addition” control and 5 mM NH_4HCO_3 (both of which had no effects) and 20 mM NH_4HCO_3 (which significantly stimulated both pressure amplitude and frequency), have been included in Fig. 3.8. Notably, the 10 mM NH_4HCO_3 treatments and 20 mM NH_4HCO_3 treatments proved to be toxic, resulting in mortality which started by 9 h of exposure in the 10 mM NH_4HCO_3 group (50% mortality), and by 6 h of exposure in the 20 mM NH_4HCO_3 group (100% mortality). Prior to these times, the fish appeared to be healthy and were not moribund, suggesting that a time-dependent toxic threshold was surpassed, as explained below. There were no mortalities in the other treatments.

The control pH in 30 ppt aerated sea water at 12°C was 8.31 ± 0.02 ($N = 6$). Addition of the various salts lowered the pH - 5 mM NH_4HCO_3 (7.95 ± 0.01), 10 mM NH_4HCO_3 (7.86 ± 0.01), 20 mM NH_4HCO_3 (7.78 ± 0.01), 10 mM NH_4Cl (7.98 ± 0.01), and 10 mM NaHCO_3 (7.97 ± 0.01) ($N = 6$). In view of the mortalities seen in the 10 mM NH_4HCO_3 treatments but not in the 10 mM NH_4Cl treatment, an additional experiment was performed to assess the possible impact of aeration on seawater pH over time (Fig. 3.9A). This experiment demonstrated that seawater pH gradually rose with time in both treatments, as well as in the 10 mM NaHCO_3 control. However, while pH in both the 10 mM NH_4Cl and 10 mM NaHCO_3 treatments stabilized at about 8.2 (i.e. slightly below the pH of control sea water) after 5 h of aeration, pH plateaued at about 8.6 over the same time frame in the 10 mM NH_4HCO_3 treatment. As a result, by the time mortalities started to occur in the 10 mM NH_4HCO_3 treatment of Series I, environmental PNH_3 levels (Fig. 3.9B) would have been approximately 3-fold higher than in the NH_4Cl treatment.

3.4.2 Series II – The effect of HEA on oxygen consumption rate

There were no mortalities in these treatments, and the animals remained healthy throughout the 15-h experiment. Notably, in this series, the water was partially replaced at 3-h intervals, and aeration was not continuous, so increases in water pH and more importantly in PNH_3 in the NH_4HCO_3 exposure would have been attenuated. $\dot{\text{M}}\text{O}_2$ tended to increase with exposure to HEA in the forms of both 10 mM NH_4Cl (doubling from 6-9 h onwards) and 10 mM NH_4HCO_3 (doubling by 0-3 h, and reaching a 4-fold stimulation by 3-6 h onwards). Only the response to 10 mM NH_4HCO_3 was significant. In the 10 mM NaHCO_3 control treatment, the fish did not significantly change their $\dot{\text{M}}\text{O}_2$ (Fig. 3.2).

3.4.3 Series III – Relationship between ventilation and changes in blood chemistry in hagfish loaded externally with ammonia

In this series, which was designed to investigate the early response of ventilation and blood chemistry to external HEA in the form of 10 mM NH_4HCO_3 , breathing was recorded simultaneously from the nostril by both flowmeter and pressure transducer. For simplicity, only the flowmeter results are shown (Fig. 3.3). The typical response was a rapid (i.e. within 5 min) decrease in ventilatory flow to close to zero (e.g. Fig. 3.3A), an effect which was sustained from 5.2 min (minimum) to 94.2 min (maximum), with a mean period of decreased flow of 38.7 ± 17.2 min ($N = 6$). Thereafter, flow would increase greatly

above the pre-treatment control levels (Fig. 3.3A). Two other examples are shown in Fig. 3.10. Overall, these changes in total ventilatory flow were significant, with the mean decrease in flow rate being about 80%, and the subsequent mean increase in flow rate being about 3-fold relative to the original pre-treatment control values (Fig 3.3B). Interestingly these changes were achieved entirely by changes in ventilatory stroke volume (Fig. 3.3D). Although breathing became very shallow, velar frequency was not reduced (Fig. 3.3C), and this was confirmed by the pressure transducer recording, which showed unchanged frequency, but marked reductions in ventilatory pressure amplitude and ventilatory index which were similar to those in stroke volume and total nostril flow respectively. Note that the initial response of greatly decreased ventilation would not have been seen in Series II where the first measurements were taken only after 3 h.

In the parallel blood sampling experiment, the control plasma ammonia concentration (T_{Amm}) of approximately $150 \mu\text{mol L}^{-1}$ had increased by about 2.3-fold by 5 min of exposure to HEA (Fig. 3.4A), a blood-sampling time which would correspond to close to the start of the period of ventilatory flow depression. However, by 180 min when breathing had rebounded and increased above control levels (Fig. 3.3), plasma T_{Amm} had increased to about $1,630 \mu\text{mol L}^{-1}$ i.e. 11-fold control levels (Fig. 3.4A). These changes in T_{Amm} were quantitatively reflected in parallel increases in PNH_3 from the control level of about $50 \mu\text{Torr}$ to about $650 \mu\text{Torr}$ at 180 min (Fig. 3.4B). There were no significant changes in either blood pH from a control level of about 8.05 (Fig. 3.4C) or PCO_2 from a control level of about 1.3 Torr (Fig. 3.4D), though plasma $[\text{HCO}_3^-]$ did increase significantly at 180 min by about 55% from a control level of 6.8 mmol L^{-1} (Fig. 3.4E).

3.4.4 Series IV – Relationship between ventilation and changes in blood chemistry in hagfish loaded internally with ammonia

Increased plasma ammonia levels appeared to be associated with hyperventilation in Series I and Series III, so we hypothesized that the increases in plasma ammonia levels were a proximate stimulus for elevated ventilation in hagfish. In order to test this hypothesis, we injected low doses of $70 \mu\text{mol kg}^{-1}$ or high doses of $1,000 \mu\text{mol kg}^{-1}$ ammonium salts (both NH_4HCO_3 and NH_4Cl) into the caudal venous sinus in order to increase plasma ammonia concentrations, and measured associated responses in blood chemistry and ventilatory parameters, with high dose injections of NaHCO_3 and NaCl as parallel controls.

After injection of both low and high doses of NH_4HCO_3 , the hagfish significantly increased ventilatory index within 1 h (Fig. 3.5C), mostly by increasing pressure amplitude (Fig. 3.5B); ventilatory

frequency did not change (Fig. 3.5A). The fish exhibited simultaneous elevations in plasma T_{Amm} (Fig. 3.6A) and PNH_3 (Fig. 3.6B) which were much greater in the high dose treatment, but plasma pH, $[\text{HCO}_3^-]$, and PCO_2 remained unchanged in both treatments (Table 3.1). These increases in plasma T_{Amm} (Fig. 3.6A) and PNH_3 (Fig. 3.6B) at 0.5 h in response to the high dose NH_4HCO_3 injections were comparable to those seen at 180 min in the 10 mM NH_4HCO_3 HEA exposures of Series III (cf. Fig. 3.4). After injection of high dose NH_4Cl , hagfish also showed significant hyperventilation (Fig. 3.5F), again mostly due to increased pressure amplitude (Fig. 3.5E). However, there were no significant ventilatory changes in response to injection of low dose NH_4Cl (Fig. 3.5D, E, F). Plasma T_{Amm} (Fig. 3.6C) and PNH_3 (Fig. 3.6D) increased proportionately in both treatments, but there were no significant changes in acid-base status (plasma pH, $[\text{HCO}_3^-]$, PCO_2 ; Table 3.1).

With respect to the control injections, high dose NaHCO_3 caused significantly increased frequency (Fig. 3.5A) while the pressure amplitude (Fig. 3.5B) was significantly decreased so the overall ventilatory index was not changed (Fig. 3.5C). Hagfish injected with high dose NaHCO_3 exhibited significant elevations in plasma pH and PCO_2 at both sample times, and a large increase in $[\text{HCO}_3^-]$ at 1 h (Table 3.1), with no changes in plasma T_{Amm} (Fig. 3.6A) and PNH_3 (Fig. 3.6B). There were no responses in ventilation (Fig. 3.5A, B, C), plasma ammonia parameters (Fig. 3.6A, B), or acid-base status (Table 3.1) to the other control treatment (high dose NaCl injection).

Two of the trials (high dose NaHCO_3 and NH_4HCO_3 injections) were repeated with measurements of ventilatory flow rather than pressure (Fig. 3.7A, B). These trials confirmed that the ventilatory index gave a reliable measure of the flow responses (cf. Fig. 3.5C); although, in this experiment there was a significant increase in frequency in response to the injection of ammonia.

Compared to animals injected with high dose NaHCO_3 , hagfish injected with a high dose of NH_4HCO_3 exhibited a significant 2.7-fold higher rate of ammonia excretion at 0 ~ 0.5 h, and a 4.1-fold higher flux at 0.5 ~ 1 h. These fish also significantly increased their urea-N excretion rate by 2.1-fold at 0.5- 1 h, but thereafter urea-N flux decreased to zero at 0.5-1 h post injection (Table 3.2). The net elevation in N-excretion over 1 h therefore amounted to about 30% of the high dose ($1,000 \mu\text{mol kg}^{-1}$) of the ammonia-N injected in the form of NH_4HCO_3 .

3.5 Discussion

3.5.1 Overview

The present study has demonstrated that ammonia stimulates ventilation in the Pacific hagfish, an animal with a deeply rooted evolutionary history in the vertebrate lineage. Ventilation in hagfish responds to both external elevations (i.e. HEA) and internal elevations of ammonia, but the hyperventilatory action of HEA appears to be through its effects on internal ammonia levels, as in other fish (*see* Introduction). Indeed, the initial response to HEA is a marked hypoventilation, perhaps mediated by external nociceptors or chemoreceptors, followed by a much later elevation of breathing when plasma levels of ammonia are greatly increased. The injection experiments demonstrated that hyperventilation in response to internal ammonia elevations is due specifically to ammonia and is not confounded by changes in blood acid-base status, again similar to the situation in other fish.

3.5.2 Ventilation changes in hagfish loaded externally with ammonia

In our previous studies on responses to HEA in seawater fish, we found that NH_4HCO_3 was preferable to NH_4Cl , because unlike the latter, it did not acidify the water (Wood and Nawata 2011; Nawata et al. 2015; De Boeck and Wood 2015). However, these studies had involved concentrations only up to 1.5 mM, whereas in the present study we were using much higher concentrations, so we thought it prudent to investigate both salts. Indeed, both treatments significantly stimulated ventilation to a comparable extent by 3 h (Fig. 3.1C). In our initial tests with the two salts at 10 mM, they had yielded virtually identical seawater pHs, as reported in the Results, so we were surprised at the mortalities occurring in the longer term only in the NH_4HCO_3 exposures (Fig. 3.8). This result was initially puzzling, because the 10 mM NaHCO_3 control treatment was without lethality. However, the mystery was solved by the subsequent finding that continued aeration of the sea water solution resulted in markedly higher water pH values, and therefore much greater PNH_3 levels in the 10 mM NH_4HCO_3 treatment (Fig. 3.8). Presumably, NH_4HCO_3 tends to dissociate to NH_3 , H_2O , and CO_2 , and the loss of CO_2 and persistence of NH_3 raises pH to a greater extent, than with NaHCO_3 or NH_4Cl -supplemented sea water, where the more moderate increases in pH are due only to the loss of CO_2 from the sea water. The higher seawater pH in the presence of 10 mM NH_4HCO_3 relative to 10 mM NH_4Cl , created by continuous aeration, results in a greater PNH_3 gradient for ammonia entry, and therefore greater internal ammonia loading. Interestingly, mortality in the 10 mM NH_4HCO_3 exposures did not occur in the MO_2 experiments of Series II, where the seawater solution was refreshed at 3-h intervals, minimizing the increases in water pH and PNH_3 . Our findings with the two salts are instructive in implicating NH_3 rather than NH_4^+ as the principal form of

ammonia entering across the body surface during HEA exposure. These concur with previous reports that ammonia loading in hagfish during HEA exposure occurs in association with an internal alkalosis, suggesting that ammonia enters the hagfish as NH_3 rather than as ionized NH_4^+ (Clifford et al. 2015). Furthermore, cutaneous ammonia conductance appears to be the prominent contributor to ammonia loading over branchial entry (Clifford et al. 2017).

Our initial experiments (Series I) demonstrated that the hagfish increased ventilation at 3 h during exposure to 10 mM HEA (or greater, as either NH_4HCO_3 or NH_4Cl); but there was no immediate response at 0 h (Fig. 3.1). However, a more detailed examination of the time course of the response (Series III) revealed that the hagfish quickly (i.e. within about 5 min) decreased ventilatory stroke volume, pressure amplitude, and ventilatory index during HEA treatment, reducing the total ventilatory flow by about 80%; velar frequency remained unchanged (Fig. 3.3). This reduction was maintained for a variable time period before ventilation finally increased significantly by 3 h (Fig. 3.3), the latter in accord with the Series I results (Fig. 3.1). In essence, the hagfish appeared to be “holding their breath” initially, possibly sensing toxic external ammonia with external chemoreceptors or nociceptors. These could be the well-developed olfactory organ with neural connections to the central nervous system (Theisen 1976; Holmes et al. 2011) or Schreiner organs which contain taste-bud-like external sensory structures in the epidermis of the head, trunk, and along the respiratory tracts (Braun 1998; Braun and Northcutt 1998). This result suggests that elevated external ammonia in itself is not a direct stimulant of ventilation.

Despite the initial hypoventilation, ammonia progressively accumulated in the bloodstream during HEA exposure (Fig. 3.4). By the time of initiation of hypoventilation (i.e. 5 min), plasma T_{Amm} was already elevated by 2.3-fold, and by the time hyperventilation was clearly instituted (3 h), plasma T_{Amm} had increased by 11-fold. It is now well established that Rh proteins [bidirectional ammonia-conductive channels (Wright and Wood 2009)] are present in both the gills and skin of hagfish (Braun and Perry 2010; Edwards et al. 2015; Clifford et al. 2017). Thus, even though water flow through the gill pouches was greatly reduced upon initial HEA exposure, ammonia could still permeate across the body surface along PNH_3 and/or NH_4^+ electrochemical gradients. Overall, we conclude that the stimulation of breathing by HEA in hagfish is likely due to its indirect action on internal chemoreceptors rather than a direct action on external chemoreceptors. In this regard, the response parallels that of teleosts (Zhang et al. 2011) and elasmobranchs (De Boeck and Wood 2015), though the absolute levels of HEA needed to elicit the hyperventilatory effect is considerably higher in the hagfish, as 5 mM NH_4CO_3 had no effect. Hagfish commonly feed by inserting their heads into decaying carrion (Martini 1998), where HEA levels may be very high (Clifford et al. 2016), so the whole sequence of events (initial breath-holding, followed

by eventual hyperventilation when blood ammonia levels pass threshold values), as well as their exceptional tolerance of HEA (Clifford et al. 2015; Clifford et al. 2017) may be adaptive for this trophic habit. The hyperventilation may be important in flushing out excess ammonia after feeding (Wilkie et al. 2017).

The experiments of Series II showed that the increases in ventilatory flow occurring during HEA treatment were effective in increasing $\dot{M}O_2$ (Fig. 3.2). Clifford et al. (2016) demonstrated that O_2 uptake occurs mainly at the gills in *E. stoutii*; the skin plays only very minor role. While the metabolic cost of breathing in hagfish has yet to be elucidated, it is possible that some of the observed increase in $\dot{M}O_2$ may have been consumed by the breathing mechanism. Breathing in hagfish consists of both the contraction of the velar pump (i.e. velum and velar chamber) for inhalation and contraction of the gill pouches for exhalation, the latter at a much lower frequency than the velum (Eom and Wood 2019; Chapter 2). Total ventilatory flow in *E. stoutii* can be altered by changes in both velar frequency and stroke volume (Eom and Wood 2019; Chapter 2). As with the initial hypoventilation, the hyperventilatory effects of HEA were exerted almost exclusively on ventilatory stroke volume; velar frequency remained unchanged in most HEA exposures, while pressure amplitude and ventilatory index increased (Figs. 3.1, 3.3, Fig. 3.8). This response pattern is similar to that seen with internal ammonia loading (Fig. 3.5). Despite the fundamental differences in breathing mechanisms in hagfish versus other fish (Strahan 1958; Malte and Lomholt 1998; Kardong 2012; Eom and Wood 2019), this is also in accord with the HEA responses of both teleosts (Zhang et al. 2011; Zhang et al. 2013) and elasmobranchs (De Boeck and Wood 2015) where only ventilatory stroke volume increases. In Pacific hagfish, Perry et al. (2009b) reported only increased velar frequency under external hypoxia and hypercapnia as ventilatory stimulants, but did not test HEA.

3.5.3 Ventilation changes in hagfish loaded internally with ammonia

After internal loading with ammonia in Series IV, either as NH_4HCO_3 or NH_4Cl , hagfish exhibited increased ventilation; the initial hypoventilation seen with external ammonia loading in HEA never occurred. The hyperventilatory response was largely due to increased ventilatory stroke volume. Pressure amplitude and ventilatory index both increased while ventilatory frequency was largely unchanged (Fig. 3.5). This response is similar to the long-term response pattern to external ammonia loading (HEA; Figs. 3.1, 3.3, Fig. 3.8), and in qualitative accord with the patterns previously reported in teleosts (Zhang and Wood 2009; Zhang et al. 2011) and elasmobranchs (De Boeck and Wood 2015)

where increases in amplitude predominated in the hyperventilatory response to internal ammonia loading. Importantly, these responses occurred in the absence of changes of blood acid-base status (Table 3.1), which have confounded interpretation in some previous studies on teleost (McKenzie et al. 1993; Zhang and Wood 2009). It is noteworthy that the one treatment showing a marked increase in frequency was the high dose NaHCO₃ control injection (Fig. 3.5A), and this was the only treatment where blood PCO₂ increased (Table 3.1), in accord with the observation of Perry et al. (2009) that external hypercapnia elevated velar frequency in *E. stoutii*.

The blood plasma measurements demonstrated that in every injection treatment where significant hyperventilation occurred (Fig. 3.5), there were corresponding significant increases in mean blood T_{Amm} and PNH₃ levels (Fig. 3.6). These measurements give an approximate indication of the threshold values needed to initiate the hyperventilatory response. Hyperventilation was marginal in the low dose injections of NH₄Cl and NH₄HCO₃ (Fig. 3.5) where mean blood plasma T_{Amm} and PNH₃ levels remained less than 100 μmol L⁻¹ and 150 μTorr respectively, but became prominent in the high dose injections where values surpassed 350 μmol L⁻¹ and 450 μTorr respectively (Fig. 3.6). In the HEA exposures of Series III, the significant hyperventilation at 3 h (Fig. 3.3) was associated with values (T_{Amm} >1,500 μmol L⁻¹; PNH₃ > 600 μTorr; Fig. 3.4) that clearly surpassed these thresholds. Overall, these plasma levels are similar to those reported to cause hyperventilation in teleosts (Zhang and Wood 2009; Zhang et al. 2011; Zhang et al. 2013), elasmobranchs (De Boeck and Wood 2015), and mammals (e.g. Wichser and Kazemi 1974; Mutch and Banister 1983). Notably, the measured plasma T_{Amm} concentrations at 0.5 h after injection (Fig. 3.6) were less than 50% of those predicted if the injected ammonia load had distributed throughout the plasma volume, and less than 20% of those predicted if it had distributed throughout the extracellular volume (*see* Methods). It was noted that only about 15% of the injected load was excreted to the external water over this time period (Table 3.2). Given that hagfish lack a complete complement of ornithine-urea cycle enzymes (Read 1975; Braun and Perry 2010), and previous studies demonstrated no increases in plasma glutamine and urea, as well as no increases in urea efflux following ammonia loading by HEA exposure (Clifford et al. 2015), biotransformation to alternative nitrogenous forms seems unlikely. Thus, we suggest that the missing ammonia partitioned into the tissues as previously demonstrated in lemon sole (*Parophrys vetulus*; Wright et al. 1988) and trout (Wright and Wood 1988).

Our experiments were not designed to distinguish whether internal PNH₃ or T_{Amm} levels (or NH₄⁺ concentrations, which are very similar to T_{Amm} concentrations) are the specific stimulants of hyperventilation in the hagfish. Regression analyses of all the paired breathing and plasma ammonia measurements in individual animals from Series IV revealed significant positive relationships of

ventilatory index with both plasma T_{Amm} ($p = 0.0037$, $r^2 = 0.1918$) and PNH_3 ($p = 0.0022$, $r^2 = 0.1945$) suggesting that either of these indicators of plasma ammonia could be the key stimulant (Fig. 3.11). However, we emphasize that correlation does not necessarily indicate causation. The experiments also did not localize the internal chemoreception sites for ammonia. In teleosts, there is strong evidence that neuroepithelial cells (NECs) in the gills are involved, serving as trimodal receptors for O_2 , CO_2 , and ammonia (Zhang et al. 2011; Zhang et al. 2015; Perry and Tzaneva 2016), as well as correlative evidence that central chemoreception of elevated ammonia concentrations in the brain may also contribute to ammonia detection (Zhang et al. 2013). In mammals, the situation is unclear, but central chemoreception of elevated brain ammonia appears to be important in the hyperventilatory response (*see* Introduction). To our knowledge, there is no information on the presence or absence of NECs in hagfish. However, NECs are believed to originate from neural crest cells which are ubiquitously found during embryogenesis of all vertebrates, including hagfish (Baker 2008; Ota et al. 2007). NECs are thought to be homologous to the glomus cells of the arterial (peripheral) chemoreceptors of higher vertebrates, and are widely distributed in respiratory epithelia ranging from fish gills to human lungs (Milsom 2012; Milsom and Burleson 2007). It would be surprising if they were not present in hagfish. [Note: At the time this paper was written, this was the prevailing view. However, the study of Hockman et al. (2017) on zebrafish casts doubt on this view, presenting evidence that the NECs of fish have a different embryonic origin (endoderm) than the neural (ectoderm) origin of glomus cells of the carotid and aortic bodies in mammals.]

3.5.4 Summary and future directions

The present study has shown that ventilation can be specifically stimulated by internal ammonia in *E. stoutii*, a representative of the oldest extant connection to the ancestral vertebrates. From experiments on this same species, Perry et al. (2009b) concluded that ventilatory responses to environmental hypoxia and hypercapnia in the vertebrates arose in the myxine lineage, and the same would appear to be true for the ventilatory responses to ammonia, the immediate product of amino acid metabolism in all animals. Therefore, the role of ammonia in stimulating breathing appears to be an ancient characteristic of the vertebrates. In mammals, it remains important in post-exercise hyperventilation and in supporting breathing during respiratory acidosis and hepatic coma (*see* Introduction). Given the unique feeding habits of the hagfish discussed earlier, the adaptive value of ammonia-induced hyperventilation appears obvious in these animals. In teleosts, elevations in plasma ammonia after both feeding and exercise (Wood 2001) have been implicated in adaptive hyperventilatory

responses (Zhang et al. 2015). In *E. stoutii*, plasma T_{Amm} concentrations ($100 \sim 200 \mu\text{mol L}^{-1}$) reported after feeding (Wilkie et al. 2017) approached the threshold concentrations for ventilatory stimulation measured in the present study. It would be of interest to measure plasma ammonia levels after exercise in this species, to see if they too are in the range needed to stimulate ventilation. Clearly additional physiological experiments and morphological analyses are now required to identify the sites of chemoreception for ammonia in hagfish, and to understand how ventilatory responses to ammonia are integrated with those to O_2 and CO_2 ; now partially addressed in Chapter 4.

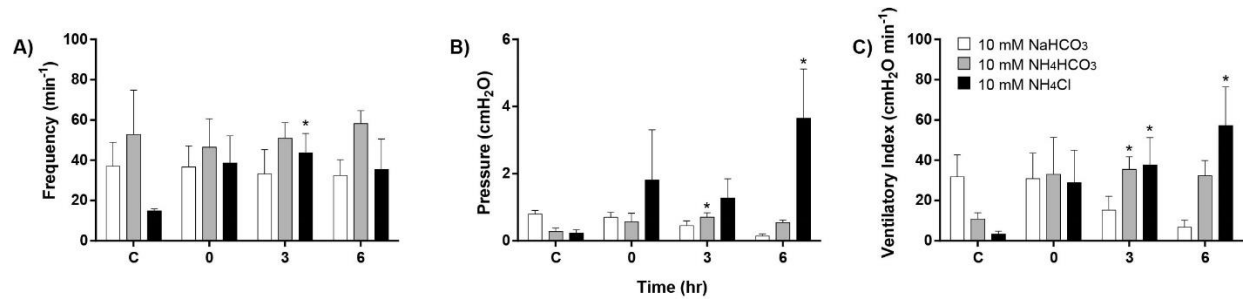


Figure 3.1 Responses over time in (A) ventilatory frequency, (B) ventilatory pressure amplitude, and (C) ventilatory index of hagfish (N = 6 per each treatment) exposed to 10 mM NaHCO₃ (bicarbonate control) and two high environmental ammonia (HEA) treatments, 10 mM NH₄HCO₃ and 10 mM NH₄Cl. Means ± 1 S.E.M. Asterisk (*) indicates significant difference (p < 0.05) from pre-exposure control value ("C").

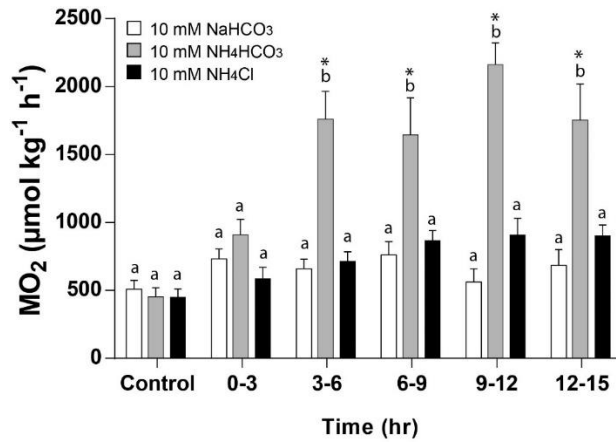


Figure 3.2 Changes in oxygen consumption rate ($\dot{M}O_2$) of hagfish in response to two different HEA treatments, 10 mM NH_4Cl ($N = 6$) or 10 mM NH_4HCO_3 ($N = 6$), as well as a control treatment with 10 mM $NaHCO_3$ ($N = 4$) in Series II. Means \pm 1 S.E.M. * indicates significant difference ($p < 0.05$) from pre-exposure control value (“C”). Different letters indicate significant differences ($p < 0.05$) among treatments within each time interval.

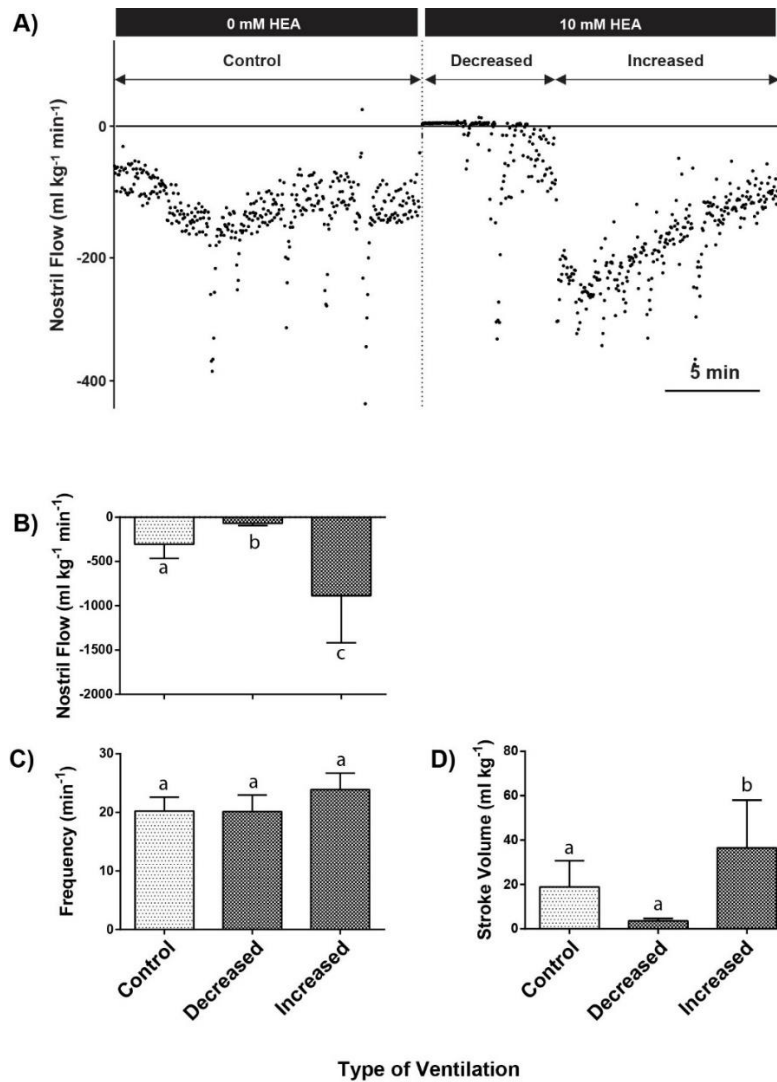


Figure 3.3 Flowmeter recordings of nostril ventilatory parameters (measured directly *via* a flow probe placed in the nostril entrance) in hagfish exposed to 10 mM NH_4HCO_3 (HEA) (A) in Series III. Note that these are flow recordings in contrast to the pressure recordings of Figs. 3.1 and 3.5. Means \pm 1 S.E.M (N = 6). The data were sampled during the pre-exposure control period and over 5-min periods representing the times of greatest initial decrease, and greatest subsequent increase in nostril ventilatory flow during the HEA treatment for each animal. In HEA, hagfish quickly decreased nostril ventilatory flow for an average of 35.6 min (range: 5.2 to 94.2 min), after which the ventilatory flow increased above the original pre-exposure control level. All these changes were achieved by changes in ventilatory stroke volume rather than in velar frequency. Different letters indicate significant differences ($p < 0.05$) among the three sampling periods.

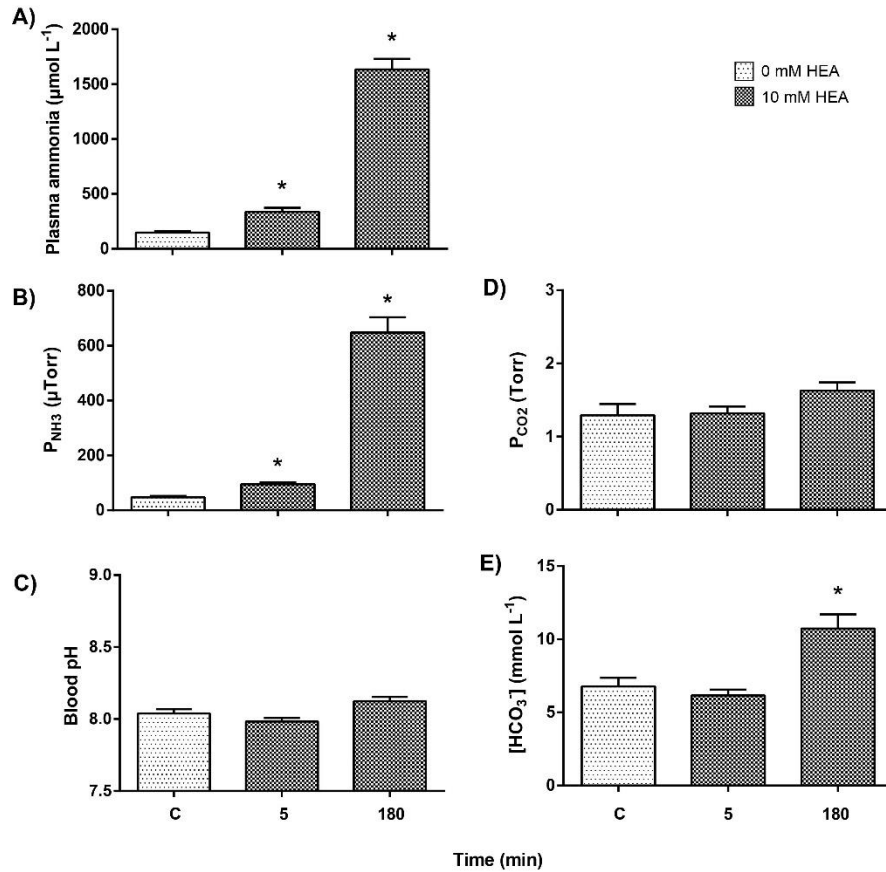


Figure 3.4 Changes in (A) plasma total ammonia concentration (T_{Amm}); (B) plasma ammonia partial pressure (P_{NH_3}); (C) plasma pH; (D) plasma carbon dioxide partial pressure (P_{CO_2}); and (E) plasma bicarbonate concentration ($[\text{HCO}_3^-]$) in hagfish ($N = 6$) in response to exposure to 10 mM NH_4HCO_3 (HEA) for 5 min or 180 min (3 h), in Series III. Means \pm 1 S.E.M. The 5-min samples were taken at a time just before ventilation decreased greatly, and the 180-min samples at a time after which ventilation had increased greatly (*see* Fig. 3.3). * indicates significant difference ($p < 0.05$) from pre-exposure control value ("C").

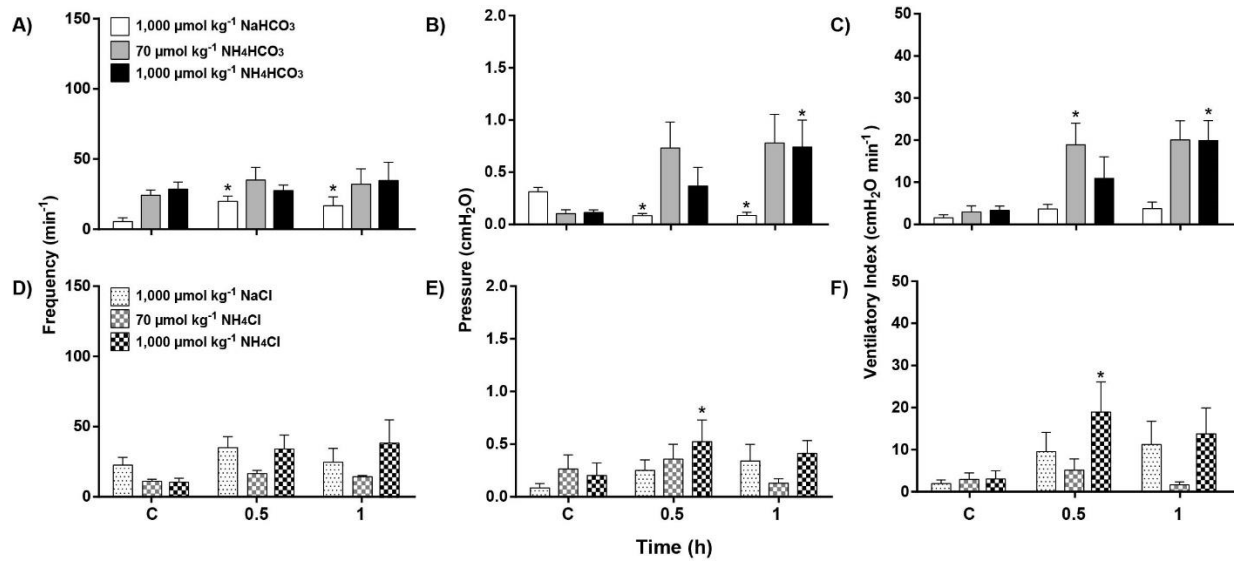


Figure 3.5 Changes in ventilatory parameters of hagfish in response to injections of ammonium salts or appropriate sodium salt controls into the venous sinus, in Series IV. NaHCO₃ and NH₄HCO₃ and responses are shown in panels (A) frequency, (B) pressure amplitude and (C) ventilatory index, while NaCl and NH₄Cl responses are shown in panels (D) frequency, (E) pressure amplitude, and (F) ventilatory index. Doses and N numbers were 1,000 μmol kg⁻¹ NaHCO₃ (N = 11), 70 μmol kg⁻¹ NH₄HCO₃ (N = 6), 1,000 μmol kg⁻¹ NH₄HCO₃ (N = 18), 1,000 μmol kg⁻¹ NaCl (N = 6), 70 μmol kg⁻¹ NH₄Cl (N = 6), and 1,000 μmol kg⁻¹ NH₄Cl (N = 6). Means ± 1 S.E.M. * indicates significant difference (p < 0.05) from pre-injection control value (“C”).

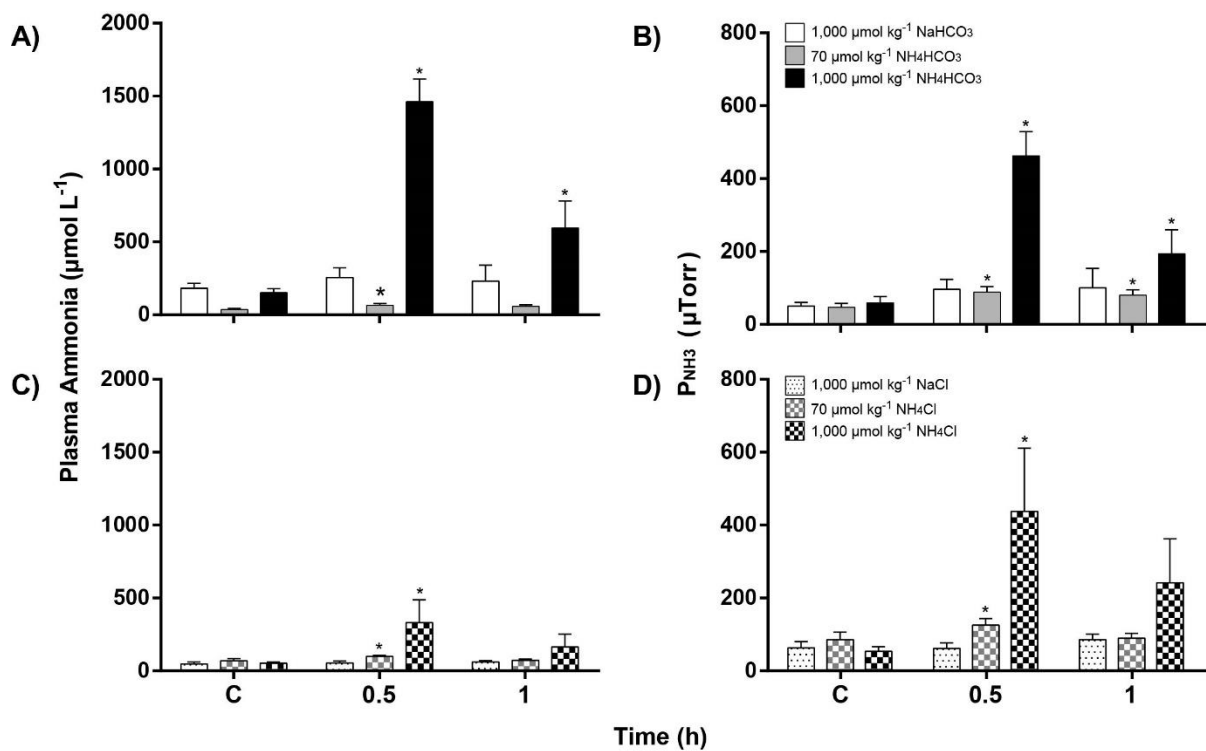


Figure 3.6 Changes in plasma total ammonia concentration (T_{Amm}) and plasma ammonia partial pressure (PNH_3) of hagfish in response to injections of ammonium salts or appropriate sodium salt controls into the venous sinus, in Series IV. NaHCO_3 and NH_4HCO_3 and responses are shown in panels (A) T_{Amm} and (B) PNH_3 , while NaCl and NH_4Cl responses are shown in panels (C) T_{Amm} and (D) PNH_3 . Doses and N numbers were 1,000 $\mu\text{mol kg}^{-1}$ NaHCO_3 (N = 11), 70 $\mu\text{mol kg}^{-1}$ NH_4HCO_3 (N = 6), 1,000 $\mu\text{mol kg}^{-1}$ NH_4HCO_3 (N = 18), 1,000 $\mu\text{mol kg}^{-1}$ NaCl (N = 6), 70 $\mu\text{mol kg}^{-1}$ NH_4Cl (N = 6), 1,000 $\mu\text{mol kg}^{-1}$ NH_4Cl (N = 6). Means \pm 1 S.E.M. * indicates significant difference ($p < 0.05$) from pre-injection control value (“C”).

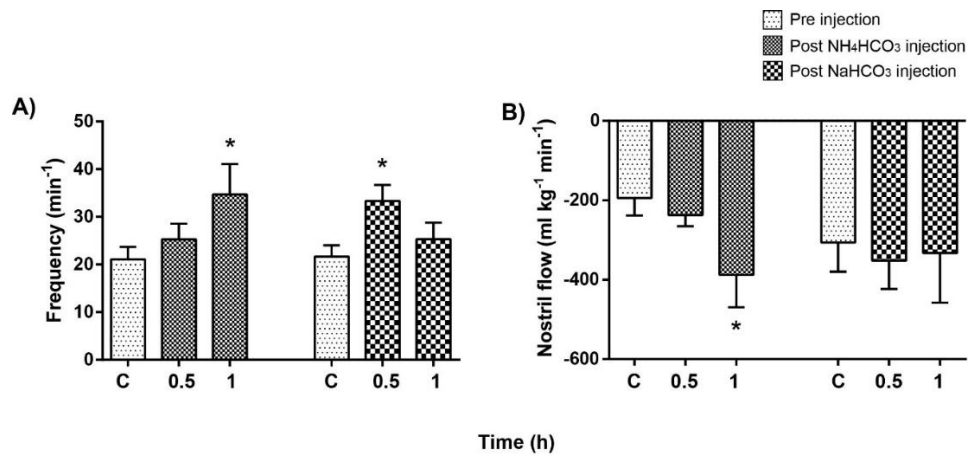


Figure 3.7 Changes in (A) ventilatory frequency and (B) ventilatory flow (measured directly *via* a flow probe placed in the nostril entrance) of hagfish in response to injections at a dose of $1,000 \mu\text{mol kg}^{-1}$ NH_4HCO_3 (dark bar, $N = 6$) and $1,000 \mu\text{mol kg}^{-1}$ NaHCO_3 (checkerboard bar, $N = 6$) into the venous sinus, in Series IV. Means ± 1 S.E.M. * indicates significant difference ($p < 0.05$) from pre-injection control value ("C").

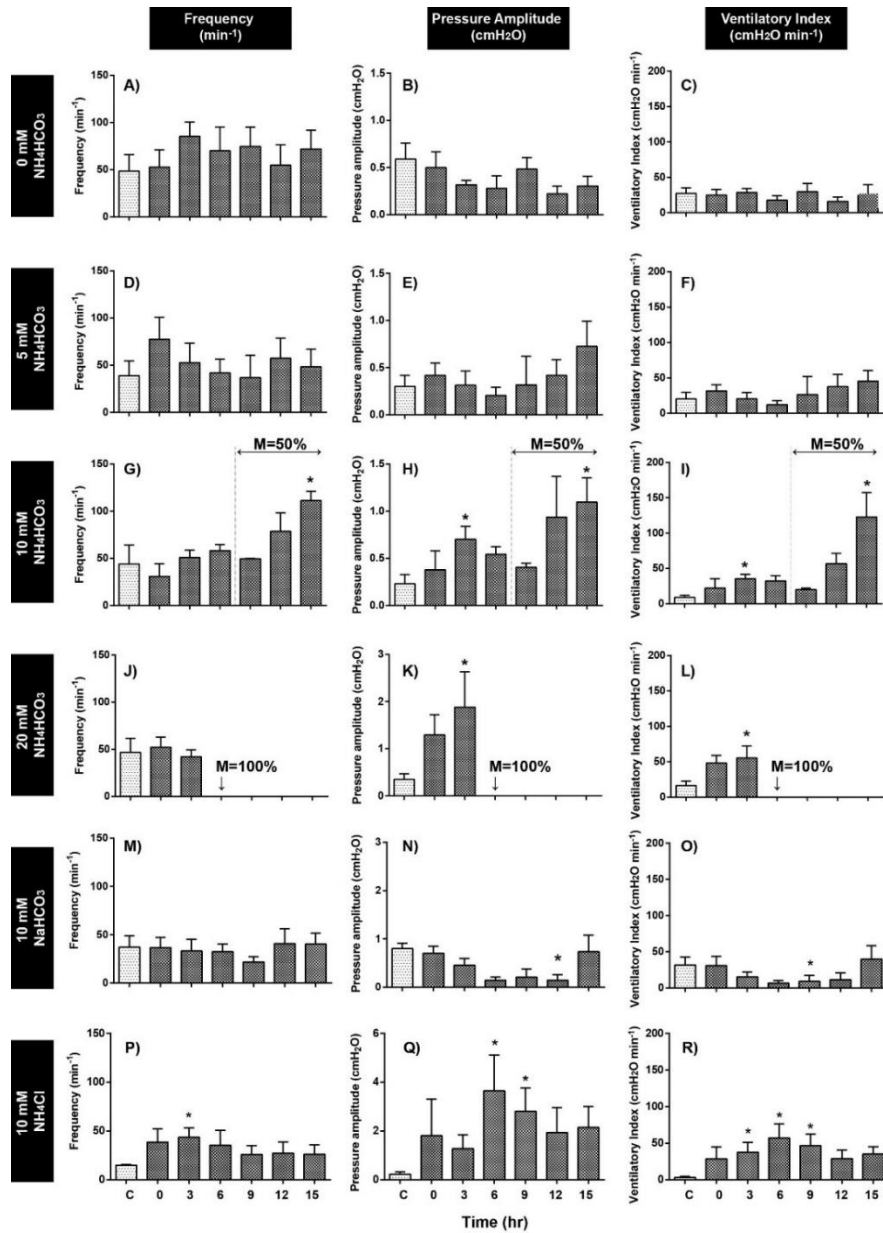


Figure 3.8 Responses over time in ventilatory parameters of hagfish ($N = 6$ per each treatment) exposed (from top to bottom) to 0 (no addition control), 5, 10, and 20 mM NH_4HCO_3 as high environmental ammonia (HEA) treatments, in Series I. Exposure to 10 mM NaHCO_3 ($N = 6$) as a bicarbonate control treatment, and 10 mM NH_4Cl ($N = 6$) as an alternate form of HEA were also evaluated. Means \pm 1 S.E.M. ‘M’ in panels G, H, I, J, K, and L indicates percent mortality out of $N = 6$. Asterisk (*) indicates significant difference ($p < 0.05$) from pre-exposure control value (“C”).

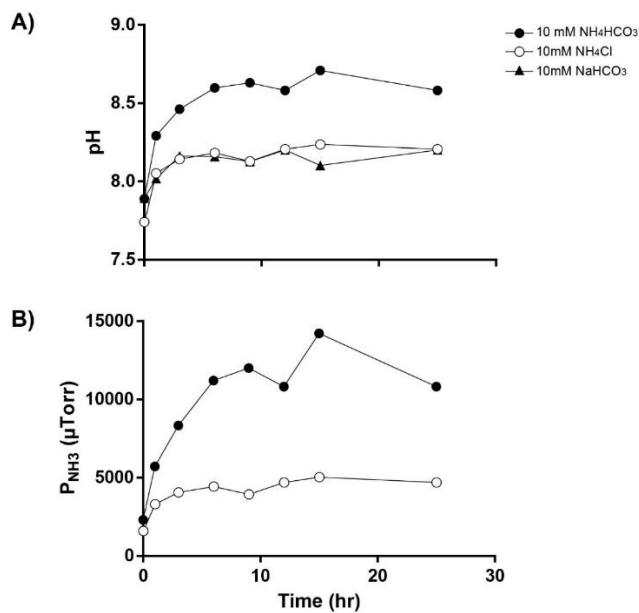


Figure 3.9 (A) Changes in pH over time of sea water (30 ppt) containing either 10 mM NH₄HCO₃, 10 mM NH₄Cl, or 10 mM NaHCO₃, and continuously bubbled with air, in Series I. The sea water containing 10 mM NH₄HCO₃, was alkalized to a greater extent than in the other two treatments. (B) Calculated P_{NH₃} levels over time in the 10 mM NH₄HCO₃ or 10 mM NH₄Cl exposures, based on the pH values recorded in panel (A).

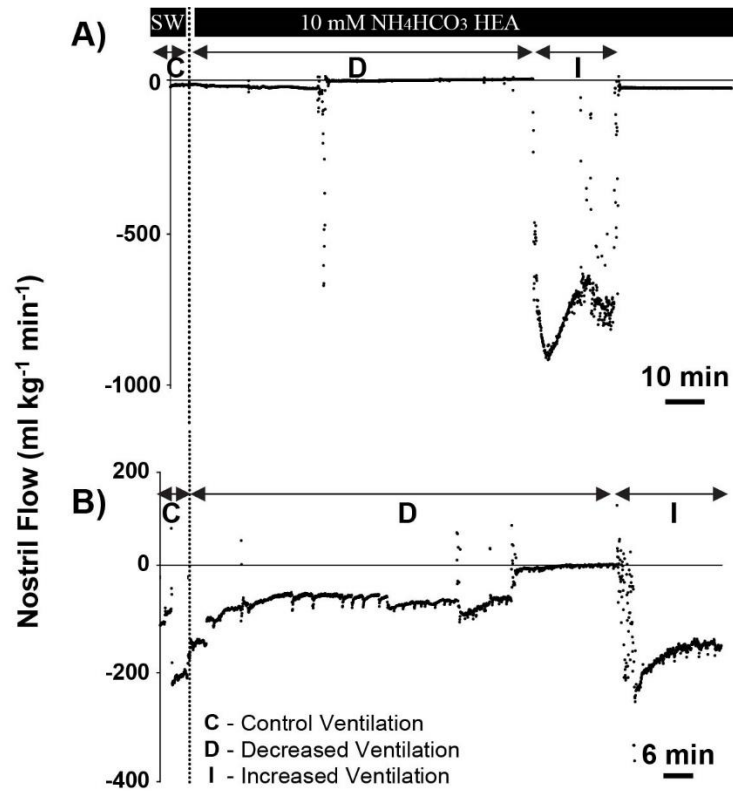


Figure 3.10 Two more examples (analogous to Fig. 3.3A) of flowmeter recordings of nostril ventilatory flow rate (measured directly *via* a flow probe placed in the nostril entrance) in hagfish exposed to 10 mM NH₄HCO₃ (HEA) in Series III. Note that these are flow recordings in contrast to the pressure recordings of Figs. 3.1 and 3.5. The data were recorded during the pre-exposure control period (“C”) during the period of greatest initial decrease (“D”), and greatest subsequent increase (“I”) in nostril ventilatory flow during the HEA treatment for each animal.

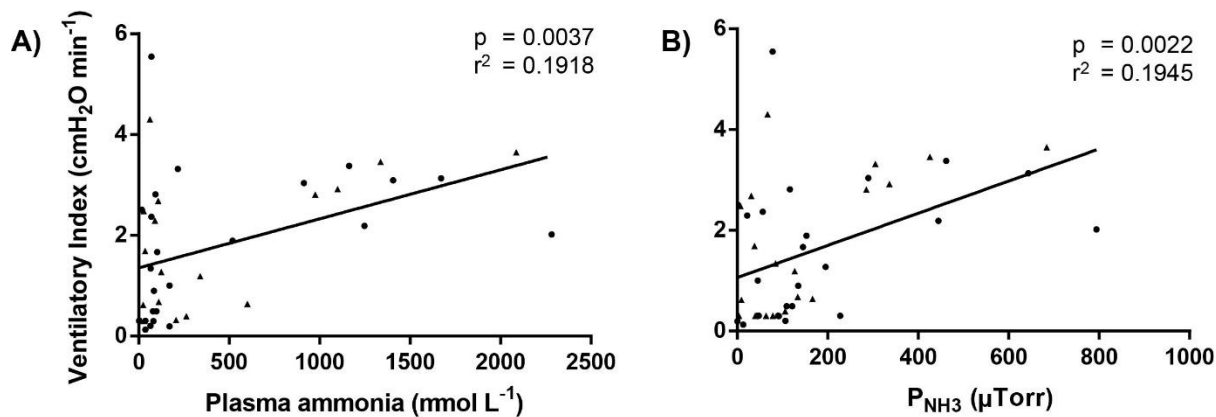


Figure 3.11 Correlation of ventilatory index with (A) total plasma ammonia concentration (T_{Amm}) and (B) gaseous ammonia tension (P_{NH_3}) in individual hagfish injected at a dose of $1,000 \mu\text{mol kg}^{-1}$ or $70 \mu\text{mol kg}^{-1}$ of ammonium salts (NH_4HCO_3 and NH_4Cl) in Series IV. The significance (p) and r^2 values are shown.

Table 3.1 Blood acid-base chemistries of hagfish before (Control) and 0.5h and 1h after (Post) injection of the respective doses of salts into the venous sinus, in Series IV. Means \pm S.E.M.

	pH			Pco ₂ (Torr)			[HCO ₃ ⁻] (mmol L ⁻¹)		
	Control	Post		Control	Post		Control	Post	
		0.5 h	1.0 h		0.5 h	1.0 h		0.5 h	1.0 h
1,000 μmol kg⁻¹ NaHCO₃ (N = 11)	7.96 \pm 0.02	8.14 \pm 0.03 *	8.12 \pm 0.02 *	1.49 \pm 0.17	1.97 \pm 0.20 *	0.87 \pm 0.09	6.74 \pm 0.79	12.75 \pm 0.95 *	5.64 \pm 0.70
1,000 μmol kg⁻¹ NH₄HCO₃ (N = 18)	8.01 \pm 0.05	8.05 \pm 0.03	8.03 \pm 0.02	1.30 \pm 0.15	1.65 \pm 0.19	1.18 \pm 0.10	7.96 \pm 1.40	9.19 \pm 1.11	6.17 \pm 0.61
70 μmol kg⁻¹ NH₄HCO₃ (N = 6)	8.14 \pm 0.02	8.19 \pm 0.02	8.19 \pm 0.02	0.90 \pm 0.02	0.88 \pm 0.03	0.81 \pm 0.02	7.99 \pm 0.78	8.58 \pm 0.67	8.01 \pm 0.96
1,000 μmol kg⁻¹ NaCl (N = 6)	8.17 \pm 0.03	8.11 \pm 0.04	8.18 \pm 0.05	0.89 \pm 0.11	1.03 \pm 0.22	0.70 \pm 0.10	8.40 \pm 1.11	7.94 \pm 1.02	6.82 \pm 0.97
1,000 μmol kg⁻¹ NH₄Cl (N = 6)	8.12 \pm 0.05	8.11 \pm 0.04	8.13 \pm 0.04	0.96 \pm 0.08	0.84 \pm 0.11	0.85 \pm 0.12	8.01 \pm 1.00	6.57 \pm 0.72	7.29 \pm 1.07
70 μmol kg⁻¹ NH₄Cl (N = 6)	8.12 \pm 0.05	8.13 \pm 0.05	8.13 \pm 0.03	0.92 \pm 0.02	0.87 \pm 0.03	0.93 \pm 0.02	7.68 \pm 0.02	7.44 \pm 0.03	7.89 \pm 0.02

Asterisk (*) indicates significant difference ($p < 0.05$) from pre-exposure control value (“C”).

Table 3.2 Ammonia flux and urea-N flux rates of hagfish after injection at a dose of 1,000 $\mu\text{mol kg}^{-1}$ NH_4HCO_3 (N = 18) or 1,000 $\mu\text{mol kg}^{-1}$ NaHCO_3 (N = 11) into the venous sinus, in Series IV. Negative values indicate excretion to the water. Means \pm S.E.M.

		NaHCO₃	NH₄HCO₃
Ammonia Flux ($\mu\text{mol kg}^{-1} \text{h}^{-1}$)	<i>0 - 0.5 h post injection</i>	-132.50 \pm 19.28	-364.20 \pm 54.71 *
	<i>0.5 - 1.0 h post injection</i>	-107.40 \pm 17.86	-435.30 \pm 85.87 *
Urea-N Flux ($\mu\text{mol kg}^{-1} \text{h}^{-1}$)	<i>0 - 0.5 h post injection</i>	-25.30 \pm 6.31	-52.23 \pm 12.78 *
	<i>0.5 - 1.0 h post injection</i>	-22.40 \pm 9.67	2.77 \pm 22.66

Asterisk (*) indicates significant difference ($p < 0.05$) between the two treatments at the same time period.

Chapter 4: Understanding ventilation and oxygen uptake of Pacific hagfish (*Eptatretus stoutii*), with particular emphasis on responses to ammonia and interactions with other respiratory gases

4.1 Summary

The hagfishes are an ancient and evolutionarily important group, with breathing mechanisms and gills very different from those of other fishes. Hagfish inhale through a single nostril *via* a velum pump, and exhale through multiple separate gill pouches. We assessed respiratory performance in *E. stoutii* (31 ppt, 12°C, 50 ~ 120 g) by measuring total ventilatory flow (\dot{V}_w) at the nostril, velar (respiratory) frequency (fr), and inspired (P_{iO_2}) and expired (P_{eO_2}) oxygen tensions at all 12 gill pouch exits plus the pharyngo-cutaneous duct (PCD) on the left side, and calculated ventilatory stroke volume (SV_w), % O₂ utilization, and oxygen consumption ($\dot{M}O_2$). At rest under normoxia, spontaneous changes in \dot{V}_w ranged from apnea to > 400 ml kg⁻¹ min⁻¹, due to variations in both fr and SV_w; “normal” \dot{V}_w averaged 137 ml kg⁻¹ min⁻¹, $\dot{M}O_2$ was 718 μmol kg⁻¹ h⁻¹, so the ventilatory convection requirement for O₂ was about 11 L mmol⁻¹. Relative to anterior gill pouches, lower P_{eO_2} values (i.e. higher utilization) occurred in the more posterior pouches and PCD. Overall O₂ utilization was 34% and did not change during hyperventilation but increased to > 90% during hypoventilation. Environmental hypoxia (P_{iO_2} ~ 8% air saturation, 1.67 kPa, 13 Torr) caused hyperventilation, but neither acute hyperoxia (P_{iO_2} ~275% air saturation, 57.6 kPa, 430 Torr) nor hypercapnia (P_{iCO_2} ~1 % CO₂, 1.0 kPa, 7.5 Torr) significantly altered \dot{V}_w . $\dot{M}O_2$ decreased in hypoxia and increased in hyperoxia but did not change in hypercapnia. Acute exposure to high environmental ammonia (HEA, 10 mM NH₄HCO₃) caused an acute decrease in \dot{V}_w , in contrast to the hyperventilation of long-term HEA exposure described in a previous study. The hypoventilatory response to HEA still occurred during hypoxia and hyperoxia, but was blunted during hypercapnia. Under all treatments, $\dot{M}O_2$ increased with increases in \dot{V}_w . Overall, there were lower convection requirements for O₂ during hyperoxia, higher requirements during hypoxia and hypercapnia, but unchanged requirements during HEA. We conclude that this “primitive” fish operates a flexible respiratory system with considerable reserve capacity.

4.2 Introduction

Modern agnathans such as the Pacific hagfish *Eptatretus stoutii* are extant representatives of what is arguably the most ancient vertebrate lineage (Goodrich 1930; Bardack 1998; Miyashita et al. 2019; Rasmussen et al. 1998; Heimberg et al. 2010; Oisi et al. 2013). Their breathing mechanism and branchial structure are fundamentally different from those of most other fishes (Bartels 1998; Johansen and Strahan

1963; Malte and Lomholt 1998; Eom and Wood 2019; now Chapter 2). Unlike teleosts, where the gills are grouped together on each side, covered by bilaterally symmetrical operculae and ventilated *via* the mouth by a buccal force - opercular suction pump (Hughes 1960; Hughes and Shelton 1962), or elasmobranchs which operate a similar system with separate gill slits (Piiper and Schumann 1968), the hagfish have multiple separate gill pouches on each side, each with a separate exit (Mallatt 1984; generally 2 rows x 12 gill pouches in *E. stoutii*). The gill pouches are internal structures surrounded by cartilaginous plates, muscle, and connective tissues (Marinelli and Strenger 1956). Water is inhaled through the single separate nostril, not the mouth, by the suction created by the up-and-down pumping action of a central velar scroll (Bartels 1998; Eom and Wood 2019; Chapter 2). The velum chamber contracts rhythmically. This forces water down a long pharynx and into the 24 separate afferent branchial ducts leading to the separate gill pouches, as well as into an apparent bypass shunting system, the pharyngo-cutaneous duct (PCD) which has a single exit on the left side in *E. stoutii*. The gill pouches contract at a much lower rate than the velum chamber and seem to play a role in driving exhalation through the 24 separate efferent branchial ducts, as well as through the PCD (termed 13th gill pouch in Wood and Eom 2019, Chapter 2). A similar expiratory pumping role for the gill pouches has been proposed for the Atlantic hagfish, *Myxine glutinosa* (Goodrich 1930; Johansen and Hol 1960). We recently characterized the breathing mechanism in *E. stoutii* as a two-phase unidirectional pumping system with a fast suction pump (velum) for inhalation through the single nostril and a much slower force pump (gill pouches and PCD) for exhalation (Eom and Wood 2019; Chapter 2). Given this apparent disconnect of the two pumps, and the fact that ventilatory flow (\dot{V}_w) can vary spontaneously from zero (apnea) to very high levels (Eom and Wood 2019; Chapter 2), the volume and residence time of water in the system may vary greatly, which would likely affect the extent of respiratory gas exchange.

Unlike the holobranchs of other fish, the hagfish has lens-shaped bi-lobed pouches with internal radial folds that in turn bear filaments and respiratory lamellae. These have been thoroughly described in *E. stoutii* by Mallatt and Paulsen (1986). While their orientation relative to the body axis is very different from other fish, these respiratory structures are surprisingly similar in architecture, blood channels, and cellular composition, and organized so as to provide a largely countercurrent flow of blood against the water. The mean effective diffusion distance is about 5 ~ 10 μm , typical of many fish (Hughes 1984). In *E. stoutii*, the gills appear to be the major sites of respiratory gas exchange, accounting for about 80% of O_2 uptake and 70% of ammonia excretion, based on divided chamber studies (Clifford et al. 2014; Clifford et al. 2016), though the skin may play a larger role in Atlantic hagfish such as *Myxine glutinosa* (Steffensen et al. 1984; Lesser et al. 1997). At present, little is known about the process of O_2 uptake ($\dot{M}\text{O}_2$) from the water, and how it might vary with flow (\dot{V}_w), or with the gas composition of the water.

Indeed, we are aware of no measurements of expired O₂ tensions (i.e. P_EO₂), how they may vary with inspired O₂ tension (P_IO₂), or the % utilization of O₂ at the gills in hagfish, either overall, or on an individual gill pouch basis. However, there is general agreement that under resting normoxic conditions, $\dot{M}O_2$ is low in *E. stoutii*, (Munz and Morris 1965; Clifford et al. 2016; Eom et al. 2019, now Chapter 3) but some disagreement as to how well it is maintained under hypoxic conditions (Perry et al. 2009b; Drazen et al. 2011; Giacomini et al. 2019b). Nevertheless, both Perry et al. (2009b) and Giacomini et al. (2019b) reported that hyperventilation occurred during environmental hypoxia, and Giacomini et al. (2019a) reported a non-significant increase in ventilation during environmental hyperoxia, the latter unlike the hypoventilatory response seen in most fish. Perry et al. (2009b) also found hyperventilation during environmental hypercapnia, and indirect evidence for the presence of both external and internal chemo-receptors based on cyanide injection. Eom et al. (2019; Chapter 3) found that elevated high environmental ammonia (HEA) caused a marked short-term (minutes) hypoventilation followed by longer term hyperventilation after several hours when blood ammonia levels increased.

In teleost, the respiratory gases (O₂, CO₂, and ammonia) are known to be detected by neuroepithelial cells (NECs) on the gills (Perry et al. 2009a). These cells are thought to be polymodal chemoreceptors responding to water and/or blood levels of these gases, as well as to surrogate stimuli such as cyanide (reviewed by Perry and Tzaneva 2016; Jonz 2018). At present, it is not known whether these peripheral chemoreceptors are present in agnathans, but the documented hyperventilatory responses to hypoxia (Perry et al. 2009b; Giacomini et al. 2019a), hypercapnia (Perry et al. 2009b), cyanide (Perry et al. 2009b) and ammonia treatments (Eom et al. 2019; Chapter 3) all suggest that NECs, or functional analogues of NECs, must be present in hagfish.

With this background in mind, in the present study, we directly measured ventilatory flow (\dot{V}_w) using an ultrasonic flowmeter (Perry et al. 2009b; Eom and Wood 2019; Chapter 2) and O₂ tensions at various sites using needle-tip optodes. We first characterized the variations in P_EO₂ and therefore % utilization of O₂ amongst the 12 gill pouches and PCD on one side. Our hypothesis was that the more posterior pouches would exhibit lower P_EO₂ and higher % utilization because of likely recycling of water from front-to-back, but that the PCD would show the highest P_EO₂ and lowest % utilization because of its role as a bypass shunt. We also hypothesized that P_EO₂ would be low and % utilization high during spontaneous hypoventilation, and *vice versa* during spontaneous hyperventilation, in light of the well-known inverse relationship between \dot{V}_w and % utilization in teleost fish (e.g. Davis and Cameron 1971; Randall 1970; Bushnell and Brill 1992). We also characterized the effects of these spontaneous changes in \dot{V}_w on $\dot{M}O_2$, as a comparator for examining \dot{V}_w *versus* $\dot{M}O_2$ relationships during experimental

manipulations of respiratory gases in the ambient water. Next, we examined the impact of acute 10 mM HEA exposure on the same parameters under normoxia. Our focus here was on the short-term hypoventilatory response as the longer term hyperventilatory response to HEA (Eom et al. 2019; Chapter 3) was too time-variable for analysis (*see* Results), and probably also less relevant to the day-to-day life of the animal. Finally, we examined these same parameters in hagfish acutely exposed to environmental hypercapnia (1% CO₂, PCO₂ = 7.5 Torr, 1.0 kPa), to severe environmental hypoxia (~8% air saturation, PO₂ = 13.0 Torr, 1.7 kPa), and to environmental hyperoxia (~275% air saturation, PO₂ = 430 Torr, 57.6 kPa), followed by simultaneous exposure to 10 mM HEA to evaluate possible interactive effects. We hypothesized that the initial responses would be similar to those documented by previous workers as outlined above – i.e. marked hyperventilation in response to hypercapnia and hypoxia, and moderate hyperventilation in response to hyperoxia. We also predicted that because it is an important defensive response to delay and therefore minimize ammonia uptake (Eom et al. 2019; Chapter 3), the hypoventilation caused by HEA would persist regardless of the presence of the other respiratory gas treatments.

4.3 Materials and Methods

4.3.1 Experimental animals

Under permits (XR-202-2016, XR-194-2017, XR-204-2018, and XR-212-2019) from the Department of Fisheries and Oceans Canada (DFO), Pacific hagfish (*Eptatretus stoutii*, 50 ~ 120 g) were captured in Trevor channel (48° 50.8440' N, 125 ° 08.3210' W) close to Bamfield Marine Sciences Centre (BMSC) located on the southwest coast of Vancouver Island, BC, Canada. Bottom-dwelling traps baited with strips of Pacific hake (*Merluccius productus*) were used. At BMSC, captured hagfish were placed in fiberglass tanks served with flowing sea water (temperature 11 to 13 °C, salinity 30 to 31 ppt) and short pieces of pipe for shelter. The animals were regularly provided with hake strips but rarely fed in captivity. Experiments were performed under animal utilization protocols (AUP) approved by the University of British Columbia (A14-0251, A18-0271) and BMSC Animal Care Committees (AUP RS-17-20, RS-18-20, RS -19-15), and followed the guidelines of the Canadian Council of Animal Care. All experiments reported here were performed on hagfish that were fasted for at least one week. After experiments, the hagfish were anesthetized by an overdose of tricaine methane sulfonate (MS-222, 5 g L⁻¹ neutralized to pH 7.8 with 5 M NaOH; Syndel laboratories, Parksville, Canada) and euthanized by evisceration to ensure death.

4.3.2 Ventilation flow recording from the nostril duct

The hagfish are nocturnal so mostly active after sunset, therefore surgical operations were performed during the day-time and most experiments were performed during the night-time in an area that was well shielded from disturbance. Prior to operation, the hagfish were anesthetized in MS-222 (0.6 g L⁻¹, neutralized to pH 7.8 with 5 M NaOH) for 1 to 2 min, placed on an operating table without gill irrigation as they were very hypoxic tolerant, and moistened with sea water wet tissue during air exposure. As previously described (Eom and Wood 2019; Eom et al. 2019; Chapters 2 and 3), a 3-cm length of transparent silicone tubing (6.35 mm O.D. and 4.32 mm I.D.) was inserted into the nostril duct of the hagfish, secured by two stitches (26 mm 1/2C taper, Perma-Hand Silk, Ethicon, Somerville, NJ, USA) laterally to the skin. After the operation, the hagfish were allowed to recover in flowing sea water. Upon recovery they almost always adopted a typical coiled posture.

Similar to the approach of Perry et al. (2009b) and Eom et al. (2019; Chapter 3), the ventilatory flow rate of hagfish (\dot{V}_w) was measured using an ultrasonic microcirculation blood flow probe (V-series, Transonic Systems Inc., Ithaca, NY, USA) attached to a dual-channel small animal blood flowmeter (T106 series, Transonic Systems Inc.) (Fig. 4.1A). The hagfish often exhibited anti-predation responses such as generating slime and knotting behavior in response to any attachments on their body including the flow probe, therefore, it was connected onto the nostril tubing only during periods of ventilation recording. The measured analogue signal was amplified (LCA-RTC, Transducer Techniques, Temecula, CA, USA), converted into digital signals in a PowerLab data integrity system (ADInstruments, Colorado Springs, CO, USA), and visualized and analyzed into ventilation flow (\dot{V}_w , ml min⁻¹) and frequency (fr, min⁻¹) in LabChart software version 7.0 (ADInstruments). The analyzed ventilation flow (ml min⁻¹) data were averaged per 30 sec intervals and divided by fish body weight to yield mass-specific \dot{V}_w (ml kg⁻¹ min⁻¹). As first noted by Perry et al. (2009b), the intrinsic calibration of the flow probe is altered in sea water, so the probe was manually recalibrated by flowing salinity 30 ppt sea water at 12°C at known rates (determined gravimetrically) through the probe attached to the 3-cm length of silicone tubing, by means of an aqua lifter vacuum pump (Cheng Gao Plastic and Hardware Electricity, Dongguan, Guangdong, China). The flow correction was incorporated by the LabChart software. The standardized \dot{V}_w was then divided by fr (frequency of velum contraction as detected in the flow trace; Eom and Wood 2019; Chapter 3) in order to calculate mean stroke volume (SV_w, ml kg⁻¹) for the period. During or after recording, electrical and/or physical non-specific noise signals were removed by a low-pass type filter in a range between 1 to 10 Hz which was incorporated in the LabChart software. The flow probe (Transonic Systems Inc.) detects the direction of flow so correct orientation of flow probe was essential.

4.3.3 Series I. Measurement of oxygen partial pressure (PO_2) from gill openings including the pharyngo-cutaneous duct (PCD)

Each individual hagfish was placed in a 2-L plastic container served with flowing normoxic sea water ($PO_2 > 75\%$ air saturation, > 118 Torr, > 15.7 kPa). Pacific hagfish generally have 12 gill pouch openings on the ventral surface on each side (~24 in total) plus the opening of the larger pharyngo-cutaneous duct (PCD) on the left side (Eom and Wood 2019; Chapter 2). Prior to measurements under normoxia, the coiled hagfish ($N = 14$ for control measurements) were gently flipped over in order to expose the ventrally placed gill openings (Fig. 4.1A). After that, an oxygen sensor (micro-optode) mounted in a #23 hypodermic needle and attached to a micro-fiber optic oxygen meter (PreSens, Microx TX 3, Precision Sensing GmbH, Regensburg, Germany) was carefully placed within 5 mm of the respective gill openings by adjusting the model M33301R three-axis micro-manipulator (Narishige, Tokyo, Japan), which was magnetically mounted on an iron plate. To move the probe between gill openings, the micro-manipulator was moved on the plate, then the micro-optode was correctly repositioned by fine adjustments with the micro-manipulator. The oxygen partial pressures (expressed as % air saturation) of the exhaled water (P_{EO_2}) at each of the 12 gill openings on one side including the PCD, as well as the inspired P_{IO_2} of water inhaled *via* the nostril duct, were measured in control normoxia initially. Ventilation is very variable in hagfish, and based on prior experience (Eom and Wood 2019; Eom et al. 2019; Chapters 2 and 3), we recognized three types of spontaneous ventilation in resting animals: normal ventilation ($75 \sim 175$ ml kg^{-1} min^{-1}), hypoventilation (< 75 ml kg^{-1} min^{-1}) and hyperventilation (> 175 ml kg^{-1} min^{-1}), in addition to apnea. Collected data were assigned to these three categories; the apnea was not included.

Following completion of the resting measurements under normoxia, comparable measurements were made in 10 mM HEA, 1% CO_2 , severe hypoxia, and hyperoxia sequentially. The methods used for creating these various respiratory gas treatments are explained in Series II and III below. In each of the treatments, the P_{EO_2} measurements from all the sites took about 0.5-h, and the order of the application of the different treatments was varied randomly among the fish, with 0.5-h between different gas treatments. It was not possible to test all gas treatments in all fish. As noted in Results, the measured P_{EO_2} from the respective gill openings typically fluctuated slightly in a rhythmic fashion over time at a much slower frequency than the velum movements, and this likely reflected ventilatory contraction of the gill pouches. The data were collected in TX3 software version 6.02 (PreSens) and the P_{EO_2} values were exported to Excel and averaged for further calculations. For example, in each hagfish, these averaged P_{EO_2} (% air

saturation) values for each gill opening and the PCD were used for calculation of O₂ % utilization by Equation 1:

$$\text{O}_2 \text{ \% Utilization} = [\text{P}_{\text{I}}\text{O}_2 (\%) - \text{P}_{\text{E}}\text{O}_2 (\%)] / \text{P}_{\text{I}}\text{O}_2 (\%) \times 100 (\%) \quad (\text{Equation 1}).$$

The routine oxygen consumption rate ($\dot{M}\text{O}_2$) was also calculated from these values using Equation 2:

$$\dot{M}\text{O}_2 = [\text{P}_{\text{I}}\text{O}_2 (\text{Torr}) - \text{P}_{\text{E}}\text{O}_2 (\text{Torr})] \times \alpha_{\text{O}_2} \times \dot{V}_w \quad (\text{Equation 2}).$$

As the individual flow rates through each of the 24 gill openings and PCD could not be determined, we used the average $\text{P}_{\text{E}}\text{O}_2$ recorded from the 13 different sites on one side for each fish. The validity of this approach is discussed subsequently. This average $\text{P}_{\text{E}}\text{O}_2$, together with the measured $\text{P}_{\text{I}}\text{O}_2$, nostril ventilatory flow rate (\dot{V}_w in $\text{L kg}^{-1} \text{ h}^{-1}$) and the appropriate O₂ solubility coefficient (α_{O_2} , $1.7747 \mu\text{mol Torr}^{-1} \text{ L}^{-1}$) for 30 ppt sea water at 12°C (Boutilier et al. 1984) were used in the calculation. Prior to $\dot{M}\text{O}_2$ calculation, PO₂ (% air saturation) values were converted into O₂ tensions in Torr, taking into account the barometric pressure and the vapour pressure of water at 12°C.

4.3.4 Series II. Basic ventilatory responses to high environmental ammonia (HEA)

Each individual hagfish (N = 9) was placed in a plastic container which was filled with 2 L of normoxic sea water (PO₂ >75 % air saturation, >118 Torr, >15.7 kPa). Animals exhibiting spontaneous apnea during the control period (*see* Eom and Wood 2019; Chapter 2) were not used. After the hagfish ventilation was stable, the ventilatory parameters (\dot{V}_w , fr) were measured (control) for about 5 min. Then, 40 ml of 500 mM of NH₄HCO₃ (Sigma-Aldrich, St. Louis, MO, USA) was added into the air-bubbled sea water of the individual hagfish container in order to prepare 10 mM HEA (PNH₃: 2,643 μTorr or 0.000352 kPa). The HEA treatment typically lasted 120 min. After HEA treatment, the hagfish were recovered by flushing normoxic sea water directly through the plastic container; the recovery period typically lasted 30 min. Ventilatory parameters (\dot{V}_w , fr, and calculated SV_w) were recorded throughout the HEA and recovery periods.

4.3.5 Series III. Ventilatory responses to other respiratory gases and interactive effects of exposure to HEA

The same measurements of ventilatory parameters (\dot{V}_w , f_r , and calculated SV_w) as in Series II were performed in individual hagfish under control normoxic conditions ($PO_2 > 75\%$ air saturation, > 118 Torr, > 15.7 kPa) and then during three different experimental treatments, each on separate hagfish. Again, animals exhibiting spontaneous apnea during the control period were not used. These treatments involved exposure to alterations in environmental PCO_2 or PO_2 for at least 1 h to allow patterns to stabilize, followed by acute exposure to 10 mM HEA as in Series II, though it lasted only for 10 min. This was followed by a 30-min recovery period when the chamber was flushed with normoxic sea water. The goal was to understand firstly the basic responses to the respiratory gas treatments, and secondly whether the presence of these other respiratory gas treatments affected the acute response to HEA – i.e. possible interactive effects. The experimental treatments included severe hypoxia ($\sim 8\%$ air saturation, $PO_2 = 13.0$ Torr, 1.67 kPa) ($N = 4$), hyperoxia ($\sim 275\%$ air saturation, $PO_2 = 430$ Torr, 57.6 kPa) ($N = 5$), or hypercapnia (1% CO_2 , $PCO_2 = 7.5$ Torr, 1.0 kPa) ($N = 7$). For hypercapnia, 1 part of 100% CO_2 (Praxair, Delta, Canada) was mixed with 99 parts of air using a Wösthoff 301aF gas-mixing pump (Bochum, Germany) so as to generate 1% CO_2 . This was directly bubbled into the hagfish container. Also, the hypoxic or hyperoxic environments were prepared by bubbling pure N_2 or O_2 (Praxair) directly into the fish container. The decreasing or increasing oxygen concentration was continuously monitored by an O_2 macro-electrode and meter (YSI, Model 55, OH, USA). Similar to Series II, for acute HEA exposure, 40 ml of 500 mM NH_4HCO_3 (Sigma-Aldrich) was added to the individual fish containers to administer 10 mM HEA in the continuing presence of the other gas treatment.

4.3.6 Statistical analyses

The measured P_{iO_2} , P_{eO_2} , \dot{V}_w and f_r , and calculated SV_w , % O_2 utilization, $\dot{M}O_2$, and convection requirement values have been reported as means \pm standard error of the mean (S.E.M.) (N) where N represents the number of fish contributing to the mean. Multiple comparisons were performed by one-way ANOVA followed by Tukey's post hoc test to identify individual differences, with appropriate transformations to achieve normality and homogeneity of variances. Regression lines were compared by ANCOVA. Student's one-tailed t-test was used to assess whether responses to individual respiratory gas stimuli were significant, where the direction of change was predicted. All tests were performed using

GraphPad Prism software version 6.0 (La Jolla, CA, USA), and a threshold for statistical significance of $p < 0.05$ was used throughout.

4.4 Results

4.4.1 Series I - Measured expired O_2 tensions and calculated O_2 utilization under normoxia and in various respiratory gas treatments

The hagfish inhaled external sea water (P_{iO_2} , $90.0 \pm 1.3\%$ air saturation; 141.3 ± 1.2 Torr; 18.8 ± 0.2 kPa, $N = 14$) *via* the nostril and exhaled *via* the gill openings after exchanging respiratory gases in the gill pouches. P_{EO_2} in the gill openings was correlated to spontaneous ventilation changes. Fig. 4.1B illustrates an experiment in which a hypoventilating hagfish with a \dot{V}_w of ~ 5 ml kg^{-1} min^{-1} suddenly initiated spontaneous hyperventilation with a \dot{V}_w of ~ 270 ml kg^{-1} min^{-1} . This caused marked changes in P_{EO_2} measured at the gill openings, and therefore in % O_2 utilization. Fig. 4.1C shows an example of a P_{EO_2} recording at one particular gill pouch, displayed on a fine scale. Very small rhythmic fluctuations of P_{EO_2} are apparent, that were visually correlated to the gill pouch contraction rhythm (typically 3 ~ 6 min^{-1}) that was much lower than the velar pumping rhythm.

As described in Methods, we classified ventilation and accompanying P_{EO_2} data collected under control normoxic conditions as either normal ventilation (\dot{V}_w : 136.7 ± 20.8 ml kg^{-1} min^{-1} , fr: 12.2 ± 1.1 min^{-1} , SVw: 11.2 ± 0.8 ml kg^{-1}), hypoventilation (\dot{V}_w : 59.5 ± 1.5 ml kg^{-1} min^{-1} , fr: 9.3 ± 2.2 min^{-1} , SVw: 6.4 ± 1.7 ml kg^{-1}), or hyperventilation (\dot{V}_w : 276.4 ± 13.3 ml kg^{-1} min^{-1} , fr: 24.4 ± 2.2 min^{-1} , SVw: 11.3 ± 3.9 ml kg^{-1}). Thus, spontaneous changes in \dot{V}_w involved changes in both fr and SVw. In general, the percentage utilization of O_2 was graded in an anterior-to-posterior direction, being higher when measured from water exiting the posterior pouches than from the anterior ones (Fig. 4.2B, D, F). This was confirmed by significance in one-way ANOVA for normal ($p = 0.0274$) and hypoventilation ($p = 0.0032$) but not for hyperventilation ($p = 0.1098$).

Note that the utilization calculation is based on comparing the measured P_{EO_2} of water exiting by each of the 13 pathways (12 gill openings, plus the opening of the PCD) with the single P_{iO_2} value of all entering water, inhaled though the only entrance, the nostril. P_{EO_2} at the PCD was similar to those at the posterior pouches, except under hypoventilation when it tended to be higher (Fig. 4.2A, C, E). However, when averaged over all hagfish, the differences were not particularly marked. For example, in normally ventilating hagfish, the greatest variation was from a minimum mean value of 25.0% utilization at the 4th

gill opening to 46.9% at the 11th gill opening (Fig. 4.2B). During normal ventilation, average $P_{E}O_2$ from exhaled water at the 12 gill openings and PCD was 56.2 ± 6.5 (7) % air saturation (Fig. 4.2A). As a result, the fish utilized 34.1 ± 6.5 (7) % of the inspired O_2 on an overall basis (Fig. 4.2B). Compared to normally ventilating hagfish, the hyperventilating hagfish exhibited similar overall O_2 utilization (37.0 ± 7.0 (6) %, Fig. 4.2C) in their gill pouches, so the fish exhaled sea water that contained a similar mean O_2 tension ($P_{E}O_2$: 54.8 ± 7.6 (6) % air saturation (Fig. 4.2D). However, these patterns were very different in spontaneously hypoventilating hagfish; the fish exhaled severely hypoxic water due to significantly increased O_2 utilization (O_2 utilization = 91.3 ± 4.3 (6) %, $P_{E}O_2$: 6.2 ± 2.7 (6) % air saturation, Figs. 4.2E, F).

Except for the severe hypoxia treatment (Fig. 4.3E, F), the other three respiratory gas treatments all resulted in similar mean O_2 utilizations ranging from 25.2% in hyperoxia (Fig. 4.3H) to 30.6% in 1% CO_2 hypercapnia (Fig. 4.3D) and 32.4% in 10 mM HEA (Fig. 4.3B); none of these were significantly different from the 34.1% in normally ventilating hagfish under normoxic control conditions (Fig. 4.2B). However, it should be noted that both mean $P_{I}O_2$ (280% air saturation) and mean $P_{E}O_2$ (197%) were much higher in the hyperoxic hagfish (Fig. 4.3G) than in the hagfish treated with 10 mM HEA (Fig. 4.3A) or 1% CO_2 hypercapnia (Fig. 4.3C), where mean $P_{I}O_2$ and $P_{E}O_2$ were about 90% and 62% air saturation respectively. Overall, similar to the situation in normoxia (Fig. 4.2), posterior gill pouches and PCD consumed more O_2 than anterior ones (as confirmed by one-way ANOVA (Fig. 4.3A: $p = 0.0403$, Fig. 4.3C: $p = 0.0061$, Fig. 4.3G: $p = 0.0243$), except in the hypoxia treatment (Fig. 4.3E: $p = 0.4965$), and hypoventilating hagfish utilized more O_2 than hyperventilating hagfish.

In light of the fairly uniform values of $P_{E}O_2$ and O_2 utilization among the different gill pouches and PCD seen within the various treatments, we proceeded to calculate routine $\dot{M}O_2$ by Equation 2 using the $P_{I}O_2$, mean \dot{V}_w , and overall mean $P_{E}O_2$ values (from the 13 measurement sites) for each fish under each condition. The spontaneous differences in ventilation seen among normally ventilating, hypoventilating, and hyperventilating hagfish under control normoxic conditions resulted in significant alterations in $\dot{M}O_2$ (Fig. 4.4A). Compared to the $\dot{M}O_2$ during normal ventilation ($718.0 \mu\text{mol kg}^{-1} \text{h}^{-1}$), $\dot{M}O_2$ was decreased by 71% in hypoventilating hagfish but increased by 87% in hyperventilating animals (Fig. 4.4A). The 10 mM HEA treatment resulted in a 64% reduction in $\dot{M}O_2$, and severe hypoxia caused a significant 85% fall, whereas hyperoxia resulted in a significant 204% elevation in $\dot{M}O_2$ (Fig. 4.4B). Hypercapnia had no significant effect on routine $\dot{M}O_2$ (Fig. 4.4B).

4.4.2 Series II - Ventilation changes in 10 mM high environmental ammonia (HEA)

In exposures to 10 mM HEA alone, hagfish initially decreased \dot{V}_w by 33% ($p = 0.0201$) (Fig. 4.5B). This decrease in \dot{V}_w was achieved by a significant decrease in f_r (Fig. 4.5A, $p = 0.0361$) while SV_w did not change (Fig. 4.5C) This effect persisted through 10 min of HEA exposure. However, when HEA was removed by the addition of fresh seawater, overall ventilatory parameters quickly returned to the original control levels (Fig. 4.5, $p = 0.0418$). The HEA exposures were typically maintained for about 2 h, but the responses during this longer time period were very variable. Some hagfish either maintained or intensified the ventilatory inhibition, whereas in others ventilation gradually rose back to or above controls with differing time courses. This is in accord with the pattern reported by Eom et al (2019; Chapter 3) where HEA acutely inhibits ventilation, and then ventilation later recovers and eventually increases above the control level as HEA is maintained up to 3 h. For this reason, in the subsequent tests with the other respiratory gases, the 10 mM HEA exposure period was limited to 10 min (with measurements at 2 min and 10 min), so as to evaluate only whether the acute inhibitory effect of 10 mM HEA on ventilation was affected by the simultaneous presence of the other respiratory gas treatment.

4.4.3 Series III - Ventilation changes in 1% hypercapnia, hypoxia, hyperoxia, and 10 mM HEA

Exposure to hypercapnia alone had minimal overall effects. In general, ventilatory responses to 1% CO_2 were variable, with some fish increasing and some decreasing \dot{V}_w ; none of the changes in this series were significant (Fig. 4.6). After the addition of 10 mM HEA in the continuing presence of 1% CO_2 , the hagfish showed a pattern of decreased \dot{V}_w due to lowered SV_w that was maintained for 10 min. These decreased ventilatory parameters gradually recovered after the addition of fresh seawater. Average frequency levels (f_r) were barely changed regardless of the different treatments (Fig. 4.6).

During the severe hypoxia treatment (mean $P_{iO_2} \sim 8\%$ air saturation, 1.67 kPa, 13 Torr) the hagfish increased \dot{V}_w by 122% ($p = 0.0272$) but the increased flow was greatly decreased below the control level ($p = 0.0058$) when acute 10 mM HEA was added in the continuing presence of hypoxia. However, thereafter, \dot{V}_w tended to increase again so this hypoventilatory effect did not persist for 10 min, and there was complete recovery back to control levels after the addition of fresh seawater (Fig. 4.7B). The pattern of changes in f_r paralleled that of \dot{V}_w . The initially increased f_r accompanying hypoxia was decreased to 76% of control levels by HEA ($p = 0.0360$) and lasted for 10 min (Fig. 4.7A). Changes in SV_w were variable and non-significant (Fig. 4.7C).

During the hyperoxia treatment (mean $P_{\text{I}O_2} \sim 275\%$ air saturation, 57.6 kPa, 430 Torr), hagfish barely changed overall ventilatory parameters but when HEA was added in the continuing presence of hyperoxia, the parameters of f_r and \dot{V}_w were immediately decreased by 40% (Fig. 4.8A, $p = 0.0483$) and 55% (Fig. 4.8B, $p = 0.0313$) respectively. A slight decrease in SV_w was not significant (Fig. 4.8C). After 10 min in 10 mM HEA plus hyperoxia, the suppressed ventilatory parameters recovered toward control levels so there was little further change upon the addition of fresh seawater.

4.5 Discussion

4.5.1 Overview

An important overall conclusion, based on this and our two preceding studies (Eom and Wood 2019; Eom et al. 2019; Chapters 2 and 3) is that when hagfish are non-stressed and allowed to exhibit normal behaviour, their respiratory physiology is very variable. \dot{V}_w can range from 0 $\text{ml kg}^{-1} \text{min}^{-1}$ (during periods of prolonged apnea) to $>400 \text{ ml kg}^{-1} \text{min}^{-1}$ (during extreme spontaneous hyperventilation). Our impression is that much of this variability disappears when the animal becomes stressed, accompanied by high continuous \dot{V}_w . The responses of resting hagfish to standardized respiratory gas stimuli are also highly variable, ranging from no or small responses to very large responses on variable time scales, and sometimes opposite responses in different animals, as seen with the 1% CO_2 treatment. In the present study, our focus was on unstressed animals, so it is unclear how highly stressed animals respond to respiratory gas stimuli.

With respect to our original goals, we found a general trend, moving from anterior to posterior gill pouches, for $P_{\text{E}O_2}$ to decrease, and therefore % utilization to increase, supporting the idea that some water may be recycled in the pharynx as it moves from front-to-back before being exhaled (Fig. 4.1B, C; Figs. 4.2, 4.3). However, as $P_{\text{E}O_2}$ was also low at the PCD, we did not confirm the idea that % utilization would be low at this bypass shunt. We also confirmed the well-known inverse relationship between \dot{V}_w and % utilization seen in teleost fish. However, it was surprising that % utilization could exceed 90% in spontaneously hypoventilating hagfish under normoxia (Fig. 4.2B), and 80% in hyperventilating hagfish under severe hypoxia (Fig. 4.3F), and also that utilization could be maintained at a constant level between normal ventilation and hyperventilation under normoxia (Fig. 4.2D, F). Clearly, $\dot{M}O_2$ depends on \dot{V}_w (Figs. 4.4, 4.9). In accord with previous studies, we found that acute exposure to HEA inhibited \dot{V}_w (Fig. 4.5), that acute hypoxia stimulated \dot{V}_w (Fig. 4.7), and we confirmed the unusual lack of a hypoventilatory response to hyperoxia (Fig. 4.8). However, there was no overall effect of hypercapnia on \dot{V}_w (Fig. 4.6),

in contrast to a previous report (Perry et al. 2009). By exploiting the wide range of individual \dot{V}_w versus $\dot{M}O_2$ measurements, we uncovered effects of respiratory gas treatments superimposed on the effects of \dot{V}_w alone (Fig. 4.9). Finally, in accord with our original prediction, the acute inhibitory influence of HEA persisted in the presence of hypoxia (Fig. 4.7) and hyperoxia (Fig. 4.8), showing its importance as a protective measure to minimize the uptake of toxic waterborne ammonia. However, the response was blunted during hypercapnia (Fig. 4.6) likely due to a water chemistry effect, as explained below. We concluded that the hagfish possesses a flexible respiratory system with considerable reserve capacity.

4.5.2 Ventilation, utilization, and $\dot{M}O_2$ under normoxia

In general, $\dot{M}O_2$ in resting hagfish was at least 4-fold lower than in teleosts (Clarke and Johnston 1999) and 2-fold lower than in elasmobranchs (Carlson et al. 2004). Our resting $\dot{M}O_2$ measurements ($\sim 700 \mu\text{mol kg}^{-1} \text{h}^{-1}$) obtained by direct measurement of \dot{V}_w and P_{iO_2} , and using an average of all 13 measurements of $P_{E O_2}$ at the different exits, would presumably have missed the small fraction (<20%) of $\dot{M}O_2$ thought to occur across the skin in this species (Clifford et al. 2016). Nevertheless, this resting $\dot{M}O_2$ agreed well with some previous measurements obtained by classic closed system respirometry of the whole animal (Weinrauch et al. 2018; Eom et al. 2019; Giacomini et al. 2019 b), but was 1.5 to 2-fold higher than in three other respirometry studies at comparable temperature (Muniz and Morris 1965; Perry et al. 2009b; Giacomini et al. 2019b). From Fig. 4.4B, it is clear that the extent of spontaneous hypoventilation or hyper-ventilation can have a large effect on resting $\dot{M}O_2$, as can periods of spontaneous apnea (Eom and Wood 2019; Chapter 2). In addition to flow effects on gas exchange in the gill pouches, it is possible that differences in $\dot{M}O_2$ associated with the differences in ventilation are also being influenced by regional O_2 consumption along the pharynx that may vary with increasing or decreasing ventilation as transit times are altered. Steffensen et al. (1984) reported much higher $\dot{M}O_2$ in non-buried *Myxine glutinosa*, approximately equal to that in hyperventilating *E. stoutii* in our experiments (Fig. 4.4B). Unlike *E. stoutii* which have a broad range of surface substrate types in the benthic deep-sea environment (McInerney and Evans 1970), *M. glutinosa* are known to bury themselves in patches of mud between rocks (Tambs-Lyche 1969) and therefore may have been stressed by the lack of immersion.

Spontaneous changes in \dot{V}_w at rest (Fig. 4.2B) involved changes in both f_r and SV_w , in accord with our previous investigations (Eom and Wood 2019; Eom et al. 2019; Chapters 2 and 3). However, changes in \dot{V}_w in response to respiratory gas stimuli involved mainly changes in f_r (Figs. 4.5, 4.6, 4.7,

4.8)., in agreement with previous studies that reported that only velar frequency (f_r) changed (Perry et al. 2009b; Coxon and Davison 2011). Under resting conditions in normoxia, “normal” \dot{V}_w was about 137 ml $\text{kg}^{-1} \text{min}^{-1}$ (Fig. 4.2) which agrees well with our previous study (125 ml $\text{kg}^{-1} \text{min}^{-1}$; Eom and Wood 2019; Chapter 2) but is lower than the 235 ml $\text{kg}^{-1} \text{min}^{-1}$ reported by Perry et al. (2009b) for *E. stoutii* at comparable temperature. In *Myxine glutinosa*, buried in sand, \dot{V}_w was 45 ml $\text{kg}^{-1} \text{min}^{-1}$ at 15°C, but this increased to 140 ml $\text{kg}^{-1} \text{min}^{-1}$ when the animals were temperature-stressed at 20°C (Steffensen et al. 1984). Taking differences in mass and temperature into account, the present value for *E. stoutii* appears to be on the low end of \dot{V}_w values recorded in teleost with similar benthic, inactive lifestyles - e.g. tench (*Tinca tinca*; Eddy 1974), carp (*Cyprinus carpio*; Lomholt and Johansen 1979), and flounder (*Platichthys stellatus*; Wood et al. 1979), that have very different ventilatory mechanisms and gill structure. These relatively low \dot{V}_w values, together with generally lower % utilization (~35%; Fig. 4.2) versus higher values in these teleosts (55 ~ 80%) explains the lower $\dot{M}O_2$ in the hagfish. However, \dot{V}_w , % utilization, and $\dot{M}O_2$ values in the big skate (*Raja ocellata*; Graham et al. 1990), an elasmobranch that also has a very different respiratory system from the hagfish, were all very similar to values in *E. stoutii*.

The utilization calculations quantify the O_2 extraction of each of the 13 pathways, comparing the measured $P_{E}O_2$ of the exiting water of each to the common single $P_{I}O_2$ value of the water inhaled through the only entrance, the nostril. While the general organization of the 13 pathways is in parallel, not in series, the general trend for increasing % utilization from anterior to posterior gill pouches (Figs. 4.2, 4.3) would be in accord with some recycling of water as it flowed posteriorly via the pharynx. Alternate or additional explanations could simply be that the posterior gills are more efficient at gas exchange, and/or that this reflects the cumulative removal of O_2 by the bordering tissues of the pharynx as the water passes posteriorly along the respiratory tract. Nevertheless, it is easy to speculate that the inhaled water moves very slowly through the pouches or may even be briefly stored in the pouch structure for respiratory gas exchange. The afferent and efferent branchial ducts are guarded by sphincters (Malte and Lomholt 1998). The gill pouches contract at a low rhythm (Fig. 4.1D; Eom and Wood 2019; Chapter 2) and in a peristaltic anterior-to-posterior manner as described in *Myxine glutinosa* (Johansen and Hol 1960; Johansen and Strahan 1963), which was visually observed in the present study. While this aids exhalation through the efferent branchial ducts, perhaps the sphincters allow some of the water to instead be forced back into the pharynx through the afferent branchial ducts, and therefore rebreathed (“recycled”) by more posterior gill pouches. The generally high % utilization at the PCD exit suggests that the PCD does not act as a by-pass shunt under resting conditions, but rather serves to collect some of this sequentially rebreathed water. It could still assume a bypass shunt function when sediment or food particles need to be cleared.

The ability of *E. stoutii* to maintain % utilization unchanged (~35%) between “normal” and spontaneous hyperventilation at rest, and to increase it above 90% during spontaneous hypoventilation (Fig. 4.2 B, D, F) indicates a respiratory system with considerable reserve capacity. In addition to the complex gill structure and moderate blood-to-water diffusion distance (Mallatt and Paulsen 1986), other key adaptations may be the counter-current flow of blood and water (Bartels 1998; Johansen and Strahan 1963; Malte and Lomholt 1998), an ability to vary blood flow distribution by opening or closing arterio-venous pathways in the gills (Bartels 1998), and a blood O₂-dissociation curve with a fairly high O₂ affinity, though to our knowledge, this has only been measured in the related *Eptatretus cirrhatus* (P50 ~ 12 Torr; Wells et al. 1986). In addition, hypoventilating hagfish may store inhaled water in their gill pouches much longer, thereby decreasing physiological dead-space and greatly increasing oxygen utilization (Hofbauer 1934).

4.5.3 Ventilation, utilization, and $\dot{M}O_2$ under respiratory gas treatments

The hagfish are mostly scavengers, browsing on carrion-dead falls (Smith 1985). They penetrate into cavities *via* soft tissues or opercular regions, and/or rasp or engulf pieces of carcass (Eom and Wood 2019; Chapter 2). In this feeding environment, the hagfish would likely experience a mixture of respiratory gas stimuli, such as depleted oxygen (hypoxia), and highly increased carbon dioxide (hypercapnia) and ammonia (HEA) emanating from the dead items. The short-term response to HEA is hypoventilation and/or apnea occurring over a time scale of minutes (Eom et al. 2019; Chapter 2), which is the response studied here (Figs. 4.5, 4.6, 4.7, and 4.8). This short-term decrease in breathing would likely be an ideal defensive mechanism to reduce inhalation of noxious water, and thereby minimize ammonia uptake across the gills, for the amount of time the hagfish would spend either immersed in or close to a rotting carcass while feeding in such an HEA environment. From our personal observations on hagfish feeding in captivity (J Eom and CM Wood, unpublished), this species does not often spend long periods inside dead prey, but rather makes short forays, dipping its head into or onto the surface of the prey, rasping off pieces that it ingests by engulfment. After ingesting at most 20 g of food, the hagfish (~100g BW) stops feeding and leaves the prey, then coils on the bottom of the tank where it stays digesting, more or less motionless, for several days. Therefore, it is believed that bouts of fairly short-term acute exposures may be more relevant to the day-to-day life of the species. Not surprisingly, as % utilization was unaltered (Fig. 4.3B), $\dot{M}O_2$ also tended to fall (Fig. 4.4B) in accord with the fall in $\dot{V}w$ (Fig. 4.5). Interestingly, the anterior-to-posterior gradient in % utilization among the gill pouches became particularly marked during HEA exposure, suggesting some re-organization of water flow (Fig. 4.3B).

The acute reduction in \dot{V}_w is thought to be initiated by external receptors as a defensive response (Eom et al. 2019; Chapter 2). While these could be chemoreceptors responsive to other respiratory gases, it is more likely that they are the well-developed olfactory rosettes (Theisen 1976; Holmes et al. 2011) or the taste-bud-like receptors of the Schreiner organs in the epidermis of the head, trunk and along the respiratory tracts (Braun 1998; Braun and Northcutt 1998). It was predicted that as a defensive response, the inhibition of \dot{V}_w by HEA would persist in the presence of other respiratory stimuli, and this indeed was observed, though its duration may have been shortened by hypoxia (Fig. 4.7) and hyperoxia (Fig. 4.8), with these drives resuming precedence over time. The response was not significant in hypercapnia (Fig. 4.6) where it may have been blunted for physico-chemical reasons. Because of the acidifying effect of CO₂, the water pH of the 10 mM HEA exposure in the presence of 1% CO₂ was approximately 7.95 and this would have lowered the PNH₃ from 5,948 μTorr (0.000793 kPa) in the normoxic situation (pH = 8.3) to 2,643 μTorr (0.000352 kPa) in the hypercapnic treatment.

Over the longer term, ammonia may build up internally after feeding, taken up from the HEA environment and/or produced metabolically by the exercise accompanying feeding and processing of the protein-rich meal (Wilkie et al. 2017). As in teleosts (Zhang et al. 2011) and elasmobranchs (De Boeck et al. 2015), the long-term response in *E. stoutii* is hyperventilation occurring over a time scale of hours (Eom et al. 2019; Chapter 3); in both hagfish and these other fish, this response can be elicited by ammonia injection and appears to be mediated by internal chemoreceptors. At least in teleosts, these ammonia-sensitive chemoreceptors appear to be the neuro-epithelial cells (NECs) in the gills which are likely polymodal receptors responsive to O₂, CO₂, ammonia and other stimuli (Perry and Tzaneva 2016; Jonz 2018), though the brain may also be involved (Zhang et al. 2013). To our knowledge, NECs have not been described in hagfish, but the cyanide injection experiments of Perry et al. (2009b) suggest that either they, or functional analogues, must be present. At least in teleosts, ammonia excretion is sensitive to convective water flow when branchial Rh proteins are activated by elevated plasma ammonia (Eom et al. 2020; now Chapter 5), so long-term hyperventilation would serve to flush out the excess ammonia *via* the Rh proteins (Braun and Perry 2010; Edwards et al. 2015; Clifford et al. 2017). By increasing \dot{V}_w , it would also facilitate greater O₂ uptake (Fig. 4.4A) and CO₂ excretion during the post-feeding period of high metabolic demand (“Specific Dynamic Action” or SDA; Weinrauch et al. 2018).

The mean level of acute hypoxia in our experiments was a P_IO₂ of about 8% air saturation (1.67 kPa, 13 Torr; Fig. 4.3E); hagfish responded by increasing \dot{V}_w by 122% (Fig. 4.7B), but appeared to remain calm, keeping their normal coiled posture. Despite a marked increase in % utilization (Fig. 4.3F), $\dot{M}O_2$ fell by 85% (Fig. 4.4A). The hyperventilatory response was qualitatively similar to that reported in

E. stoutii by Perry et al. (2009b) using a similar level of hypoxia and similar measurement methods. Exact comparison is difficult, as Perry et al. (2009b) normalized their data to $\Delta\dot{V}_w$ above baseline, but the present response would appear much smaller. These same authors, using a more moderate level of hypoxia (33% air saturation) in separate closed-system respirometry experiments, reported that $\dot{M}O_2$ was maintained constant, but Giacomini et al. (2019a), using an intermediate level of hypoxia (20% air saturation), reported a significant rise in the ventilatory index (a proxy for \dot{V}_w) and a 49% fall in $\dot{M}O_2$ by closed-system respirometry. Overall, these data are congruent with recent findings that under identical conditions, the P_{crit} of *E. stoutii*, where $\dot{M}O_2$ becomes dependent upon P_{iO_2} is about 11.2% air saturation (2.33 kPa, 17.5 Torr; A Clifford and CM Wood, unpublished data), and the report of Drazen et al. (2011) that it is about 6.8 % air saturation (1.43 kPa, 11 Torr) at a lower temperature (5°C). Therefore, the differences in the $\dot{M}O_2$ responses among Perry et al. (2009), Giacomini et al. (2019a), and the present study (Fig. 4.4A) reflect the differences in the levels of hypoxia employed.

Note that the hagfish in all these studies were acclimated to normoxia, and this may not be representative of the deep-sea benthic environment in which these animals normally live, as noted by Drazen et al. (2011). Indeed, the hagfish used in the present experiments were captured at depth of ~100 m (10.4°C) in Trevor channel close to BMSC. The mean PO_2 measured in the water next to the traps was 14.5% air saturation (23 Torr, 3.0 kPa) (CellOx325, WTW GmbH & Co., Weiheim, Germany) (personal communication, Ora Johannsson).

The mean level of acute hyperoxia in our experiments was a P_{iO_2} of about 275% air saturation, (57.6 kPa, 430 Torr). Contrary to the pattern of hypoventilation seen in most other fish (e.g. Wood and Jackson 1980; Heisler et al. 1988), \dot{V}_w did not change during hyperoxia in the hagfish (Fig. 4.8), in agreement with Giacomini et al. (2019b) who reported a non-significant rise in the ventilatory index, and a significant increase in f_r . Indeed, we noticed that the hagfish became restless during hyperoxia exposure and often uncoiled, as though it were an irritant, while Giacomini et al. (2019b) reported associated disturbances in ion and acid-base status. With unchanged mean ventilatory flow and unchanged % utilization despite the greatly increased P_{iO_2} (Fig. 4.3F), $\dot{M}O_2$ was elevated 3-fold in the present study (Fig. 4.4B). Again, all these unusual responses may reflect the fact that *E. stoutii* normally lives in a very hypoxic benthic environment and rarely encounter high O_2 levels. However, live hagfish are commonly sold in Asian wet markets (Homma 1998) where they are held in oxygen-bubbled seawater; this in fact may be detrimental to their wellbeing.

Environmental hypercapnia (1% CO_2 , 1.0 kPa, 7.5 Torr) had no consistent effect on ventilation, such that \dot{V}_w , f_r , SV_w (Fig. 4.6) and $\dot{M}O_2$ (Fig. 4.4B) all remained statistically unchanged. However, this

disguise great variability in responses with some animals hyperventilating, interspersed with short periods of apnea, while others tended to reduce \dot{V}_w , so that when averaged, there were no changes. This contrasts with the report of Perry et al. (2009b) where exposure to 1% CO₂ elicited a consistent increase in \dot{V}_w in *E. stoutii*, though the response appeared to be smaller than that elicited by hypoxia. One experimental difference of our study from that of Perry et al. (2009) is that we randomized the order of the various respiratory gas treatments. It is possible that this contributed to the different results. Our results also contrast with the responses of most other fish, where high external PCO₂ elicits hyperventilation (Gilmour 2001). Note however that the hagfish were acclimated to normocapnia; it would be interesting to measure the PCO₂ in their hypoxic benthic environment. *E. stoutii* is known to be very tolerant of high PCO₂ (Baker et al. 2015; Clifford et al. 2018).

4.5.4 The relationship between $\dot{M}O_2$ and ventilation under different respiratory gas treatments

Given the ability of *E. stoutii* to maintain % utilization unchanged during spontaneous hyperventilation under normoxia, it is not surprising that $\dot{M}O_2$ increased with \dot{V}_w (Fig. 4.4A). However, by just looking at the means (Figs. 4.4B, 4.5, 4.6, 4.7, and 4.8) from different experimental series, it is difficult to see how the relationship changed under the different respiratory gas treatments. Therefore, in Fig. 4.9 we have exploited the wide range of simultaneous individual \dot{V}_w versus $\dot{M}O_2$ measurement pairs made in Series 1 and 2, to examine possible effects of the respiratory gas treatments superimposed on the effects of changing \dot{V}_w alone.

When $\dot{M}O_2$ (Y-axis) was regressed against \dot{V}_w (X-axis), there were significant positive linear relationships in all of the respiratory gas treatments, and none of the intercepts at $\dot{V}_w = 0$ were significantly different from each other or from zero (Fig. 4.9A). However, the slope of the hyperoxia relationship was about 2.3-fold greater than that of the normoxia relationship, whereas the slope of the hypoxia relationship was only about 17% of that of the normoxia relationship; both differences were significant. This analysis clearly demonstrated the effects of the elevated P₁O₂ in hyperoxia and reduced P₁O₂ in hypoxia (and comparably affected driving PO₂ gradients) on $\dot{M}O_2$, separate from the effects of differences in \dot{V}_w (Figs 4.7, 4.8). Furthermore, although 10 M HEA inhibited \dot{V}_w (Fig. 4.5), the analysis also revealed that it did not affect the efficiency of $\dot{M}O_2$ per unit flow, as the slope was not significantly different from that of the normoxic control. A simple interpretation is that HEA did not affect the ability of the gill to transfer O₂ or the ability of the blood to take it up. This contrasts with the 1% CO₂ hypercapnia treatment, where the slope was significantly depressed by about 45% relative to that of the

normoxic control. Thus, the efficiency of $\dot{M}O_2$ per unit flow was reduced. One possible explanation would be decreased O_2 affinity of the blood due to the Bohr effect, which has been observed in the whole blood of the congeneric *E. cirrhatus* (Wells et al. 1986).

Using mean values of \dot{V}_w ($137 \text{ ml kg}^{-1} \text{ min}^{-1}$) and $\dot{M}O_2$ ($718 \text{ } \mu\text{mol kg}^{-1} \text{ h}^{-1}$) for hagfish exhibiting “normal ventilation” under normoxic control conditions, the ventilatory convection requirement for O_2 (\dot{V}_w per unit $\dot{M}O_2$) was about 11 L mmol^{-1} . This value is less than one-third of that (35 L mmol^{-1}) reported by Perry et al (2019b) for *E. stoutii* under normoxia. Certainly, the present data suggest a more efficient system, comparable to that (10 L mmol^{-1}) in the skate (Graham et al. 1990), but still less efficient than those ($5\text{-}6 \text{ L mmol}^{-1}$) in tench (Eddy 1973), common carp (Lomholt and Johansen 1979), and starry flounder (Wood et al. 1979). By reversing the axes of Fig. 4.9A and rationalizing the units to a common basis, it is possible to calculate the mean ventilatory convection requirement for O_2 (L mmol^{-1}) across a wide range of ventilatory flows, as the slopes of regressions of \dot{V}_w (Y-axis) against $\dot{M}O_2$ (X-axis) - i.e. $\Delta\dot{V}_w$ per $\Delta\dot{M}O_2$ (Fig. 4.9B). Under normoxia, this overall convection requirement was about 9 L mmol^{-1} , very similar to the single point estimate above. This decreased significantly during hyperoxia to about 5 L mmol^{-1} . However, the overall convection requirement increased significantly by 9-fold during hypoxia to about 80 L mmol^{-1} , and by 2.5-fold during 1% CO_2 hypercapnia to about 22 L mmol^{-1} , but did not change during 10 mM HEA exposure, in accord with our earlier explanations. In future, studies on the effects of both CO_2 and ammonia on blood O_2 -binding and transport in *E. stoutii*, as well as the influence of all three respiratory gases on the distribution of ventilatory flow among gill pouches, would be illuminating.

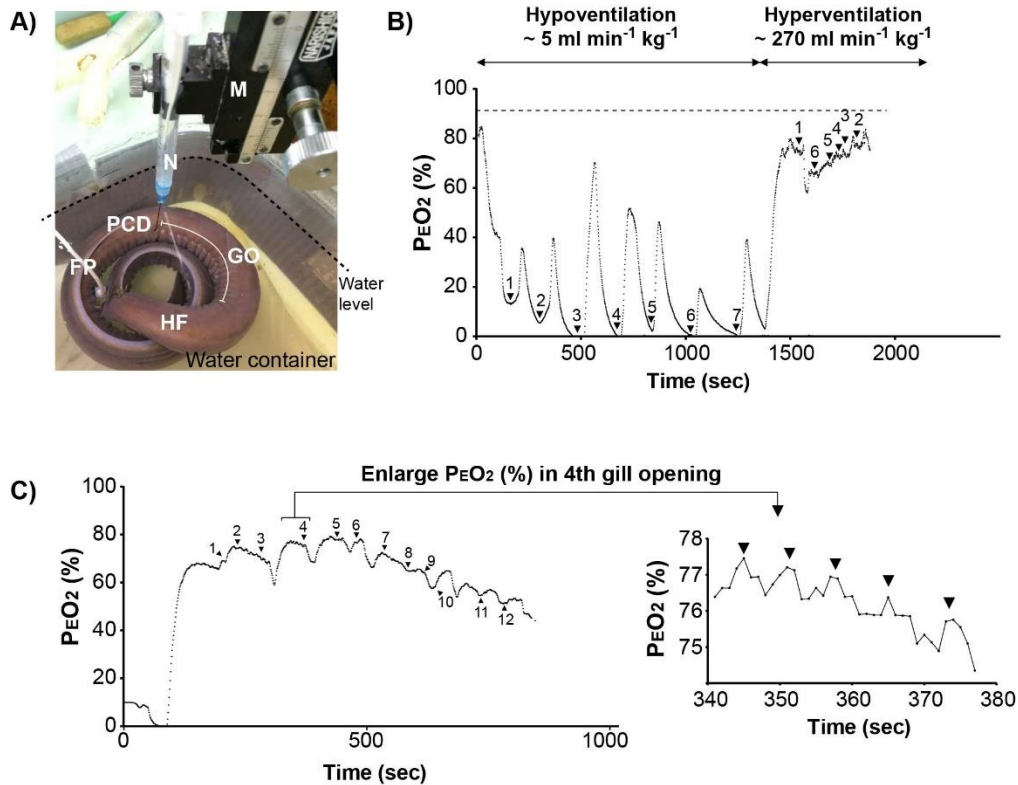


Figure 4.1 A) On the flipped over hagfish (HF), which was submerged in water, expired oxygen tension ($P_{E}O_2$) was measured at the gill openings (GO) including the pharyngo-cutaneous duct (PCD) by a needle-type oxygen probe (N) attached on a micro-manipulator (M), which was magnetically mounted on an iron plate. The oxygen probe could be moved between gill openings by moving the micro-manipulator. Simultaneously, ventilation flow (\dot{V}_w) was also measured using a flow probe (FP) attached on silicone tubing in the nostril duct. B) In this example of $P_{E}O_2$ measurements, the hagfish was initially exhibiting hypoventilation. The needle-type oxygen probe was moved sequentially between different numbered gill openings, with 1 being the most anterior, and subsequent numbers being more and more posterior openings. The points marked by arrow heads represent the true $P_{E}O_2$ measurements at each numbered gill pouch opening. Note the lower $P_{E}O_2$ values as the probe was moved to more posterior gill openings. At approximately 1400 sec, the hagfish spontaneously changed to hyperventilation. $P_{E}O_2$ values increased markedly, but the trend whereby more posterior openings exhibited lower $P_{E}O_2$ values continued. C) In this example, the trend for lower $P_{E}O_2$ in posterior gill pouches is clearly seen; again, the arrowheads represent the points where the probe was correctly positioned to measure true $P_{E}O_2$ values at the respective numbered gill openings. In the time scale expansion of recording at the 4th gill opening, the measured $P_{E}O_2$ fluctuated slightly, probably reflecting the slow rhythmic contractions of the gill pouches.

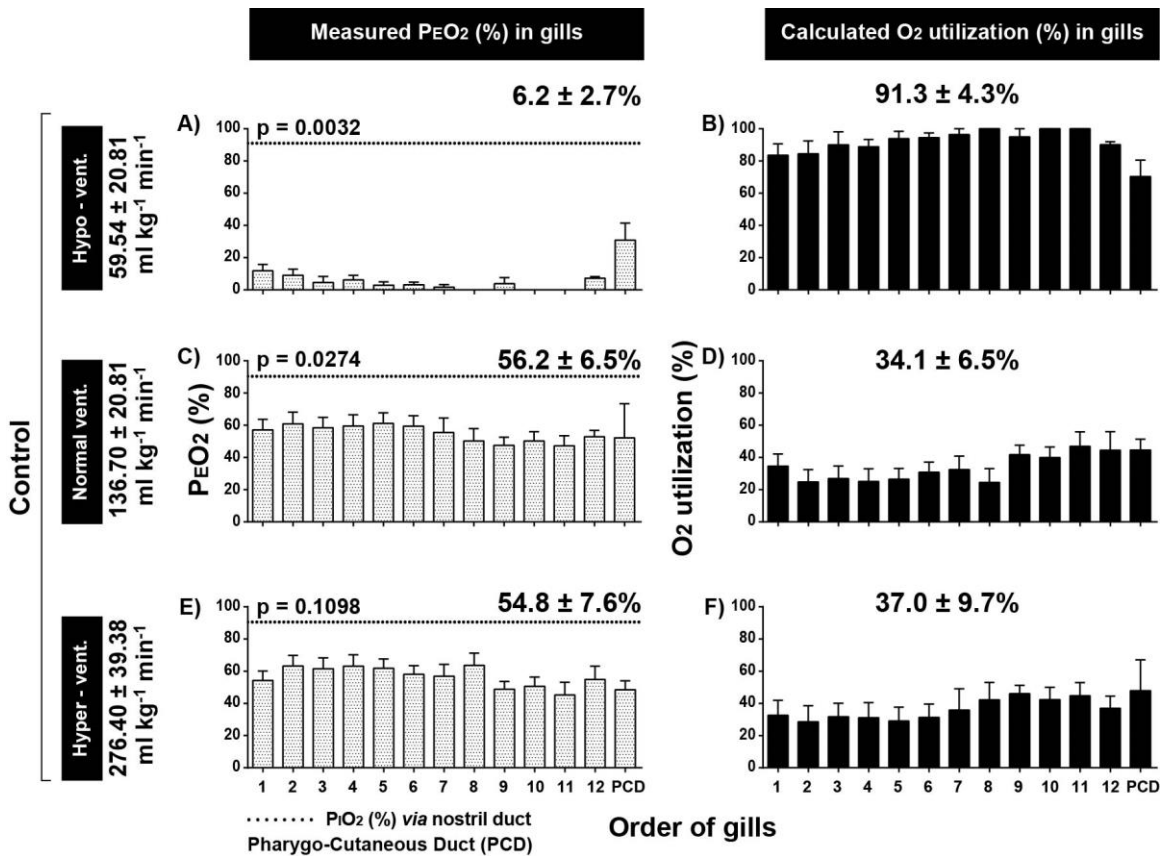


Figure 4.2 Expired O_2 tensions ($P_{E}O_2$, % air saturation) and % utilization of O_2 (calculated by Equation 1) from the respective gill openings including the pharyngo-cutaneous duct (PCD) in control normoxic hagfish, which showed three different ventilation magnitudes (<75 , $75 \sim 175$, and >175 $ml\ kg^{-1}\ min^{-1}$, *see* Methods): A, B) hypoventilation (\dot{V}_w : 59.5 ± 20.8 $ml\ kg^{-1}\ min^{-1}$); C, D) normal ventilation (\dot{V}_w : 136.7 ± 20.8 $ml\ kg^{-1}\ min^{-1}$); and E, F) hyperventilation (\dot{V}_w : 276.4 ± 39.4 $ml\ kg^{-1}\ min^{-1}$). These values are also shown on the left-hand axis. In Panels A, C, and E, the dashed line illustrates the mean P_iO_2 . Means \pm 1 S.E.M. ($N = 6 - 7$). The significance of anterior-to-posterior differences for $P_{E}O_2$ was confirmed by one-way ANOVA for panels A ($p = 0.0032$), and C ($p = 0.0274$), but not E ($p = 0.1098$).

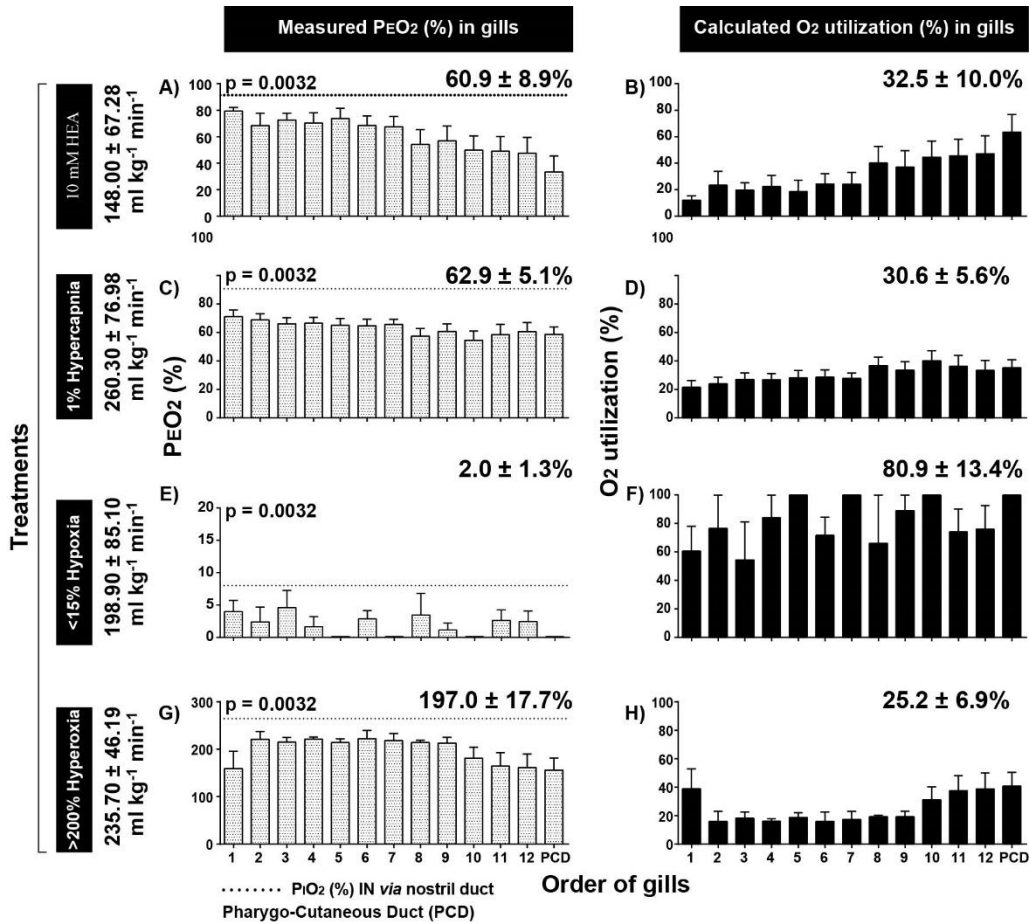


Figure 4.3 Expired oxygen tension ($P_{E}O_2$) and % utilization of O_2 (calculated by Equation 1) from the respective gill openings including pharyngo-cutaneous duct (PCD) of hagfish treated with A, B) high environmental ammonia (10 mM HEA), C, D) hypercapnia (1% CO_2), E, F) severe hypoxia (<15% air saturation), and G, H) hyperoxia (>200% air saturation). The \dot{V}_w (means \pm 1 S.E.M.) during the measurements is shown on the left-hand axis. In Panels A, C, E, and G, the dashed line illustrates the mean $P_{i}O_2$. Means \pm S.E.M. (N = 5 - 8). The significance of anterior-to-posterior differences for $P_{E}O_2$ was confirmed by one-way ANOVA for panels A ($p = 0.0403$), C ($p = 0.0061$), and G ($p = 0.0243$), but not for E ($p = 0.4965$).

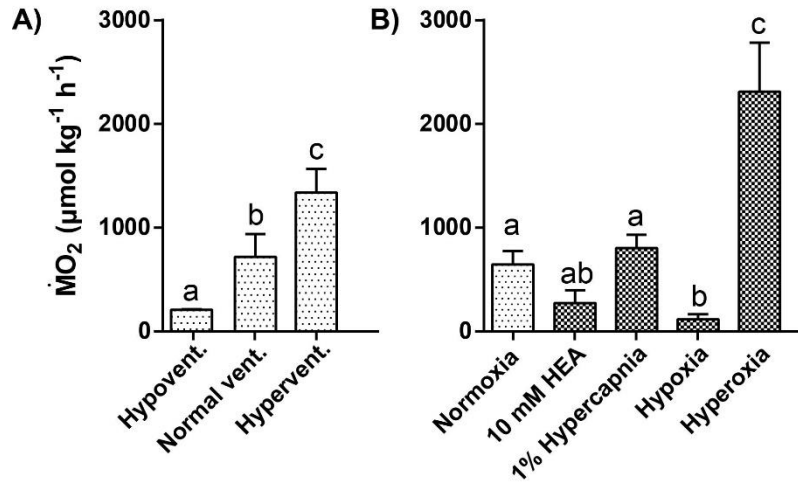


Figure 4.4 Routine $\dot{M}O_2$ calculated by Equation 2 using the P_{iO_2} , mean \dot{V}_w , and overall mean $P_{E}O_2$ values (from the 13 measurement sites) for each fish under each experimental condition. A) In control normoxic conditions, with data classified according to whether they were recorded during normal ventilation, hypoventilation, or hyperventilation (<75 , $75 \sim 175$, and $>175 \text{ ml kg}^{-1} \text{ min}^{-1}$, *see* Methods). B) In various respiratory gas treatments – control normoxia, high environmental ammonia (10 mM HEA), hypercapnia (1% CO_2), severe hypoxia ($<15\%$ air saturation), and hyperoxia ($>200\%$ air saturation). Within a panel, means not sharing the same letter are significantly different from one another. Means \pm S.E.M. (N = 9).

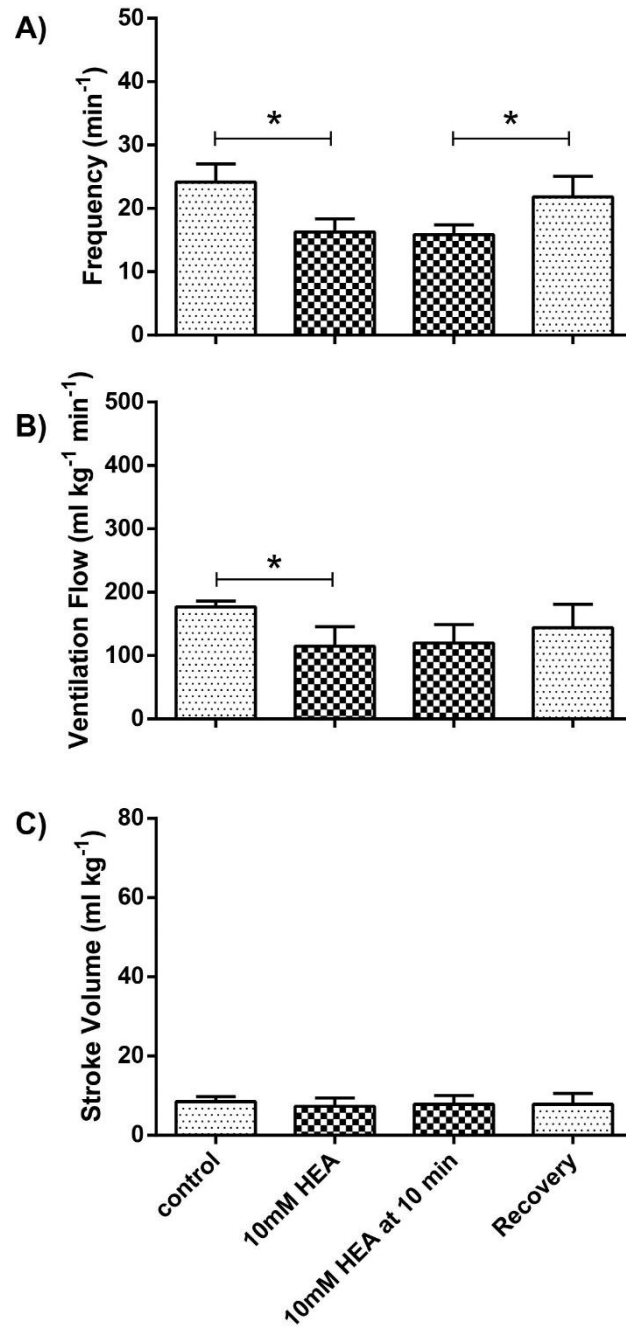


Figure 4.5 Changes in ventilatory parameters A) frequency (fr), B) total ventilatory flow (\dot{V}_w), and C) ventilatory stroke volume (SV_w) in hagfish acutely exposed to 10 mM high environmental ammonia (HEA) in normoxia. The chamber was flushed with fresh normoxic seawater for recovery. Means \pm S.E.M. (N = 9). * signifies significant change from the preceding condition (p < 0.05).

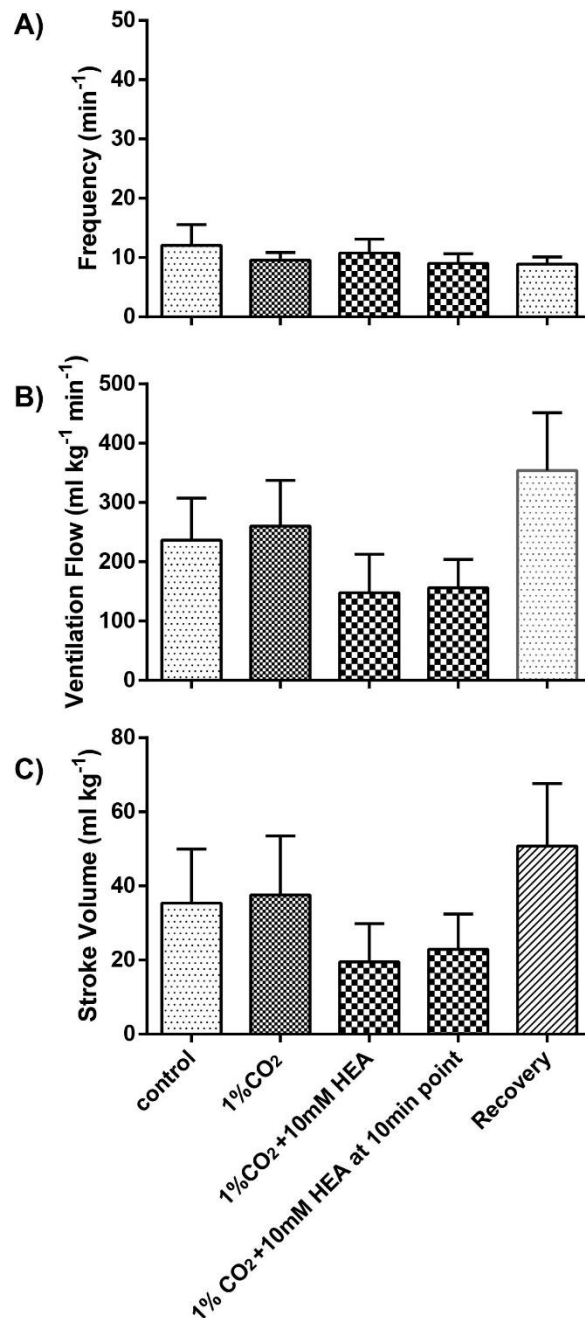


Figure 4.6 Changes in ventilatory parameters A) frequency (fr), B) total ventilatory flow (\dot{V}_w), and C) ventilatory stroke volume (SV_w) in hagfish exposed to hypercapnia (1% CO₂) and then subsequently acutely exposed to 10 mM high environmental ammonia (HEA) in the continuing presence of hypercapnia. The chamber was flushed with fresh normoxic seawater for recovery. Means \pm S.E.M. (N = 7). None of the changes were statistically significant (i.e. $p > 0.05$).

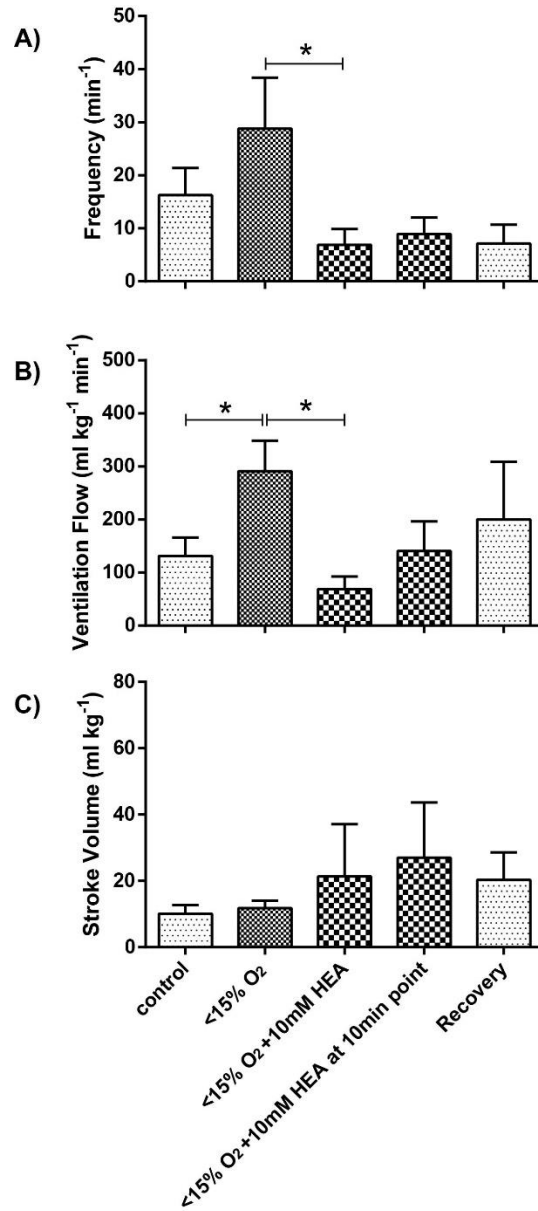


Figure 4.7 Changes in ventilatory parameters A) frequency (fr), B) total ventilatory flow (\dot{V}_w), and C) ventilatory stroke volume (SV_w) in hagfish exposed to severe hypoxia ($\text{PO}_2 < 15\%$ air saturation) and then subsequently acutely exposed to 10 mM high environmental ammonia (HEA) in the continuing presence of hypoxia. The chamber was flushed with fresh normoxic seawater for recovery. Means \pm S.E.M. (N = 4). * signifies significant change from the preceding condition ($p < 0.05$).

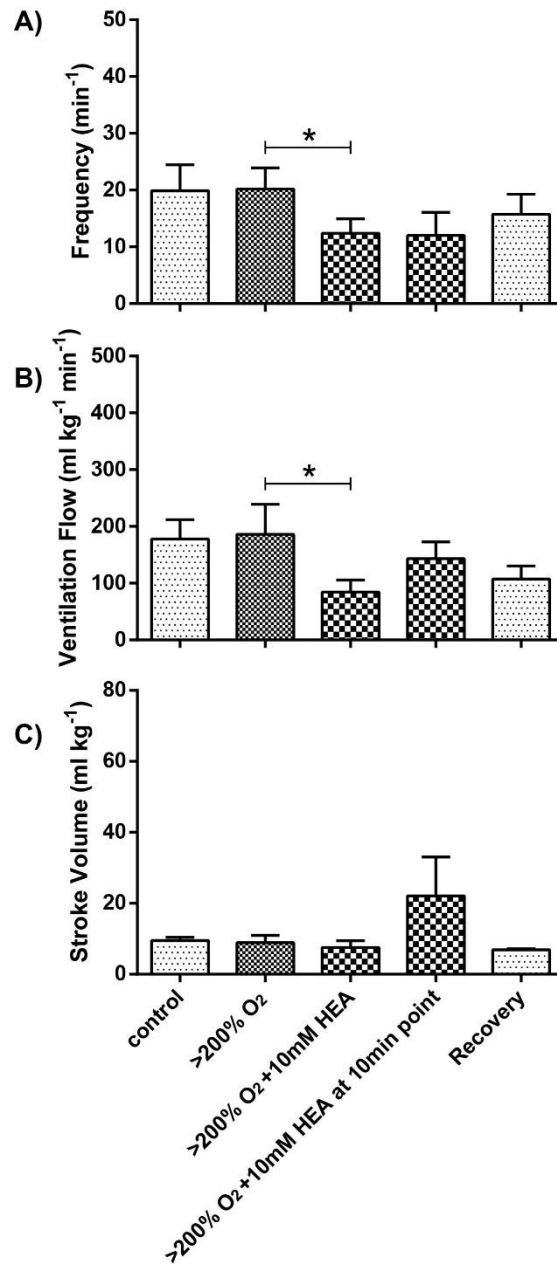


Figure 4.8 Changes in ventilatory parameters A) frequency (fr), B) total ventilatory flow (\dot{V}_w), and C) ventilatory stroke volume (SV_w) in hagfish exposed to hyperoxia ($PO_2 > 200\%$ air saturation) and then subsequently acutely exposed to 10 mM high environmental ammonia (HEA) in the continuing presence of hyperoxia. The chamber was flushed with fresh normoxic seawater for recovery. Means \pm S.E.M. (N = 5). * signifies significant change from the preceding condition ($p < 0.05$).

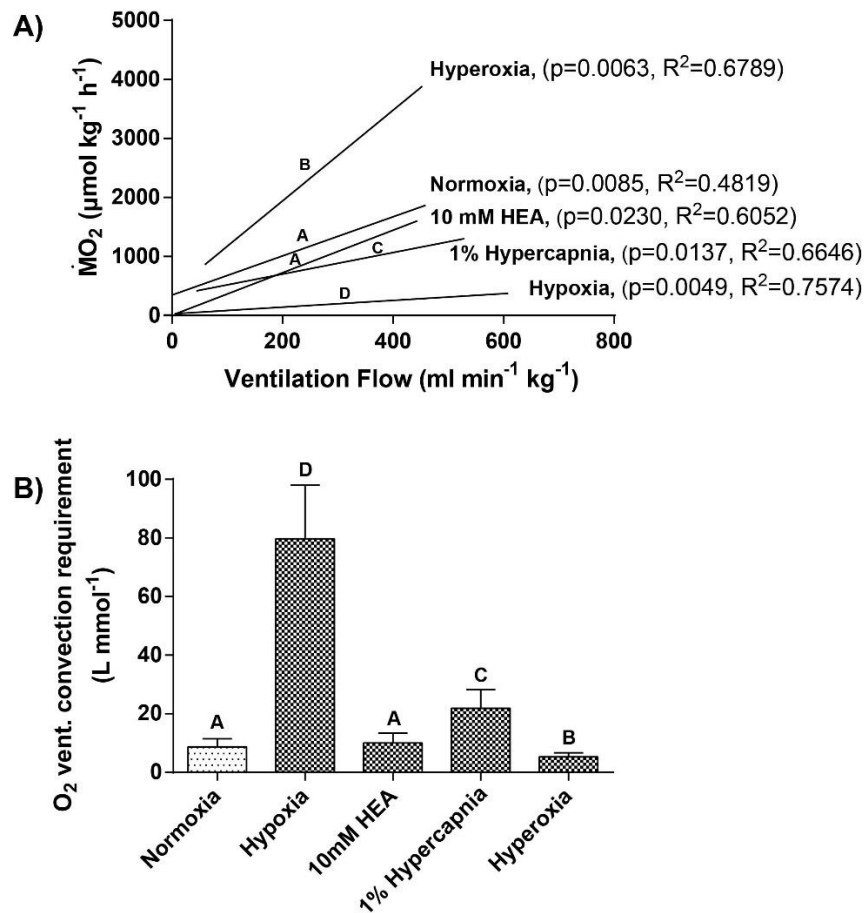


Figure 4.9 (A) Regressions between routine oxygen consumption rate ($\dot{M}O_2$, Y-axis) and total ventilatory flow ($\dot{V}w$, X-axis) in hagfish under different respiratory gas treatments. The r^2 and p values are shown.

The equations are:

Normoxia: $\dot{M}O_2 = 3.315 \dot{V}w + 337.4$ (N = 13)

10 mM HEA: $\dot{M}O_2 = 3.602 \dot{V}w - 4.26$ (N = 8)

1% CO_2 Hypercapnia: $\dot{M}O_2 = 1.825 \dot{V}w + 329.23$ (N = 8)

Hypoxia: $\dot{M}O_2 = 0.570 \dot{V}w + 22.15$ (N = 8)

Hyperoxia: $\dot{M}O_2 = 7.683 \dot{V}w + 391.9$ (N = 9)

By ANCOVA, none of the intercepts are significantly different from one another, whereas letters indicate significant differences in slope ($p < 0.05$). (B) The convection requirement for O_2 , (L mmol^{-1}) calculated from the slopes of regressions between total ventilatory flow ($\dot{V}w$, Y axis) and routine oxygen consumption rate ($\dot{M}O_2$, X axis) in the same hagfish under different respiratory gas treatments. Means \pm S.E.M. (N), where N is the same as in panel (A). Letters indicate significant differences ($p < 0.05$).

Chapter 5: Is ammonia excretion affected by gill ventilation in the rainbow trout *Oncorhynchus mykiss*?

5.1 Summary

Ammonia ($\text{NH}_3 + \text{NH}_4^+$) is the major nitrogenous waste in teleost fish. NH_3 is also the third respiratory gas, playing a role in ventilatory control. However, it is also highly toxic. Normally, ammonia excretion through the gills occurs at about the same rate as its metabolic production, but the branchial transport mechanisms have long been controversial. An influential review (Randall and Ip 2006) has claimed that ammonia excretion in fish is probably limited by diffusion rather than by convection, so that increases in ventilation would have negligible effect on the rate of ammonia excretion. Why then should elevated plasma ammonia stimulate ventilation? The diffusion-limitation argument was made before the discovery of Rhesus (Rh) glycoproteins and the associated metabolon in the gills, which serve to greatly increase branchial ammonia permeability under conditions of ammonia loading. Therefore, we hypothesized here that (i) in accord with the diffusion-limitation concept, changes in ventilation would not affect the rate of ammonia excretion under conditions where branchial Rh metabolon function would be low (resting trout with low plasma ammonia levels). However, we also hypothesized that (ii) in accord with convective limitation, changes in ventilation would influence the rate of ammonia excretion under conditions where diffusion limitation was removed because branchial Rh metabolon function would be high (ammonia-loaded trout with high plasma ammonia levels). We used variations in environmental O_2 levels to manipulate ventilation in trout under control or ammonia-loaded conditions – i.e. hyperventilation in moderate hypoxia or hypoventilation in moderate hyperoxia. In accord with hypothesis (i), under resting conditions, ammonia excretion was insensitive to experimentally induced changes in ventilation. Ammonia-loading by NH_4HCO_3 infusion for 30 h+ increased the gill mRNA expressions of two key metabolon components (Rhcg2, V-H⁺-ATPase or HAT), together with a 7.5-fold increase in plasma ammonia concentration and a 3-fold increase in ammonia excretion rate. In accord with hypothesis (ii), in these fish, hypoxia-induced increases in ventilation elevated the ammonia excretion rate and lowered plasma ammonia, while hyperoxia-induced decreases in ventilation reduced the ammonia excretion rate, and elevated plasma ammonia concentration. We conclude that under conditions of natural ammonia loading (e.g. meal digestion, post-exercise recovery), diffusion-limitation is removed by Rh metabolon upregulation, such that the stimulation of ventilation by elevated plasma ammonia can play an important role in clearing the potentially toxic ammonia load.

5.2 Introduction

Since ammonia excretion through the gills of fish was first measured by Homer Smith (1929), the transport mechanisms have been controversial. Ammonia movement has been variously explained by simple diffusion of NH_3 along pNH_3 gradients, by NH_4^+ diffusion along electrochemical gradients, by direct exchange of Na^+ for NH_4^+ (first suggested by August Krogh 1938), or NH_4^+ movement *via* K^+ channels and transporters (for reviews *see* Evans and Cameron 1986; Wood 1993; Wilkie 1997, 2002; Evans et al. 2005; Fehsenfeld and Weihrauch 2016). However, since 2000, the paradigm has shifted with the discovery that in mammals, Rh glycoproteins can serve as selective channels which greatly facilitate the diffusion of ammonia across cell membranes (Marini et al. 2000; Westhoff et al. 2002; Ripoche et al. 2004). Weihrauch et al. (2004) first showed that homologues of these Rh proteins are expressed in the gills of crabs, then Nakada et al. (2007a, b), Hung et al. (2007), and Nawata et al. (2007) demonstrated their presence in the gills of teleost fish. Their importance in ammonia excretion was reinforced by the discovery that the mRNA expression levels of Rh proteins in the gills were upregulated by external (Nawata et al. 2007; Wood and Nawata 2011) or internal ammonia loading (Nawata and Wood 2009) in trout, and that molecular knockdown of Rh protein expression severely reduced ammonia excretion in larval zebrafish (Braun et al. 2009). The ammonia transport function of trout Rh proteins was conclusively proven by *in vitro* oocyte expression studies (Nawata et al. 2010b).

The Rh proteins now play a key role in current models for branchial ammonia excretion in teleost fish (Tsui et al. 2009; Wright and Wood 2009, 2012; Weihrauch et al. 2009; Ito et al. 2013). While some ammonia may pass by simple diffusion through the lipoprotein cell membranes, a significant portion may also pass by facilitated diffusion through Rh protein channels, and this fraction is thought to increase when Rh protein expression is induced by ammonia loading. Indeed active outward transport of ammonia by an Rh-mediated metabolon linked to Na^+ uptake and acid excretion (Wright and Wood 2009, 2012) has been proposed to explain the increased ammonia excretion after feeding, exercise, or ammonia infusion, as well as the restoration of ammonia excretion when the normal outwardly directed pNH_3 and electrochemical NH_4^+ gradients are reversed by high external ammonia (Nawata et al. 2007; Nawata and Wood 2009; Zimmer et al. 2010; Wood and Nawata 2011; Sinha et al. 2013; Zhang et al. 2015).

Hyperventilation in response to high external ammonia has been frequently observed in fish, and often interpreted as a general stress response to a toxicant (e.g. Smart 1978; Lang et al. 1987; Fivelstad and Binde 1994; Knoph 1996). However, there is evidence that ventilation is also stimulated by elevation of internal ammonia levels (Hillaby and Randall 1979; McKenzie et al. 1993). More recent studies on trout have proven that this effect can occur independently of changes in blood O_2 , CO_2 , and acid-base

status (Zhang and Wood 2009), and that it is mediated at least in part by neuroepithelial cells (NECs) on the 1st and 2nd gill arches (Zhang et al. 2011, 2015). Indeed, as ammonia is produced at about 10-20% the rate of CO₂, it is essentially the third respiratory gas in ammoniotelic teleost fish (Randall and Ip 2006). Therefore, it makes sense that ammonia should be detected by the same receptor systems as for O₂ and CO₂ (Zhang et al. 2015; Perry and Tzaneva 2016). Central detection by sensing of brain ammonia buildup may also be involved (Zhang et al. 2013). Blood ammonia levels are markedly elevated after feeding (Bucking et al. 2008; Wicks and Randall 2002; Zimmer et al. 2010) and exhaustive exercise (Wood 1988; Mommsen and Hochachka 1988; Wang et al. 1994), so ammonia-stimulated hyperventilation would be a very appropriate response if it helped to increase ammonia excretion.

However, in a seminal review, Randall and Ip (2006) argued that ammonia excretion in fish is probably limited by diffusion rather than by blood perfusion or water convection, so “*that increases in ventilation would have negligible effect on the rate of ammonia excretion, and therefore represent a non-physiological response on the part of the fish*”. This seems counterintuitive. Diffusion limitation would mean that only the ammonia gradients (PNH₃ and/or NH₄⁺ electrochemical gradients) and the effective permeability of the gills to ammonia would affect excretion rate; convective flow of blood or water would not have any influence. However, it is important to note that this was a theoretical prediction formulated in the absence of any evidence whether (or not) changes in ventilation affected ammonia excretion, and it was made just one year before the discovery of Rh proteins in fish gills (Nakada et al. 2007a, b; Hung et al. 2007; Nawata et al. 2007). If Rh proteins serve to facilitate ammonia movement through the gill epithelium, diffusion limitation may not apply, and this argument may be invalid. However, to our knowledge, this idea has never been experimentally tested.

In the present study, we evaluated two hypotheses in adult rainbow trout. The first was that in accord with the diffusion-limitation concept of Randall and Ip (2006), changes in ventilation would not affect the rate of ammonia excretion under conditions where branchial Rh protein expression would be minimal (fasted, resting fish with low plasma ammonia levels). The second hypothesis we tested was the convection-limitation hypothesis where changes in ventilation would influence the rate of ammonia excretion under conditions where branchial Rh protein expression would be high (ammonia-loaded fish with high plasma ammonia levels), i.e. no diffusion limitation for ammonia.

Ammonia loading was created by chronic intravascular infusion of ammonia (140 mM NH₄HCO₃), a treatment previously shown to upregulate branchial Rh protein expression in trout (Nawata and Wood 2009), and ventilation was experimentally manipulated using moderate hypoxia (50% air saturation) to achieve hyperventilation, and hyperoxia (> 300%) to induce hypoventilation. Cortisol

levels were measured, as there is circumstantial evidence that they contribute to regulation of the branchial Rh metabolon (Tsui et al. 2009; Nawata and Wood 2009). Ammonia excretion was monitored throughout, plasma ammonia concentrations were measured, and mRNA abundances of three key genes of the Rh metabolon (Rhcg2, NHE2, and V-H⁺-ATPase or HAT) were quantified in the gills using quantitative real-time PCR (qPCR).

5.3 Materials and Methods

5.3.1 Experimental animals

Rainbow trout (*Oncorhynchus mykiss*, 203.4 ± 6.5 g, 24.9 ± 0.3 cm) were transported from Miracle Springs Inc. Trout Hatchery (Fraser Valley, BC, Canada) to aquatic facilities at the University of British Columbia. There, the fish were held in 90-L glass aquaria served with flow-through charcoal-filtered dechlorinated Vancouver City tap water ([Na⁺], 0.17 mmol L⁻¹; [Cl⁻], 0.21 mmol L⁻¹; hardness, 30 mg L⁻¹ as CaCO₃; pH 7.0; temperature, 6.5 to 9.0 °C). The fish were fed with commercial pellets (EWOS, Surrey, BC, Canada) but were fasted for a week prior to experiment to minimize the influence of feeding on ammonia metabolism. The fish were treated in accordance with the University of British Columbia animal care protocol #A14-0251, and the guidelines of the Canadian Council on Animal Care. At the end of experiments, the fish were euthanized by an overdose (120 mg L⁻¹) of tricaine methanesulfonate (MS-222, Western Chemicals Inc., Ferndale, WA, USA; pH was adjusted to ~7.0 with 1 mmol L⁻¹ of NaOH).

5.3.2 Fish operations

In order to monitor ventilatory pressure amplitude and frequency in both Series I and Series II, trout were implanted with buccal catheters as described by Holeton and Randall (1967), with minor modifications. In brief, fish were anesthetized in 60 mg L⁻¹ MS-222 (pH neutralized to ~7.0 as described above), and irrigated on an operating table. A hole was drilled in the roof of the mouth using an 18G needle, taking care to avoid the nares, and a 3-cm sleeve of PE 160 polyethylene tubing (Clay-Adams, Sparks, MD, USA; O.D. 1.57 x I.D. 1.14 mm), flared at the mouth end, was inserted. A 30-cm length of PE 50 tubing (O.D. 0.97 x I.D. 0.58 mm), again flared at the mouth end, was fitted through the PE 160 sleeve and cemented to it using cyanoacrylate glue (Krazy Glue, High Point, NC, USA). Silk suture was used to hold the catheter in place by knots at the outside and stitches through the dorsal fin of the fish.

In both Series I and II, a pair of enameled copper wires was implanted externally, one on each side of the pericardium, for measurement of the electro-cardiogram (ECG) as an indicator of heart rate, to give a bipolar recording as described by Roberts et al. (1975). The wires were anchored in place by a suture placed on the dorsal fin of the fish.

In Series II, trout were additionally fitted with arterial catheters for ammonia infusion, using a modification of the method of Soivio et al. (1972). A second PE 160 sleeve was fitted through another hole in the roof of the mouth next to buccal catheter. The dorsal aorta was cannulated between the 2nd and 3rd gill arches using a 30-cm length of PE 50 tubing, cut sharp at the insertion end, and filled with Cortland saline (124 mmol L⁻¹ NaCl, 5.1 mmol L⁻¹ KCl, 1.6 mmol L⁻¹ CaCl₂, 0.9 mmol L⁻¹ MgSO₄, 11.9 mmol L⁻¹ NaHCO₃, 3.0 mmol L⁻¹ NaH₂PO₄, 5.6 mmol L⁻¹ glucose; Wolf 1963) which was heparinized at 50 international units ml⁻¹ with sodium heparin (Sigma-Aldrich, St. Louis, MO, USA). After penetration of the artery was confirmed by blood appearance in the tubing, the catheter was advanced ~5 cm deep into the dorsal aorta at a ~10 ° angle, almost parallel to roof of the mouth, and secured in place by a silk suture stitch. Then, the other end of the PE 50 tubing was passed through the PE 160 sleeve, drawn taught, sealed with a pin, and secured in place with cyanoacrylate glue and silk suture as described for the buccal catheter. After operation, fish were recovered overnight in individual black plexiglass chambers (length 38 cm x width 10 cm x height 18 cm) served with 500 ml min⁻¹ of aerated flowing water.

5.3.3 Experimental series

In both series, the experiments were performed in the same individual black plexiglass chambers in which the fish had been allowed to recover from surgery. To allow rapid manipulation of PO₂ levels in the water, the bottoms of the chambers were fitted with multi-pored airline tubing which facilitated bubbling of air for normoxia, pure nitrogen for hypoxia, or pure oxygen for hyperoxia. During experiments, the chambers were aerated but water flow-through was suspended, and the water volume was set to 3.4 L. The individual chambers were submerged in a flowing reservoir to maintain water temperature between 6.5 ~ 9.0 °C.

5.3.3.1 Series I – Relationship between ventilation and ammonia excretion in fish under baseline conditions

This experiment was performed over two days (9 h per day) following recovery from surgery, and fish were randomly treated with either hypoxia on day 1 and hyperoxia on day 2, or hyperoxia on day 1 and hypoxia on day 2. Within each day, a 3-h control period under normoxia (bubbling with air), was followed by a 3-h experimental period (bubbling with nitrogen for hypoxia, or oxygen for hyperoxia), and then a 3-h recovery period under normoxia (bubbling with air again). Within each period, water PO₂, ventilation, and the rate of ammonia excretion were monitored, and between each period, a 0.5-h interval was used to flush the chambers to keep ammonia concentrations low, and to reset water PO₂ to the desired levels which were 100% air saturation in normoxia and recovery, 50% saturation in hypoxia, and >300% saturation in hyperoxia. These PO₂ levels were selected based on our preliminary experiments which demonstrated that they caused the desired changes in ventilation and could be tolerated indefinitely by the fish at this temperature (6.5 to 9.0 °C). Between days 1 and 2, the flow-through (500 ml min⁻¹) of normoxic water was restored.

5.3.3.2 Series II – Relationship between ventilation and ammonia excretion in ammonia-loaded fish

This series was also performed over two days following recovery from surgery, but each fish was subjected to only one experimental treatment (hypoxia or hyperoxia) on day 2. On day 1, control measurements of ventilation, and the rate of ammonia excretion were made on each fish over a 3-h period under baseline conditions in normoxia, as in Series 1, prior to the start of ammonia infusion. These values are designated as “control(-)” in Table 5.1 and Figs. 5.3 and 5.4, A-D. Immediately thereafter, the chamber was flushed, flow-through conditions were re-established, and a blood sample (200 µL, with saline replacement and re-infusion of red blood cells) was taken from the dorsal aortic catheter for the measurement of plasma total ammonia concentration. The sample was immediately centrifuged (5,000 g x 2 min), and the plasma was flash-frozen in liquid N₂ and stored at -80°C until analysis. Infusion with 140 mmol L⁻¹ NH₄HCO₃ *via* the dorsal aorta was then started at a rate of 2.98 ± 0.13 ml kg⁻¹ h⁻¹ using a Minipuls2 Peristaltic Pump (Gilson, Middleton, WI, USA) in order to raise the plasma ammonia concentration. This infusion was continued for 33 h – i.e. into day 2. Starting at 24 h, control measurements were made under normoxia in these ammonia-loaded fish. These values are designated “control(+)” in Table 5.1B and Figs. 5.3 and 5.4, A-D. The chambers were then flushed, a second blood sample was taken, and either hypoxic or hyperoxic conditions were established for a 3-h experimental

period, and a final blood sample, followed by a 3-h normoxic recovery period. Ammonia loading was continued throughout, and measurements of water PO₂, ventilation, and ammonia excretion rate were made in all periods.

5.3.3.3 Series III – Influence of ammonia-loading on gene expression in the gills

The protocol was identical to that of Series II, except that the fish were kept in normoxia throughout. There were with two infusion treatments (3 ml kg⁻¹ h⁻¹), 140 mmol L⁻¹ NH₄HCO₃ and 140 mmol L⁻¹ NaCl, ending at 33 h. At this time, the fish were rapidly euthanized as described above, the second gill arches were harvested, and the filaments were immediately cut off and transferred to ice-cold RNAlater™ (Ambion Inc., Austin, TX, USA) for storage at -20°C.

5.3.4 Analytical techniques

For measurements of ventilatory frequency (sec⁻¹) and pressure amplitude (cmH₂O, as an indicator of stroke volume), the buccal catheter, filled with water, was connected to a pressure transducer (Utah Medical Products, Midvale, UT, USA) which had been calibrated against a column of water. The analogue signal of the pressure transducer was amplified using an LCA-RTC amplifier (Transducer Techniques, Temecula, CA, USA) and converted into a digital signal *via* a PowerLab data integrity system (ADInstruments, Colorado Springs, CO, USA). The recorded digital signal was analyzed using LabChart™ version 7.0 software (ADInstruments). The ventilatory index (cmH₂O sec⁻¹, as an indicator of total ventilatory water flow) was calculated as the product of mean ventilatory pressure amplitude (cmH₂O) and mean frequency (sec⁻¹). The copper wires were connected to the same recording and analysis system for measurement of heart rate (sec⁻¹). Within each 3-h period, data taken from 0.5 to 3.0-h were generally stable and were averaged; the first 0.5 h was discarded as a period of transition.

Water PO₂ levels in the experimental chambers were continuously monitored using a Radiometer E-5036 polarographic electrode (Radiometer, Copenhagen, Denmark) connected to a polarographic amplifier (Model 1900, A-M Systems, Sequim, WA, USA) and captured by the PowerLab data integrity system (ADInstruments).

Water samples (5 ml) were taken at 0.5-h intervals throughout each 3-h period for total ammonia measurements by the colorimetric sodium salicylate method of Verdouw et al. (1978). The mean rate of ammonia excretion (μmol kg⁻¹ h⁻¹) was calculated from the linear regression slope (μmol L⁻¹ h⁻¹) of a plot

of water ammonia concentration ($\mu\text{mol L}^{-1}$) versus time (0.5 to 3.0-h), factored by body mass (kg) and water volume (L). Plasma total ammonia concentration ($\mu\text{mol L}^{-1}$) was measured using an enzymatic reagent kit based on the glutamate dehydrogenase/NAD method (RaichemTM R85446, Cliniqua, San Marcos, CA, USA). The same standards used for the water ammonia assay were employed. Plasma cortisol concentrations were assayed with an ELISA Kit (07M-21602, MP Biomedicals, Solon, OH, USA), according to the manufacturer's instructions.

For measurement of mRNA expression of V-type proton ATPase B subunit (HAT, AF14002), Na^+/H^+ exchanger-2 (NHE2, EF446605), and elongation factor 1- α total (EF1 α , AF498320) in gills, forward and reverse primer sequences tabulated by Wood and Nawata (2011) for *Oncorhynchus mykiss* were used. For measurement of *Oncorhynchus mykiss* rhesus glycoprotein type c (Rhcg2, AY619986.1), forward: GGTAGTCTGCTTCGTCTGGC, reverse: TCATGGGCCTTGGTCTCTAC primers were used. RNA was extracted from the RNAlaterTM fixed 2nd gill filaments with Trizol (Invitrogen, Burlington, ON, Canada). After removing potential DNA contamination with DNaseI (Invitrogen), RNA was quantified and quality assessed on a Nanodrop spectrophotometer (NanoDrop 2000, Thermo Scientific, Wilmington, DE, USA). Absence of DNA traces were verified by regular PCR on EF1- α . 1 μg of purified total RNA was then reversely transcribed into cDNA with the iScriptTM cDNA synthesis kit (Bio-Rad, Mississauga, ON, Canada). Quantitative real-time PCR (qPCR) reactions were performed using SsoFastTM EvaGreen[®] Supermix (Bio-Rad) and the CFXConnectTM real-time system (Bio-Rad). The qPCR protocol consisted of an initial step at 98°C for 2 min to activate the enzyme, and then 40 cycles of 5 s at 98°C for denaturation and 20 s at 60°C for annealing. Reactions were set up in a final volume of 15 μL using 2 μL of cDNA template and a final primer concentration of 0.4 $\mu\text{mol L}^{-1}$. Products were verified to result in a single specific amplicon by melt curve analysis (65 ~ 95°C, steps of 0.5°C for 5 s). A standard curve using a 1:2 serial dilution of gill cDNA was included for quantification and to ensure performance of the reaction (efficiency = 97.6%; $r^2 = 0.995$). Analyses were performed with the CFX manager software ver. 3.1 (Bio-Rad). EF1- α expression, which did not vary with treatment, was used for normalization.

5.3.5 Data analysis

Data have been reported as means \pm S.E.M. (N) where N represents the number of fish. One-way repeated-measures ANOVA followed by Dunnett's test was applied to compare the respiratory parameters, heart rates, and ammonia excretion rates, against control values within Series I and II experiments. Relationships between parameters were examined by linear and non-linear regression.

Student's t-tests two-tailed t-tests, with Bonferroni correction when required, were employed to compare the plasma total ammonia and cortisol concentrations among treatments (Series II) as well as gene expression (Series III). GraphPad Prism 6.0 (La Jolla, CA, USA) was used for all analyses. The threshold for statistical significance was $p < 0.05$.

5.4 Results

5.4.1 Series I – Relationship between ventilation and ammonia excretion in fish under baseline conditions

When water oxygen concentration was experimentally lowered from 97% air saturation control(-) to 48% for a 3-h period of hypoxia, trout ($N = 6$) significantly increased both ventilatory pressure amplitude by 28% (Fig. 5.1A) and frequency by 15% (Fig. 5.1B). Together, the increased pressure and frequency resulted in a 50% elevation of total ventilatory index (Fig. 5.1C). However, there was no significant change in ammonia flux rate (Fig. 5.1D). After restoration of normoxia (98% saturation), all ventilatory parameters returned to control(-) levels and there was no change in ammonia flux rate. During hypoxia, heart rate decreased by 16%, but recovered to control(-) levels after restoration of normoxia (Table 5.1A).

When water oxygen concentration was experimentally raised from 97% saturation control(-) to 334% for a 3-h period of hyperoxia, trout ($N = 6$) significantly decreased both ventilatory pressure amplitude by 18% (Fig. 5.2A) and ventilatory frequency by 9% (Fig. 5.2B). In combination, these resulted in a 26% reduction of total ventilatory index (Fig. 5.2C). After restoration of normoxia (100% saturation) there was no change in ammonia excretion rate, but all ventilatory parameters returned to control(-) levels. During hyperoxia, heart rate did not change (Table 5.1A).

Overall, under baseline conditions, trout were responsive to low and high oxygen levels in water by increasing and decreasing ventilation respectively, but these changes did not affect their rates of ammonia excretion, as summarized in Fig. 5.5A.

5.4.2 Series II – Relationship between ventilation and ammonia excretion in ammonia-loaded fish

Infusion with 140 mmol L^{-1} of NH_4HCO_3 at a rate of $2.98 \pm 0.13 \text{ ml kg}^{-1} \text{ h}^{-1}$ for 30 h raised the plasma ammonia concentration by about 7.5-fold from the control(-) level of $267 \text{ } \mu\text{mol L}^{-1}$ to a control(+) level close to $2000 \text{ } \mu\text{mol L}^{-1}$ (Fig. 5.6A). This was accompanied by a 3-fold elevation in the rate of

ammonia excretion as indicated by the significant increases from control(-) to control(+) values (Figs. 5.3D, 5.4D). Ammonia infusion also resulted in significant increases in total ventilatory index by about 40% which were achieved solely by elevations in ventilatory pressure without significant changes in frequency (Figs 5.3, 5.4). Ammonia infusion had no effect on heart rate (Table 5.1B). These infused fish control (+) with chronically elevated levels of plasma total ammonia, ammonia excretion, and ventilation were then subjected to the same experimental treatments as in Series I, during which time infusion was continued.

Reductions in water oxygen concentration from 94% saturation control(+) to 48% (hypoxia) for 3-h in these ammonia-infused trout (N = 10) resulted in hyperventilation, with significant increases of all ventilatory parameters amounting to 113% in pressure amplitude (Fig. 5.3A), 5% in frequency (Fig. 5.3B), and 135% in total ventilatory index (Fig. 5.3C). This elevation in ventilation was accompanied by a highly significant 53% increase in ammonia flux rate (Fig. 5.3D). After hypoxia, fish were returned to normoxic water (94% saturation) which resulted in decreases of all ventilatory parameters (Figs. 5.3A, B, C), which returned to levels not significantly different from control(+) values. Notably, ammonia excretion also decreased to a rate close to control(+) levels (Fig. 5.3D), in parallel to the decrease in ventilation. During hypoxia in these ammonia-loaded fish, heart rate decreased by 29% but recovered to control(+) levels after restoration of normoxia (Table 5.1B).

Elevations in water oxygen concentrations from 88% saturation control(+) to 475% (hyperoxia) in ammonia-infused trout (N = 7) resulted in hypoventilation with significant decreases in all ventilatory parameters, amounting to 17% in pressure amplitude (Fig. 5.4A), 7% in frequency (Fig. 5.4B), and 24% in total ventilatory index (Fig. 5.4C). This reduction in ventilation was accompanied by a highly significant 33% reduction in ammonia flux rate (Fig. 5.4D). After hyperoxia, fish were returned to normoxic water (93% saturation) which resulted in increases in ventilatory parameters, all of which returned to levels which were not different from control(+) values. Ammonia excretion also increased to a rate close to control(+) levels, in parallel to the increase in ventilation. Hyperoxia had no effect on heart rate in these ammonia-loaded fish (Table 5.1B).

Overall, chronic ammonia loading by infusion caused increased ventilation, increased plasma ammonia concentrations, and increased rates of ammonia excretion. When ventilation was subsequently manipulated by hypoxia and hyperoxia treatments, the rate of ammonia excretion became sensitive to ventilation, increasing with hyperventilation, and decreasing with hypoventilation, as summarized in Fig. 5.5B. Furthermore, measurements of plasma total ammonia revealed significantly lower concentrations in the trout subjected to hypoxia-induced hyperventilation (hypoxia) relative to those subjected to

hyperoxia-induced hypoventilation (Fig. 5.6B). Interestingly, the hyperoxia-treated trout also had significantly lower plasma cortisol concentrations (5.45 ± 1.72 ng dl⁻¹) than the hypoxia treated animals (13.85 ± 4.30 ng dl⁻¹). The plasma cortisol concentration in control(+) fish was 16.33 ± 4.61 ng dl⁻¹.

5.4.3 Series III – The influence of ammonia loading on gene expression in the gills

Chronic infusion with 140 mM NH₄HCO₃ for 33-h, parallel to the ammonia-loading treatment in Series II, was compared to chronic infusion with 140 mM NaCl for the same time period. Ammonia-loading resulted in significant increases in the expression of Rhcg2 (Fig. 5.7A) in the gills by 2.29-fold and HAT (Fig. 5.7B) by 1.26-fold respectively, relative to the NaCl treatment. The expression level of NHE2 was not significantly affected (Fig. 5.7C).

5.5 Discussion

5.5.1 Overview

The present results have confirmed our two hypotheses, showing that the prediction of Randall and Ip (2006) (“diffusion limitation”) was correct for resting trout with low concentrations of plasma ammonia (Series I), but became incorrect when trout were chronically loaded with ammonia (Series II). Thus, experimental manipulations of ventilation using moderate hypoxia and hyperoxia had no effect on ammonia excretion rate in resting trout, but these same treatments caused large changes in ammonia excretion when plasma ammonia concentrations were greatly elevated. The probable explanation is that diffusion limitation was removed because elevated plasma ammonia activated the Rh protein metabolon in the gills, thereby effectively increasing the ammonia permeability of the branchial epithelium. This would involve opening up facilitated diffusion channels and increasing the provision of protons for diffusion trapping of ammonia in the gill water boundary layer (Wright and Wood 2009, 2012). Thus, greater convection of water could carry away more ammonia. It is also possible that under these circumstances, ammonia excretion would become sensitive to the convective flow of blood through the gills, though this was not evaluated in the present study. Heart rate did not change significantly in response to either ammonia loading or hyperoxia, but it fell during hypoxia. This classic bradycardia would change the temporal pattern of blood flow through the gills, but not necessarily the absolute flow rate. Regardless, it is now clear that the ability of elevated plasma ammonia concentrations to stimulate ventilation can play a functional role in augmenting the excretion rate of potentially toxic ammonia under

conditions of natural ammonia loading such as during digestion of a meal (Buckling et al. 2008; Wicks and Randall 2002; Zimmer et al. 2010) and during recovery from exhaustive exercise (Wood 1988; Mommsen and Hochachka 1988; Wang et al. 1994). Gene expression data indicate that the Rh metabolon is likely activated in trout in both circumstances, though at present confirmatory protein expression data are lacking (Zimmer et al. 2010; Zhang et al. 2015).

5.5.2 Ammonia permeability in gills

In both Series I and Series II experiments, the fish changed ventilation in response to hypoxia and hyperoxia, but the ammonia excretion rates were only affected in fish infused with ammonia (Series II). This means that the internally elevated ammonia increased the permeability of the gills to ammonia. There is circumstantial evidence that cortisol may also play a role in activating the branchial Rh metabolon (Tsui et al. 2009; Nawata and Wood 2009). In this regard, it is interesting that in the ammonia-loaded fish of Series II, plasma cortisol levels in the hypoxia-treated group were significantly greater than in the hyperoxia-treated group, a difference which paralleled the greater ammonia excretion rate in the former.

In the freshwater rainbow trout, components of the Rh metabolon include Rhcg2 (the apical ammonia channel), an as yet uncharacterized apical Na⁺ channel, apical NHE2, intracellular carbonic anhydrase and HAT (the apical H⁺ pump) (Tsui et al. 2009; Wright and Wood 2009, 2012). When the metabolon is activated, Na⁺ uptake and ammonia excretion increase, and ammonia can be excreted even against prevailing gradients (Nawata et al. 2007; Nawata and Wood 2009; Zimmer et al. 2010; Wood and Nawata 2011; Nawata et al. 2010a; Sinha et al. 2013). In the present study, the mRNA abundance of two key genes (Rhcg2 and HAT) in the gills were elevated by chronic ammonia loading, in accord with the earlier findings of Nawata and Wood (2009), who used a similar 140 mM NH₄HCO₃ infusion protocol. The lack of significant change in NHE2 expression is in accord with previous studies showing that this generally has a less pronounced response than HAT to ammonia loading in freshwater trout (Nawata et al. 2007; Nawata and Wood 2009; Wood and Nawata 2011). However, an important cautionary note is that changes in gene expression do not necessarily indicate changes at the protein level. Therefore, in the future, protein expression levels of these transporters should be studied. The metabolon is thought to work by facilitating NH₃ diffusion through the apical Rh channel and increasing the export of H⁺ across the apical membrane to allow diffusion trapping of NH₃ and its conversion to NH₄⁺ in the gill water boundary layer. The H⁺ ions are generated by intracellular carbonic anhydrase. At the same time, HAT

creates an electrochemical gradient across the apical membrane to increase active Na^+ uptake from the water, thereby maintaining electroneutrality. The excreted NH_4^+ ions cannot diffuse back, and as long as the fish continues to hyperventilate, they will be washed away. The fish gain benefits in several different ways. These include increased ammonia excretion which becomes responsive to ventilation, increased H^+ excretion, and greater active Na^+ uptake at times (e.g. after feeding or exercise) when elevated metabolism is generating more ammonia and acidic equivalents, accompanied by greater diffusive Na^+ losses through the osmorepiratory compromise (Randall et al. 1972; Nilsson 1986).

5.5.3 Possible ammonia sensing organs in fish

We employed experimental ammonia-loading to elevate plasma ammonia concentrations. The fish gills and/or brain are thought to be the organs involved in detecting elevated internal ammonia concentrations. Zhang et al. (2011) provided evidence that serotonin (5-HT)-immunoreactive neuroepithelial cells (NECs) on gills of arches 1 and 2, which are known to also be O_2 and CO_2 sensors (Burlison and Milsom 1993; Jonz et al. 2004; Burlison et al. 2006; Coolidge et al. 2008; Perry et al. 2009; Abdallah et al. 2012; Zachar and Jonz 2012; Perry and Tzaneva 2016), serve as potential ammonia chemoreceptors, displaying intracellular Ca^{2+} signals in response to physiological levels of extracellular NH_4^+ . This was reinforced by the discovery that Rh glycoproteins are expressed in these cells (Zhang et al. 2015), thereby providing a route for ammonia entry. Serotonergic neural pathways would transmit the signals back to respiratory control centers in the brain, and in turn motor outflow along cranial nerves to the breathing muscles would increase ventilation. Zhang and Wood (2009) and Zhang et al. (2011) also showed that the hyperventilatory response to elevated internal ammonia was almost immediate, while that to elevated external ammonia was somewhat slower in the trout, and this was later reinforced by parallel observations in an elasmobranch (De Boeck and Wood 2015). These suggest that the NECs primarily sense internal plasma ammonia and that the response to high environmental ammonia (HEA) in the external water is indirect (i.e. after ammonia entry into the bloodstream), but further research is needed on this issue.

Zhang et al. (2013) also suggested the brain as a potential ammonia-sensing organ, because brain ammonia levels directly matched the hyperventilatory response to HEA in trout. This is in accord with earlier evidence that the brain in mammals plays a role in ammonia sensing (Vanamee et al. 1955; Warren 1958; Cooper et al. 1987; Wichser and Kazemi 1974). The evidence for central chemoreceptors for CO_2 , pH, and O_2 in fish is not strong (Wilson et al. 2000; Hedrick et al. 1991, Milsom 2012).

However, there is abundant evidence that elevated plasma ammonia permeates the blood brain-barrier in fish, and for this reason there are powerful detoxifying mechanisms for ammonia in the brain which convert it to glutamine (Schenone et al. 1982; Wright et al. 2007; Sanderson et al. 2010; Zhang et al. 2013) so as to avoid central neurotoxicity (Randall and Tsui 2002; Walsh et al. 2007). Rh glycoproteins are also expressed in trout brain tissue and respond to ammonia loading (Nawata et al. 2007; Zhang et al. 2013). In the future, we suggest that simple ammonia injection experiments into the brain while simultaneously measuring ventilation may be instructive. (This approach was used in Chapter 7).

5.5.4 Interaction of ammonia with O₂ in ventilatory control

The experimental design of Series II provides some indication of how ammonia and O₂ interact in ventilatory control. Clearly, the well-established ventilatory responses of fish to hypoxia and hyperoxia (Shelton et al. 1986; Perry et al. 2009), involving only small changes in frequency and larger changes in ventilatory pressure amplitude (i.e. stroke volume) persisted even when ventilation was stimulated by chronic ammonia loading. Ammonia similarly acted almost entirely by increasing amplitude, in accord with previous studies (Zhang and Wood 2009; Zhang et al. 2011). It is interesting that the hyperventilatory response to hypoxia in the ammonia-loaded fish of Series II appeared to be greater than that in the non-infused fish of Series I (compare Figs 5.3C versus 5.1C). This suggests that high ammonia and low O₂ may act synergistically to stimulate breathing, an interesting topic for future investigation.

5.5.5 Perspectives

We propose the following scenario. Elevated internal ammonia levels stimulate increased expression of components of the branchial Rh metabolon that can accelerate ammonia excretion at the gills, thereby effectively increasing their ammonia permeability. Meanwhile, increased plasma ammonia can be sensed by NECs in the gills and/or by the brain. These ammonia-stimulated signals would be transmitted to integrating centers in the central nervous system that control breathing, generating hyperventilation. Analogous to the model of Knepper and Agre (2004) which was originally proposed for more primitive ammonia channels, the excretion pathway for elevated plasma ammonia will involve conversion of ionized ammonium (NH₄⁺, the dominant form in the plasma) into gaseous ammonia (NH₃) at the Rh channel entrance. Upon exit at the apical surface, it is immediately converted back to NH₄⁺ by protons that acidify the boundary layer, in this case provided by increased activity of V-H⁺-ATPase

(HAT). The excreted ionic NH_4^+ is in turn eliminated by increased convective water flow in hyperventilating fish.

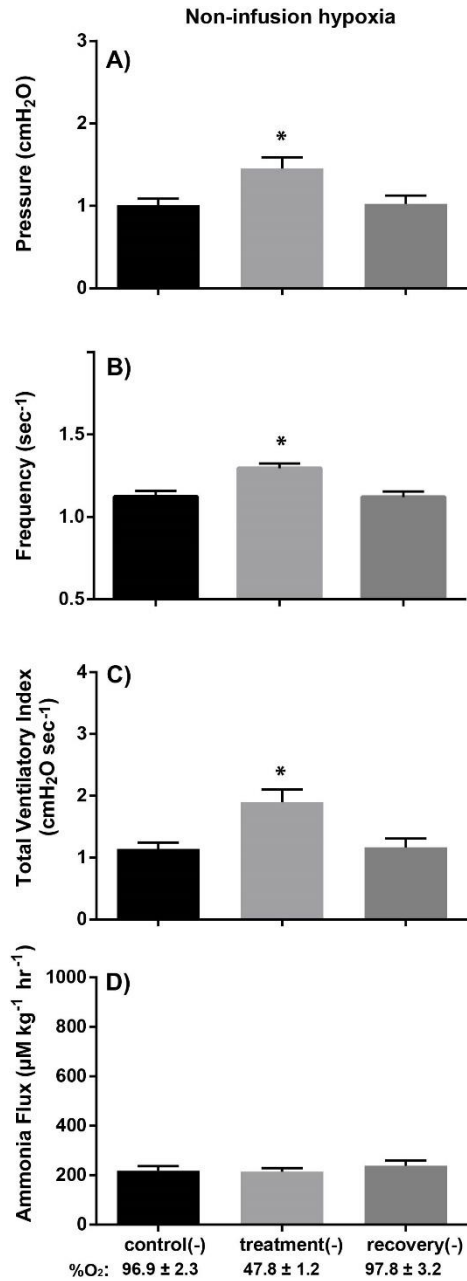


Figure 5.1 Changes in A) ventilation pressure amplitude, B) frequency, C) total ventilatory index (frequency x pressure amplitude), and D) ammonia excretion flux rate in non-infused rainbow trout (N = 6) during hypoxia in Series I. Asterisks indicate means that are significantly different from control(-) value. Symbol of (-) represents non-infused control value. Although fish significantly increased ventilation (one-way ANOVA, $p = 0.0177$) during hypoxia (48% air saturation in water), ammonia flux rate was not affected ($p = 0.3391$). Ventilation recovered to control levels in 98% air saturation water without changes in ammonia flux rate.

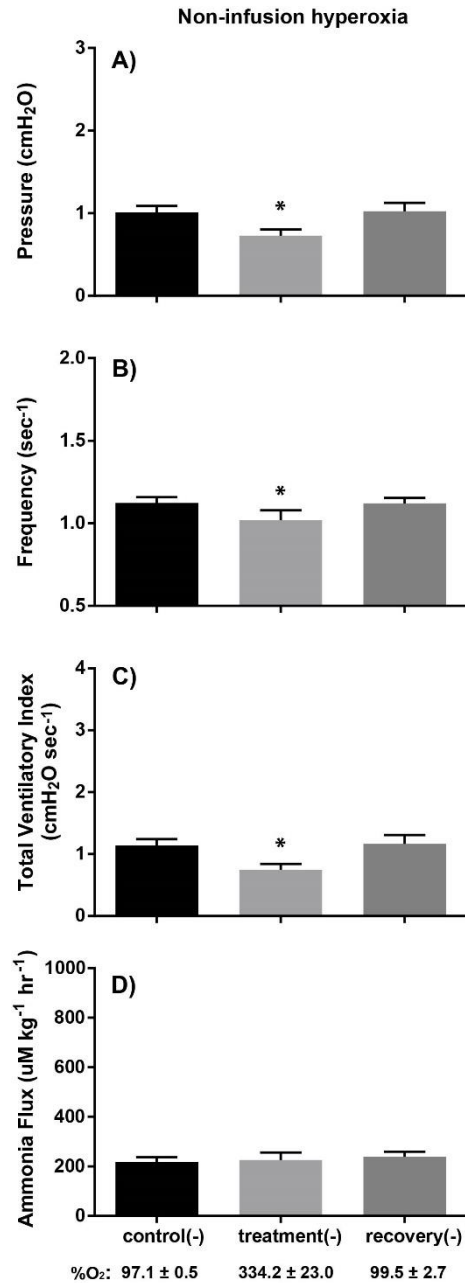


Figure 5.2 Changes in A) ventilation pressure amplitude, B) frequency, C) total ventilatory index (frequency x pressure amplitude), and D) ammonia excretion flux rate in non-infused rainbow trout (N = 6) during hyperoxia in Series I. Asterisks indicate means that are significantly different from control(-) value. Symbol of (-) represents non-infused control value. Although fish significantly decreased ventilation (one-way ANOVA, $p = 0.0033$) during hyperoxia (334% air saturation in water), ammonia flux rate was not affected ($p = 0.5166$). Ventilation recovered to control levels in 98% air saturation water without changes in ammonia flux rate.

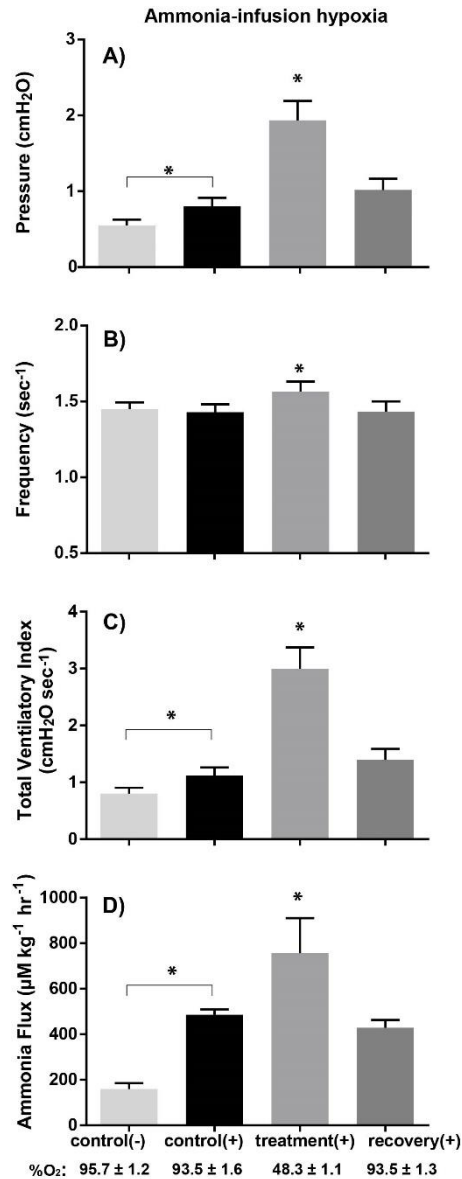


Figure 5.3 Changes in A) ventilation pressure amplitude, B) frequency, C) total ventilatory index (frequency x pressure amplitude), and D) ammonia excretion flux rate in non-infused rainbow trout (N = 10) in response to ammonia infusion and subsequent treatment with hypoxia during continuing ammonia infusion in Series II. Asterisks indicate significant differences from respective controls. Symbol of (-) represents non-infusion control and symbol of (+) indicates infusion control. With ammonia infusion, fish significantly increased ammonia flux rate and ventilation relative to control(-) values. During hypoxia, fish increased ventilation further (one-way ANOVA, $p < 0.0001$) with an accompanying elevation in ammonia flux rate ($p = 0.0005$). Ventilation and ammonia flux rate recovered to control(+) levels in 94% air saturation water.

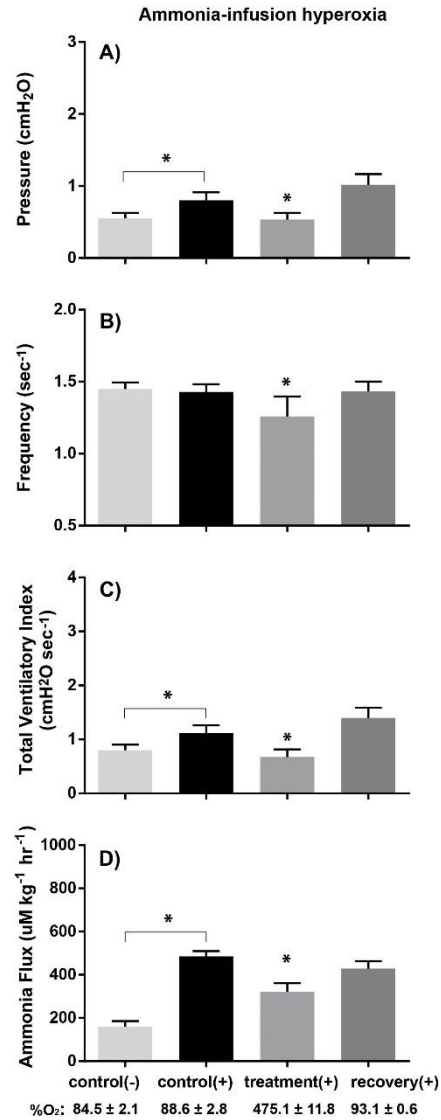


Figure 5.4 Changes in A) ventilation pressure amplitude, B) frequency, C) total ventilatory index (frequency x pressure amplitude), and D) ammonia excretion flux rate in non-infused rainbow trout (N = 10) in response to ammonia infusion and subsequent treatment with hyperoxia during continuing ammonia infusion in Series II. Asterisks indicate significant differences from respective controls. Symbol of (-) represents non-infusion control and symbol of (+) indicates infusion control. With ammonia infusion, fish significantly increased ammonia flux rate and ventilation relative to control(-) values. During hyperoxia, fish decreased ventilation (one way ANOVA, $p < 0.0084$) with an accompanying decrease in ammonia flux rate ($p = 0.0005$) relative to control(+) values. Ventilation and ammonia flux rate recovered to control(+) levels in 94% air saturation water.

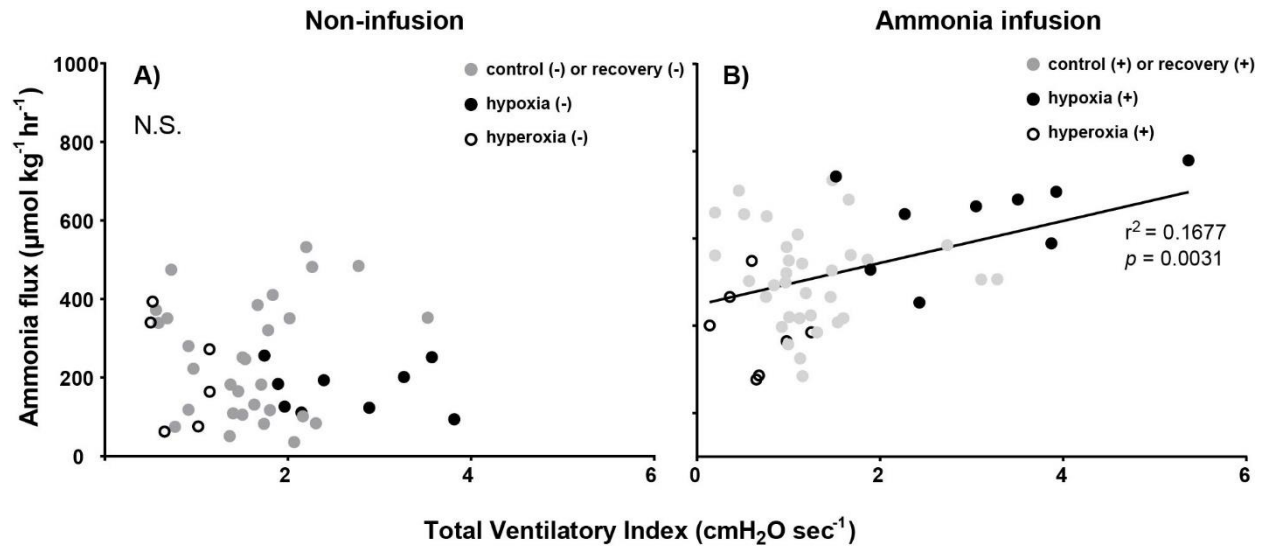


Figure 5.5 A) Hyperventilation (during hypoxia) or hypoventilation (during hyperoxia) in Series I did not affect ammonia excretion flux rate in non-infused fish that were not loaded with ammonia. Therefore, there was no significant relationship between ammonia excretion rate and ventilatory index. B) However, when fish were loaded with ammonia by infusion in Series II, hyperventilation (during hypoxia) increased ammonia excretion rate, and hypoventilation (during hyperoxia) decreased ammonia excretion rate, resulting in a significant relationship between ammonia excretion rate and ventilatory index. Symbol of (-) represents non-infused fish and symbol of (+) represents ammonia-infused fish. N.S. represents “not significant.”

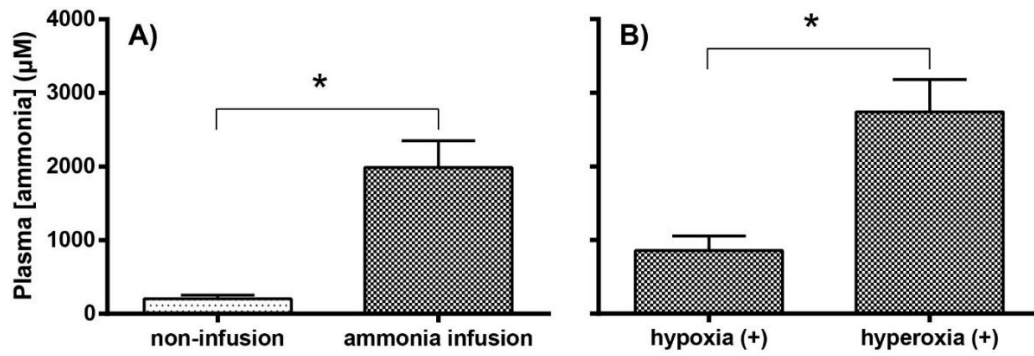


Figure 5.6 A) After ammonia infusion in Series II, plasma [ammonia] significantly increased in rainbow trout (N = 17) (Student's t-test, $p < 0.0001$). With continued ammonia infusion, B) hyperventilating fish in hypoxia (N = 8) showed significantly lower plasma [ammonia] than hypoventilating fish in hyperoxia (N = 9) ($p = 0.0058$). Symbol of (+) represents ammonia-infused fish.

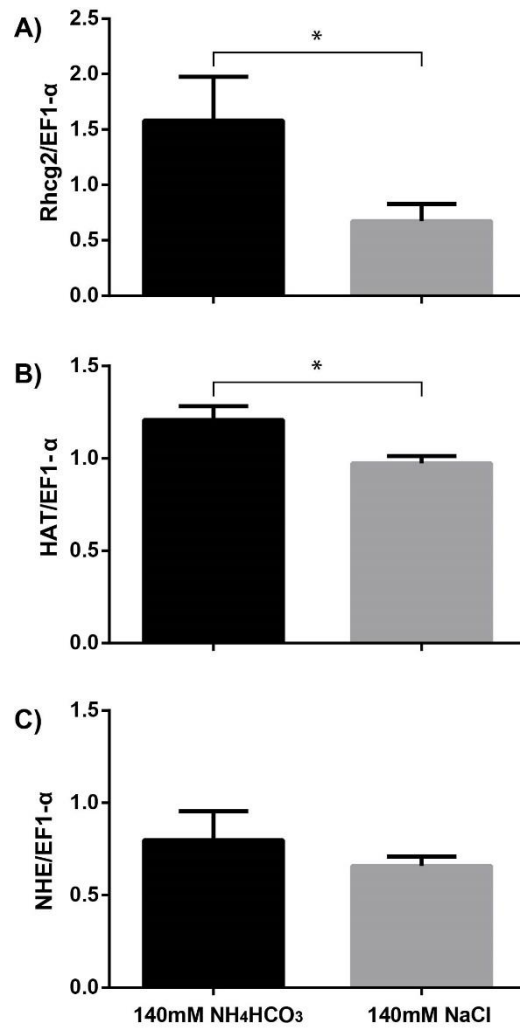


Figure 5.7 Expression levels of Rhcg2, HAT, and NHE2 genes in the gills of rainbow trout infused with 140 mM NH₄HCO₃ or 140 mM NaCl for 33 h in Series III.

Table 5.1 Heart rates (beats sec⁻¹, *via* ECG) under A) baseline conditions (Series I) and B) ammonia-loading (Series II).

A) Heart rate in series I (Baseline condition)			
control(-)	treatment(-)	recovery(-)	
0.77 ± 0.02	0.65 ± 0.01*	0.76 ± 0.02 hypoxia	
0.74 ± 0.03	0.71 ± 0.04	0.74 ± 0.03 hyperoxia	

B) Heart rate in series II (Ammonia-loaded)			
control(-)	control(+)	treatment(+)	recovery(+)
0.87 ± 0.02	0.85 ± 0.05	0.60 ± 0.05*	0.98 ± 0.06
		hypoxia	
0.81 ± 0.04	0.75 ± 0.08	0.70 ± 0.06	0.82 ± 0.04
		hyperoxia	

(unit: sec⁻¹)

Asterisks (*) indicate significant differences from A) control(-) in Series I or B) control(+) in Series II. Symbol of (-) represents baseline condition without ammonia-loading, while symbol of (+) represents baseline condition with ammonia-loading. Regardless of ammonia-loading, heart rate significantly decreased with hypoxia in both Series I (one-way ANOVA, $p = 0.0067$, $N = 6$) and Series II ($p = 0.0018$, $N = 7$). In hyperoxia, the heart rate did not change in either Series I ($N = 6$) or Series II ($N = 7$).

Chapter 6: A less invasive system for the direct measurement of ventilation in fish

6.1 Summary

Most previous systems for quantifying ventilatory flow in fish involve prior anesthesia and difficult surgery to sew or glue membranes to the animal, and are undoubtedly stressful. By modification of the original “van Dam” box design, and incorporation of an ultrasonic blood flow-probe, we have developed a less invasive system which avoids these problems and provides breath-to-breath measurements of ventilatory flow in real time. The fish can be quickly moved in and out of the apparatus, facilitating repeated measurements on the same animal after different treatments. We have used the system to document the hyperventilatory and hypoventilatory responses to environmental hypoxia and hyperoxia respectively in both 400-g trout and 10-g goldfish; the method is easily adaptable to fish of other sizes. Separate experiments on trout have demonstrated that responses in buccal pressure amplitude, breathing frequency, and ventilation index to these treatments are not altered by the apparatus. This less invasive methodology may prove more acceptable to animal ethics committees.

6.2 Introduction

The measurement of \dot{V}_w , the total ventilatory flow of water (“ventilation volume”) through the gills, is fundamental to understanding the respiratory physiology of fish, but is not easy to accomplish without stress to both the fish and the investigator. Ideally, \dot{V}_w should be measured directly and non-invasively. The classic study of Hall (1931) appears to be the first direct measurement, capitalizing on the discrete opercular openings of the pufferfish, attaching them by glass tubes to constant-level overflow chambers so that \dot{V}_w could be directly determined by timed volumetric collection, though opercular closure was undoubtedly impeded. The anatomies of most fish are not amenable to this approach, though in the dragonet (Hughes and Umezawa 1968a), rays (Cameron et al. 1971; Graham et al. 1990), and dogfish (Lenfant and Johansen 1966; Piiper and Schumann 1967; Hughes and Umezawa 1968b), similar but improved systems were applied by sewing and/or gluing latex funnels externally around the opercular openings so as to attach them to constant level overflows without impeding opercular closure. A more widely used direct measurement system was pioneered by van Dam (1938) who developed a divided chamber fitted with constant-level overflows; a rubber dam fitting tightly around the head of the fish (trout or eel) separated the buccal inflow (anterior chamber) from the opercular outflow so that the water

exhaled into the posterior chamber could be quantified by timed collection. Various versions of the “van Dam box” were subsequently customized for fish of different anatomies - for example dogfish (Hanson and Johansen 1970), flatfish (Watters and Smith 1973; Wood et al. 1979), catfish (Gerald and Cech 1970), mullet (Cech and Wohlschlag 1973), suckers (Wilkes et al. 1981), carp (Takeda 1990) and particularly salmonids (e.g. Hughes and Shelton 1957; Cameron and Davis 1970; Davis and Cameron 1971; Wood and Jackson 1980; McKim and Goeden 1982; Smith and Jones 1982; Randall and Cameron 1973; Playle et al. 1990; Kinkead and Perry 1990), for which it was frequently used for about two decades.

As technology improved, ultrasonic flow probes originally designed for measuring blood flow were employed for instantaneous ventilatory flow determinations. Initially, funnels fitted with flow-probes were sealed into the sand so as to overlay the protruding heads of flatfish (Kerstens et al. 1979) and hagfish (Steffensen et al. 1984) that had burrowed into sandy substrates. Flow-probes were also substituted for timed overflow collection, thereby providing breath-to-breath rather than time-averaged measurements of ventilatory outflow from the opercular openings of carp (Lomholt and Johansen 1979) and flatfish (Wood et al. 1979). Glass et al. (1990) made an important advance by attaching flow probes to the entrance of a rubber mask sutured around the mouth of the carp, and more recently, very direct measurements of instantaneous inflow were made by attaching the flow-meter to a tube sutured into the single inhalant nostril of hagfish (Perry et al. 2009; Eom and Wood 2019; now Chapter 2). Except for the “funnel in sand” studies, virtually all of these mask, funnel, tubing, and membrane techniques have required prior anesthesia and surgery (often quite difficult), in order to suture or glue the device(s) to the fish. An extensive post-operative recovery period in a restraining device is needed, success rates are problematic, and the fish is undoubtedly stressed, which may affect the measurements. It has become increasingly difficult to have such techniques approved by animal ethics committees, which may explain why such direct approaches have been rarely used in recent years.

Less invasive alternatives exist, but they provide only indirect measurement of \dot{V}_w , and all again require prior surgery to implant cannulae into the buccal and/or opercular cavities for water sampling or pressure measurements. Classic indirect methods include dye dilution approaches (Millen et al. 1966; Jones et al. 1990) and more commonly used Fick principle calculations (e.g. Saunders 1962; Holeyton and Randall 1967; Wood and Munger 1994; Kalinen et al. 2000). In the latter, \dot{V}_w is calculated from simultaneous measurements of whole animal O_2 consumption, and PO_2 in inspired and expired water. There are errors associated with multiple PO_2 determinations, and expired PO_2 measurements, which are critically important, can be particularly variable (Garey 1967; Davis and Watters 1970). The ventilatory

index, calculated as the product of ventilatory pressure amplitude and breathing frequency (measured by pressure transducers attached to buccal or opercular catheters) has also been used as a \dot{V}_w surrogate (e.g. Zhang et al. 2013; Wood et al. 2019; Eom et al. 2020; now Chapter 3). At best, all of these indirect approaches yield only relative measures of changes in \dot{V}_w .

With this background in mind, our goal was to develop a less invasive system that provided direct \dot{V}_w measurements on a breath-to-breath basis, one that avoided the need for anesthesia, suturing or gluing, that was manually simple for the investigator, and into which the fish could be quickly introduced and released. A thorough reading of Van Dam (1938) suggests that he was able to avoid using anesthesia, sutures, or glue by careful design of the chamber. Here, we have returned to the van Dam approach, combining it with an ultrasonic flow probe on the inflow (Glass et al. 1990), and a design allowing sealing and simple assembly, so that an unanesthetized fish can be quickly introduced with minimal disturbance. Using our system, we have successfully measured \dot{V}_w in both 400-g rainbow trout and 10-g goldfish under moderate hypoxia and hyperoxia, proving that the fish show the expected hyperventilation and hypoventilation respectively. In a separate series on trout, we have also demonstrated that responses in ventilatory pressure amplitude, breathing frequency, and ventilatory index were unaffected by the system, suggesting that breathing was not constrained. Overall, this system is easy to use for collecting \dot{V}_w data, and may prove useful for fish respiration researchers in the future.

6.3 Materials and Methods

6.3.1 Experimental animals

Experiments were performed under an approved UBC animal care protocol # A17-0301 following the guidelines of the Canadian Council on Animal Care. After completion of experiments, fish were euthanized by an overdose (120 mg L⁻¹) of tricaine methanesulfonate (MS-222, Western Chemicals Inc., Ferndale, WA, USA; pH was adjusted to 7.0 by titrating with 1 mmol L⁻¹ NaOH).

Rainbow trout (*Oncorhynchus mykiss*, 260 g ~ 501 g,) from Nanaimo River Hatchery (Nanaimo, BC, Canada) and goldfish (*Carassius auratus*, 9.8 g ~ 10.1 g) from Noah's Ark (Vancouver, BC, Canada) were held in charcoal-filtered dechlorinated Vancouver City tap water ([Na⁺], 0.17 mmol L⁻¹; [Cl⁻], 0.21 mmol L⁻¹; hardness, 30 mg L⁻¹ as CaCO₃; pH 7.0; temperature, 6.5 to 9.0 °C for rainbow trout, 15°C for goldfish) in flow-through systems at the University of British Columbia. These same

temperatures were used in the subsequent experiments. Fish were fed with commercial pellets (EWOS, Surrey, BC, Canada) three times per week, and fasted for one week prior to experiments.

6.3.2 Rainbow trout operations

It was not necessary to perform any surgery or cannulation on trout used in the new ventilation measurement system. However, to check whether the system affected the fish's resting ventilation and/or ventilatory responses to hypoxia and hyperoxia, buccal cannulation was performed on a separate group of trout using the method of Holeton and Randall (1967) so as to measure buccal pressure amplitude and frequency. Prior to cannulation, the fish were anesthetized in 60 mg L⁻¹ MS-222 (pH neutralized to ~7.0 as described above) and irrigated via the gills on an operating table. Using an 18-gauge needle, a hole was drilled in the roof of the mouth, and a 3-cm sleeve of polyethylene tubing (PE 160, Clay-Adams, Sparks, MD, USA; O.D. 1.57 mm and I.D. 1.14 mm) which had been heat-flared at the mouth end was inserted. Another flared 30-cm length of PE 50 tubing (Clay-Adams, O.D. 0.97 mm and I.D. 0.58 mm) was fitted through the PE 160 sleeve and cemented with cyanoacrylate glue (Krazy Glue, High Point, NC, USA). The connection between PE 160 and PE 50 was knotted at the outside with silk sutures. The operated fish were recovered overnight in flowing, aerated freshwater.

6.3.3 System set-up for rainbow trout

Fig. 6.1 shows the system set-up used for 260 ~ 501 g trout, and Media 6.1 (<https://doi.org/10.1139/cjfas-2020-0177>) shows a video of how unanesthetized trout are installed in the system. The set-up was submerged in an aerated 8-L water bath (reservoir) at the acclimation temperature (6.5 ~ 9.0 °C). Prior to fish placement, the centre-cut rubber piece layer which was cut from a balloon (BPL in Fig. 6.1, Dollarama, Vancouver, BC, Canada) was layered over the front end of the anterior 2.0" small PVC piece, which was then plugged into the 2.5" hollow PVC pipe. The fish was placed into the 2.5" PVC, its dorsal fin was positioned so as to fit through the dorsal slit in the 2.5" PVC pipe, and the head was pushed through the centre-cut BPL to a point just posterior to the eyes so as to separate the mouth from the operculae. The free movement of the lower jaw is very important for normal ventilation in rainbow trout, so an additional BPL cut was made if the fish showed any symptoms of irregular ventilation. The position of the posterior 2" PVC pipe was adjusted as necessary to minimize the anterior-posterior movement of the fish, which was also limited by the slit for the protruding dorsal fin. After

making these adjustments, a silicone collapsible funnel (SCF, Daiso, Vancouver, BC, Canada) was placed over the extended portion of the fish's head by stretching it over the anterior 2.0" PVC piece, completely sealing the anterior part of system. The open anterior end of the SCF was plugged with a rubber stopper (RS) penetrated by silicone tubing (ST, O.D. 6.35 mm and I.D. 4.32 mm, length 20 mm). Therefore, the anterior part of system was completely sealed except for the ST, through which the generated \dot{V}_w flowed and was measured by the attached flow probe (FP). Using dye, the possibility of leakage was checked after installation of the fish into the system.

When buccal pressure measurements were made, the water-filled PE 50 tubing was inserted through a pin-hole prepared in the SCF, and connected to a pressure transducer (DTP-100, Utah Medical Products, Midvale, UT, USA). The analogue buccal pressure signal was amplified (CLA-RTC, Transducer Techniques, Temecula, CA, USA) and converted into a digital signal in the digitizer (ADInstruments, Colorado Springs, CO, USA), recorded, and analyzed using two points calibration between 0 cmH₂O and 2 cmH₂O in the LabChart software (ADInstruments).

6.3.4 System set-up for goldfish

The reservoir temperature was set to 15°C. The overall system set-up was reduced in size by using a 1" PVC pipe rather than a 2.5" pipe. Instead of using anterior and posterior PVC plugs, the cut-lined BPL was directly stretched over the 1" PVC pipe end and the goldfish was placed into the pipe (Fig. 6.1). The fish's mouth extended through the cut-lined BP, with the eyes remaining behind the BPL. Instead of moving the lower jaw, the goldfish opens and closes the mouth by moving the mouth skeletal structure forward and backwards, therefore, less BPL cut line was required. The 1" PVC coupling was fitted over the extended fish's mouth, and the other side of the coupling was sealed with a 1" RS penetrated with the ST (O.D. 6.35 mm and I.D. 4.32 mm, length 20 mm). Again, the attached FP measured the \dot{V}_w . The buccal pressure was not measured in goldfish tests. Media 6.2 (<https://doi.org/10.1139/cjfas-2020-0177>) shows a video of how unanesthetized goldfish are installed in the system.

6.3.5 Flow-meter calibration

In accord with previous reports (Perry et al., 2009; Eom and Wood, 2019; Chapter 2), the internal machine calibration of the flow-meter (T106 series, Transonic Systems Inc., Ithaca, NY, USA) was not

applicable as it was designed for measuring blood flow, so we manually recalibrated with known flow rates of Vancouver water at the experimental temperature. In practice, we first internally calibrated the flow-meter using the two-point machine calibration, and then manually recalibrated it. Fig. 6.5 shows an example calibration relationship for correcting the measured \dot{V}_w . We also measured the hydraulic resistance of the ST. At a flow rate ($426.6 \pm 1.5 \text{ ml min}^{-1}$, $N = 83$) comparable to the highest instantaneous \dot{V}_w recorded in our study, the pressure differential across the ST was $0.047 \pm 0.009 \text{ cmH}_2\text{O}$ ($N = 83$), whereas at lower flow rates (means of 64.6 ml min^{-1} , $108.2 \text{ ml min}^{-1}$, and $227.0 \text{ ml min}^{-1}$), the measured pressure differentials were actually slightly negative ($\sim -0.04 \text{ cmH}_2\text{O}$), perhaps reflecting turbulence and/or the Venturi effect. Regardless, these values are negligible relative to buccal pressure amplitudes of several cmH_2O (see Fig.6.3A, D), so the resistance of the ST was insignificant.

6.3.6 Experimental procedures

In Series I, the rainbow trout ($N = 6$) and goldfish ($N = 3$), which had not been operated, were placed in their respective measurement systems first. The pipe systems were then placed in the black plexiglass boxes (8-L reservoir for rainbow trout, 4-L reservoir for goldfish). The fish were allowed to settle overnight in the apparatus, and then control ventilatory flow parameters in normoxic water were measured over a 0.5-h period. By bubbling pure nitrogen (N_2) gas or oxygen (O_2) gas, oxygen tension (PO_2) of the reservoir in the box was quickly adjusted to either 50% air saturation (hypoxia) or over 200% air saturation (hyperoxia). The PO_2 of reservoir was continuously monitored by a dissolved oxygen meter (Model 55, YSI, Yellow Springs, OH, USA). The ventilatory parameters were continuously measured over a 1-h treatment period of hypoxia or hyperoxia. At the end of exposure, the water in the reservoir was quickly replaced with normoxic water, and ventilatory parameters were further recorded over a 0.5-h recovery period.

In Series II, the basic experimental protocol was identical but buccal pressure measurements were made throughout. The operated rainbow trout were placed in the 2.5" PVC pipe system either with ($N = 6$) or without ($N = 6$) the BPL and SCF attachment. After overnight settling, buccal pressure measurements were made in normoxia (0.5 h), then hypoxia or hyperoxia (1.0 h), and finally during normoxic recovery (0.5h).

In both Series I and II, the fish were randomly treated first under hypoxia or first under hyperoxia, then allowed to recover overnight, and used again under the alternate treatment.

6.3.7 Data analysis

The measured ventilatory flow (\dot{V}_w) and buccal pressure parameters were analyzed using LabChart version 7.0 (ADInstruments). Employing the “Multiple Add to Data Pad” function in LabChart, flow traces were analyzed into ventilation flow (ml min^{-1}) and breathing frequency (min^{-1}), and pressure traces into buccal pressure amplitude (cmH_2O) and breathing frequency (min^{-1}) respectively. The collected ventilatory parameters were averaged every 3 sec in LabChart and exported to Excel, for calculation of ventilatory flow per unit body weight (\dot{V}_w , $\text{ml kg}^{-1} \text{min}^{-1}$), stroke volume (ml kg^{-1} , using an equation of “ $\dot{V}_w / \text{frequency}$ ”), and ventilatory index ($\text{cmH}_2\text{O min}^{-1}$, using an equation of “buccal pressure amplitude x frequency”). GraphPad Prism 6.0 (La Jolla, CA, USA) was used for plotting and statistically analyzing the measured and calculated parameters. Using repeated measures one-way ANOVA in Series I and two-way ANOVA (factors: oxygen, presence/absence of attachments), as well as Student’s two tailed t-test in Series II, overall significance of averaged ventilatory parameters among control, oxygen (hypoxia or hyperoxia), and recovery period were statistically tested. Also, changed ventilatory parameters in treatments and recovery were compared to averaged control using Dunnett’s post hoc test. Throughout, data have been expressed as means \pm 1 SEM (N). The threshold for statistical significance was $p < 0.05$.

6.4 Results

Using our less invasive system, ventilatory flow measurements were made in Series I on rainbow trout under normoxic control conditions, and then in 50% saturation (hypoxia) or in $>200\%$ saturation (hyperoxia) (Figs. 6.2A, B, C). Representative recordings are shown in Fig. 6.4A, B, C, D. Mean resting \dot{V}_w under normoxia was about $140 \text{ ml kg}^{-1} \text{min}^{-1}$ with a frequency of about 70 min^{-1} and a stroke volume of about 2 ml kg^{-1} (at $6.5 - 9^\circ\text{C}$). When challenged with hypoxia (50% saturation) our trout exhibited a significant and sustained 30% increase in \dot{V}_w ($p = 0.0008$; Fig. 6.2A), achieved almost entirely by an increase in ventilatory stroke volume (Fig. 6.2C); there was no change in frequency (Fig. 6.2B). Ventilatory parameters returned to normal after about 10 min of normoxia restoration. During hyperoxia, our trout decreased \dot{V}_w by about 40% ($p = 0.0017$; Fig. 6.2A), achieved by a large decrease in stroke volume ($p = 0.0104$; Fig. 6.2C) and a very small decrease in frequency ($p = 0.0502$; Fig. 6.2B). \dot{V}_w returned to normal within 15 min of restoration of normoxia, though there were some ongoing small disturbances of stroke volume and frequency.

We down-sized our system to see if it could be adapted to much smaller fish, such as 10-g goldfish (Fig. 6.2D, E, F; Fig. 6.4E, F, G, H). Mean resting \dot{V}_w under normoxia was about 110 ml kg⁻¹ min⁻¹, with a frequency of 90 min⁻¹ and stroke volume of 1.2 ml kg⁻¹ h⁻¹ (15°C). Goldfish also showed hyper- and hypo-ventilation in hypoxia and hyperoxia respectively, but the relative changes were larger than in the rainbow trout. Thus, \dot{V}_w increased by 230% during hypoxia ($p = 0.0304$), and recovered only partially during 30 min of normoxia restoration (Fig. 6.2D). This hyperventilation was achieved by significant increases in both frequency (by 25%, $p = 0.0403$; Fig. 6.2E) and stroke volume (by 170%, $p = 0.0522$; Fig. 6.2F). During hyperoxia, mean \dot{V}_w decreased by 55% ($p = 0.0330$; Fig. 6.2D). Breathing became intermittent with frequent pauses (Fig. 6.4G, H), so frequency and calculated stroke volume both became very variable, with the former significantly declining by about 80% (Fig. 6.2E) and the latter increasing many-fold (Fig. 6.2F) but these changes were not significant due to large variation and low N-number.

Using rainbow trout, the experiments of Series II addressed the possibility that our system might restrict the fish's resting ventilation and/or ventilatory responses to hypoxia and hyperoxia. Buccal pressure amplitude (Fig. 6.3A, D) and ventilatory frequency (Fig. 6.3B, E) were measured in separate trout either with or without the BPL and SCF attachments. There were no significant differences at any time in pressure amplitude (cmH₂O), frequency (min⁻¹), or their product (ventilatory index, cmH₂O min⁻¹) between the two treatments. In case any differences between the two treatments were missed in the two-way ANOVA, they were also checked by Student's two tailed t-test at each time; there were no significant differences. Furthermore, the patterns of ventilatory index changes [35% increase during hypoxia (Fig. 6.3C), 45% decrease during hyperoxia (Fig. 6.3F)] were virtually identical to those seen in \dot{V}_w in Series I [30% increase, 40% decrease (Fig. 6.2A)].

6.5 Discussion

Overall, our measured ventilation flow values in our less invasive system were close to those reported by Davis and Cameron (1971) in comparably sized trout at similar temperature (8.6°C) in Vancouver water. Davis and Cameron (1971) used a modified "van Dam box" with the rubber membrane sewn to the fish's lips. In van Dam's original study (van Dam 1938), where there was no sewing, his single 900-g trout also pumped the same control \dot{V}_w under normoxia at a frequency of 90 min⁻¹ in slightly warmer water (10 to 12° C). Our trout exhibited a significant and sustained 30% increase in \dot{V}_w when acutely exposed to hypoxia (50% saturation) (Fig. 6.2A), achieved almost entirely by an increase in

ventilatory stroke volume (Fig. 6.2C). van Dam's trout exhibited an 80 to 100% increase in \dot{V}_w at the same level of hypoxia (50% saturation), again mainly achieved by increased stroke volume. However, by way of contrast, Davis and Cameron (1971) reported a 600% increase in \dot{V}_w at 40% saturation, and Kinkead and Perry (1990) reported a 200% increase in \dot{V}_w at 46% saturation (10 to 19°C), both using sewn-on membranes. Holeton and Randall (1967) reported a 900% increase in \dot{V}_w at 50% saturation (15°C) calculated by the Fick principle in trout fitted with many catheters. A tentative conclusion is that more invasive techniques tend to amplify the responses to hypoxia.

In response to acute hyperoxia, our trout decreased \dot{V}_w by about 40% (Fig. 6.2A), mainly due to a large decrease in stroke volume Fig.6.2C. By way of comparison, in trout fitted with sewn-on membranes, reported decreases in \dot{V}_w were about 65% at 10 to 19°C (Kinkead and Perry 1990) and 40 to 60% at 12 to 16°C (Wood and Jackson 1980), again achieved almost entirely by reductions in stroke volume.

During hypoxia, our goldfish increased \dot{V}_w by 230% during hypoxia (Fig. 6.2D) achieved by 25% increases in frequency (Fig. 6.2E) and much larger 170% elevations in stroke volume (Fig. 6.2F). We are aware of no previous direct measurements of \dot{V}_w at goldfish. However, in the related common carp (*Cyprinus carpio*), Glass et al. (1990), using their stitched mask and flow-meter system (*see* Introduction) reported 160% and 240% increases in \dot{V}_w in response to the same hypoxia level (50% saturation) at 10°C and 20°C respectively. Stroke volume elevations dominated the response at 10°C, while frequency elevations were more important at 20°C. Tzaneva and Perry (2010) used impedance techniques to monitor ventilation in goldfish, and found that a more severe acute hypoxia (20% saturation) caused 40% increases in ventilatory frequency and 90% increases in amplitude respectively, at both 7°C and 25°C. Goldfish are known to normally exploit surface "air gulping" during hypoxia (Burggren 1982), an opportunity which was prevented by the systems used in all three studies, including the present one. This may help explain their large responses to hypoxia. With respect to hyperoxia, Takeda (1990), using a "van Dam box" system and a stitched mask, found that hyperoxia decreased \dot{V}_w by about 60% in the related common carp at 25°C. Our measurements appear to be in general accord with all these studies.

Interestingly, in goldfish exposed to hyperoxia, ventilation became consistently intermittent with frequent pauses (Fig. 6.4G, H), a pattern we also saw occasionally during normoxia, but never in hypoxia (Fig. 6.4E, F). In two other cyprinids, Glass et al. (1990) and Vulesevic et al. (2006) observed episodic ventilation patterns during normoxia in common carp and zebrafish respectively, and in the latter, these episodes became more common during hyperoxia, and less common during hypoxia, as in the present

study. We found that breaths became large, and there was a brief moment where the flow was reversed, or in other words became bidirectional (Fig. 6.4H). This did not occur in the common carp, where the instantaneous flow trace never became negative (Glass et al. 1990). At present we are unsure whether the flow reversal in hyperoxic goldfish is real, or an artifact, because we noticed that the fish tended to move its mouth forward when taking a large breath. In the closed anterior chamber, this could momentarily reverse the flow through the probe without reversing flow across the gills. Further research is required.

In conclusion, our less invasive system is easy to use, does not involve anesthesia or surgery, and produces reasonable measures of \dot{V}_w on a breath-to-breath basis in both large trout and small goldfish. It will be easily adaptable to fish of different sizes, and with careful design of the BPL and SCF attachments, it could be adapted to other fish with different morphologies. PO_2 , PCO_2 , and pH sensors can be easily mounted in the inflow and outflow compartments to monitor respiratory gas exchange. As illustrated in Supplementary Media 6.1 and 6.2, the fish can be quickly moved in and out of the system, so it is possible to make repeated measurements on the same animal after different treatments – for example after feeding, or a bout of exercise. Furthermore, as the procedures are less invasive, the fish is less stressed, so the measurements are more reliable, and the protocol may prove more acceptable to animal ethics committees.

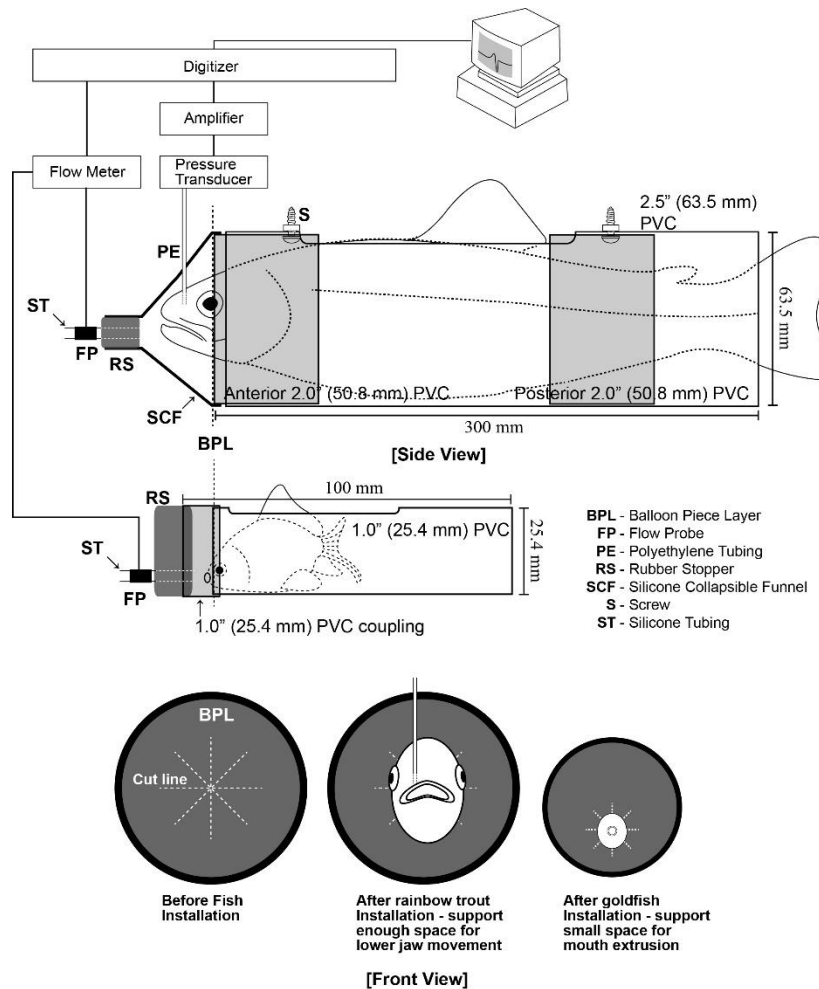


Figure 6.1 A diagram of the system set-up, in rainbow trout and goldfish. For the trout, the system is shown with a buccal cannula in place. The trout is placed in a 2.5" (63.5 mm) diameter PVC pipe. Two 2.0" (50.8 mm) PVC pieces are anteriorly and posteriorly plugged in place and later secured with screws (S) for stabilizing the fish. The centre-cut balloon piece layer (BPL) is stretched over the anterior 2.0" PVC piece, and plugged into the 2.5" PVC pipe in order to separate the buccal and opercular cavities. Once the trout is placed in the 2.5" PVC pipe, the silicone collapsible funnel (SCF) is stretched over the anterior 2.0" PVC piece. At this point, it is essential to adjust the BPL so as to allow enough space for lower jaw movement. The anterior opening of the SCF is sealed with a rubber stopper (RS) penetrated with the silicone tubing (ST). The inset shows how the overall system is scaled down using a 1" PVC pipe for ventilatory flow measurements in goldfish. In both the trout and goldfish systems, the fish's head is completely sealed in the anterior chamber, so that water inflow during ventilation is only allowed through the ST and is measured by the attached flow-probe.

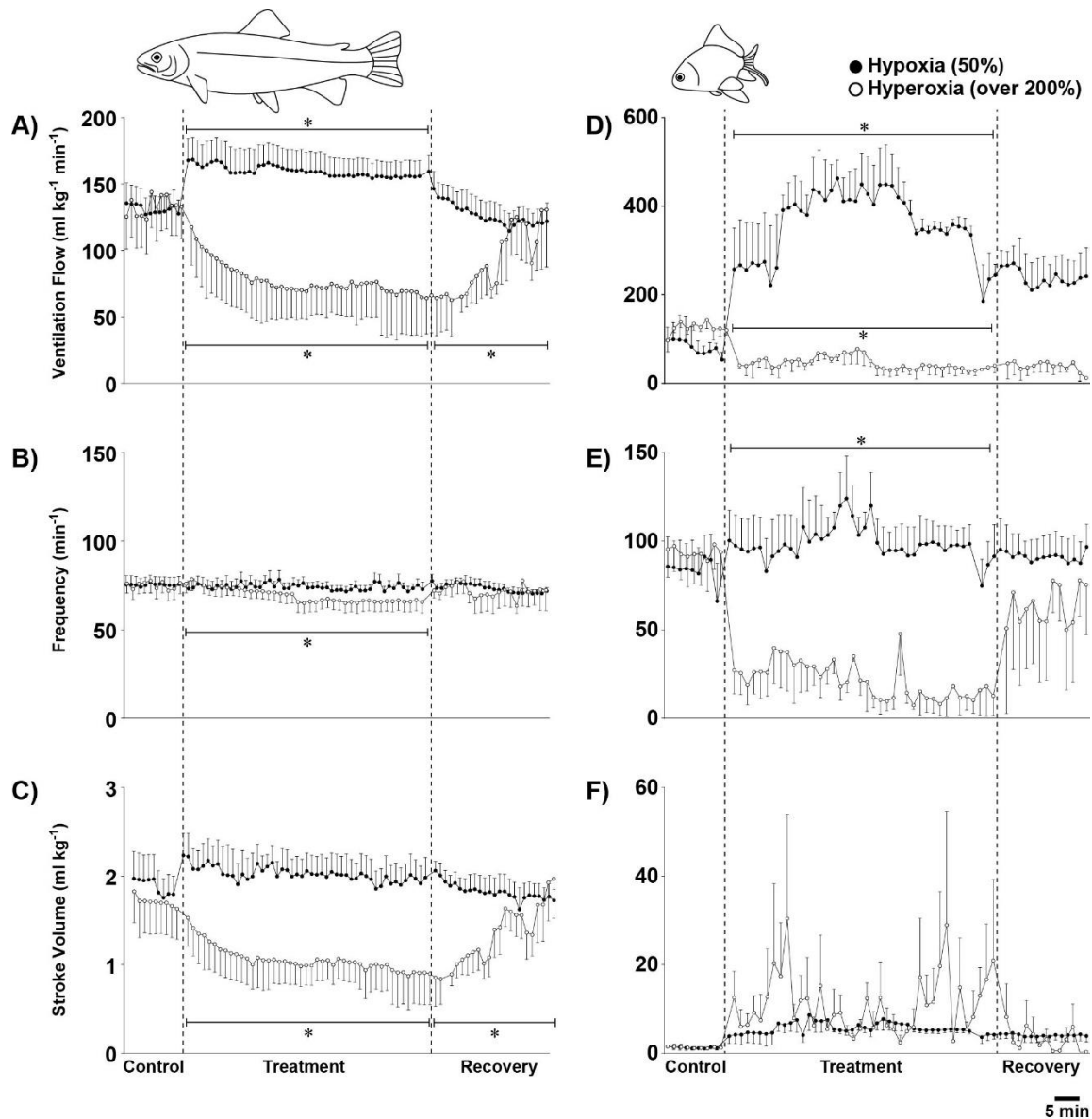


Figure 6.2 Ventilatory flow parameters measured during control normoxia, during 1 h in either hypoxia (50% saturation, closed symbols) or hyperoxia (> 200% saturation, open symbols), and during recovery in normoxia in rainbow trout (N = 6, left hand panels) and goldfish (N = 3, right hand panels): A, D) ventilatory flow (\dot{V}_w), B, E) ventilatory frequency, C, F) ventilatory stroke volume. Means \pm 1 S.E.M. Asterisks indicate periods during which the measured parameters were significantly different from the mean normoxic control value. Measured parameters were averaged every 60 sec and plotted. The high variation in the calculated stroke volumes in the goldfish originated from the episodic breathing which occurred during this treatment.

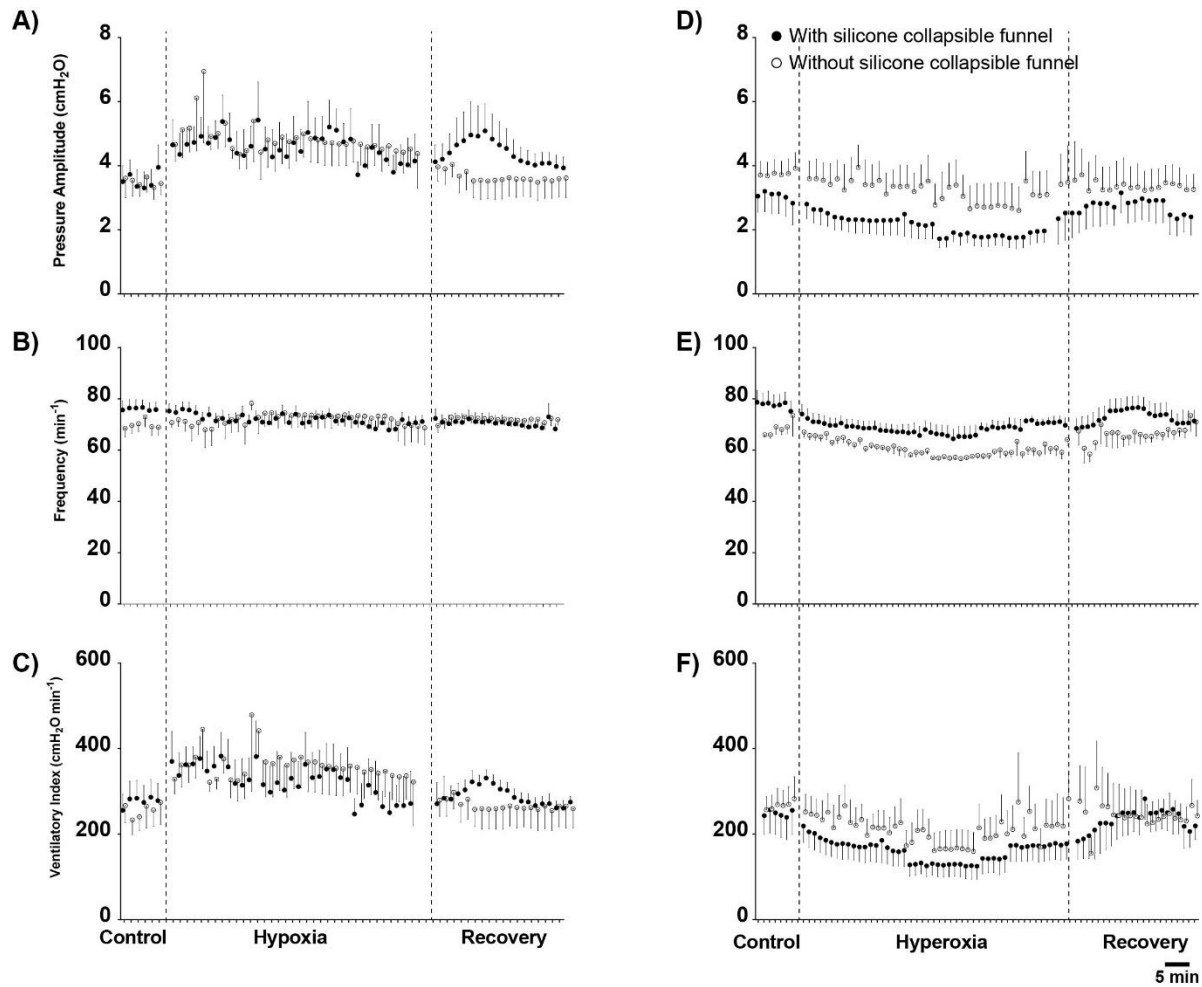


Figure 6.3 Changes in A, D) buccal pressure amplitude, B, E) breathing frequency, and C, F) ventilatory index in rainbow trout with (solid symbols) or without (open symbols) the silicone collapsible funnel (SCF) and balloon piece layer (BPL) in place. Measurements were made during control normoxia, during 1 h in either hypoxia (50% saturation, left hand panels) or hyperoxia (>200% saturation, right hand panels) and during recovery in normoxia. Means \pm S.E.M. (N = 6). There were no significant differences between the two treatments (with SCL and BPL *versus* without SCL and BPL) at any time.

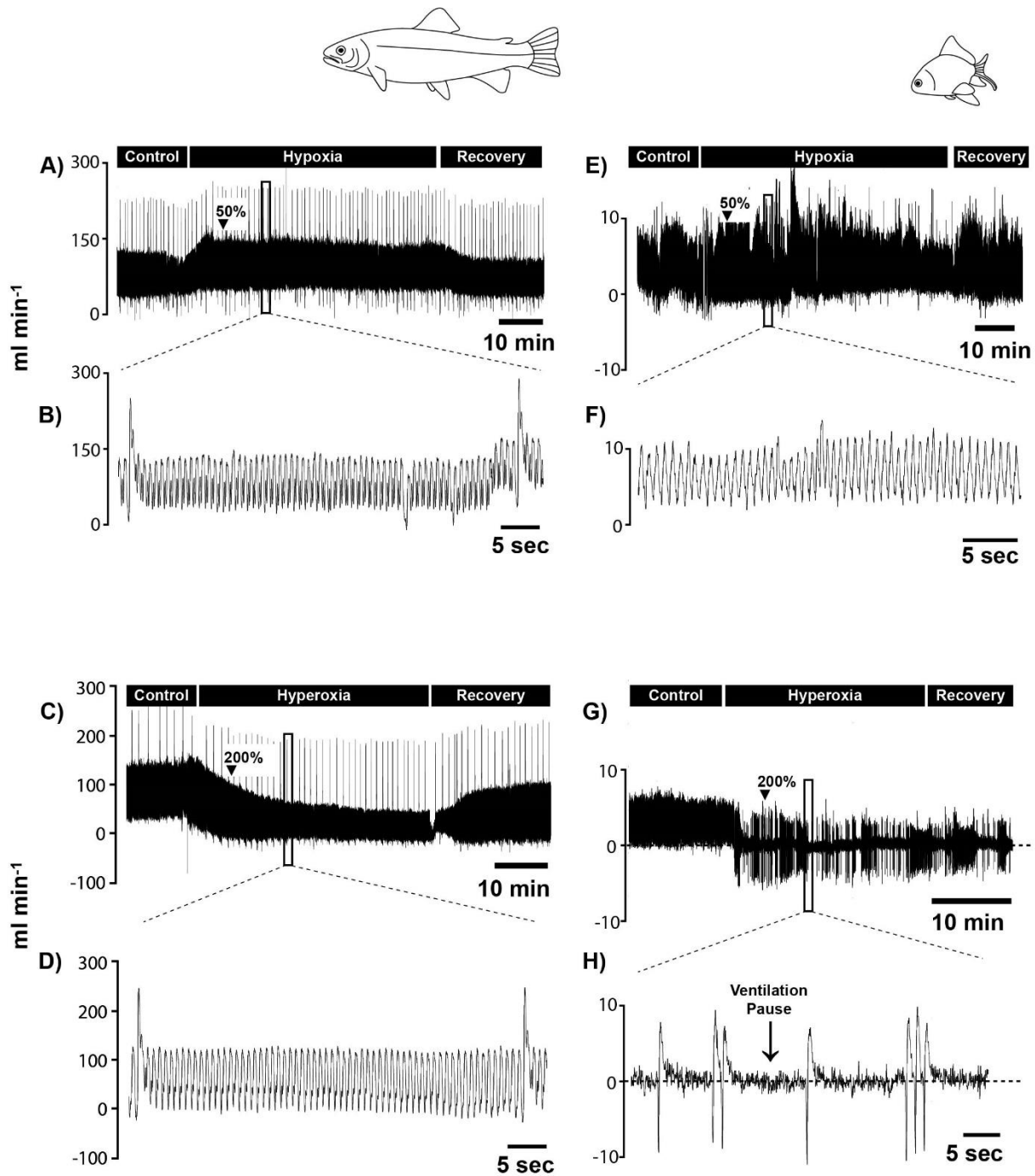


Figure 6.4 Ventilatory flow traces of rainbow trout (N = 1) and goldfish (N = 1) in 50% hypoxia (50% saturation) and hyperoxia (>200% saturation). Note the episodic breathing patterns in hyperoxia-treated goldfish.

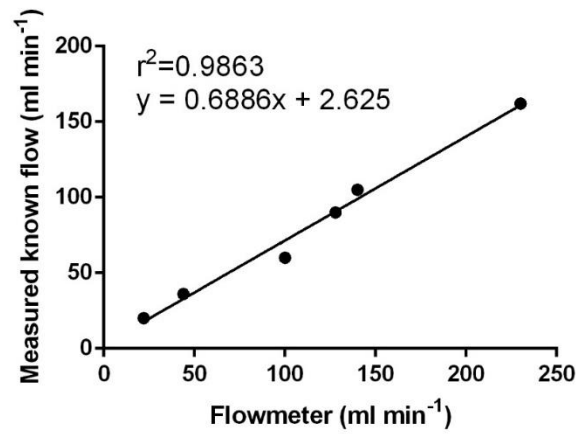
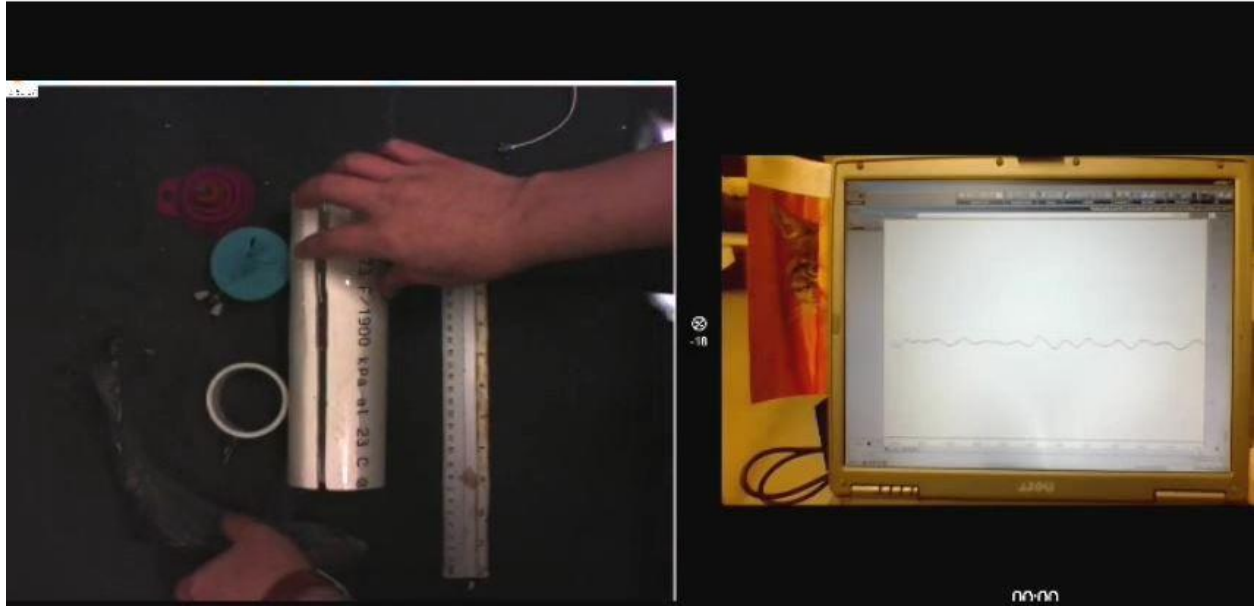
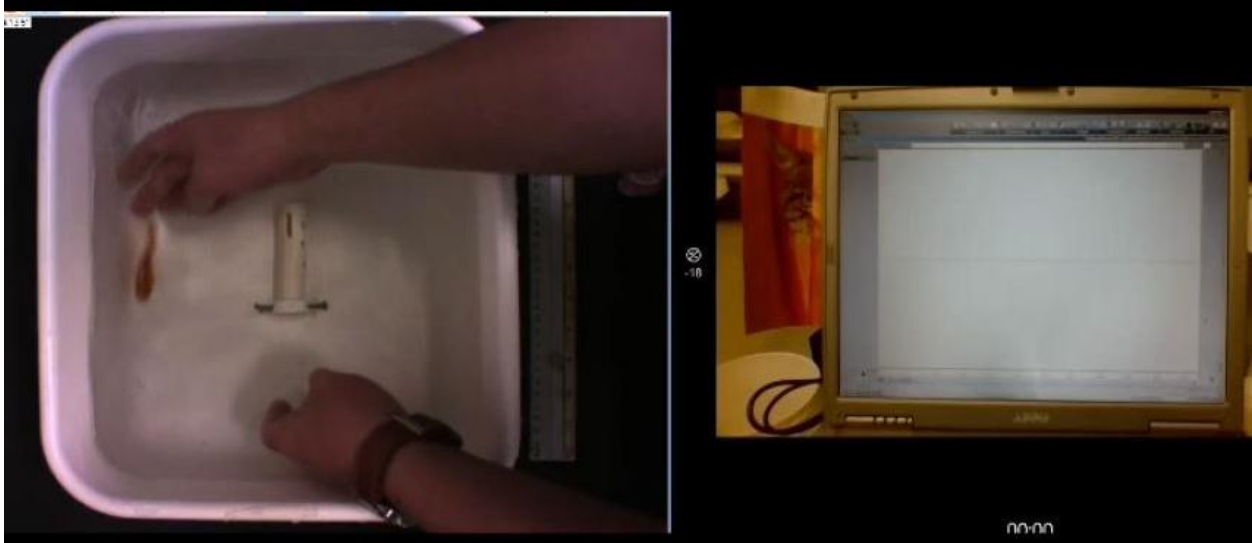


Figure 6.5 An example of a manual calibration curve for the flow-probe. Ventilatory flow rate measured by the flowmeter was plotted against the known water flow rate. The equation of the relationship was used to correct the collected ventilatory flow data.



Media 6.1 System set-up procedure in 350-g rainbow trout.



Media 6.2 System set-up procedure in 10-g goldfish.

Chapter 7: Brain and gills as internal and external ammonia sensing organs for ventilatory control in rainbow trout, *Oncorhynchus mykiss*

7.1 Summary

Ammonia is both a respiratory gas and a toxicant in teleost fish. Hyperventilation is a well-known response to elevations of both external and internal ammonia levels. Branchial neuroepithelial cells (NECs) are thought to serve as internal sensors of plasma ammonia (peripheral chemoreceptors), but little is known about other possible ammonia-sensors. Here, we investigated whether trout possess external sensors and/or internal central chemoreceptors for ammonia. For external sensors, we analyzed the time course of ventilatory changes at the start of exposure to 1 mM high environmental ammonia (HEA). Hyperventilation developed gradually over 20 min, suggesting that it was a response to internal ammonia elevation. We also directly perfused ammonia solutions (0.01 to 1 mM) to the external surfaces of the first gill arches. Immediate hypo-ventilation occurred. For central chemoreceptors, we injected ammonia solutions (0.5 to 1.0 mM) directly onto the surface of the hindbrain of anaesthetized trout. Immediate hyper-ventilation occurred. This is the first evidence of central chemoreception in teleost fish. We conclude that trout possess both external ammonia sensors, and dual internal ammonia sensors (perhaps for redundancy), but their roles differ. External sensors cause short term hypoventilation, which would help limit toxic waterborne ammonia uptake. When fish cannot avoid HEA, the diffusion of waterborne ammonia into the blood will stimulate both peripheral (NECs) and central (brain) chemoreceptors, resulting in hyper-ventilation. This hyperventilation will be beneficial in increasing ammonia excretion *via* the Rh metabolon system in the gills not only after HEA exposure, but also after endogenous ammonia loading from feeding or exercise.

7.1 Introduction

Fish are known to hyperventilate in response to elevations in environmental ammonia (Smart 1978; Lang et al. 1987; Fivelstad and Binde 1994; Knoph 1996). While this is often interpreted as a general stress response to a toxicant, it may in fact reflect activation of a key mechanism for controlling ventilation. As teleost fish are ammoniotelic, they metabolically produce and excrete large amounts of ammonia, at a rate amounting to 10 ~ 20% of O₂ consumption and CO₂ production. For this reason, ammonia, which like carbon dioxide (CO₂ + HCO₃⁻) exists in both unionized (NH₃) and ionized (NH₄⁺)

forms, is considered the third respiratory gas in fish (Randall and Ip 2006). Rh glycoproteins are widely distributed in fish tissues, especially the gills (Nawata et al. 2007; Nakada et al. 2007a; Wright and Wood 2009), serving to facilitate ammonia movement across membranes. Using the rainbow trout as a model system, it has been established that increases in blood ammonia can stimulate ventilation (McKenzie et al. 1993), that this effect is independent of changes in the other respiratory gases (Zhang and Wood 2009), and that the hyperventilation is effective in increasing ammonia excretion across the gills, once diffusive limitation (Randall and Ip 2006) has been removed by activation of the Rh metabolon system (Eom et al. 2020; now Chapter 5).

The neuro-epithelial cells (NECs) on the first and second gill arches, which are known to be polymodal receptors for the other respiratory gases (reviewed by Milsom 2012; Perry and Tzaneva 2016; Jonz 2018) appear to play a key role in sensing blood ammonia levels (Zhang et al. 2011; Zhang et al. 2015). In mammals, it has long been known that elevations in blood ammonia can stimulate ventilation (Poppell et al. 1956; Roberts et al. 1956; Warren, 1958; Campbell et al. 1973) probably by actions on central chemo-sensors in the brain (Wichser and Kazemi 1974). Detection in the brain may also play a role in fish, as Zhang et al. (2013) showed a close association between increases in ventilation and increases in brain total ammonia levels in trout during various experimental treatments. However, the evidence was only correlational. It is less clear how elevations in external ammonia are sensed. The hyper-ventilatory response to high environmental ammonia (HEA) seems to develop gradually over time (Zhang et al. 2013), in contrast to the almost instantaneous response to injections of ammonia into the blood stream (McKenzie et al. 1993; Zhang and Wood 2009; Zhang et al. 2011). This could suggest that ammonia is not detected externally, and that ventilation rises during HEA exposure only once blood ammonia increases by inward diffusion across the gills to a level sufficient to stimulate internal receptors (NECs and/or brain). Indeed, this appears to be the case in the hagfish, a primitive ancestral vertebrate (Eom et al. 2019; now Chapter 3) and in the elasmobranch dogfish, a representative of another ancient lineage (DeBoeck and Wood 2015).

The present study focuses on short-term ventilatory responses to ammonia in trout, in order to understand whether ammonia is detected externally, and whether the brain serves as an ammonia sensor. In Series I, we exposed the fish to HEA, and closely followed the initial time course of the ventilatory responses. As previous studies had made only indirect measurements (buccal pressure amplitude and frequency) of ventilatory flow (\dot{V}_w), we additionally measured \dot{V}_w directly using a flow-meter system. In Series II, we measured ventilation changes in response to direct perfusion of ammonia onto the external surfaces of the gill arches. In Series III, we measured ventilation changes in response to injections of

ammonia in mock extradural fluid (EDF) directly onto the surface of the brain. Our overall hypothesis was that fish would have both external and multiple (gill NECs and brain) internal ammonia receptors so as to make appropriate ventilatory responses to this respiratory gas and widespread toxicant.

7.2 Materials and Methods

7.2.1 Experimental animals

Rainbow trout (100 ~ 300 g) were obtained from a hatchery (Miracle Springs Inc., Fraser Valley, BC, Canada) and held in 900-L fibreglass tanks, served with flow-through, charcoal-filtered dechlorinated Vancouver City tap water ($[\text{Na}^+]$ 0.17 mmol L⁻¹; $[\text{Cl}^-]$ 0.21 mmol L⁻¹; hardness 30 mg L⁻¹ as CaCO₃; pH 7.0; temperature 6.5 to 9.0°C) at the University of British Columbia. The fish were regularly fed with commercial food pellets (EWOS, Surrey, BC, Canada) three times per week but they were fasted for a week prior to experiments in order to minimize the internally increased ammonia metabolism after feeding. The experiments were approved by the University of British Columbia under animal care protocol AUP# A17-0301 following the guidelines of the Canadian Council on Animal Care. After completion of the experiments, the fish were humanely euthanized using an over-dose (360 mg L⁻¹) of tricaine methanesulfonate (MS-222, Western Chemicals Inc., Ferndale, WA, USA; pH was adjusted to 7.0 with 5 M NaOH).

7.2.2 Fish cannulations and analytical techniques

Three different series of experiments were performed. Series I (N = 7) used both flow and buccal pressure measurements to monitor the immediate ventilatory responses of the fish to high environmental ammonia (HEA) in the external water. Series II (N = 5) employed buccal pressure measurements to examine the ventilatory responses to a logarithmic series of increasing ammonia concentrations perfused directly onto the external surfaces of the gill arches. Series III (N = 6) explored the effects on ventilation (monitored by buccal pressure measurements) of injection of different concentrations of ammonia onto the surface of the hindbrain (Fig. 7.1).

In all series, fish were surgically prepared under deep anaesthesia (180 mg L⁻¹ MS-222, pH neutralized to ~7.0 with 5.0 M NaOH), and in Series I and II, during surgery, VaselineTM-impregnated cotton balls were inserted into both nares to block the nostril entrance so as remove olfactory complications. After completion of surgery in these first two series, the fish were allowed to recover overnight in individual boxes (black plexiglass chambers, length 380 mm x width 100 mm x height 180

mm) served with 500 ml min⁻¹ of aerated flowing dechlorinated water at the acclimation temperature, (6.5 to 9.0 °C). In Series I, as described below, after overnight recovery, the fish were transferred to a newly developed system for the direct measurement of ventilation flow (\dot{V}_w) (Eom and Wood 2020; now Chapter 6). In Series II, the fish were maintained in their individual boxes. In Series III, the fish were again maintained in their individual boxes for experimentation. However, surgery was performed under deep anaesthesia, and then the fish were switched to a lighter level of anaesthesia (60 mg L⁻¹ MS-222, pH neutralized) for 2 ~ 3 h of recovery, and this lighter anaesthesia was maintained during the subsequent experiments.

In Series I, the fish were anesthetized and placed on an operating table while neutralized MS-222 solution was irrigated over the gills *via* the opercular openings. Using a #18G needle, a hole was drilled through the roof of mouth cavity, taking care to avoid the nares, and a 3-cm sleeve of PE 160 tubing (Clay-Adams, Sparks, MD, USA; 1.57 mm O.D. and 1.14 mm I.D.), heat-flared at the buccal side, was inserted through the hole. An additional 30-cm length of PE 50 tubing (Clay-Adams, 0.97 mm O.D. and 0.58 mm I.D.), again heat-flared at the buccal side, was inserted through the PE 160 which was already fitted into mouth cavity. The cannulae were cemented together using cyanoacrylate glue (Krazy Glue, High Point, NC, USA). In order to prevent movement of the cemented tubing, the outside of cemented tubing was tightened with a large silk suture knot. The catheter was used to monitor the frequency and buccal pressure amplitude of ventilation (Holeton and Randall 1967). The overnight recovered fish were then transferred into a newly developed flow-measuring device which has been described in detail by Eom and Wood (2020; Chapter 6); *see* Fig. 6.1 in that chapter. The system is designed for measuring ventilatory flow (\dot{V}_w) without any further surgical operation, and is submerged in an 8-L temperature-controlled, recirculating reservoir. In brief, the apparatus is based on the original mask-system of van Dam (1938). However, instead of a constant-level overflow, the system incorporates an ultrasonic blood flow probe (Transonic Systems Inc., Ithaca, NY, USA) coupled to a flow-meter (T106 series, Transonic Systems Inc.) into the front of the form-fitting mask for the continuous recording of ventilatory water flow. As in van Dam (1938), no stitches or gluing are used to attach the mask. However, the fish is restricted inside a hollow polyvinyl chloride tube which minimizes side-to-side and back-and-forth movement.

In Series II, the first buccal catheter was placed as in Series I, and a second buccal catheter was placed for perfusing ammonia directly onto the external gill arches, using a technique similar to that of Daxboeck and Holeton (1978). For the latter, a second hole was drilled through the other side of the roof of the mouth cavity using the #18G needle, again avoiding the nares. Another heat-flared 3-cm PE 160 sleeve was placed, and a 30-cm length of PE 50 tubing was inserted through the PE 160 sleeve. A Y-

shaped connector (1.59 mm I.D., Cole-Parmer, St. Montreal, QC, Canada) was joined to the PE 50 tubing at the buccal cavity end; the size gap between the PE 50 tubing and Y-connector was filled by wrapping the parafilm around the PE 50 so as to make a tight seal. The device was positioned so that the open Y-ends targeted the 1st pair of gill arches, and was tightly sutured to the roof of the mouth. The other end of the tubing was connected to a Minipuls2 peristaltic pump (Gilson, Middleton, WI, USA) in order to apply a series of increasing ammonia concentrations directly to the external surfaces of the two gill arches simultaneously. The buccal pressure changes associated with breathing could be monitored using the first buccal catheter, as in Series I.

In Series III, a buccal catheter was placed as in Series I for monitoring ventilation. Another cannula was placed in order to precisely inject ammonia solutions onto the hind brain. A #26G needle was cut off at 2-cm length, and bent at two points: 90° and -90° at 1/3 and 2/3 of the distance along the cut needle. The sharp-end of cut needle was gently inserted through the translucent cartilage of the cranium, using predetermined co-ordinates based on the dissection of dead trout, so as to penetrate into the cranial cavity and terminate directly over the hind-brain. The blunt-end of the needle was connected to 5-cm length of PE 20 tubing (Clay-Adams, 1.09 mm O.D. and 0.38 mm I.D.), facilitating the injection of ammonia solutions prepared in mock extradural fluid (EDF; 120 mmol L⁻¹ NaCl, 4 mmol L⁻¹ KCl, 1 mmol L⁻¹ MgSO₄, 1 mmol L⁻¹ CaCl₂, 10 mmol L⁻¹ NaHCO₃) (Hedrick et al. 1991) into the hindbrain cavity. The PE 20 and connected needle were always filled with mock EDF, and plugged with a stainless-steel pin to prevent brain damage from external freshwater contamination. After completion of the experiment, the fish were humanely euthanized and the position of needle was confirmed at autopsy.

In all series, the extended PE 50 tubing from the buccal catheter was filled with freshwater and connected to a medical pressure transducer (Utah Medical Products, Midvale, UT, USA) which had been two-point calibrated against the experimental water surface (0 cmH₂O) and 2 cm above the water surface (2 cmH₂O). The buccal pressure fluctuations were amplified by an LCA-RTC amplifier (Transducer Techniques, Temecula, CA, USA) and converted into a digital signal by a Powerlab data integrity system (ADInstruments, Colorado, Springs, CO, USA). Using LabChart version 7.0 (ADInstruments), the converted pressure signals were analyzed into pressure amplitude (cmH₂O) and frequency (min⁻¹). These ventilation parameters were then exported to Excel (Microsoft, Redmond, WA, USA) for further calculation of ventilatory index (cmH₂O min⁻¹) as the product of buccal pressure amplitude times frequency, which is a commonly used indicator of total ventilatory flow in fish (e.g. Zhang et al. 2013; Eom and Wood 2020; Chapter 5).

In Series I, the ventilatory flow (\dot{V}_w) was also digitized into the above Powerlab data integrity system (ADInstruments) and the recorded data were exported to Excel (Microsoft) for further calculation

of stroke volume (ml kg^{-1}) as the product of buccal \dot{V}_w divided by frequency. However, at the time these experiments were performed, the ventilatory flow-measuring device was only a prototype still under development, and we are not confident that the actual flow calibration was correct, whereas we are confident in the relative changes. For this reason, the experimental flow (\dot{V}_w) and stroke volume measurements during the experimental HEA treatment have been normalized as a percentage of the preceding control measurements (100%) for each fish.

7.2.3 Experimental series

7.2.3.1 Series I – Acute responses to high environmental ammonia (HEA) in the external water

After overnight recovery from surgery, the fish were gently transferred to the ventilatory flow-measuring device, while aeration continued in the water reservoir. The buccal catheter and flow probe were connected to the pressure transducer and flow-meter respectively, simultaneously measuring buccal pressure and ventilation flow (\dot{V}_w) until stable recordings were achieved for a control period of 10 ~ 20 min. Then, 16 ml of freshwater were removed and 16 ml of 500 mmol L^{-1} NH_4HCO_3 (Sigma-Aldrich, St. Louis, MO, USA) were added to the air bubbling site to prepare 1 mM of high environmental ammonia (HEA, $N = 7$); buccal pressure and \dot{V}_w were measured continuously for the first 20 min of the HEA treatment.

7.2.3.2 Series II – Ammonia perfusion to external gill arches

The black plexiglass boxes were maintained on flow-through. Prior to experiments ($N = 5$), each concentrated NH_4HCO_3 ammonia solution was prepared in a 500-ml glass beaker and placed in the same flow-through water reservoir as for the fish chambers in order to keep the temperature of the solution equal to that of the fish. Also, the correct distribution of solutions pumped through the Y-tube system was checked using commercial food dye (McCormick & Company, Inc., Hunt Valley, MD, USA). Ventilatory parameters were monitored throughout the experiment by pressure recordings from the first buccal catheter, as in Series I. For control measurements, the intake end of the PE 50 tubing connected to the Y-tube system was submerged in the fish box so that freshwater was continually pumped to left and right gill 1st arches *via* the peristaltic pump at a rate of 2.28 ml min^{-1} . By subsequently shifting the intake of the tubing from 0.01, 0.1, and finally 1 mM NH_4HCO_3 , the external surfaces of the gills of fish were exposed to progressively higher ammonia solutions. Ammonia perfusions were for 5 min for each concentration, separated by approximately 5 min of freshwater perfusion, so as to completely remove the previous solution from the gill region.

7.2.3.3 Series III– Ammonia injection onto the hindbrain

After completion of surgery in Series III, the fish were transitioned to lighter anaesthesia (60 mg L⁻¹ neutralized MS-222), representing Stage 4 of McFarland (1959), and allowed to stabilize for several hours, with the flow-through maintained by a recirculating system. Stage 4 represents: “*total loss of equilibrium, reaction only to strong stimuli, opercular movements slightly depressed,*” and was maintained throughout the experiments. The fish were breathing continuously, generally unresponsive, but still showed strong ventilatory responses to stimuli injected into the cranial cavity. Prior to experiments (N = 6), injection solutions were equilibrated to the experimental temperature and atmospheric PO₂. Using a gas-tight glass syringe (Hamilton, Reno, NV, USA), 15 µl of mock EDF (control), or NH₄HCO₃ solutions (0.1 mmol L⁻¹, 0.5 mmol L⁻¹, and 1 mmol L⁻¹ NH₄HCO₃ in mock EDF, pH 7.8) were gently injected to the hindbrain over 1 sec through the PE 20 cannula. Injections were administered in random order at intervals >5 min. Meanwhile, the ventilatory parameters were simultaneously measured from the buccal catheter as in the other two series.

7.2.3.4 Statistical analysis

Data have been reported as means ± S.E.M (N). One-way repeated-measures ANOVA followed by Dunnett’s post hoc test was applied for comparing ventilatory parameters back to reference or control levels in the three experimental series (GraphPad Prism 6.0, San Diego, CA, USA). In addition, in Series I, comparisons back the pre-exposure control were also made using two-tailed paired Student’s t-tests as a more sensitive method to detect when changes in ventilatory parameters first became apparent. In Series III, a two-tailed paired Student’s t-test was used to evaluate if there were any significant ventilatory changes to injections of mock EDF alone, and as the small increases were not significant, the response to mock EDF alone was used as the reference control level. The threshold for statistical significance was p <0.05.

7.3 Results

During 20 min of acute 1 mM HEA treatment in Series I, the fish gradually increased ventilatory flow (\dot{V}_w), ventilatory stroke volume, and buccal pressure amplitude. After perfusion of ammonia to the external gill arches in Series II, there was an immediate dose-dependent hypoventilation, whereas in Series III, internal injections of ammonia into the hindbrain cavity elicited immediate dose-dependent hyperventilation.

7.3.1 Series I - Acute responses over time to high environmental ammonia (HEA) in the external water

In response to acute 1 mM HEA exposure, the fish gradually increased \dot{V}_w over 20 min (Fig. 7.2A). By repeated measures one-way ANOVA, the overall response was significant ($p = 0.0045$), and by Dunnett's test, the change became significant at 12 ~ 16 min whereas the more sensitive t-test detected significance at 10 ~ 18 min, where it peaked at about a 34% increase. The ventilatory stroke volume exhibited a similar increasing pattern (Fig. 7.2B), but the overall response was not significant by Dunnett's test whereas the t-test detected significance at 12 ~ 16 min, with a peak increase of 33%. During 1 mM HEA exposure, the fish also increased buccal ventilatory index (Fig. 7.2C; control: 307.4 ± 66.2 cmH₂O min⁻¹), a response which was significant overall by repeated measures one-way ANOVA ($p = 0.0003$) and significant by Dunnett's test only at 8 min, though at 8 ~ 16 min by the t-test, with a maximum increase of 34%. This was due to gradually increasing buccal pressure amplitude (Fig. 7.2D; control: 4.1 ± 0.9 cmH₂O). However, the increase in buccal pressure was not significant by repeated measures one-way ANOVA ($p = 0.2017$), though interestingly was significant by t-test from 2 min through to 16 min. At 2 min, the mean elevation in buccal pressure amplitude was only 3%, but this gradually increased to 25%. Regardless, the ventilation frequency was stable during 1 mM HEA (Fig. 7.2E, control: 71.9 ± 2.7 min⁻¹). The overall decline at 18 ~ 20 min in some of the mean responses (Fig. 7.2A, B) reflected decreases in 2 of the 7 fish, whereas ventilation remained elevated in the other 5 trout.

7.3.2 Series II – Ammonia perfusion to external gill arches

During the control period, the fish exhibited the following mean ventilatory parameters: ventilation pressure amplitude of 1.2 ± 0.1 cmH₂O, frequency of 66.2 ± 7.1 min⁻¹, and ventilatory index of 77.2 ± 13.3 cmH₂O min⁻¹. Representative responses of the ventilatory index in a single trout to perfusion of the external surfaces of the gill arches with ammonia are shown in Fig. 7.3, and mean responses of all ventilatory parameters in Fig. 7.4. In response to 0.01 mM ammonia perfusion directly to the external surfaces of the first pair of gill arches, the fish decreased the pressure amplitude by 17% (Fig. 7.4B, repeated measures one-way ANOVA and Dunnett's test, $p = 0.0109$) and the ventilatory index by 18% (Fig. 7.4C, $p = 0.0007$). When the external ammonia concentration was increased to 0.1 mM, the hypoventilatory responses increased and the trout decreased the buccal pressure amplitude by 34% (Fig. 7.4B, $p = 0.0109$) and the ventilatory index by 35% (Fig. 7.4C, $p = 0.0007$). At 1 mM ammonia, the response slightly attenuated but remained significant, averaging about 29% inhibitions for both pressure amplitude (Fig. 7.4B) and ventilatory index (Fig. 7.4C, $p = 0.0230$). Regardless of the concentration of

ammonia perfused to the external gill arches, the fish barely changed the breathing frequency (Fig. 7.4A, control: $66.2 \pm 7.1 \text{ min}^{-1}$).

7.3.3 Series III – Ammonia injection into the hind-brain cavity.

Overall, the fish increased ventilation in response to injections of ammonia (prepared in mock EDF) onto the hindbrain. Original recordings illustrating the range of responses observed are shown in Fig. 7.4, and mean responses are summarized in Fig. 7.5. Responses typically increased over about 30 sec, then attenuated over the following 30 sec.

Although trout slightly increased mean ventilatory parameters after injections of mock EDF alone relative to the pre-injection control values, the responses were not significant ($p = 0.5183$, Fig. 7.5). After injections of mock EDF alone, the fish showed the following mean ventilatory parameters: ventilation pressure amplitude of $1.6 \pm 0.2 \text{ cmH}_2\text{O}$, frequency of $54.6 \pm 4.0 \text{ min}^{-1}$, and ventilatory index of $82.6 \pm 17.4 \text{ cmH}_2\text{O min}^{-1}$. Responses to ammonia injections were compared to these values. Trout barely changed their ventilatory parameters in response to the lowest concentration of ammonia (0.1 mM) in mock EDF. However, in response to a 5-fold higher concentration (0.5 mM) of injected ammonia, both ventilatory pressure amplitude and ventilatory index increased significantly by 21% (Fig. 7.6B, repeated measures one-way ANOVA plus Dunnett's test, $p = 0.0442$) and 25 % (Fig. 7.6C, $p = 0.0342$). After 1 mM ammonia injection, there were further increases in both parameters, reaching about 28% ($p = 0.0246$) and 45% ($p = 0.0332$) in buccal pressure and ventilatory index respectively (Figs. 7.6B, C). Regardless of the concentration, the fish barely changed the breathing frequency (Fig. 7.6A).

7.4 Discussion

7.4.1 Overview

The present results provide support for our overall hypothesis that trout would have both external and multiple internal receptors (gill NECs and brain) for ammonia, so as to make appropriate ventilatory responses to a substance that is both a respiratory gas and a toxicant. Previous studies (summarized in the Introduction) have shown that the NECs on the first two gill arches play a key role in sensing elevated blood (i.e. internal) ammonia levels, thereby triggering hyper-ventilation. Using direct \dot{V}_w measurements and a fine time course analysis, Series I supplied confirmation that the hyper-ventilation in response to exposure of the whole animal to elevated external ammonia (HEA) is not immediate, but develops gradually over time, suggesting that it is driven by internal ammonia receptors responding to elevated

blood ammonia, rather than by external ammonia receptors. Indeed, Series II showed for the first time that the immediate effect of ammonia exposure, when limited to the external surfaces of the first gill arches, is hypoventilation rather than hyperventilation. This would be an appropriate response to a short-term exposure to a waterborne toxicant, so as to minimize uptake while behavioral escape occurs. Series III provided evidence that elevated internal ammonia can be sensed directly by the brain, thereby eliciting hyperventilation. To our knowledge, this is the first demonstration of central chemo-sensing of a respiratory gas in a teleost fish, but is in accord with central chemo-sensing of ammonia in mammals (*see* Introduction). These findings indicate that there are both peripheral (gill NECs) and central chemoreceptors for ammonia in fish.

7.4.2 External and internal ammonia sensing in gills

In both Series I and II, the fish were exposed to high environment ammonia (HEA) but showed hyperventilation in Series I (Fig. 7.2) but hypoventilation in Series II (Fig. 7.4). However, the natures of the HEA exposures were different – only to the external surfaces of the first gill arches for a short period in Series II, but to the whole gill and body surface for a longer period in Series I. The time courses of the responses also differed – virtually immediate in Series II (Fig. 7.3), but slowly developing in Series I (Fig. 7.2).

As the fish of Series I could not avoid the HEA, the entire surface area of the external gill arches and body would have been evenly exposed to 1 mM ammonia. Therefore, it would diffuse along PNH_3 and NH_4^+ electrochemical gradients (Wood and Nawata 2011) into the blood plasma across the respiratory lamellae and perhaps also across the skin (Zimmer et al. 2010), resulting in elevated blood ammonia levels that have been documented in many similar HEA exposures of trout (e.g. Nawata et al. 2007; Wood and Nawata 2011; Zhang et al. 2011). In turn, high internal ammonia levels would be sensed by gill NECs (peripheral chemoreceptors; Zhang et al. 2009; Zhang et al. 2011; Zhang et al. 2015) and/or by the brain (central chemoreceptors; Zhang et al. 2013, and present study, Figs. 7.5, 7.6), resulting in a gradually increasing ventilation (Fig. 7.2). The situation appears to be similar in elasmobranch dogfish (De Boeck and Wood 2015) and agnathan hagfish (Eom et al. 2019), though the internal receptor sites have not been identified in these ancient fishes.

In contrast, in Series II, the ammonia perfused onto the surfaces of the first pair of gill arches would likely have been diluted by ventilated water which would quickly flush it away. As the normal \dot{V}_w in these 100 ~ 300g trout would have been about 30 ml min^{-1} (Eom and Wood 2020, Chapter 6) and the

ammonia perfusion rate was only 2.28 ml min^{-1} , there would have been little chance of uptake into the bloodstream. Yet hypo-ventilation occurred, even at a very low ammonia concentration (0.01 mM). The present technique was similar to that used by Daxboeck and Holeton (1978) to identify external O_2 sensors on the first gill arches responsible for the bradycardia response to environmental hypoxia. Today, it is generally believed that these O_2 sensors affecting heart rate in trout are externally-oriented NECs (Milsom 2012; Perry and Tzaneva 2016; Jonz 2018). These may differ from the more widely distributed, internally-oriented NECs located on the basal membranes of gill filaments, facing the plasma. The latter appear to monitor blood O_2 levels, and elicit hyperventilation during environmental hypoxia, as first shown in trout by Smith and Jones (1982), though external O_2 receptors may also be involved in hypoxic hyperventilation (Milsom 2012). Thus, there may be a parallel to peripheral O_2 chemoreception, with the external ammonia-sensing NECs responsible for ventilatory inhibition being analogous to those causing hypoxic bradycardia, while the internal ammonia-sensing NECs responsible for ventilatory stimulation being analogous to those causing hypoxic hyperventilation. However, further complicating interpretation is that CO_2 -sensing NECs involved in hypercapnic hyperventilation appear to be exclusively external in orientation (Milsom 2012), so by this scheme, externally oriented NECs could cause either hypo-ventilation (to ammonia) or hyperventilation (to CO_2) depending on the stimulus, or there could be two different types of external NECs. Of course, as discussed in Section 4.3, external nociceptors could alternately or additionally be responsible for the hypoventilatory response.

This hypoventilatory response to HEA does not appear to have been reported previously. There are several likely explanations. Perhaps it is normally so transient, a sort of short-term breath-holding, that it has been overlooked. In this regard we have seen hypoventilation in some trout right at the start of HEA exposure, whereas others show no immediate response or hyper-ventilation (J Eom and CM Wood, personal observations). Additionally, when the whole animal, rather than just the first pair of gill arches is exposed to HEA, the ventilatory inhibition may be overwhelmed by the ventilatory stimulation elicited by gradually rising internal ammonia levels. This was first detectable at 2 min in buccal pressure amplitude, but became apparent in \dot{V}_w , stroke volume and buccal ventilatory index only at 8 min or later (Fig. 7.2).

7.4.3 Nociceptors as possible external ammonia-sensing receptors

In natural environments, as opposed to anthropogenically manipulated ones such as aquaculture or polluted waters, HEA is probably less common than hypoxia and hypercapnia, so it is possible that fish do not have specific external receptors for ammonia, but rather are using sensors responsive to a variety

of waterborne toxicants, including ammonia. Nasal chemo-sensors could not have been involved in the responses of Series I or II as the nostrils were plugged. However, nociceptors remain a possibility for the hypoventilation caused by ammonia application to the external surfaces of the first pair of gill arches in Series II (Figs. 7.3, 7.4). Nociceptors are known to prevent damage to sensory and other systems by detecting noxious threats, resulting in defensive behavioral and physiological responses in a wide variety of animals (Walters 1996), including amphibia (Spray 1976), birds (Gentle 2000), mammals (Yeomans and Proudfit 1996), and fish (reviewed by Sneddon 2019). In mammals, various classes of nociceptors have been described such as mechano-thermal nociceptors for noxious heat, and polymodal nociceptors for noxious chemicals (Lynn 1996). The mechano-thermal and polymodal nociceptors are also found in fish, and respond to noxious heat and chemicals such as acetic acid (Sneddon 2003; Mettam et al. 2012; Sneddon 2019). In addition to electrophysiological responses to noxious stimuli, increases (rather than decreases) in opercular movements have been observed (Sneddon 2003). These would likely be coupled to overall increases in ventilation (Hughes and Shelton 1962). Furthermore, the nociceptors on the surface of the head of the trout, which are innervated by the trigeminal nerve, are unresponsive to 0.02 mM ammonium chloride (Mettam et al. 2012). It is not clear whether there are nociceptors on the first pair of gill arches, and if present, whether they receive trigeminal innervation. More research is needed to clarify if nociceptors play a role in ventilatory control, such as ammonia-induced hypoventilation (Figs. 7.3, 7.4).

7.4.4 Internal ammonia sensing in the central nervous system

The results of Series III, where ammonia solutions were injected directly onto the surface of the hindbrain, provided direct evidence of central ammonia-sensing, resulting in hyperventilation (Figs. 7.5, 7.6). As reviewed by Milsom (2012) and Florindo et al. (2018), there is only sparse prior evidence (e.g. Wilson et al. 2000) for central chemoreception in fish other than sarcopterygians, some negative reports (Rovainen 1977; Hedrick et al. 1991), and apparently no evidence at all on this possibility in teleost fish. However, these previous studies have not examined ammonia, which appears to be detected centrally in mammals (Wichser and Kazemi 1974), eliciting a hyperventilatory response (Poppell et al. 1956; Roberts et al. 1956; Warren 1958; Campbell et al. 1973). Earlier, Zhang et al. (2013) showed that ammonia readily permeates the blood-brain barrier in trout. Furthermore, based on correlation of brain intracellular ammonia concentrations with hyperventilation during HEA treatments, these workers proposed a role for central chemoreception of ammonia in fish. The present data confirm this idea. The ammonia concentrations (in mock EDF) applied to the brain surface that were effective in the present study were

0.5 and 1.0 mM (Fig. 7.6), and these were well within the ranges of both blood plasma and cerebrospinal fluid concentrations measured in HEA-exposed rainbow trout by Zhang et al. (2013). The relative roles, time courses of response, specific sites of ammonia-sensing, and integration of afferent neural pathways of branchial NECs versus the brain need to be worked out, and there is a clear need for further research on these topics. Nevertheless, working in combination with peripheral chemoreceptors, central chemoreceptors would provide important redundancy to ensure that hyperventilation occurs when internal ammonia levels are elevated.

7.4.5 Why do fish regulate ventilation in response to elevated external or internal ammonia?

The regulation of ventilation through multiple detection sites would be beneficial for avoiding waterborne ammonia toxicity and for excreting increased plasma ammonia in fish. Very short-term hyperventilation as seen in Series II would help minimize ammonia uptake when the fish first encounters HEA, providing time for behavioral escape. This is similar to the marked reduction in \dot{V}_w (sometimes complete apnea) seen in hagfish at the start of HEA exposure, prior to a later hyperventilatory response which takes over as blood ammonia levels eventually increase (Eom et al. 2019; Chapter 3). Recently, we have shown in trout (Eom et al. 2020; Chapter 5) that hyperventilation is effective in increasing ammonia excretion only after plasma ammonia levels have been elevated for some time so as to activate the Rh glycoprotein metabolon system (Wright and Wood 2009) in the gills, thereby removing diffusive limitations on ammonia flux (Randall and Ip 2006). Prolonged elevations in plasma ammonia concentrations of endogenous origin occur after exercise (Wood 1988; Mommsen and Hochachka 1988; Wang et al. 1994) and feeding (Wicks and Randall 2002; Bucking and Wood 2008), which are times when elevated \dot{V}_w is needed not only to excrete ammonia, but also to help provide increased O_2 uptake for the post-exercise “ O_2 debt” (Scarabello et al. 1991) and post-feeding “Specific Dynamic Action” (Seth et al. 2009) in trout. Elevated ventilation is also useful after chronic HEA exposure in order to get rid of the accumulated internal ammonia burden. In all these circumstances, the Rh metabolon system is upregulated in the gills (Nawata et al. 2007; Zimmer et al. 2010; Zhang et al. 2015) so the increased ventilation will help to excrete the excess ammonia. The fact that there are two receptor systems for elevated internal ammonia (gill NECs and brain) suggests that the homeostatic regulation of this respiratory gas, which is also a toxicant, is of critical importance.

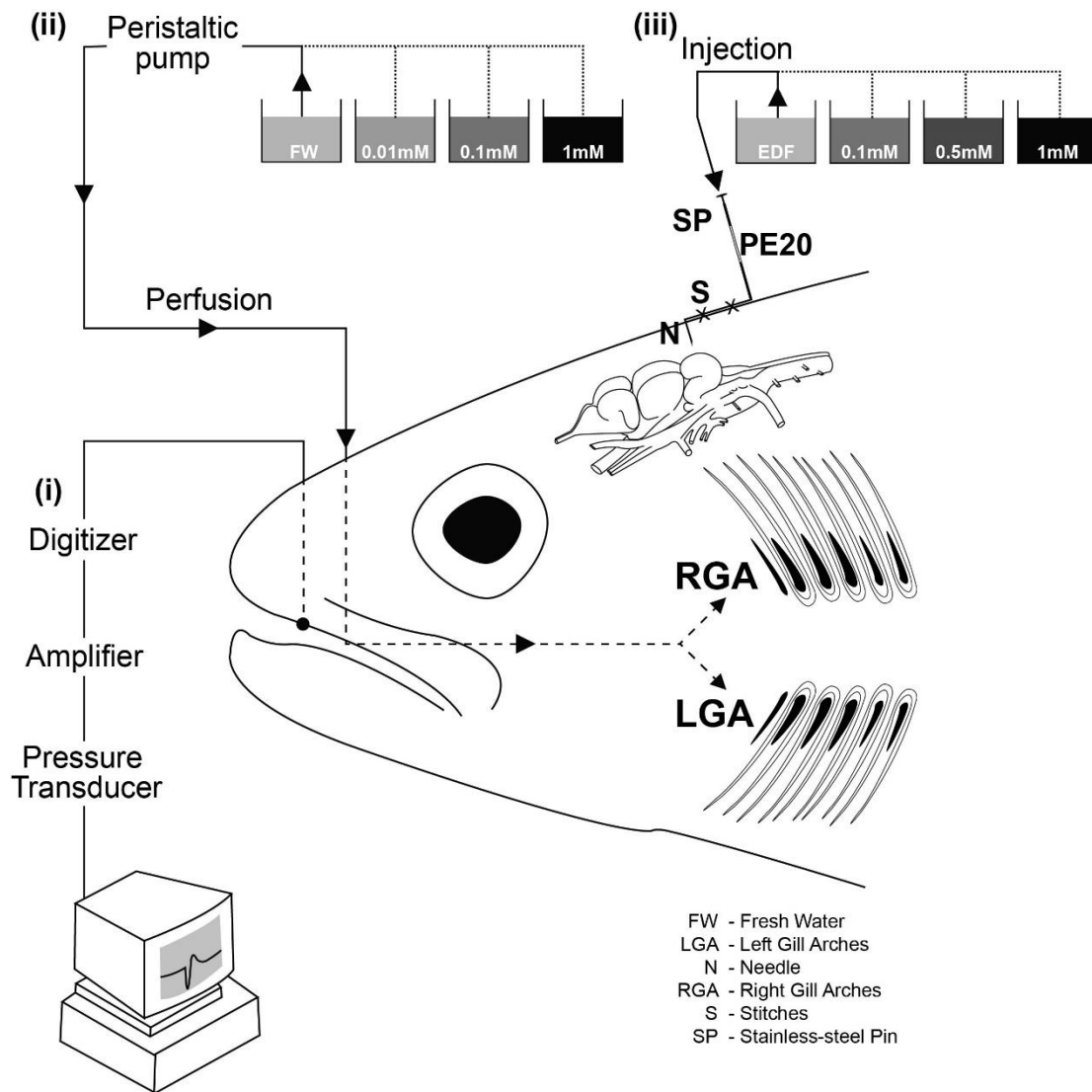


Figure 7.1 Schematic diagram of the experimental setups. Two cannulations were placed in the buccal cavity: (i) for measuring buccal ventilation in Series I, II, and III, and (ii) for additionally perfusing a logarithmic series of increasing ammonia concentration between 0.01 mM and 1 mM directly to external surfaces of the 1st gill arches in Series II. In Series III, (iii) another cannulation was performed, placing a needle-tip into the cranial cavity over the hind-brain for injecting ammonia concentrations between 0.1 mM and 1 mM prepared in mock EDF directly onto the brain surface.

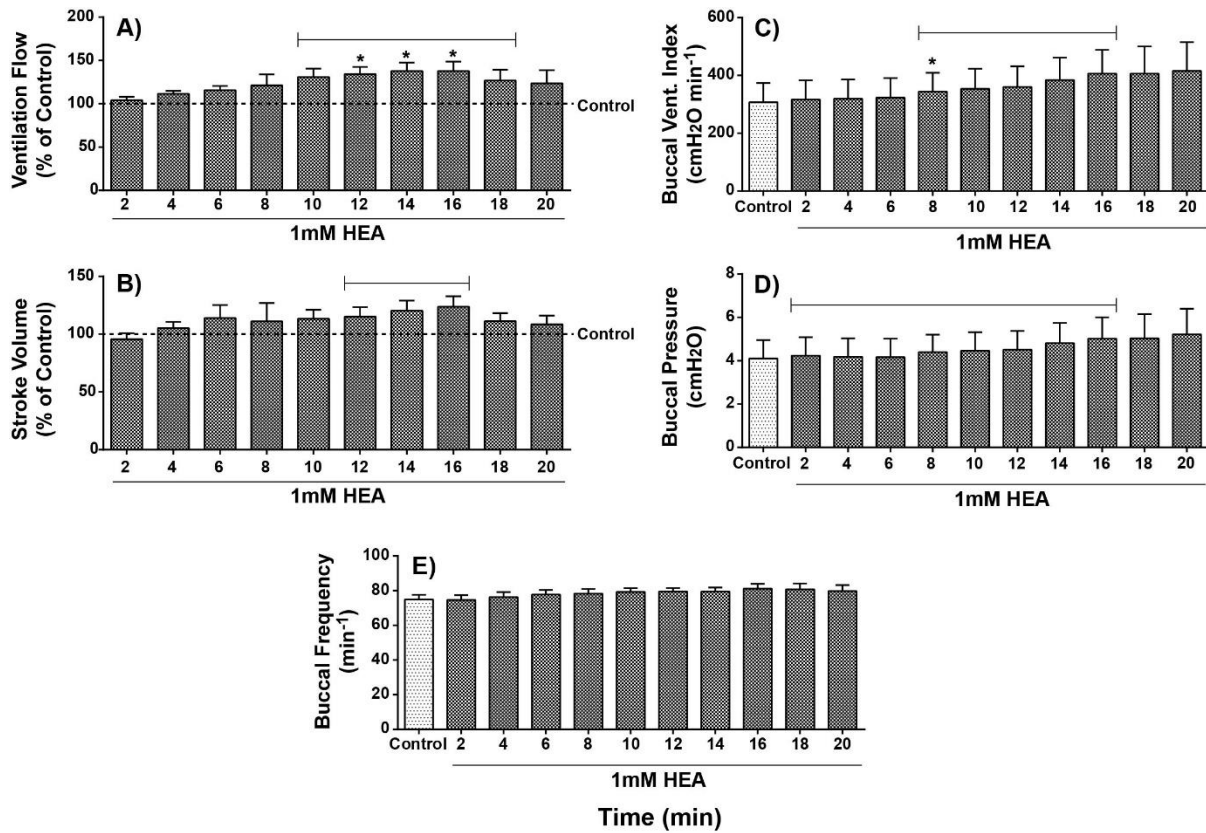


Figure 7.2 The immediate time course of ventilatory responses to 1 mM HEA (NH_4HCO_3) exposure in rainbow trout in Series I. (A) relative ventilation flow (\dot{V}_w); (B) relative ventilatory stroke volume (SV_w); (C) buccal ventilatory index; (D) buccal pressure amplitude; and (E) buccal frequency. Means \pm S.E.M. ($N = 7$). The dashed line indicates the control level (100%) prior to HEA exposure in panels A and B. Asterisks indicate significant differences ($p < 0.05$) from control by repeated measures one-way ANOVA and Dunnett's test. The overlying lines indicates significant differences from control by Student's two-tailed paired t-test.

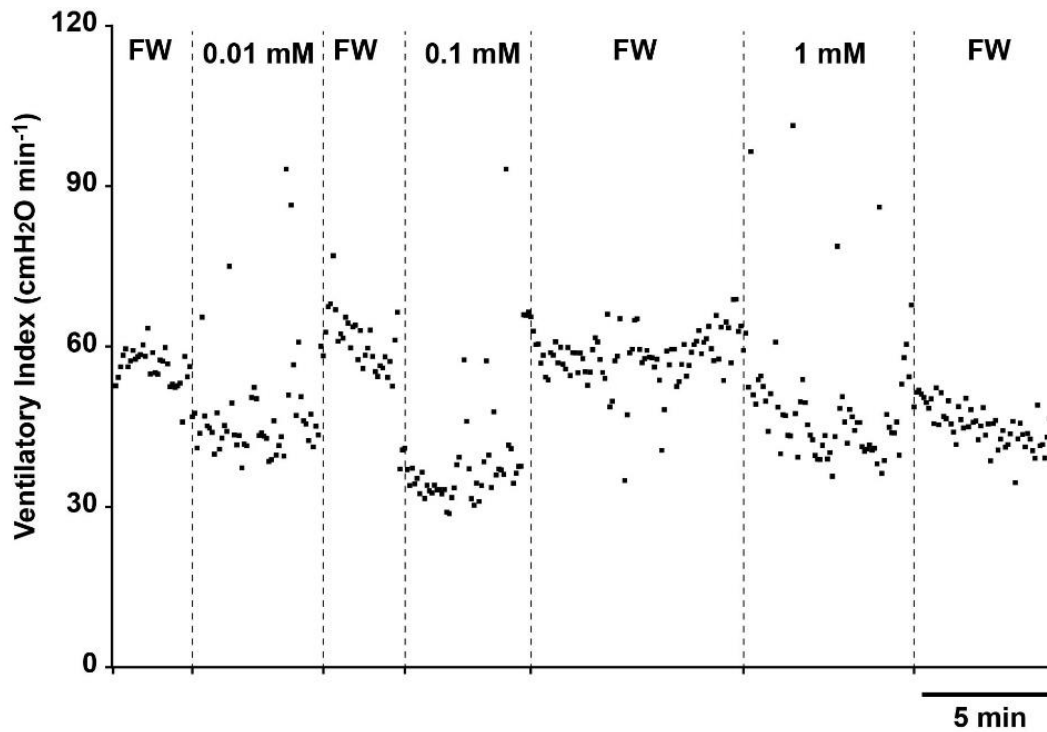


Figure 7.3 Representative variations of buccal ventilatory index in a single trout of Series II in response to perfusion of a logarithmic series of increasing ammonia concentrations directly to the external surfaces of the 1st gill arches. Compared to control levels, the fish immediately decreased ventilatory index in response to 0.01 mM ammonia perfusion, and the extent of hypo-ventilation tended to increase with increased ammonia concentration. Each dot represents averaged ventilatory index per 3 sec, whereas the bar below shows a 5-min time scale.

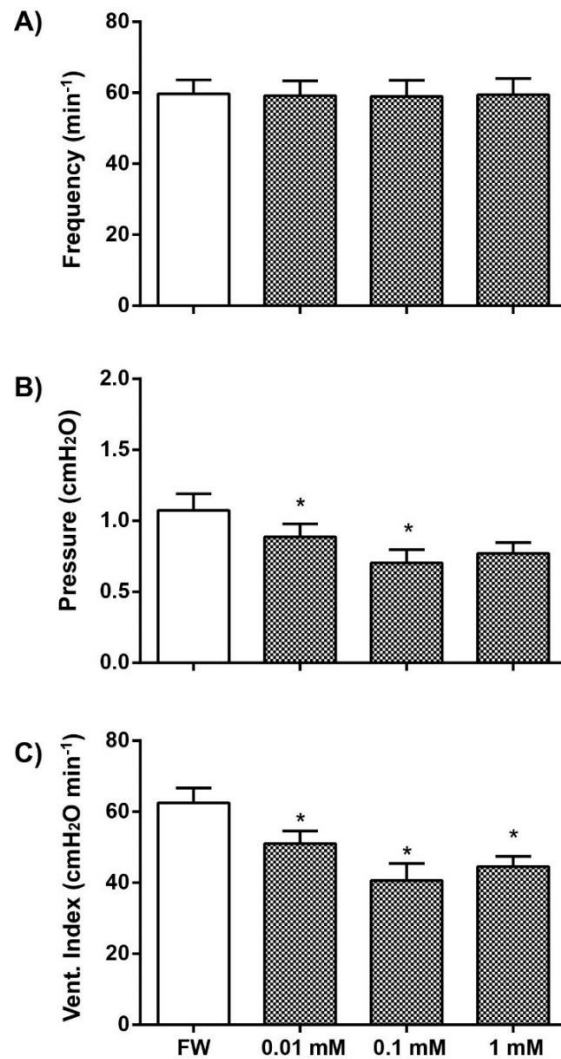


Figure 7.4 Mean ventilatory parameters in Series II in response to perfusion of increasing ammonia concentrations to the external surfaces of the 1st gill arches. Means \pm S.E.M. (N = 5). The fish (A) barely changed overall frequency levels, but (B) significantly decreased buccal pressure amplitude and its level became lower as the perfused ammonia concentration increased (repeated measures one-way ANOVA, $p = 0.0047$). In (C), these responses in pressure amplitude were reflected in similar patterns in buccal ventilatory index ($p < 0.0001$). Asterisks indicate individual means significantly different from control by Dunnett's test.

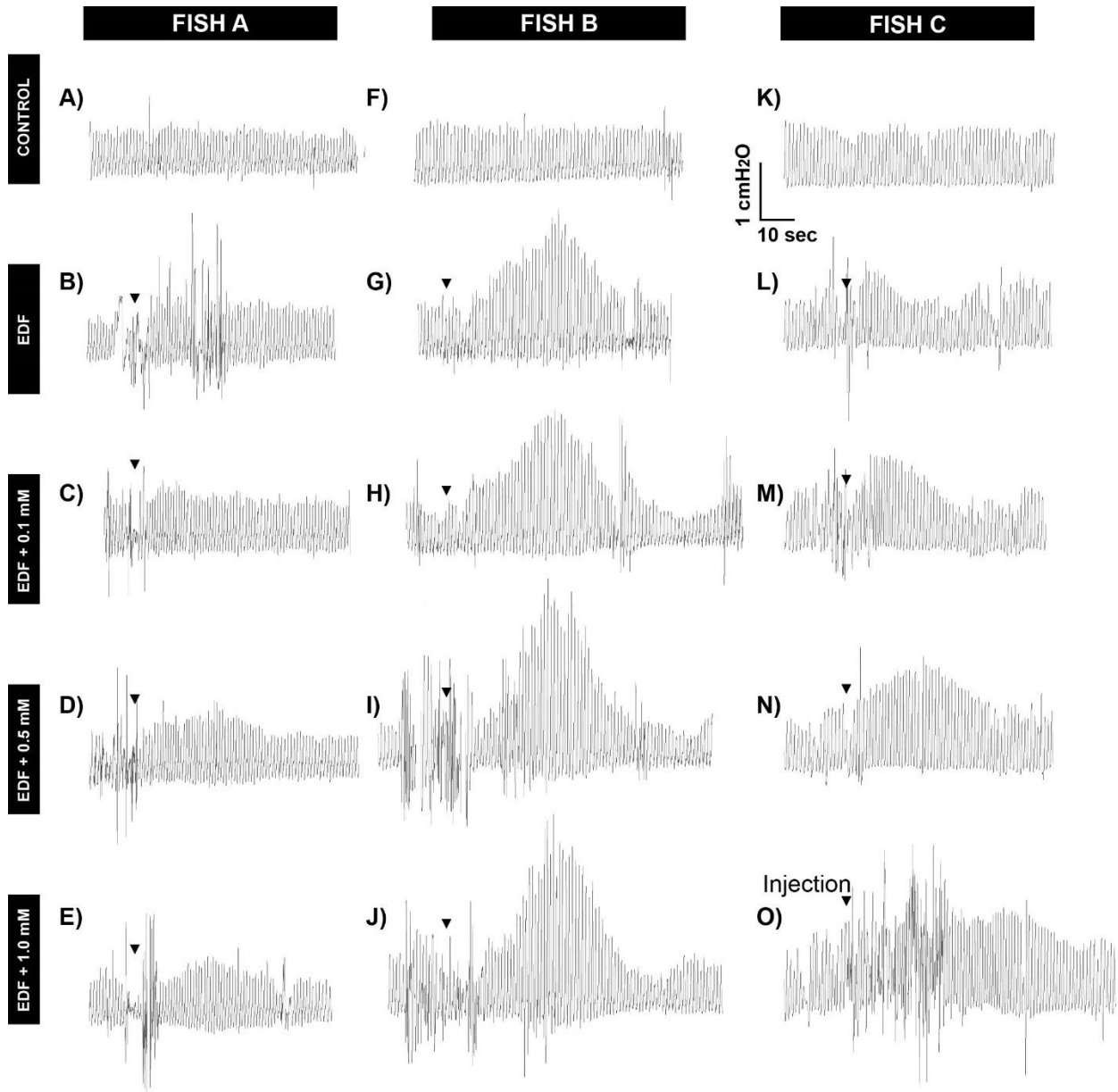


Figure 7.5 Representative ventilation traces (buccal pressure recordings) in three trout of Series III after random injections ($15 \mu\text{l}$) of mock EDF solutions, and ammonia concentrations in mock EDF, directly to the hind-brain cavity of rainbow trout. Arrowhead indicates time of injection. Increases in buccal pressure amplitude lasted for approximately 60 sec, with progressive increases in first 30 sec, followed by progressive decreases back to control levels over another 30 sec.

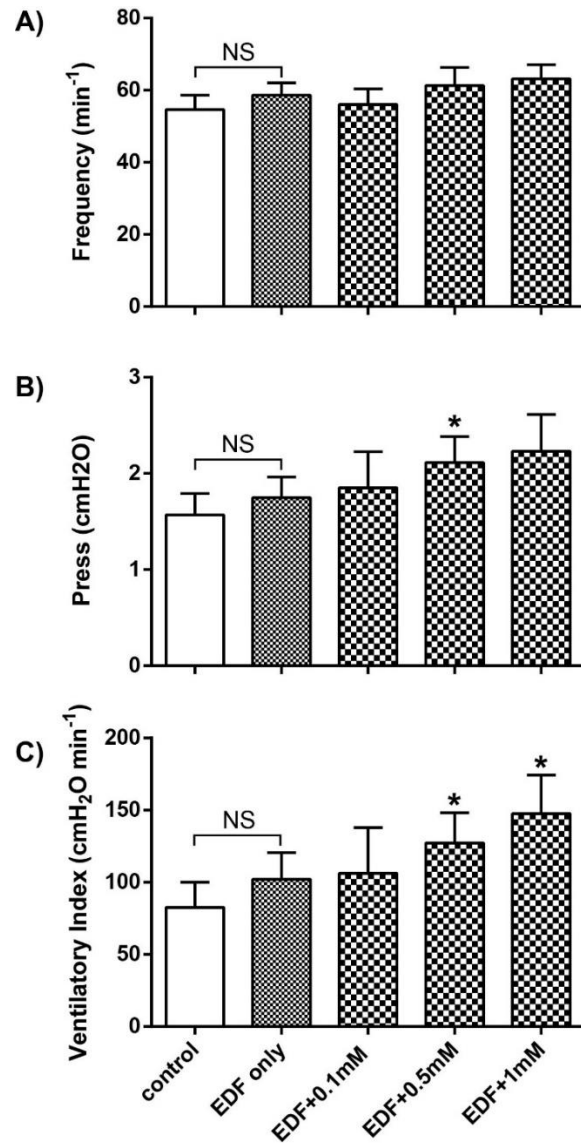


Figure 7.6 Variations of ventilatory parameters after randomly ordered injections of ammonia concentrations (in mock EDF) to the hind-brain cavity in Series III (Means \pm S.E.M., N = 6). The fish (A) barely changed overall frequency levels, but (B) there was a strong influence of injected ammonia concentration to increase buccal pressure amplitude (repeated measures one-way ANOVA, $p = 0.0525$) and (C) this resulted in a pattern of significantly increasing buccal ventilatory index ($p = 0.0325$). Asterisks indicate mean values significantly different from the injections of mock EDF alone by Dunnett's test. Although fish slightly increased mean ventilatory parameters in response to mock EDF injections alone, relative to the pre-injection control values, the responses were not significant (NS) (Student's t-test, $p = 0.5183$).

Chapter 8: General Discussion and Conclusions

My thesis has shown that both hagfish (Chapter 3 and 4) and trout (Chapters 5,7) respond to elevations in ammonia in the blood plasma, as well as in the external environment (HEA) by altering ventilation. In both species, the increases in plasma ammonia appears to be sensed directly, resulting in hyperventilation (Chapters 3, 5). In trout, I have also demonstrated that this hyperventilation helps increase the excretion of ammonia under physiologically relevant conditions (Chapter 5). While HEA exposure also results in increased breathing, the evidence from both my work and preceding studies by other investigators suggests that the response is an indirect one, reflecting diffusive entry of ammonia from the external environment, with the rise in internal ammonia concentration providing the actual direct stimulus for hyperventilation (Chapters 3, 5,7). Indeed, the immediate direct response to HEA appears to be inhibition of breathing (Chapters 3, 4, 7). Here I will briefly integrate my findings with recent literature to explain how these responses may occur, why they are beneficial to the survival of the fish, and to place them in an evolutionary perspective.

8.1 Role of ammonia in controlling ventilation of hagfish

My idea was to look for a possible role of ammonia in controlling breathing in an animal representing the closest extant connection to the ancestral vertebrates. However, before tackling this issue, the experiments of Chapter 2 were necessary to better understand the basic breathing mechanism of the hagfish, and were complemented by experiments of Chapter 4 which characterized the performance of its complex respiratory system in O₂ uptake. Prior to my work, relatively little was known about ventilatory control in hagfish or about the details of respiratory gas exchange, and there was no information at all on the possible effects of ammonia. As hagfish feed on rotting carcasses, it seemed likely that they would be exposed naturally to HEA at times. Immediately prior to and during the period of my thesis research, information appeared that hagfish were well equipped to deal with HEA. These findings included a demonstrated ability to excrete ammonia mainly through the gills (Clifford et al. 2016), and that this occurred at very high rates after ammonia injection or HEA exposure (Braun and Perry 2010; Edwards et al. 2015) or after feeding (Wilkie et al. 2017; Weinrauch et al. 2018). In both situations, plasma ammonia levels were elevated. Additionally, there were several reports that hagfish could excrete ammonia against external gradients (Clifford et al. 2015; Clifford et al. 2017), perhaps by active transport mechanisms involving Rh proteins, as there was molecular evidence for the presence of these ammonia channels in gills and skin (Braun and Perry 2010; Edwards et al. 2015; Clifford et al.

2017; Suzuki et al. 2017). My findings were able to put these findings into perspective by showing that HEA exposure induces a biphasic response in ventilation. This comprises a short-term hypoventilation, followed by longer term hyperventilation, whereas experimental elevation of blood ammonia by injection of ammonium salts elicits only hyperventilation.

The short-term hypoventilation caused by HEA (Chapter 3) was similar to the spontaneous apnea that I had described as a frequent occurrence in hagfish under control conditions in Chapter 2, and which had not been reported previously. When exposed to HEA, hagfish decreased or stopped breathing within 5 min, and this “breath-holding” response continued for a variable time period (5 to 90 min). However, by 3 h, this had been replaced by a sustained hyperventilation at several-fold above control levels. Injections of ammonium salts elicited only hyperventilation, and this seemed to be a specific effect of ammonia as it was observed even when blood acid-base status was unchanged. As outlined in the following Section 8.2, both the short-term hypoventilation and longer-term hyperventilation of hagfish have parallels in the ventilatory responses to HEA in a more modern fish, the rainbow trout, and may reflect the evolutionary antecedents of these. Therefore Fig. 8.1 presents a schematic, somewhat hypothetical model of the HEA response in hagfish, which relies to some extent on our greater understanding in trout.

I propose that initially, the hagfish detects the elevated ammonia in the water inhaled through the nostrils using as yet unidentified external receptors somewhere in the respiratory tract. This reduces or stops breathing so that water flow over the gills is diminished, and the diffusive uptake of ammonia into the blood is minimized. This would be a protective response. Nevertheless, as the HEA exposure continues, some ammonia does diffuse into the blood across skin and gills, and eventually, this reaches a sufficient threshold to stimulate internal ammonia receptors which stop the “breath-holding” and activate hyperventilation. I have no evidence on the location of the internal ammonia sensors; they could be on NECs and/or centrally located in the brain as in trout – or elsewhere. Regardless, I hypothesize that the increase in ventilation is helpful in excreting some of the internal ammonia load and thereby lowering blood ammonia levels. I propose that this would occur because, by this time, the ammonia loading would have turned on the active transport system at the gills so that ammonia excretion against the gradient becomes possible (Clifford et al. 2015; Clifford et al. 2017). Under these circumstances, diffusion limitation would not apply, and the increased flow of water would help flush away the excreted ammonia. This system would keep blood ammonia concentration well below the concentration in the HEA environment, as demonstrated in these studies. It is tempting to suggest that the Rh channel system is part of the active transport system. When Edwards et al. (2015) injected the Atlantic hagfish (*Myxine*

glutinosa) with an NH_4Cl load that raised the blood plasma total ammonia concentration to approximately the same level ($\sim 1,200 \mu\text{mol L}^{-1}$) as I recorded at 3 h ($\sim 1,600 \mu\text{mol L}^{-1}$) in HEA-exposed *Eptatretus stoutii* (Chapter 3), Rhcg mRNA expression in the gills was upregulated within 0.25 h, and Rhcg protein expression was activated within 2 h. Unfortunately, however, Clifford et al. (2015) and Clifford et al. (2017) saw no change in Rhcg protein expression during HEA treatments, even over much longer time scales, in *Eptatretus stoutii*, so this idea remains speculative.

Internal ammonia loading is also known to occur after feeding in hagfish (Wilkie et al. 2017; Weinrauch et al. 2018), and perhaps also after exercise due to oxidative deamination of amino acids and the purine nucleotide cycle, as described in Chapter 1. Certainly, hagfish become very active at the time of feeding, and although ventilation increases with swimming (Chapter 2), ventilation is likely impeded during the feeding event itself (Chapter 2), which also would cause ammonia retention. Fig. 8.2 presents a speculative model as to how internal ammonia loading resulting from feeding and/or exercise interacts with ventilation.

I propose that this internal ammonia buildup is important in activating and maintaining high ventilation, and thereby helping to repay any “ O_2 debt” that is incurred during an exercise event by “Excess Post-Exercise Oxygen Consumption” (EPOC), and also to maintain an elevated $\dot{\text{M}}\text{O}_2$ to satisfy the Specific Dynamic Action (SDA) costs (McCue 2006; Secor 2009) of processing a meal (Fig. 8.2). At least based on research with teleosts (*see* Section 8.2), SDA lasts much longer than EPOC. In Chapter 3, I showed that HEA exposure resulted in both hyperventilation and elevated $\dot{\text{M}}\text{O}_2$. According to Wilkie et al. (2017), blood ammonia concentrations remain elevated for up to 72 h after feeding and ammonia excretion remains elevated for more than 24 h. Weinrauch et al. (2018) used a different feeding protocol and found that ammonia excretion was elevated for at least 36 h. $\dot{\text{M}}\text{O}_2$ had peaked earlier but was still elevated non-significantly by 50% at this time. Thus, elevated plasma ammonia can provide a sustained signal to maintain hyperventilation, thereby facilitating the high $\dot{\text{M}}\text{O}_2$ required at this time. As proposed for HEA exposure, high plasma ammonia would also keep the transport system for ammonia activated at the gills, so that diffusion limitation would not apply, and the greater convection of water would also facilitate ammonia excretion (Fig. 8.2).

8.2 Role of ammonia in controlling ventilation of trout

Once Rh glycoproteins were discovered in the gill epithelia of teleost fish, together with evidence that they could facilitate ammonia excretion and were involved in apparent active ammonia excretion

against gradients (Nakada et al. 2007b; Nawata et al. 2007; Nawata et al. 2010a, b; Wood and Nawata 2011; Sinha et al. 2012), researchers realized that the permeability of the branchial epithelium to ammonia could be regulated (Wright and Wood 2009; Wright and Wood 2012; Weihrauch et al. 2009). Therefore, the apparent diffusion limitation on ammonia excretion articulated by Randall and Ip (2006) might not always apply, and convection might be important in altering ammonia excretion. Indeed, this would explain the common observation that teleosts hyperventilate in response to both HEA exposure (e.g. Smart 1978; Lang et al. 1987; Fivelstad and Binde 1994; Knoph 1996) and internal elevations of blood plasma ammonia (McKenzie et al. 2003; Zhang et al. 2009; Zhang et al. 2011; Zhang et al. 2013). If this were the case, we would predict that hyperventilation would be beneficial to increase ammonia excretion at times when the fish are dealing with an increased ammonia load. However, this possibility had never been tested. The experiments of Chapter 5 were the first to evaluate this idea.

In brief, I demonstrated that in rainbow trout under resting conditions (no loading with ammonia), experimentally induced increases or decreases in ventilation had no effect on branchial ammonia excretion, in accord with the diffusion-limitation hypothesis of Randall and Ip (2006). However, after chronic internal loading by ammonia infusion, a treatment that greatly increased ventilation and also increased the gene expression of the Rh channels and associated transporters in the gills, ammonia excretion became very sensitive to experimental increases or decreases in ventilation (Chapter 5). Thus ventilation-limitation seems to apply under these conditions, and the greater water convection associated with ammonia-induced hyperventilation is beneficial in increasing ammonia excretion.

Previous studies had shown that the NECs are located in first and second gill arches of trout, and that these are the sites at which internal ammonia is detected, resulting in hyperventilation (Zhang et al. 2011; Zhang et al. 2015). This was in the accord with the concept that they are polymodal peripheral chemoreceptors responding to a range of respiratory signals (O₂, CO₂, pH, and ammonia; Perry and Tzaneva 2016; Jonz 2018). However, it was unclear whether the NECs also detected elevations in external ammonia (HEA) directly, or whether they only detected the increase in blood plasma ammonia, after the HEA had diffused into the animal. It was also unclear whether there were central chemoreceptors for ammonia in the brain, for which Zhang et al. (2013) had provided only correlational evidence. The experiments of Chapter 7 investigated these issues.

Direct application of HEA selectively to the external surfaces of the 1st gill arches resulted in an immediate hypoventilation (Chapter 7), rather than the expected hyperventilation. While this was somewhat surprising, as it had not been reported previously, it may be a parallel response to the long

lasting (5 ~ 90 min) hypoventilation seen in response to HEA exposure in hagfish (Chapter 3). I have no evidence on whether this response to external ammonia is due to externally oriented NECs, or to some other type of receptors, such as nociceptors. It may not have been seen in previous studies because generally much higher concentrations (≥ 1 mM) at higher water pH (and therefore higher PNH_3) have been used, whereas in Chapter 7, significant hypoventilation occurred at only 0.01 mM, an ammonia level that is much more environmentally relevant. Alternatively or additionally, the immediate hypoventilation may not have been reported previously because it is transient, and soon overwhelmed by the internal response as blood ammonia levels rise and stimulate internal ammonia sensors such as gill NECs. In trout placed in our less invasive ventilation-measuring device (developed in Chapter 6) and exposed to 1 mM HEA, only a slowly developing hyperventilation over 20 min was seen (Chapter 7), which supports this interpretation.

The other major finding of Chapter 7 was that direct application of ammonia to the surface of the hindbrain (at physiologically relevant concentrations in mock extradural fluid) resulted in hyperventilation. This is the first evidence for central chemoreception of any respiratory gas in any teleost fish (Milsom 2012), and supports the interpretation of Zhang et al. (2013) of a direct relationship between the levels of total ammonia in brain tissue and the degree of hyperventilation in HEA-exposed trout. It is also in accord with mammalian data indicating that the brain is the site of ammonia detection (Wichser and Kazemi 1974). Thus, increases in internal ammonia are sensed by two sites. Likely the internal NECs in the gills respond first to elevations in blood plasma ammonia, whereas the central chemoreceptors in the hindbrain are activated more gradually, and maintain the long term hyperventilatory response, as seen for example in Chapter 5. Based on this evidence, Fig. 8.3 presents a model for the ventilatory response to HEA in trout that is partly hypothetical, but less so than in hagfish.

I propose that the trout initially detects the waterborne ammonia via sensors on the external surface of the 1st gill arches, and thereby immediately decrease water flow over the gills (Fig. 8.3). Teleosts are well known to behaviourally avoid HEA environments (e.g. Richardson et al. 2001; Eddy 2005), so this may be a protective response (“breath-holding”) to minimize ammonia uptake while the fish escapes to clean water. Nevertheless, unlike the hagfish which sometimes stops breathing altogether, if it cannot escape, the trout continues to breathe at a reduced rate, so blood ammonia levels will rise gradually as ammonia diffuses in across the gills (Fig. 8.3). This first stimulates internal NECs in the gills and later the central chemoreceptors in the hindbrain, both of which will cause hyperventilation. In combination with upregulation of the Rh metabolon system in the gills that removes diffusive limitation

and allows active excretion against a gradient, the increased convection facilitates greater ammonia excretion, allowing blood ammonia levels to stabilize and eventually fall (Fig. 8.3).

Similar to hagfish, trout are also known to load ammonia into their plasma after feeding due to oxidative deamination of amino acids (Bucking and Wood 2008) and/or after exercise due to the purine nucleotide cycle (Mommsen and Hochachka 1988). It is very difficult to record breathing during feeding because of “noise”, but ventilatory water flow probably goes up somewhat as trout become very active at this time, with occasional impediments as food is swallowed. I am aware of no ventilation measurements after feeding, but $\dot{M}O_2$ may be elevated for as much as 40 h after a meal in trout (Eliason and Farrell 2014). As for hagfish, this represents the SDA costs of processing and metabolizing the meal (McCue 2006; Secor 2009). Both plasma total ammonia concentration and ammonia excretion rates are also elevated for 24 ~ 48 h after feeding (Bucking and Wood 2008). During exercise, it has been well established that ventilatory flow goes up greatly (Stevens and Randall 1968; Kiceniuk and Jones 1977). At least in part, this is due to “ram ventilation” (Steffensen 1985). After exhaustive exercise in trout, ventilation is still greatly elevated after 2 h of recovery (Wood and Munger 1994), and $\dot{M}O_2$ is elevated for about 4 h as the “ O_2 debt” incurred during exercise is paid off by “Excess Post-Exercise O_2 Consumption” (EPOC; Scarabello et al. 1990). Plasma total ammonia concentration and branchial ammonia excretion rates are also greatly elevated, and both recover over a similar 4-h time course (Wood 1988; Wang et al. 2004).

Integrating this information with my findings in Chapters 5 and 7, I propose in Fig. 8.4 a model in which hyperventilation after both feeding and exercise is promoted and then maintained by internal ammonia buildup, mediated by peripheral (gill NECs) and central (hindbrain) chemoreceptors. This is likely very important in supplying the increased ventilatory flow that is needed to support the increased $\dot{M}O_2$ demands of EPOC and the SDA. I am not aware of arterial blood PO_2 and O_2 content measurements during the post-feeding SDA period, but after exhaustive exercise in trout, these do not change greatly (Primmett et al. 1986; Milligan and Wood 1987). It is problematic whether they could provide as strong a stimulus for ventilation as plasma ammonia which is elevated several-fold. It is also known that both exhaustive exercise (Zhang et al. 2015) and feeding (Zimmer et al. 2010; Zhang et al. 2015) stimulate the mRNA expression of Rh proteins and associated transporters in gills, presumably associated with the increases in plasma ammonia. As argued earlier, augmented ammonia flux *via* these proteins would remove diffusive limitation, such that the increased convection would facilitate the large increases in ammonia excretion (Fig. 8.4).

8.3 Evolutionary perspective

The present study has shown parallel roles of ammonia in controlling ventilation between the hagfish, representing the oldest extant connection to the ancestral vertebrates, and a more modern teleost fish, the rainbow trout. In both, the long-term effect of ammonia loading is ventilatory stimulation, mediated by internal receptors. A similar internally mediated response to ammonia has been identified in the spiny dogfish (*Squalus acanthias suckleyi*), a representative of another ancient fish group, the elasmobranchs (De Boeck and Wood 2015). The functionality of the response in facilitating ammonia excretion depends on the presence of Rh proteins, so as to remove diffusive limitations. It is interesting to look back to the invertebrates, to see if evolutionary precursors of the response can be seen in these early animals. A recent comprehensive review on ammonia excretion in invertebrates (Weihrauch and Allen 2018) noted that Rh proteins are widely distributed, as are the distantly related AMT proteins which also serve as ammonia transporters in invertebrates. The review also noted examples of apparent active ammonia excretion against gradients but made no mention of any study showing that ammonia could stimulate ventilation. However, one study was highlighted (Thomsen et al. 2016). In mytilid mussels (*Mytilus edulis*), the plicate organ and gills contain Rh proteins and v-type H⁺ ATPase, and appear to be the major sites of ammonia excretion. When ventilatory flow (created by cilia) is experimentally slowed, the rate of ammonia excretion decreases, suggesting that convection is important. It would be interesting to test if ventilation is stimulated by ammonia loading in these organisms.

It is also interesting to look laterally to lampreys and up to higher vertebrates. There seems to be no information on the possible role of ammonia in ventilatory control in lampreys, lungfish, amphibians, reptiles, or birds. Recent information suggests that the NECs of fish have a different embryonic origin (endoderm, Hockman et al. 2017) than the primary peripheral chemoreceptors of higher vertebrates, the type 1 (glomus) cells of the carotid and aortic bodies that are derived from the neural crest. We therefore may not expect to find ammonia sensitivity in peripheral chemoreceptors of higher vertebrates. Nevertheless, in mammals, particularly humans, elevations in blood ammonia are well known to stimulate breathing (Poppell et al., 1956; Roberts et al., 1956; Warren, 1958; Campbell et al., 1973) probably by actions on central chemo-sensors in the brain (Wichser and Kazemi, 1974). Indeed, it is this ventilatory stimulation that may keep patients with liver failure alive during periods of hepatic coma, by offsetting (via respiratory alkalosis) the lactacidosis that often accompanies hepatotoxicity. Perhaps the origin of this response can be found in fish, as my experiments in Chapter 7, as well as the earlier work of Zhang et al. (2013), point to a role for central chemoreceptors in the trout hindbrain in mediating ammonia-induced hyperventilation.

8.4 Future directions

As with any research, my thesis has raised as many questions as it has answered, probably more. I list here four important future directions.

1. Finding the nature and location of chemoreceptors in hagfish. Physiological experiments are very difficult in hagfish because of their knotting and sliming behaviour, and their ability to displace any attachments. Ideally, stimuli should be delivered to precise internal and external locations by catheters, but I believe this will only be possible on deeply anaesthetized animals that may not exhibit normal ventilatory responses. Nevertheless, the approach should be tried. Alternately, a search using immunohistochemical techniques to identify NECS may prove successful, as well as isolated brain preparations where fictive ventilation is measured (see point 3 below).

2. Understanding prolonged apnea in hagfish. About 35% of the hagfish examined at rest exhibited apnea (Chapter 2), and apnea was induced by HEA exposure (Chapter 3). Recent observations with remotely operated underwater vehicles (ROV) have documented periods of prolonged apnea in the teleost Family Chaunacidae (Order Lophiiformes, coffinfishes), and have related the phenomenon to the need for energy conservation in the nutrient-poor, often hypoxic deep-sea environment (Long and Farina, 2019). The branchial chamber volume is enormous in coffinfishes. Considering the multiple separate branchial chambers and their associated “plumbing”, including the PCD, in *Eptatretus stoutii*, the volume of the respiratory system is also high in this deep-sea hagfish. It would be interesting to examine the extent of apnea in the hagfish at depth in their natural habitat by ROV experiments and to understand if internal water circulation and O₂ extraction occur during apnea.

3. An examination of central chemosensitivity for other respiratory gases in trout. As discussed in Chapter 7, my experiments with injections of ammonia in small volumes of mock EDF onto the hindbrain of anaesthetized trout provided the first evidence of central chemoreceptors in a teleost fish. Now that the technique has been worked out, it would be relatively easy to repeat these experiments with CO₂, O₂, and pH stimuli. If the results are positive, the topic could be followed up with isolated brainstem experiments in which fictive ventilation is recorded, as was done successfully by Wilson et al. (2000) in the holostean gar (*Lepisosteus osseus*).

4. Understanding how other respiratory gases interact with the hyperventilatory response to ammonia in both hagfish and trout. In journal referee reports on several of the papers from my thesis, I have noticed that reviewers object to my referring to ammonia as “a respiratory gas”, so this information may help clarify whether ammonia really has this status in fish, at least from the viewpoint of normal ventilatory control. In Chapter 4, I demonstrated that there were relatively minimal interactions of O₂ and CO₂ stimuli on the short-term hypoventilatory response to ammonia in hagfish. However, the ammonia sensors involved in the hypoventilatory response remain unknown. It would be useful to evaluate if interactions of O₂ and CO₂ occur with the longer-term hyperventilatory response to ammonia in both animals, which appears to be driven by both peripheral (NECs) and central (hindbrain) chemoreceptors. Interestingly, in Chapter 5 I found that in trout, hypoxia-induced hyperventilation was more intense when combined with elevation of plasma ammonia concentration, suggesting that positive interactions may occur.

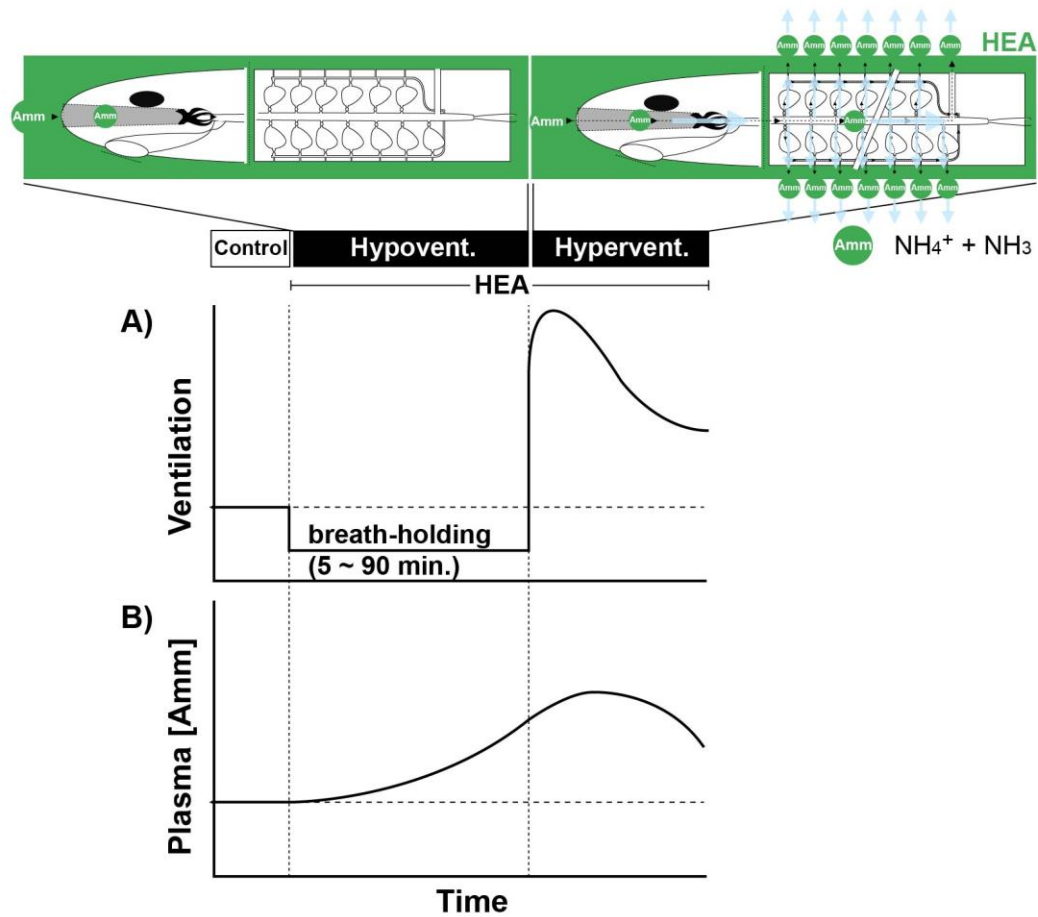
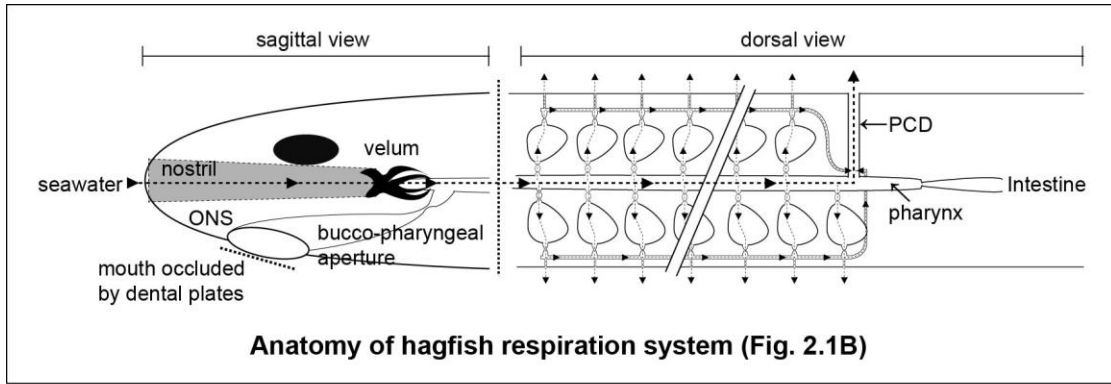


Figure 8.1 Hypothetical model of the role of high external ammonia (HEA) in controlling hagfish ventilation. In HEA, hagfish exhibit A) apnea-like decreased ventilation for 5-90 min but thereafter increase ventilation because B) the rise in plasma ammonia concentration stimulates internal ammonia sensors. The A) increase in ventilation at this time, in combination with the activation of a mechanism for the active outward transport of ammonia at the gills would B) help lower plasma ammonia levels.

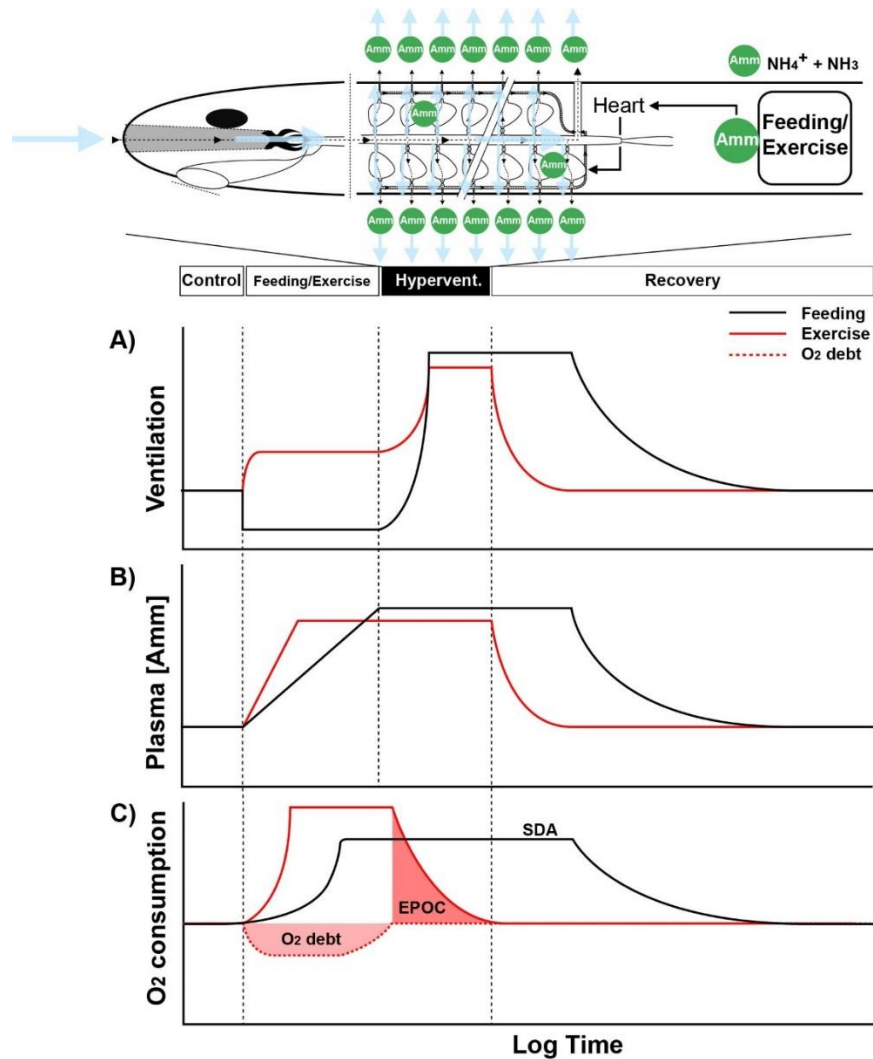


Figure 8.2 Hypothetical model of the role of internal ammonia in controlling hagfish ventilation after feeding and/or exercise (swimming). A) Hagfish increase their ventilation during swimming, but probably decrease ventilation during feeding due to obstruction of the nostril. C) An “O₂ debt” is probably incurred during swimming, and perhaps to a small extent during feeding. B) Increased ammonia production as a result of the purine nucleotide cycle during and after exercise, and as a result of the metabolism of protein-rich prey during and after feeding, results in a rise in plasma ammonia levels. This stimulates internal ammonia sensors which cause A) hyperventilation during the recovery period. The increase in plasma ammonia concentration may also B) activate the ammonia excretion mechanism at the gills. In combination, these help to increase ammonia excretion and thereby stabilize and eventually lower plasma ammonia levels. The A) hyperventilation is important in C) increasing MO₂, thereby helping to pay off the “O₂ debt” by “Excess Post-Exercise O₂ consumption (EPOC)” as well as to satisfy the O₂ requirements of “Specific Dynamic Action” (SDA) to process the ingested foodstuffs.

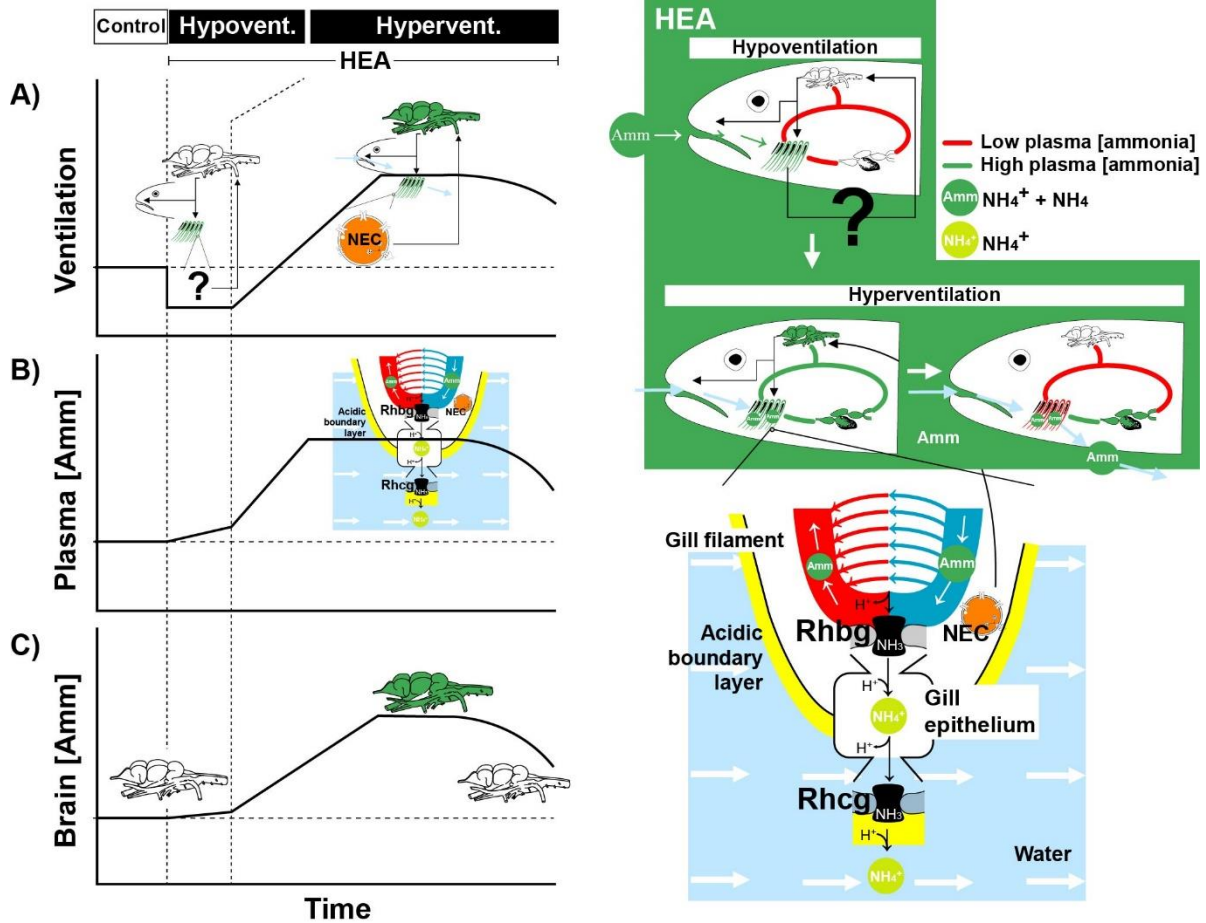


Figure 8.3 Hypothetical model of the role of high external ammonia (HEA) in controlling ventilation in trout. In response to HEA, trout show A) brief hypoventilation but the external sensing mechanism is not known. Ammonia gradually diffuses in across the gills and B) accumulates in plasma. This stimulates first A) the internal NECs (peripheral chemoreceptors) and later as C) brain ammonia levels build up, the A) central chemoreceptors, so that ventilation rises and stays high for some time. High plasma ammonia also activates B) the active excretion ammonia excretion mechanism on the gills. This helps to excrete ammonia, so that B) plasma ammonia levels decrease and A) ventilation is reduced back towards control levels.

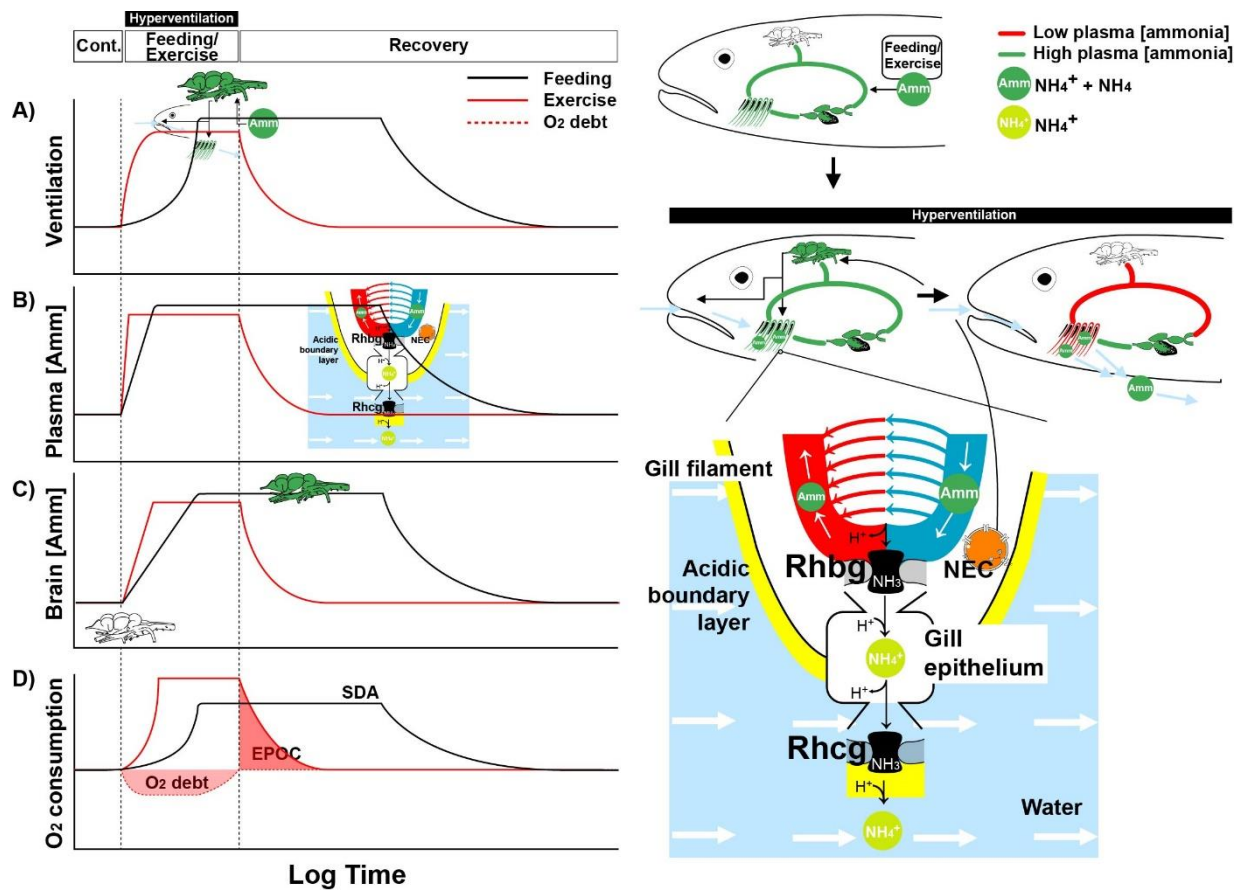


Figure 8.4 Hypothetical model of the role of internal ammonia in controlling ventilation in trout after feeding and/or exercise (swimming). A) Trout increase their ventilation during swimming, and probably to a lesser extent during feeding. D) An “O₂” debt is incurred during exercise. Increased ammonia production as a result of the purine nucleotide cycle during and after exercise, and as a result of the metabolism of protein-rich prey during and after feeding, results in B) a rise in plasma ammonia levels. This stimulates internal ammonia sensors (NECS in gills and central chemoreceptors in the brain) which cause A) hyperventilation during the recovery period. The elevation of B) plasma ammonia is of shorter duration after exercise, but longer-lasting after feeding because of continuing ammonia production by the metabolism of protein nutrients. Therefore, A) ventilation follows a similar time course, lasting long enough to pay off the “O₂ debt” by “Excess Post-Exercise Oxygen Consumption (EPOC)”, but is sustained after feeding to satisfy the continuing O₂ requirements of “Specific Dynamic Action” (SDA) to process the ingested foodstuffs. The increase in plasma ammonia concentration may B) also activate the ammonia excretion mechanism at the gills. In combination, these help to increase ammonia excretion and thereby stabilize and eventually lower plasma ammonia levels, so that A) ventilation also returns towards control levels.

References

- Abdallah SJ, Perry SF, Jonz MG (2012) CO₂ signaling in chemosensory neuroepithelial cells of the zebrafish gill filaments: Role of intracellular Ca₂⁺ and pH. In: *Arterial chemoreception, advances in experimental medicine and biology*. (Ed.), C Nurce, C Gonzalez, C Peers, N Prabhakar, pp. 143-148. New York, Springer Press.
- Ballantyne JS (2001) Amino acid metabolism. In: *Fish physiology* Vol. 20, pp. (Ed.), WS Hoar, JD Randall, pp. 77-107. Orlando, Academic Press.
- Baker CVH (2008) The evolution and elaboration of vertebrate neural crest cells. *Curr. Opin. Genet. Dev.*, **18**, 536-543.
- Baker DW, Sardella B, Rummer JL, Sackville M, Brauner CJ (2015) Hagfish: Champions of CO₂ tolerance question the origins of vertebrate gill function. *Science Rep.*, **5**, 11182.
- Bardack D (1998) Relationships of living and fossil hagfishes. In: *The Biology of Hagfishes* (Ed.), JM Jorgensen, JP Lomholt, RE Weber, H Malte, pp. 3-14. London, Chapman and Hall.
- Bartels H (1998) The gills of hagfishes. In: *The Biology of Hagfishes* (Ed.), JM Jorgensen, RE Weber, H Malte, pp. 205-222. New York, NY, Chapman & Hall.
- Boutilier RG, Heming TA, Iwama GK (1984) Appendix: Physicochemical parameters for use in fish respiratory physiology. In: *Gills Anatomy, Gas Transfer, and Acid-Base Regulation, Fish Physiology* Vol. 10B (Ed.), WS Hoar, DJ Randall, pp. 403-430. Orlando, Elsevier.
- Braun CB (1998) Schreiner organs: a new craniate chemosensory modality in hagfishes. *J. Comp. Neurol.*, **392**, 135-163.
- Braun CB, Northcutt GR (1998) Cutaneous exteroceptors and their innervation in hagfishes. In: *The Biology of Hagfishes* (Ed.), JM Jorgensen, JP Lomholt, RE Weber, H Malte, pp. 512-532. London, Chapman & Hall.
- Braun MH, Perry SF (2010) Ammonia and urea excretion in the Pacific hagfish *Eptatretus stoutii*: Evidence for the involvement of Rh and UT proteins. *Comp. Biochem. Physiol. A.*, **157**, 405-415.
- Braun MH, Steele SL, Perry SF (2009) The responses of zebrafish (*Danio rerio*) to high external ammonia and urea transporter inhibition: nitrogen excretion and expression of rhesus glycoproteins and urea transporter proteins. *J. Exp. Biol.*, **212**, 3846-3856.

- Braun CB, Northcutt GR (1998) Cutaneous exteroceptors and their innervation in hagfishes. In: *The Biology of Hagfishes* (Ed.), JM Jorgensen, JP Lomholt, RE Weber, H Malte, pp. 512-532. London, Chapman & Hall.
- Braun MH, Perry SF (2010) Ammonia and urea excretion in the Pacific hagfish *Eptatretus stoutii*: Evidence for the involvement of Rh and UT proteins. *J. Comp. Biochem. Physiol. A.*, **157**, 405–415.
- Bucking C, Wood CM (2008) The alkaline tide and ammonia excretion after voluntary feeding in freshwater rainbow trout. *J. Exp. Biol.*, **211**, 2533-2541.
- Burleson ML, Mercer SE, Wilk-Blaszczak MA (2006) Isolation and characterization of putative O₂ chemoreceptor cells from the gills of channel catfish (*Ictalurus punctatus*). *Brain Res.*, **1092**, 100-107.
- Burleson ML, Milsom WK (1990) Propranolol inhibits O₂-sensitive chemoreceptor activity in trout gills. *Am. J. Physiol.*, **258**, R1089-R1091.
- Burleson ML, Milsom WK (1993) Sensory receptors in the first gill arch of rainbow trout. *Respir. Physiol.*, **93**, 97-110.
- Bushnell PG, Brill RW (1992) Oxygen transport and cardiovascular responses in skipjack tuna (*Katsuwonus pelamis*) and yellowfin tuna (*Thunnus albacares*) exposed to acute hypoxia. *J. Comp. Physiol. B.*, **162**, 131-143.
- Burggren WW (1982) "Air gulping" improves blood oxygen transport during aquatic hypoxia in the goldfish, *Carassius auratus*. *Physiol. Zool.*, **55**, 327-334.
- Burleson ML, Mercer SE, Wilk-Blaszczak MA (2006) Isolation and characterization of putative O₂ chemoreceptor cells from the gills of channel catfish (*Ictalurus punctatus*). *Brain Res.*, **1092**, 100-107.
- Burleson ML, Milsom WK (1990) Propranolol inhibits O₂-sensitive chemoreceptor activity in trout gills. *J. Physiol. Soc.*, **27**, R1089-R1091.
- Burleson ML, Milsom WK (1993) Sensory receptors in the first gill arch of rainbow trout. *Res. Physiol.*, **93**, 97-110.
- Bury NR, Wood CM (1999) Mechanism of branchial apical silver uptake by rainbow trout is via the proton-coupled Na⁺ channel. *Am. Physiol. Soc.*, **46**, R1385-R1391.
- Bushnell PG, Jones DR (1994) Cardiovascular and respiratory physiology of tuna: adaptations for support of exceptionally high metabolic rates. *Environ. Biol. Fish.*, **40**, 303-318.

- Cameron JN, Davis JC (1970) Gas exchange in rainbow trout (*Salmo gairdneri*) with varying blood oxygen capacity. *J. Fisher. Board Can.*, **27**, 1069-1085.
- Cameron JN, Heisler N (1983) Studies of ammonia in the rainbow trout physico-chemical parameters, acid-base behavior and respiratory clearance. *J. Exp. Biol.*, **105**, 107-125.
- Cameron JN, Randall DJ, Davis JC (1971) Regulation of the ventilation-perfusion ratio in the gills of *Dasyatis sabina* and *Squalus suckleyi* (L.). *J. Comp. Biochem. Physiol. A*, **39**, 505-519.
- Campbell AGM, Rosenberg LE, Snodgrass PJ, Nuzum CT (1973) Ornithine transcarbamylase deficiency: a cause of lethal neonatal hyperammonemia in males. *New Engl. J. Med.*, **288**, 1-5.
- Carlson JK, Goldman KJ, Lowe CG (2004) Metabolism, energetic demand, and endothermy. In: *Biology of sharks and their relatives* (Ed.), JC Carrier, JA Musick, MR Heithaus, pp. 203-224. New York, CRC Press.
- Cech JJ, Wohlschlag DE (1973) Respiratory responses of the striped mullet, *Mugil cephalus* (L.), to hypoxic conditions. *J. Fish Biol.*, **5**, 421-428.
- Clifford AM, Goss GG, Wilkie MP (2015) Adaptations for a deepsea scavenger: extreme ammonia tolerance and active NH₄⁺ excretion by the Pacific hagfish (*Eptatretus stoutii*). *J. Comp. Biochem. Physiol. A.*, **182**, 64-74.
- Clifford AM, Weinrauch AM, Edwards SL, Wilkie MP, Goss GG (2017) Flexible ammonia handling strategies using both cutaneous and branchial epithelia in the highly ammonia-tolerant Pacific hagfish. *Am. J. Physiol. Regul. Integr. Comp. Physiol.*, **313**, R78-R90.
- Clifford AM, Guffey SC, Goss GG (2014) Extra-branchial mechanisms of systemic pH recovery in hagfish (*Eptatretus stoutii*). *Comp. Biochem. Physiol. A Mol. Integr. Physiol.*, **168**, 82-89.
- Clifford AM, Weinrauch AM, Goss GG (2018) Dropping the base: recovery from extreme hypercarbia in the CO₂ tolerant Pacific hagfish (*Eptatretus stoutii*). *J. Comp. Physiol. B.*, **188**, 421-435.
- Clifford AM, Zimmer AM, Wood CM, Goss GG (2016) It's all in the gills: evaluation of O₂ uptake in Pacific hagfish refutes a major respiratory role for the skin. *J. Exp. Biol.*, **219**, 2814-2818.
- Clarke A, Johnston NM (1999) Scaling of metabolic rate with body mass and temperature in teleost fish. *J. Anim. Ecol.*, **68**, 893-905.
- Cole FJ (1905) A monograph on the general morphology of the Myxinoid fishes based on a study of

- Myxine*. Part I. The anatomy of the skeleton. *Trans. R. Soc. Edinburgh.*, **41**, 749-788.
- Coolidge EH, Ciuhandu CS, Milsom WK (2008) A comparative analysis of putative oxygen-sensing cells in the fish gill. *J. Exp. Biol.*, **211**, 1231-1242.
- Cooper AJ, Plum F (1987) Biochemistry and physiology of brain ammonia. *Physiol. Rev.*, **67**, 440-519.
- Cox GK, Sandblom E, Farrell AP (2010) Cardiac responses to anoxia in the Pacific hagfish, *Eptatretus stoutii*. *J. Exp. Biol.*, **213**, 3692-3698.
- Cox GK, Sandblom E, Richards JG, Farrell AP (2011) Anoxic survival of the Pacific hagfish (*Eptatretus stoutii*). *J. Comp. Physiol. B*, **181**, 361-371.
- Coxon SE, Davison W (2011) Structure and function of the velar muscle in the New Zealand hagfish *Eptatretus cirrhatus*: response to temperature change and hypoxia. *J. Fish Biol.*, **79**, 280-289.
- Davis JC, Cameron JN (1971) Water flow and gas exchange at the gills of rainbow trout, *Salmo gairdneri*. *J. Exp. Biol.*, **54**, 1-18.
- Daxboeck C, Holeton GF (1978) Oxygen receptors in the rainbow trout, *Salmo gairdneri*. *Can. J. Zool.*, **56**, 1254-1259.
- Davis JC, Cameron JN (1971) Water flow and gas exchange at the gills of rainbow trout, *Salmo gairdneri*. *J. Exp. Biol.*, **54**, 1-18.
- Dawson JA (1963) The oral cavity, the 'Jaws' and the horny teeth of *Myxine glutinosa*. In: *Biology of Myxine* (Ed.), A Brodal, R Fange, pp. 231-255. Oslo, Universitetsforlaget.
- DeBoeck G, Wood CM (2015) Does ammonia trigger hyperventilation in the elasmobranch, *Squalus acanthias suckleyi*? *Respir. Physiol. Neurobiol.*, **206**, 25-35.
- Drazen JC, Yeh J, Friedman J, Condon N (2011) Metabolism and enzyme activities of hagfish from shallow and deep water of the Pacific Ocean. *J. Comp. Biochem. Physiol. A*, **159**, 182-187.
- Dymowska AK, Hwang PP, Goss GG (2012) Structure and function of ionocytes in the freshwater fish gill. *Respir. Physiol. Neurobiol.*, **184**, 282-292.
- Eddy FB (1974) Blood gases of the tench (*Tinca tinca*) in well aerated and oxygen-deficient waters. *J. Exp. Biol.*, **60**, 71-83.
- Eddy FB (2005) Ammonia in estuaries and effects on fish. *J. Fish Biol.*, **67**, 1495-1513.
- Edwards SL, Arnold J, Blair SD, Pray M, Bradley R, Erikson O, Walsh PJ (2015) Ammonia excretion in the Atlantic hagfish (*Myxine glutinosa*) and responses of an Rhc glycoprotein. *Am. J. Physiol.*, **308**, R769-R778.

- Eliason EJ, Farrell AP (2014) Effect of hypoxia on specific dynamic action and postprandial cardiovascular physiology in rainbow trout (*Oncorhynchus mykiss*). *J. Comp. Biochem. Physiol. A*, **171**, 44-50.
- Eom J, Wood CM (2019) The ventilation mechanism of the Pacific hagfish *Eptatretus stoutii*. *J. Fish Biol.*, **94**, 261-276.
- Eom J, Fehsenfeld S, Wood CM (2020) Is ammonia excretion affected by gill ventilation in the rainbow trout *Oncorhynchus mykiss*? *Respir. Physiol. Neurobiol.*, **275**, 103385
- Eom J, Giacomini M, Clifford AM, Goss GG, Wood CM (2019) Ventilatory sensitivity to ammonia in the Pacific hagfish (*Eptatretus stoutii*), a representative of the oldest extant connection to the ancestral vertebrates. *J. Exp. Biol.*, **222**, jeb199794.
- Eom J, Wood CM (2020) A less invasive system for the direct measurement of ventilation in fish. *Can. J. Fisher. Aquat. Sci.*, **77**, 1870-1877.
- Eom J, Wood CM (2021a) Brain and gills as internal and external ammonia sensing organs for ventilatory control in rainbow trout *Oncorhynchus mykiss*. *Comp. Biochem. Physiol. A*, **254**, 110896. doi.10.1016/j.cbpa.2021.110896.
- Eom J, Wood CM (2021b) Understanding ventilation and oxygen uptake of Pacific hagfish (*Eptatretus stoutii*), with particular emphasis on responses to ammonia and interaction with other respiratory gases. *J. Comp. Physiol. B*, **191**, 255–271 doi.org/10.1007/s00360-020-01329-7.
- Evans DH, Cameron JN (1986) Gill ammonia transport. *J. Exp. Zool.*, **239**, 17-23.
- Evans DH, Piermarini PM, Choe KP (2005) The multifunctional fish gill: dominant site of gas exchange, osmoregulation, acid-base regulation, and excretion of nitrogenous waste. *Physiol. Rev.*, **85**, 97-177.
- Fehsenfeld S, Weihrauch D (2016) The role of ancestral hyperpolarization-activated cyclic nucleotide-gated K⁺ channel in branchial acid-base regulation in the green crab, *Carcinus maenas*. *J. Exp. Biol.*, **219**, 887-896.
- Felipo V, Butterworth RF (2002) Neurobiology of ammonia. *Prog. Neurobiol.*, **67**, 259-279.
- Florindo LH, Armelin VA, McKenzie DJ, Rantin FT (2018) Control of air-breathing in fishes: Central and peripheral receptors. *Acta Histochemica.*, **120**, 642-653.
- Fivelstad S, Binde M (1994) Effects of reduced waterflow (increased loading) in soft water on Atlantic salmon smolts (*Salmo salar* L.) while maintaining oxygen at constant level by oxygenation of the inlet water. *Aquacul. Engin.*, **13**, 211-218.

- Forster ME, Davison W, Axelsson M, Farrell AP (1992) Cardiovascular responses to hypoxia in the hagfish, *Eptatretus cirrhatus*. *Respir. Physiol.*, **88**, 373-386.
- Forster ME, Russell MJ, Hambleton DC, Olson KR (2001) Blood and extracellular fluid volume in whole body and tissues of the Pacific hagfish, *Eptatretus stoutii*. *Physiol. Biochem. Zool.*, **74**, 750-756.
- Garey WF (1967) Gas exchange, cardiac output and blood pressure in free-swimming carp (*Cyprinus carpio*). Ph. D. dissertation, Department of Physiology, University of New York at Buffalo, New York, N.Y.
- Gentle MJ, Tilston VL (2000) Nociceptors in the legs of poultry: implications for potential pain in pre-slaughter shackling. *Anim. Welfare*, **9**, 227-236.
- Gerald JW, Cech Jr. JJ (1970) Respiratory responses of juvenile catfish (*Ictalurus punctatus*) to hypoxic conditions. *Physio. Zool.*, **43**, 47-54.
- Giacomin M, Dal Pont G, Eom J, Schulte PM, Wood CM (2019a) The effects of salinity and hypoxia exposure on oxygen consumption, ventilation, diffusive water exchange and ionoregulation in the Pacific hagfish (*Eptatretus stoutii*). *J. Comp. Biochem. Physiol. A*, **232**:47-59.
- Giacomin M, Eom J, Schulte PM, Wood CM (2019b) Acute temperature effects on metabolic rate, ventilation, diffusive water exchange, osmoregulation and acid-base status in the Pacific hagfish (*Eptatretus stoutii*). *J. Comp. Physiol. B*, **189**, 17-35.
- Gilmour KM (2001) The CO₂/pH ventilatory drive in fish. *Comp. Biochem. Physiol. A*: 130, 219-240.
- Glass ML, Andersen NA, Kruhøffer M, Williams EM, Heisler N (1990) Combined effects of environmental PO₂ and temperature on ventilation and blood gases in the carp *Cyprinus carpio* L. *J. Exp. Biol.*, **148**, 1-17.
- Glover C, Blewett TA, Wood CM (2016) Determining the functional role of waterborne amino acid uptake in hagfish nutrition: a constitutive pathway when fasting or a supplementary pathway when feeding? *J. Comp. Physiol. B*, **186**, 843-853.
- Glover C, Bucking C (2016) Feeding, digestion and nutrient absorption in hagfish. In: *Hagfish biology*. (Ed.), SL Edward, GG Goss, pp. 287-308. Boca Raton, CRC Press.
- Glover C, Bucking C, Wood CM (2011) Adaptations to *in situ* feeding: novel nutrient acquisition pathways in an ancient vertebrate. *Proc. R. Soc. B*, **278**, 3096-3101.

- Glover CN, weinrauch AM, Bynevelt S, Bucking C (2019) Feeding in *Eptatretus cirrhatus*: effects on metabolism, gut structure and digestive processes, and the influence of post-prandial dissolved oxygen availability. *J. Comp. Biochem. Physiol. A*, **229**, 52-59.
- Goodrich ES (1930) Studies on the structure and development of vertebrates. London, MacMillan and Co. Limited.
- Goss GG, Adamia S, Galvez F (2001) Peanut lectin binds to a subpopulation of mitochondria-rich cells in the rainbow trout gill epithelium. *Am. J. Physiol.*, **281**, 1718-1725.
- Graham MS, Turner JD, Wood CM (1990) Control of ventilation in the hypercapnic skate *Raja ocellata*. I. Blood and extradural fluid. *Respir. Physiol.*, **80**, 259-277.
- Gustafson G (1935) On the biology of *Myxine glutinosa*. *Arkiv for Zoologie* **28**, 1-8.
- Hall FG (1931) The respiration of puffer fish. *Biol. Bull.*, **61**, 457-467.
- Hanson D, Johansen K (1970) Relationship of gill ventilation and perfusion in Pacific dogfish, *Squalus suckleyi*. *J. Fish. Res. Board Can.*, **27**, 551-564.
- Hedrick MS, Bursleson ML, Jones DR, Milsom WK (1991) An examination of central chemosensitivity in an air-breathing fish (*Amia calva*). *J. Exp. Biol.*, **135**, 165-174.
- Heimberg AM, Cowper-Sal R, Semon M, Donoghue PCJ, Peterson KJ (2010) microRNAs reveal the interrelationship of hagfish, lampreys, and gnathostomes and the nature of the ancestral vertebrate. *Proc. Natl. Acad. Sci. USA*, **107**, 19379-19383.
- Heisler N, Toews DP, Holeton GF (1988) Regulation of ventilation and acid-base status in the elasmobranch *Scyliorhinus stellaris* during hyperoxia-induced hypercapnia. *Respir. Physiol.*, **71**, 227-246.
- Hillaby BA, Randall DJ (1979) Acute ammonia toxicity and ammonia excretion in rainbow trout (*Salmo gairdneri*). *J. Fish. Res. Board Can.*, **36**, 621-629.
- Hills AG (1973) pH and the Henderson-Hasselbalch equation. *Am. J. Medic.*, **55**, 131-133.
- Hockman D, Burns AJ, Schlosser G, Gates KP, Jevans B, Mongera A, Fisher S, Unlu G, Knapik EW, Kaufman CK, Mosimann C (2017) Evolution of the hypoxia-sensitive cells involved in amniote respiratory reflexes. *Elife*, **6**, p.e21231.
- Hofbauer M (1934) Anatomischer und histologischer Bau der Kiemensäcke von *Myxine glutinosa*. *Biol. General.*, **12**, 330-348.

- Holeton GF, Randall DJ (1967) The effect of hypoxia upon the partial pressure of gases in the blood and water afferent and efferent to the gills of rainbow trout. *J. Exp. Biol.*, **46**, 317-327.
- Holmes WM, Cotton R, Xuan VB, Rygg AD, Craven BA, Abel RL, Slack R, Cox JPL (2011) Three-dimensional structure of the nasal passageway of a hagfish and its implications for olfaction. *Anatom. Rec.*, **294**, 1045-1056.
- Hughes GM (1960) A comparative study of gill ventilation in marine teleosts. *J. Exp. Biol.*, **37**, 28-45.
- Hughes GM, Ballintijn CM (1968) Electromyography of the respiratory muscles and gill water flow in the dragonet. *J. Exp. Biol.*, **49**, 593-602.
- Hughes GM, Shelton G (1957) Pressure changes during the respiratory movements of Teleostean fishes. *Nature*, **4553**, 255.
- Hughes GM, Shelton G (1962) Respiratory mechanisms and their nervous control. *Adv. Comp. Physiol. Biochem.*, **1**, 275-364.
- Hung CYC, Tsui KNT, Wilson JM, Nawata CM, Wood CM, Wright PA (2007) Rhesus glycoprotein gene expression in the mangrove killifish *Kryptolebias marmoratus* exposed to elevated environmental ammonia levels and air. *J. Exp. Biol.*, **210**, 2419-2429.
- Hughes GM, Umezawa SI (1968a) On respiration in the dragonet *Callionymus lyra* (L.). *J. Exp. Biol.*, **49**, 565-582.
- Ito Y, Kobayashi S, Nakamura N, Miyagi H, Esaki M, Hoshijima K, Hirose S (2013) Close association of carbonic anhydrase (CA2a and CA15a), Na⁺/H⁺ exchanger (Nhe3b), and ammonia transporter Rhcg1 in zebrafish ionocytes responsible for Na⁺ uptake. *Front. Physiol.*, **4**, 59-76.
- Johansen K, Hol RA (1960) A cineradiographic study of respiration in *Myxine glutinosa*. *J. Exp. Biol.*, **37**, 474-480.
- Johansen K, Strahan R (1963) The respiratory system of *Myxine glutinosa* L. In: *Biology of Myxine* (Ed.), FR Brodal, pp. 352-371. Oslo, Universitetsforlaget.
- Jones DR, Brill RW, Butler PJ, Bushnell PG, Heieis MRA (1990) Measurement of ventilation volume in swimming tunas. *J. Exp. Biol.*, **149**, 491-498.
- Jonz MG (2018) Insights into the evolution of polymodal chemoreceptors. *Acta Histochem.*, **120**, 623-629.
- Jonz MG, Fearon IM, Nurse CA (2004) Neuroepithelial oxygen chemoreceptors of the zebrafish gill. *J. Physiol.*, **560**, 737-752.

- Jung EH, Smich J, Rubino JG, Wood CM (2020) An *in vitro* study of urea and ammonia production and transport by the intestinal tract of fed and fasted rainbow trout: responses to luminal glutamine and ammonia loading. *J. Comp. Physiol. B*, doi: 10.1007/s00360-020-01335-9.
- Kalinin AL, Severi W, Guerra CDR, Costa MJ, Rantin FT (2000) Ventilatory flow relative to intrabuccal and intraopercular volumes in the serrasalmid fish *Piaractus mesopotamicus* during normoxia and exposed to graded hypoxia. *Rev. Bras. Biol.*, **60**, 249-254.
- Kardong KV (2012) *Vertebrates: Comparative Anatomy, Function, Evolution*. New York, McGraw-Hill.
- Kerstens A, Lomholt JP, Johansen K (1979) The ventilation, extraction and uptake of oxygen in undisturbed flounders *Platichthys flesus*: responses to hypoxia acclimation. *J. Exp. Biol.*, **83**, 169-179.
- Kiceniuk JW, Jones DR (1977) The oxygen transport system in trout (*Salmo gairdneri*) during sustained exercise. *J. Exp. Biol.* **69**, 247-260.
- Kinkead R, Perry SF (1990) An investigation of the role of circulating catecholamines in the control of ventilation during acute moderate hypoxia in rainbow trout (*Oncorhynchus mykiss*). *J. Comp. Physiol. B*, **160**, 441-448.
- Knepper MA, Agre P (2004) The atomic architecture of a gas channel. *Science*, **305**, 1573-1574.
- Knoph MB (1996) Gill ventilation frequency and mortality of Atlantic salmon (*Salmo salar* L.) exposed to high ammonia levels in seawater. *Water Res.*, **30**, 837-842.
- Knoph MB, Thorud K (1996) Toxicity of ammonia to Atlantic salmon (*Salmo salar* L.) in seawater – Effects on plasma osmolality, ion, ammonia, urea and glucose levels and hematological parameters. *J. Comp. Biochem. Physiol. A*, **113**, 375-381.
- Krogh A (1938) The active absorption of ions in some freshwater animals. *Zeitschrift für vergleichende Physiologie*, **25**, 335-350.
- Krogh A (1939) *Osmotic regulation in aquatic animals*. Cambridge: Cambridge University Press.
- Lang T, Peters G, Hoffmann R, Mayer EI (1987) Experimental investigations on the toxicity of ammonia: effects on ventilation frequency, growth, epidermal mucous cells, and gill structure of rainbow trout *Salmo gairdneri*. *Dis. Aquat. Org.*, **3**, 159-165.
- Laurent P (1984) Gill internal morphology. In: *Fish physiology Volume 10* (Ed.), WS Hoar, DJ Randall, pp. 73-183. Florida, Academic Press.
- Laurent P, Dunel S (1980) Morphology of gill epithelia in fish. *Am. Physiol. Soc.*, **238**, 147-159.

- Lesser MP, Martini FH, Heiser JB (1997) Ecology of the hagfish, *Myxine glutinosa* L. in the Gulf of Maine I. Metabolic rates and energetics. *J. Exp. Mar. Biol. Ecol.*, **208**, 215-225.
- Lin H, Randall DJ (1993) H⁺-ATPase activity in crude homogenates of fish gill tissue: inhibitor sensitivity and environmental and hormonal regulation. *J. Exp. Biol.*, **180**, 163-174.
- Lisser DF, Lister ZM, Pham-Ho PQH, Scott GR, Wilkie MP (2017) Relationship between oxidative stress and brain swelling in goldfish (*Carassius auratus*) exposed to high environmental ammonia. *Am. J. Physiol. Regul. Integr. Comp. Physiol.*, **312**, R114-R124.
- Lomholt JP, Johansen K (1979) Hypoxia acclimation in carp. How it affects O₂ uptake, ventilation and O₂ excretion from water. *Physiol. Zool.*, **52**, 38-49.
- Long, JH, Adcock B, Root RG (2002) Force transmission via axial tendons in undulating fish: a dynamic analysis. *Comp. Biochem. Physiol. A*, **133**, 911-929.
- Long NP, Farina SC (2019) Enormous gill chambers of deep-sea coffinfishes (Lophiiformes: Chaunacidae) support unique ventilatory specialisations such as breath holding and extreme inflation. *J. Fish Biol.* **95**, 502-509.
- Lynn B (1996) Principles of classification and nomenclature relevant to studies of nociceptive neurons. In: *Neurobiology of Nociceptors*, (Ed.), C Cervero, F Belmonte, pp. 1-2. London, Oxford University Press.
- Mahe Y, Garcia-Romeu F, Motais R (1985) Inhibition by amiloride of both adenylate cyclase activity and the Na⁺/H⁺ antiporter in fish erythrocytes. *Europ. J. Pharmacol.*, **116**, 199-206.
- Mallatt J (1984) Early vertebrate evolution: pharyngeal structure and the origin of gnathostomes. *J. Zool. Soc. London.*, **204**, 169-183.
- Mallatt J, Paulsen C (1986) Gill ultrastructure of the Pacific hagfish *Eptatretus stoutii*. *Am. J. Anatom.*, **177**, 243-269.
- Malte H, Lomholt JP (1998) Ventilation and gas exchange. In: *Biology of Hagfishes* (Ed.), JM Jorgensen, JP Lomholt, RE Weber, H Malte, pp. 223-234. London, Chapman and Hall.
- Marinelli W, Strenger A (1956) *Myxine glutinosa* (L.). Vergleichende Anatomie und Morphologie der Wirbeltiere, Franz Deuticke, Vienna, Bd II.
- Marini AM, Matassi G, Raynal V, Andre B, Cartron JP, Cherif-Zahar B (2000) The human Rhesus-associated RhAG protein and a kidney homologue promote ammonium transport in yeast. *Nature Genetics*, **26**, 341-344.

- Martini FH (1998) The ecology of hagfishes. In: *The Biology of Hagfishes* (Ed.), JM Jorgensen, JP Lomholt, RE Weber, H Malte, pp. 57-78. London, Chapman and Hall.
- McCue MD (2006) Specific dynamic action: a century of investigation. *J. Comp. Biochem. Physiol. A*, **144**, 381-394.
- McFarland WN (1959) A study of the effects of anesthetics on the behaviour and physiology of fishes. *Publ. Inst. Mar. Sci. Univ. Tex.*, **6**, 23-55.
- McInerney JE, Evans DO (1970) Habitat characteristics of the Pacific hagfish, *Polistotrema stoutii*. *J. Fish. Res. Bd Canada.*, **27**, 966-968.
- McKenzie DJ, Randall DJ, Lin H, Aota S (1993) Effects of changes in plasma pH, CO₂, and ammonia on ventilation in trout. *Fish Physiol. Biochem.*, **10**, 507-515.
- McKim JM, Goeden HM (1982) A direct measure of the uptake efficiency of a xenobiotic chemical across the gills of brook trout (*Salvelinus fontinalis*) under normoxic and hypoxic conditions. *J. Comp. Biochem. Physiol. C*, **72**, 65-74.
- Mettam JJ, McCrohan CR, Sneddon LU (2012) Characterization of chemosensory trigeminal receptors in the rainbow trout, *Oncorhynchus mykiss*: responses to chemical irritants and carbon dioxide. *J. Exp. Biol.*, **215**, 685-693.
- Millen JE, Murdaugh Jr. HV, Hearn DC, Robin ED (1966) Measurement of gill water flow in *Squalus acanthias* using the dye-dilution technique. *Am. J. Physiol.*, **211**, 11-14.
- Milligan CL, Wood CM (1987) Regulation of blood oxygen transport and red cell pHi after exhaustive activity in rainbow trout (*Salmo gairdneri*) and starry flounder (*Platichthys stellatus*). *J. Exp. Biol.*, **133**, 263-282.
- Milsom WK (2012) New insights into gill chemoreception: Receptor distribution and roles in water and air breathing fish. *Respir. Physiol. Neurobiol.*, **184**, 326-339.
- Milsom WK, Bursleson ML (2007) Peripheral arterial chemoreceptors and the evolution of the carotid body. *Respir. Physiol. Neurobiol.*, **157**, 4-11.
- Milsom WK (2012) New insights into gill chemoreception: receptor distribution and roles in water and air breathing fish. *Respir. Physiol. Neurobiol.*, **184**, 326-339.
- Miyashita T, Coates MI, Farrar R, Larson P, Manning PL, Wogelius RA, Edwards NP, Anne J, Bermann U, Palmer RA, Currie PJ (2019) Hagfish from the Cretaceous Tethys sea and a reconciliation of

- the morphological-molecular conflict in early vertebrate phylogeny. *Proc. Natl. Acad. Sci. USA*, **116**, 2146-2151.
- Mommsen TP, Hochachka PW (1988) The purine nucleotide cycle as two temporally separated metabolic units: a study on trout muscle. *Metabolism.*, **37**, 552-556.
- Munz FW, Morris R (1965) Metabolic rate of the hagfish, *Eptatretus stoutii* (Lockington) 1878. *Comp. Biochem. Physiol.*, **16**, 1-6.
- Mutch BJ, Banister E (1983) Ammonia metabolism in exercise and fatigue: a review. *Med. Sci. Sports. Exerc.*, **15**, 41-50.
- Nakada T, Hoshijima K, Esaki M, Nagayoshi S, Kawakami K, Hirose S (2007a) Localization of ammonia transporter Rhcg1 in mitochondrion rich cells of yolk sac, gill and kidney of zebrafish and its ionic strength-dependent expression. *Am. J. Physiol.*, **293**, R1743-R1753.
- Nakada T, Westhoff CM, Kato A, Hirose S (2007b) ammonia secretion from fish gill depends on a set of Rh glycoproteins. *FASEB*, **21**, 1067-1074.
- Nawata CM, Huang CCY, Tsui TKN, Wilson JM, Wright PA, Wood CM (2007) Ammonia excretion in rainbow trout (*Oncorhynchus mykiss*): evidence for Rh glycoprotein and H⁺-ATPase involvement. *Am. J. Physiol. Soc.*, **31**, 463-474.
- Nawata CM, Hirose S, Nakada T, Wood CM, Kato A (2010a) Rh glycoprotein expression is modulated in pufferfish (*Takifugu rubripes*) during high environmental ammonia exposure. *J. Exp. Biol.*, **213**, 3150-3160.
- Nawata CM, Walsh PJ, Wood CM (2015) Physiological and molecular responses of the spiny dogfish shark (*Squalus acanthias*) to high environmental ammonia: scavenging for nitrogen. *J. Exp. Biol.*, **281**, 238-248.
- Nawata CM, Wood CM, O'Donnell MJ (2010b) Functional characterization of Rhesus glycoproteins from an ammoniotelic teleost, the rainbow trout, using oocyte expression and SIET analysis. *J. Exp. Biol.*, **213**, 1049-1059.
- Nawata CM, Wood CM (2009) mRNA expression analysis of the physiological responses to ammonia infusion in rainbow trout. *J. Comp. Physiol. B*, **179**, 799-810.
- Nilsson S (1986) Control of gill blood flow. In: *Fish Physiology: Recent Advances* (Ed.), S Nilsson, S Holmgren, pp. 87-101. London, Croom Helm.
- Oisi Y, Ota KG, Kuraku S, Fujimoto S, Kuratani S (2013) Craniofacial development of hagfishes and the evolution of vertebrates. *Nature*. 493, 175-181.

- Olson KR (2002). Vascular anatomy of the fish gill. *J. Exp. Zool.*, **293**, 214-231.
- Ota KG, Kuraku S, Kuratani S (2007) Hagfish embryology with reference to the evolution of the neural crest. *Nature*, **446**, 672-675.
- Perry SF, Davie PS, Daxboeck C, Ellis AG, Smith DG (1984) Perfusion methods for the study of gill physiology. In: *Fish Physiology*. (Ed.), DJ Randall, WS Hoar, pp. 325-388. New York, Academic Press.
- Perry SF, Jonz MG, Gilmour KM (2009a) Oxygen sensing and the hypoxic ventilatory response. In: *Fish Physiology* (Ed.), JG Richards, AP Farrell, CJ Brauner, pp. 193-253. San Diego, Academic Press.
- Perry SF, Tzaneva V (2016) The sensing of respiratory gases in fish: mechanisms and signalling pathways. *Respir. Physiol. Neurobiol.*, **224**, 71-79.
- Perry SF, Vulesevic B, Braun M, Gilmour KM (2009b) Ventilation in Pacific hagfish (*Eptatretus stoutii*) during exposure to acute hypoxia or hypercapnia. *Respir. Physiol. Neurobiol.*, **167**, 227-234.
- Peters T, Gros G (1988) Transport of bicarbonate, other ions and substrates across the red blood cell membrane of hagfishes. In: *Biology of hagfishes*. (Ed.), JM Jorgensen, JP Lomholt, RE Weber, H Malte, pp. 307-320. London, Chapman and Hall.
- Piiper J, Schumann DB (1968) Effectiveness of O₂ and CO₂ exchange in the gills of the dogfish (*Scyliorhinus stellaris*). *Res. Physiol.*, **5**, 338-349.
- Playle RC, Munger RS, Wood CM (1990) Effects of catecholamines on gas exchange and ventilation in rainbow trout (*Salmo gairdneri*). *J. Exp. Biol.*, **152**, 353-367.
- Poppell JW, Cuajunco JS, Horsley JS, Randall HT, Roberts KE (1956) Renal arteriovenous ammonium difference and total renal ammonia production in normal, acidotic and alkalotic dogs. *Clin. Res.*, **4**, 137.
- Poppell JW, Roberts KE, Thompson RF, Vanamee P (1956) Respiratory alkalosis accompanying ammonium toxicity. *J. Appl. Physiol.*, **9**, 367-370.
- Porteus C, Kumai Y, Abdallah SJ, Yew HM, Kwong RW, Pan Y, Milsom WK, Perry SF (2020) Respiratory responses to external ammonia in zebrafish (*Danio rerio*). *J. Comp. Biochem. Physiol. A*. **251**, 110822.
- Primmitt DR, Randall DJ, Mazeaud M, Boutilier RG (1986) The role of catecholamines in erythrocyte pH regulation and oxygen transport in rainbow trout (*Salmo gairdneri*) during exercise. *J. Exp. Biol.*, **122**, 139-148.

- Rahmatullah M, Boyde TRC (1980) Improvements in the determination of urea using diacetyl monoxime; methods with and without deproteinisation. *Clin. Chim. Acta.*, **107**, 3-9.
- Randall DJ (1970) Gas exchange in fish. In: *Fish Physiology* (Ed.), WS Hoar, DJ Randall, pp. 253-292. Cambridge, Academic Press.
- Randall DJ, Baumgarten D, Malyusz M (1972) The relationship between gas and ion transfer across the gills of fishes. *J. Comp. Biochem. Physiol. A*, **41**, 629-637.
- Randall DT, Cameron JN (1973) Respiratory control of arterial pH as temperature changes in rainbow trout *Salmo gairdneri*. *Am. J. Physiol.*, **225**, 997-1002.
- Randall DJ, Ip YK (2006) Ammonia as a respiratory gas in water and air-breathing fishes. *Respir. Physiol. Neurobiol.*, **154**, 216-225.
- Randall DJ, Taylor E (1988) Circulating catecholamines and the control of ventilation in the decerebrate dogfish. *J. Physiol. Lond.*, **412**, 63.
- Randall DJ, Tsui TKN (2002) Ammonia toxicity in fish. *Mar. Pollut. Bull.*, **45**, 17-23.
- Rasmussen AS, Janke A, Arnason U (1998) The mitochondrial DNA molecule of the hagfish (*Myxine glutinosa*) and vertebrate phylogeny. *J. Molecul. Evol.*, **46**, 382-388.
- Read LJ (1975) Absence of ureogenic pathways in liver of the hagfish *Bdellostoma cirrhatum*. *J. Comp. Biochem. Physiol. B*, **51**, 139-141.
- Richardson J, Williams EK, Hickey CW (2001) Avoidance behaviour of freshwater fish and shrimp exposed to ammonia and low dissolved oxygen separately and in combination. *N. Z. J. Mar. Freshwater Res.*, **35**, 625-633.
- Ripoche P, Bertrand O, Gane P, Birkenmeier C, Colin Y, Cartron JP (2004) Human Rhesus-associated glycoprotein mediates facilitated transport of NH₃ into red blood cells. *Proc. Natl. Acad. Sci. USA*. **101**, 17222-17227.
- Roberts JL (1975) Active branchial and ram gill ventilation in fishes. *Biol. Bull.*, **148**, 85-105.
- Roberts KE, Thompson GF, Poppell WJ, Vanamee P (1956) Respiratory alkalosis accompanying ammonia toxicity. *J. Appl. Physiol.*, **9**, 367-370.
- Rovainen CM (1977) Neural control of ventilation in the lamprey. *Fed. Proceed.*, **36**, 2386-2389.
- Salama A, Morgan IJ, Wood CM (1999) The linkage between Na⁺ uptake and ammonia excretion in rainbow trout: kinetic analysis, the effects of (NH₄)₂SO₄ and NH₄HCO₃ infusion and the influence of gill boundary layer pH. *J. Exp. Biol.*, **202**, 697-709.

- Sanderson LA, Wright PA, Robinson JW, Ballantyne JS, Bernier NJ (2010) Inhibition of glutamine synthetase during ammonia exposure in rainbow trout indicates a high reserve capacity to prevent brain ammonia toxicity. *J. Exp. Biol.*, **213**, 2343-2353.
- Saunders RL (1962) The irrigation of the gills in fishes: II. Efficiency of oxygen uptake in relation to respiratory flow activity and concentrations of oxygen and carbon dioxide. *Can. J. Zool.*, **40**, 817-862.
- Scarabello M, Heigenhauser GJF, Wood CM (1991) The oxygen debt hypothesis in juvenile rainbow trout after exhaustive exercise. *Respir. Physiol.*, **84**, 245-259.
- Schenone G, Arillo A, Margiocco C, Melodia F, Mensi P (1982) Biochemical basis for environmental adaptation in goldfish (*Carassius auratus*): resistance to ammonia. *Ecotoxicol. Environ. Safety*, **6**, 479-488.
- Secor SM (2009) Specific dynamic action: a review of the postprandial metabolic response. *J. Comp. Physiol. B*, **179**, 1-56.
- Seth H, Sandblom E, Axelsson M (2009) Nutrient-induced gastrointestinal hyperemia and specific dynamic action in rainbow trout (*Oncorhynchus mykiss*)—importance of proteins and lipids. *Am. J. Physiol. Regul. Integrat. Comp. Physiol.*, **296**, R345-R352.
- Shelton G, Jones DR, Milsom WK (1986) Control of breathing in ectothermic vertebrates. In: *Handbook of Physiology, Section 3; The Respiratory System, Vol II: Control of Breathing, Part 2*. (Ed.), NS Cherniak, JG Widdicombe, MD Bethesda, pp. 857-909. Rockville, American Physiological Society.
- Sidell BD, Stowe DB, Hansen CA (1984) Carbohydrate is the preferred metabolic fuel of the hagfish (*Myxine glutinosa*) heart. *Physiol. Zool.*, **57**, 266-273.
- Sinha AK, Liew HJ, Nawata CM, Blust R, Wood CM, De Boeck G (2013) Modulation of Rh glycoproteins, ammonia excretion and Na⁺ fluxes in three freshwater teleosts when exposed chronically to high environmental ammonia. *J. Exp. Biol.*, **216**, 2917-2930.
- Smart GR (1978) Investigations of the toxic mechanisms of ammonia to fish-gas exchange in rainbow trout (*Salmo gairdneri*) exposed to acutely lethal concentrations. *J. Fish Biol.*, **12**, 93-104.
- Smith HW (1929) The excretion of ammonia and urea by the gills of fish. *J. Biol. Chem.*, **81**, 727-742.
- Smith CR (1985) Food for the deep sea: utilization, dispersal, and flux of nekton falls at the Santa Catalina Basin. *Deep Sea Res.*, **32**, 417-442.

- Smith FM, Jones DR (1982) The effect of changes in blood oxygen-carrying capacity on ventilation volume in the rainbow trout (*Salmo gairdneri*). *J. Exp. Biol.*, **97**, 325–334.
- Sneddon LU (2003) Trigeminal somatosensory innervation of the head of a teleost fish. *Brain Res.*, **972**, 44-52.
- Sneddon LU (2019) Evolution of nociception and pain: evidence from fish models. *Philos. Trans. R. Soc. Lond. B*, **374**, 20190290.
- Spray DC (1976) Pain and temperature receptors of anurans. In: *Frog neurobiology* (Ed.), R Llinas, W Precht, pp. 607-628. Berlin, Springer.
- Soivio A, Westman K, Nyholm K (1972) Improved method of dorsal aorta catheterization: Hematological effects followed for three weeks in rainbow trout (*Salmo gairdneri*). *Finn. Fish. Rep.*, **1**, 11-21.
- Steffensen JF (1985) Ram ventilation in fishes: Energetic consequences and dependence on water oxygen tension. *J. Exp. Biol.*, **114**, 141-150.
- Steffensen JF, Johansen K, Sindberg CD, Sørensen JH, Møller JL (1984) Ventilation and oxygen consumption in the hagfish, *Myxine glutinosa* L. *J. Exp. Mar. Biol. Ecol.*, **84**, 173-178.
- Stevens ED, Randall DJ (1967) Changes of gas concentrations in blood and water during moderate swimming activity in rainbow trout. *J. Exp. Biol.*, **46**, 329-337.
- Strahan R (1958) The velum and the respiratory current of *Myxine*. *Acta Zoologica* **39**, 227-240.
- Suzuki A, Komata H, Iwashita S, Seto S, Ikeya H, Tabata M, Kitano T (2017) Evolution of the Rh gene family in vertebrates revealed by brown hagfish (*Eptatretus atami*) genome sequences. *Molecul. Phylogenet. Evol.*, **107**, 1-9.
- Takeda T (1990) Ventilation, cardiac output and blood respiratory parameters in the carp, *Cyprinus carpio*, during hyperoxia. *Respir. Physiol.*, **81**, 227-239.
- Tambs-Lyche H (1969) Notes on the distribution and ecology of *Myxine glutinosa* L. *Fisk. skrifter serie havundersøkelser*, **15**, 179-184.
- Taylor EW (1992) Nervous control of the heart and cardiorespiratory interactions. In: *Fish Physiology Volume 12 Part B* (Ed.), WS Hoar, DJ Randall, AP Farrell, pp. 343-387. Florida, Academic Press.
- Taylor JR, Cooper CA, Mommsen TP (2011) Implications of GI function for gas exchange, acid-base balance and nitrogen metabolism. In: *The multifunctional gut, Fish physiology, Volume 30* (Ed.),

- M Grosell, AP Farrell, CJ Brauner, pp. 213-259. San Diego, Academic Press.
- Theisen B (1976) The olfactory system in the Pacific hagfishes *Eptatretus stoutii*, *Eptatretus deani*, and *Myxine circifrons*. *Acta Zool.*, **57**, 167-173.
- Thomsen J, Himmerkus N, Holland N, Sartoris FJ, Bleich M, Tresguerres M (2016) Ammonia excretion in mytilid mussels is facilitated by ciliary beating. *J. Exp. Biol.*, **219**, 2300-2310.
- Tsui TKN, Hung CYC, Nawata CM, Wilson JM, Wright PA, Wood CM (2009) Ammonia transport in cultured gill epithelium of freshwater rainbow trout: the importance of Rhesus glycoproteins and the presence of an apical Na⁺/NH₄⁺ exchange complex. *J. Exp. Biol.*, **212**, 878–892.
- Tzaneva V, Perry SF (2010) The control of breathing in goldfish (*Carassius auratus*) experiencing thermally induced gill remodeling. *J. Exp. Biol.*, **213**, 3666-3675.
- Van Dam L (1938) On the utilization of oxygen and regulation of breathing in some aquatic animals. Doctoral dissertation. University of Groningen, Groningen, Netherlands.
- Vanamee P, Poppell JW, Glicksman AS, Randall HT, Roberts KE (1955) Respiratory alkalosis in hepatic coma. *JAMA Inter. Med.*, **97**, 762-767.
- Verdouw H, van Eched CJA, Dekkers EMJ (1978) Ammonia determination based on indophenol formation with sodium salicylate. *Water Res.*, **12**, 399-402.
- von Doring M, Andres K (1988) Skin sensory organs in the Atlantic hagfish *Myxine glutinosa*. In: *Biology of Hagfishes* (Ed.), M Jorgensen, RE Weber, H Malte, pp. 499-511. London, Chapman and Hall of Thomson Science.
- Vulesevic B, McNeill B, Perry SF (2006) Chemoreceptor plasticity and respiratory acclimation in the zebrafish *Danio rerio*. *J. Exp. Biol.*, **209**, 1261-1273.
- Walsh PJ, Veauvy CM, McDonald MD, Pamerter ME, Buck LT, Wilkie MP (2007) Piscine insights into comparisons of anoxia tolerance, ammonia toxicity, stroke and hepatic encephalopathy. *J. Comp. Biochem. Physiol. A*, **147**, 332–343.
- Walsh PJ, Wang Y, Campbell CE, DeBoeck G, Wood CM (2001) Patterns of nitrogenous waste excretion and gill urea transporter mRNA expression in several species of marine fish. *Mar. Biol.*, **139**, 839-844.
- Walters ET (1996) Comparative and evolutionary aspects of nociceptor function. In: *Neurobiology of nociceptors*. (Ed.), C Belmonte, F Cervero, pp. 92-116. London, Oxford University Press.

- Wang Y, Heigenhauser GJF, Wood CM (1994) Integrated responses to exhaustive exercise and recovery in rainbow trout white muscle: acid-base, phosphogen, carbohydrate, lipid, ammonia, fluid volume and electrolyte metabolism. *J. Exp. Biol.*, **195**, 227–258.
- Warren KW (1958) The differential toxicity of ammonium salts. *J. Clin. Invest.*, **37**, 497-501.
- Weinrauch AM, Clifford AM, Goss GG (2018) Post-prandial physiology and intestinal morphology of the Pacific hagfish (*Eptatretus stoutii*). *J. Comp. Physiol. B*, **188**, 101-112.
- Weihrauch D, Allen GJ (2018) Ammonia excretion in aquatic invertebrates: new insights and questions. *J. Exp. Biol.*, **221**, jeb178673.
- Weihrauch D, Morris S, Towle DW (2004) Ammonia excretion in aquatic and terrestrial crabs. *J. Exp. Biol.*, **207**, 4491-4504.
- Weihrauch D, Wilkie MP, Walsh PJ (2009) Ammonia and urea transporters in gills of fish and aquatic crustaceans. *J. Exp. Biol.*, **212**, 1716-1730.
- Wells RM, Forster ME, Davison W, Taylor HH, Davie PS, Satchell GH (1986) Blood oxygen transport in the free-swimming hagfish, *Eptatretus cirrhatus*. *J. Exp. Biol.*, **43**, 43-53.
- Westhoff CM, Ferreri-Jacobia M, Mak DOD, Foskett JK (2002) Identification of the erythrocyte Rh blood group glycoprotein as a mammalian ammonium transporter. *J. Biol. Chem.*, **277**, 12499-12502.
- Wicks BJ, Randall DJ (2002) The effect of feeding and fasting on ammonia toxicity in juvenile rainbow trout, *Oncorhynchus mykiss*. *Aquat. Toxicol.*, **59**, 71-82.
- Wichser J, Kazemi H (1974) Ammonia and ventilation: Site and mechanism of action. *Res. Physiol.*, **20**, 393-406.
- Wicks BJ, Randall DJ (2002) The effect of feeding and fasting on ammonia toxicity in juvenile rainbow trout, *Oncorhynchus mykiss*. *Aquat. Toxicol.*, **59**, 71–82.
- Wilkie MP (1997) Mechanisms of ammonia excretion across fish gills. *J. Comp. Biochem Physiol. A*, **118**, 39-50.
- Wilkie MP (2002) Ammonia excretion and urea handling by fish gills: present understanding and future research challenges. *J. Exp. Biol.*, **293**, 284-301.
- Wilkie MP, Clifford A, Edwards SL, Goss GG (2017) Wide scope of ammonia and urea excretion in foraging Pacific hagfish. *Mar. Biol.*, **164**, 126.
- Wilson RJA, Harris MB, Remmers JE, Perry SF (2000) Evolution of air-breathing and central CO₂/H⁺

- respiratory chemosensitivity: new insights from an old fish? *J. Exp. Biol.*, **203**, 3505–3512.
- Wilkie MP, Pamenter ME, Duquette S, Dhiyebi H, Sangha N, Skelton G, Smith MD, Buck LT (2011) The relationship between NMDA receptor function and the high ammonia tolerance of anoxia-tolerant goldfish. *J. Exp. Biol.*, **214**, 4107-4120.
- Wilkes PRH, Walker RL, McDonald DG, Wood CM (1981) Respiratory, ventilatory, acid-base and ionoregulatory physiology of the white sucker (*Catostomus commersoni*): the influence of hyperoxia. *J. Exp. Biol.*, **91**, 239-254.
- Wilson RW, Wright PM, Munger S, Wood CM (1994) Ammonia excretion in freshwater rainbow trout (*Oncorhynchus mykiss*) and the importance of gill boundary layer acidification: lack of evidence for $\text{Na}^+/\text{NH}_4^+$ exchange. *J. Exp. Biol.*, **191**, 37-58.
- Wolf K (1963) Physiological salines for fresh-water teleosts. *Progress. Fish-Cultur.*, **25**, 135-140.
- Wood CM (1988) Acid-base and ionic exchanges at gills and kidney after exhaustive exercise in the rainbow trout. *J. Exp. Biol.*, **136**, 461-481.
- Wood CM (1993) Ammonia and urea metabolism and excretion. In: *The Physiology of Fishes*. (Ed.), D Evans, pp. 379-425. Boca Raton, CRC Press.
- Wood CM (2001) The influence of feeding, exercise, and temperature on nitrogen metabolism and excretion. In: *Fish Physiology Volume 20* (Ed.), WP Anderson, PA Wright, pp. 201-238. Orlando, Academic Press.
- Wood CM, Jackson EB (1980) Blood acid-base regulation during environmental hyperoxia in the rainbow trout (*Salmo gairdneri*). *Respir. Physiol.*, **42**, 351-372.
- Wood CM, McMahon BR, McDonald DG (1979) Respiratory gas exchange in the resting starry flounder, *Platichthys stellatus*: a comparison with other teleosts. *J. Exp. Biol.*, **78**, 167-179.
- Wood CM, Munger R (1994) Carbonic anhydrase injection provides evidence for the role of blood acid-base status in stimulating ventilation after exhaustive exercise in rainbow trout. *J. Exp. Biol.* **194**, 225-253.
- Wood CM, Nawata CM (2011) A nose-to-nose comparison of the physiological and molecular responses of rainbow trout to high environmental ammonia in sea water versus fresh water. *J. Exp. Biol.*, **214**, 3557–3569.

- Wood CM, Ruhr IM, Schauer KL, Wang Y, Mager EM, McDonald MD, Stanton B, Grosell M (2019) The osmorepiratory compromise in the euryhaline killifish: water regulation during hypoxia. *J. Exp. Biol.*, 222: pii: jeb204818.
- Wright PA, Randall DJ, Wood CM (1988) The distribution of ammonia and H⁺ ions between tissue compartments in lemon sole (*Parophrys vetulus*) at rest, during hypercapnia, and following exercise. *J. Exp. Biol.*, **136**, 149-175.
- Wright PA, Steele SL, Huitema A, Bernier NJ (2007) Induction of four glutamine synthetase genes in brain of rainbow trout in response to elevated environmental ammonia. *J. Exp. Biol.*, **210**, 2905-2911.
- Wright PA, Wood CM (1988) Muscle ammonia stores are not determined by pH gradients. *Fish Physiol. Biochem.*, **5**, 159-162.
- Wright PA, Wood CM (2009) A new paradigm for ammonia excretion in aquatic animals: role of Rhesus (Rh) glycoproteins. *J. Exp. Biol.*, **212**, 2303-2312.
- Wright PA, Wood CM (2012) Seven things fish know about ammonia and we don't. *Respir. Physiol. Neurobiol.*, **184**, 231-240.
- Yeomans DC, Proudfit HK (1996) Nociceptive responses to high and low rates of noxious cutaneous heating are mediated by different nociceptors in the rat: electrophysiological evidence. *Pain*, **68**, 141-150.
- Zachar PC, Jonz MG (2012) Neuroepithelial cells of the gill and their role in oxygen sensing. *Respir. Physiol. Neurobiol.*, **184**, 301-308.
- Zhang L, Nawata CM, Wood CM (2013) Sensitivity in ventilation and brain metabolism to ammonia exposure in rainbow trout, *Oncorhynchus mykiss*. *J. Exp. Biol.*, **216**, 4025-4037.
- Zhang L, Nurse CA, Jonz MG, Wood CM (2011) Ammonia sensing by neuroepithelial cells and ventilatory responses to ammonia in rainbow trout. *J. Exp. Biol.*, **214**, 2678-2689.
- Zhang L, Nawata MC, Wood CM (2013) Sensitivity of ventilation and brain metabolism to ammonia exposure in rainbow trout, *Oncorhynchus mykiss*. *J. Exp. Biol.*, **216**, 4025-4037.
- Zhang L, Nawata MC, De Boeck G, Wood CM (2015) Rh protein expression in branchial neuroepithelial cells, and the role of ammonia in ventilatory control in fish. *Comp. Biochem. Physiol. A*, **186**, 39-51.
- Zhang L, Wood CM (2009) Ammonia as a stimulant to ventilation in rainbow trout *Oncorhynchus mykiss*. *Respir. Physiol. Neurobiol.*, **168**, 261-271.

Zimmer A, Nawata CM, Wood CM (2010) Physiological and molecular analysis of the interactive effects of feeding and high environmental ammonia on branchial ammonia excretion and Na⁺ uptake in freshwater rainbow trout. *J. Comp. Physiol. B*, **180**, 1191–1204.